CSPalpha as a novel pathological marker for synapse loss in neurodegenerative disease

Rupawala, Huzefa

Awarding institution:
King's College London

CSPalpha as a Novel Pathological Marker for Synapse Loss in Neurodegenerative Disease

Huzefa Jujar Rupawala

Thesis submitted in fulfilment of the degree of Doctor of Philosophy

Basic and Clinical Neuroscience
Institute of Psychiatry, Psychology and Neuroscience
King's College London

June 2021

Declaration

I declare that all the work presented in this thesis is my own, except for the following:

Post-mortem Human Tissues:

- Immunohistochemical staining of post-mortem brains was in part carried out by Lucy Granat (King's College London) (Chapter 3, Section 3.4.6).
- Homogenisation of hippocampal brain for immunoblotting in Chapter 4 was carried out by Natalie Meeson (King's College London) (Chapter 2, Section 2.4.3)

Array Tomography:

- Analysis scripts were written by Dr Marti Colom-Cadena (University of Edinburgh) and Caitlin Davies (University of Edinburgh).

Mouse Experiments:

- 3-, 9- and 12-month-old WT/ 5xFAD mice were genotyped and perfused by Xianhui Peng (King's College London) (Chapter 6, Fig 6.2)
- 6-7-month-old mice were genotyped by Manal Aljuhani (King's College London) and perfused with the assistance of Dr Keiko Mizuno (King's College London) (Chapter 2, Section 2.11.1).

Huzefa Rupawala

June 2021

Abstract

Synapse loss in Alzheimer's disease (AD) is the best correlate of cognitive impairment. However, the processes underlying synapse loss in AD are still not sufficiently understood. Synaptic proteins have been traditionally used as markers to investigate synaptic degeneration and loss, however, these have not been fully able to predict when changes in disease first occur. The neuroprotective co-chaperone protein, cysteine string protein (CSP) alpha is involved in the maintenance of protein folding, neurotransmitter release and synaptic stability. Further, it has been shown that CSPalpha can be secreted in association with neurodegenerative disease proteins such as tau, a process likely linked with "prion-like" propagation of protein aggregates across AD brain. Previous work in the Giese laboratory suggested a protective role for CSPalpha during the early stages of presynaptic degeneration in AD. This thesis builds on these findings to add new data showing the accumulation of CSPalpha near AD-associated Aβ plaques in post-mortem human brain and describes the relationship between CSPalpha and amyloid pathology.

Results are presented showing amorphous accumulations of CSPalpha near the core of Aβ deposits, that partially colocalise with hyperphosphorylated tau, dystrophic neurites and in glial cells proximal to plaques. CSPalpha is highly expressed in presynaptic terminals, and the accumulations of CSPalpha were found to localise to some, but not all dystrophic presynaptic structures, suggesting a possible or intra- or extracellular localisation. Using super resolution microscopy and array tomography, CSPalpha accumulations were found to exist in close proximity to Aβ deposits, to a greater extent than other presynaptic proteins such as synaptophysin. Varying levels of CSPalpha protein expression was identified in other neurodegenerative diseases including mixed dementia, frontotemporal lobar dementia and dementia with Lewy

bodies, along with evidence of CSPalpha accumulations but only in the presence of amyloid plaques. Furthermore, in the brains of the 5x familial AD (FAD) mice, which display memory impairments related to Aβ over-production and the development of amyloid plaques, it was found that virtually all of the Aβ-positive deposits were associated with aberrant CSPalpha accumulations.

These findings suggest a novel role for CSPalpha as a pathological marker of presynaptic damage that is associated with Aβ pathology. These findings are in-line with published reports of dystrophic presynaptic terminal structures and presynaptic protein deposits surrounding amyloid plaques. However, CSPalpha accumulations were more abundant and were also found distal from the amyloid plaque centre in comparison to other presynaptic proteins. Together these data indicate that CSPalpha may be the earliest known pathological marker of pre-synapse loss in diseases that feature Aβ deposition and may also mediate neuroprotective and/or neurodegenerative mechanisms in disease. These findings further support pre-synaptic die-back theories in AD and provide a better understanding of synapse degeneration in several neurodegenerative diseases.

Acknowledgements

Firstly, I would like to thank my primary co-supervisors, Professor Peter Giese and Dr Wendy Noble. Peter has always provided me with constant support, advice and scientific guidance throughout this PhD. He has been a great mentor and has always motivated me to grow into the scientist I am today. Wendy has provided me with the skills to think critically as an independent researcher and her scientific input has been so valuable throughout this study. I am so grateful to Wendy for encouraging me to explore novel research ideas along with undertaking exciting extracurricular opportunities.

I would like to thank Dr Keiko Mizuno and Dr Anshua Ghosh for being incredible mentors and laboratory partners, teaching and developing my scientific skills from the start of my academic journey. A huge thanks to 'Team Tau', my friends and colleagues who have given me the best advice and a social life too! Thanks to Professor Diane Hanger, Dr Maria Jimenez-Sanchez and Dr Bea Perez-Nievas for their scientific input. To my dearest friend Rebecca, who started this incredible PhD journey with me, you have always provided happiness even in the darkest of times (Albus Dumbledore) and have encouraged me every step of the way. Cindy, you have been such a massive support, bringing out the best in me and always being there to push me that extra mile. To Louisa and Paula, the best laboratory friends who know when it's time for a coffee and treating me with amazing cake bakes! To my senior mentors, Dr Lizzie Glennon and Dr Dawn Lau, for teaching and guiding me throughout this PhD. Thanks to the friends and colleagues at the Maurice Wohl, Dr Ariana Gatt, Lucy, my fellow backbencher, Frecks (Sarah) and Dr Sachin Tiwari, you have always been there for me when it was most needed.

Thanks to my past supervisors, Dr Martin Broadstock, Professor Paul Francis, Dr Wajeeha Aziz, Dr Sarah Thomas and Professor Chris Miller along with my personal tutor, Dr Sandrine Thuret, who have always believed in me to accomplish what I am today. To Dr John Pizzey, Dr Anna Battaglia and Dr Isabella Gavazzi for being the most amazing tutors who have always given me the opportunity to progress in my academic career. A special thanks to my collaborator's Dr Tara Spires-Jones, Dr Po Wah So, Professor Alan Morgan, the London Neurodegenerative diseases Brain Bank team, Edinburgh and Oxford Brain Banks, who I have had the pleasure to work with during this PhD. I would like to thank the Spires-Jones group, especially Caitlin, Jamie, Marti, Hattie and Makis, for the most memorable experiences in Edinburgh. Additionally, thanks to George and Chen at the KCL WCIC imaging facility assisting with microscopy work.

This PhD would not have been possible without the KCL MRC DTP and extended family of colleagues and support staff that have trained me during this incredible journey. Along with this, the opportunity to travel and present at amazing conferences and placement opportunities would not have been possible without funders including, MRC DTP, MRC flexible supplement and KCL ARUK network.

I would like to thank my parents, who have been there for me throughout this process, who have given up time for me and I am forever grateful for their care and love. To the Haanis and H K Family, I am always thankful for your love and affection as well as the curiosity you share with me in my work. To close friends, Karan, Suneet, Mariska, Shreeya and the Akhis and partners for giving me the best of times!

Finally, I would like to dedicate this work to my wife, Zahra. This journey has been for the both of us from the start. It has been your motivation, patience, love and happiness that has kept me going till the very end. I love you!

Table of Contents

List of Figures

List of Tables

Publications

Rupawala, H., Davies, C., Granat, L., Colom-Cadena, M., Shah, K., Aljuhani, M., Mizuno, K., Troakes, C., Rose, J., Morgan, A., So, P., Hortobagyi, T., Spires-Jones, T., Noble, W., Giese, K. P. (2021). CSPalpha accumulations discovered in beta-amyloid diseases. (In preparation)

Lau, D., Paillusson, S., Hartopp, N., **Rupawala, H**., Morotz, G., Gomez-Suaga, P., Greig, J., Troakes, C., Noble, W., Miller, C. (2020). Disruption of ER-mitochondria tethering proteins in post-mortem Alzheimer's disease brain. *Neurobiology of Disease.143.*

Sekhar, G. N., Fleckney, A., Boyanova, S., **Rupawala, H**., Lo, R., Wang, H., Farag, D., Rahman, K. M., Broadstock, M., Reeves, S. J. & Thomas, S. A. (2019). Region-specific blood-brain barrier transporter changes leads to increased sensitivity to amisulpride in Alzheimer's disease. *Fluid and Barriers of the CNS. 16.*

Aziz, W., Kraev, I., Mizuno, K., Kirby, A. J., Fang, T., **Rupawala, H**., Kasbi, K., Rothe, S., Jozsa, F., Rosenblum, K., Stewart, M. & Giese, K. P. (2019). Multi-input synapses, but not LTP-strengthened synapses, correlate with hippocampal memory storage in ages mice. *Current biology. 29.* 3600-3610.

Burford, C., Pasha, T., Iver, P., **Rupawala, H.**, Andreica, E. C. & Huett, M. (2019). Initiatives to reduce neurophobia in medical students: a novel neuroscience conference model. *Journal of the Neurological Sciences. 398.* 119-120.

Abbreviations

3D	3-Dimensions
Aβ	Beta-amyloid
AβPP	Aβ precursor protein
AD	Alzheimer's disease
ADAM	A disintegrin and metalloproteinase
AICD	APP intracellular domain
ALS	Amyotrophic lateral sclerosis
AMPA	3-hydroxy-5-methyl-4- isoxazolepropionic acid
ANCL	Adult neuronal ceroid lipofuscinosis
ANOVA	Analysis of variance
ApoE	Apolipoprotein E
APS	Ammonium persulphate
APP	Amyloid precursor protein
AT	Array tomography
ATP	Adenosine triphosphate
A.U.	Arbitrary units
BA9	Brodmann Area 9
BACE	β-site APP cleaving enzyme
BCA	Bicinchoninic acid
BIN-1	Bridging integrator 1 gene
BK	Large-conductance calcium-activated potassium
BNE	BrainNet Europe
Bp	Base pair
CA1	*Cornu Ammonis* area 1
CA3	*Cornu Ammonis* area 3

CAA	Cerebral amyloid angiopathy
CaMKII	Calmodulin-dependent kinase II
cAMP	Cyclic adenosine monophosphate
CBD	Corticobasal degeneration
C-*elegans*	Caenorhabditis *Elegans*
CERAD	Consortium to establish a registry for Alzheimer's disease
CSD	Cysteine-string domain
CSF	Cerebrospinal fluid
CSP	Cysteine string protein
C-terminus	Carboxyl-terminus
CTFα	C-terminal fragment alpha
C99	C-terminal fragment of 99 amino acids
DAB	3,3′-diaminobenzidine chromogen
DAPI	4′,6-diamidino-2--phenylindole
DLB	Dementia with Lewy Bodies
DNA	Deoxyribonucleic acid
DS	Down syndrome
DTT	Dithiothreitol
ECL	Enhanced chemiluminescence
EDTA	Ethylenediaminetetraacetic acid
ELISA	Enzyme-linked immunosorbent assay
EOAD	Early-onset Alzheimer’s disease
Ephb2	Ephrin type-B receptor 2
ER	Endoplasmic reticulum
FAD	Familial Alzheimer’s disease
FBD	Familial British dementia
FDD	Familial Danish dementia
FTLD	Frontotemporal lobar dementia

GABA	Gamma aminobutyric acid
GAD	Glutamic acid decarboxylase
GFAP	Glial cell fibrillary acid
GSK3	Glycogen synthase kinase 3
HCl	Hydrochloric acid
HD	Huntington's disease
Hsc	Heat shock cognate
Htau	Human tau
HPD	Histidine-Proline-Aspartic acid
Hsp	Heat shock protein
Iba-1	Ionised calcium binding adapter molecule 1
KCl	Potassium chloride
kDa	Kilodaltons
KO	Knockout
LAMP-1	Lysosomal-associated membrane protein 1
LE	Late endosome
Leu	Leucine
LOAD	Late-onset Alzheimer's disease
LTD	Long-term depression
LTP	Long-term potentiation
Lys	Lysine
MAPS	Misfolding-associated protein secretion
MAPT	Microtubule-associated protein tau
MCI	Mild cognitive impairment
mGluR5	Metabotropic glutamate receptor type 5
Min	Minutes
MRC	Medical Research Council
mRNA	Messenger ribonucleic acid

MRI	Magnetic resonance imaging
NaCl	Sodium chloride
NGS	Normal goat serum
NMDA	N-methyl-D-aspartate
NR2B	N-methyl-D-aspartate receptor subtype 2B
NSE	Neuron specific enolase
NSS	Normal Swine Serum
N-terminus	Amino-terminus
NFTs	Neurofibrillary tangles
PAGE	Polyacrylamide gel electrophoresis
PBS	Phosphate-buffered saline
PBS-T	Phosphate-buffered saline Tween 20
PCR	Polymerase chain reaction
PD	Parkinson's disease
PFA	Paraformaldehyde
PHF	Paired helical filaments
PIC	Protease inhibitor cocktail
PiD	Pick's disease
PKA	Protein kinase A
PMD	Post-mortem delay
PP2A	Protein phosphatase 2A
PS1	Presenilin-1
PS2	Presenilin-2
PSD-95	Post-synaptic density 95
PSP	Progressive supranuclear palsy
S	Seconds
sAPPα	Soluble amyloid precursor protein alpha
sAPPβ	Soluble amyloid precursor protein beta

Sarkosyl	N-Lauroylsarcosine
SEM	Standard error of the mean
SDS	Sodium dodecyl sulphate
Ser	Serine
SGT	Small glutamine-rich tetratricopeptide repeat-containing protein
SNAP25	Synaptosome- associated protein of 25 kDa
SNAP23	Synaptosome- associated protein of 23 kDa
SNARE	N-ethylmaleimide-sensitive attachment receptors
STG	Superior temporal gyrus
SVD	Small vessel disease
TBS	Tris buffered saline
TBS-T	Tris buffered Saline Tween 20
TDP-43	Tar-DNA binding protein 43
TEMED	N,N,N',N' tetramethylethylenediamine
Tg	Transgenic
Thioflavin S	Thio-S
Thr	Threonine
UK	United Kingdom
USP19	Ubiquitin-specific protease 19
V	Volts
VaD	Vascular dementia
VAMP	Vesicle-associated membrane protein
VGLUT-1	Vesicular glutamate transporter 1
WT	Wild type
WM	White matter

Chapter 1: Introduction

1.1 Alzheimer's Disease

Alzheimer's disease (AD) is a progressive, age-related neurodegenerative disorder first described by the German psychiatrist Alois Alzheimer in 1906 (Stelzmann et al., 1995). Alzheimer reported the unusual case of a fifty-one-year-old woman, Auguste D, who presented with symptoms of paranoia, aggression, confusion and cognitive deficits until her death at the age of 55. Histopathological analysis of her brain showed a "peculiar severe disease process of the cerebral cortex" (Hippius and Neundörfer, 2003). The brain was severely atrophied and presented with "miliar foci" - deposits consisting of a special substance and also tangle-like fibrils to which is now known to be extracellular beta-amyloid (Aβ) deposits and intracellular neurofibrillary (tau) tangles (NFTs), pathological hallmarks used to diagnose the disease today post-mortem (Stelzmann et al., 1995; Strassnig and Ganguli, 2005). More than 100 years since this first discovery, much has been revealed about the pathology of this devastating disease, however much is still unknown about the molecular mechanisms that underlie it and have yet to find a suitable treatment or cure for the disease.

1.2 Prevalence and Economic Burden of AD

AD is the most common form of dementia, estimated to contribute to about 60–70% of cases (Barker et al., 2002). Epidemiological statistics of the global prevalence of AD from the World Alzheimer's Report 2018 estimate 50 million people currently living with the disease (Patterson, 2018). Since age is the largest risk factor for AD, and as the aging population are now living longer due to recent advancements in medical research, this number is projected to rise to 152 million by 2050, yet surprisingly rates have been reported to be in decline in western countries (Satizabal et al., 2016). As

the number of individuals being diagnosed with AD continues to rise, the associated costs will also increase. As such, in 2018 the total worldwide cost of dementia was estimated to be $1 trillion with costs estimated to rise to more than $2 trillion by 2030 (Patterson, 2018).

In the United Kingdom (UK), there are currently 850,000 people living with dementia (Prince et al., 2014). This figure will drastically increase to over two million by 2050 (Prince et al., 2014). AD is a major social and economic burden and hence the UK economy is severely impacted with costs surmounting to more than £26 billion every year with £4.3 billion going towards the National Health Service (Prince et al., 2014). These statistics highlight the urgent need to understand underlying mechanisms of AD aetiology and to develop better early-stage diagnostic tools and therapies.

1.3 Symptoms and Diagnosis

Development of guidelines for the clinical presentation of the stages of AD was led by the National Institutes of Health and the Alzheimer's Association which built upon the original 1984 diagnostic criteria (Dubois et al., 2014). Due to the advancements of medical technologies and early detection, current research identifies three stages of AD: preclinical AD, mild cognitive impairment (MCI) due to AD, and dementia due to AD which can be broken down into mild, moderate and severe stages of dementia severity (Fig 1.1) (Albert et al., 2011; Jack Jr et al., 2011; McKhann et al., 2011; Sperling et al., 2011).

Preclinical AD is the first stage of a clinical diagnosis for AD. This stage is asymptomatic, meaning there are no apparent symptoms such as memory loss, however individuals can present measurable brain changes and altered biomarker profiles. These indicators mark early signs of AD which include amyloid deposition detectable using positron emission tomography scans, amyloid and tau changes in

cerebrospinal fluid (CSF), and atrophy of brain areas affected in AD observed with structural magnetic resonance imaging (MRI), yet at this stage it remains uncertain whether the patient will go on to develop AD (Dubois et al., 2010; Lashley et al., 2018). The second stage is MCI, marked by measurable clinical symptoms of memory loss and cognitive decline that do not compromise an individual's daily activities (Dubois et al., 2010). This also includes biomarker evidence of AD-related brain changes. Individuals with MCI are more likely to develop AD or another form of dementia without MCI, but in some cases, MCI can revert to normal cognition (Kantarci et al., 2009).

Finally, the last stage is classified as dementia due to AD where individuals present increasingly impaired cognition, memory loss and behavioural symptoms that impair a person's daily life. The progression can be further broken into three stages of mild, moderate and severe AD. The mild stage of AD can last between 2-5 years and is characteristic of memory impairment (short term memory loss), aphasia (language dysfunction), occasional depression, visuospatial difficulty and personality changes, yet patients can still perform some routine tasks without disruption (Holtzman et al., 2011). Individuals with moderate AD, where the disease has progressed further, can present with more obvious difficulties in memory (long-term memory loss) along with other cognitive symptoms such as agnosia (failure of recognition), apraxia (movement difficulties), and behavioural changes such as agitation. This stage can last a further 2-4 years, and patients become more dependent on their friends and family to assistant in their daily activities (Holtzman et al., 2011; van der Flier et al., 2011). The final stage of dementia due to AD is the severe stage, where patients are fully dependent on caregivers for all daily activities. Symptoms include severe cognitive and memory deficits, disphagia (problems in swallowing), inability to control bladder and bowel function, vulnerability to infections and organ failure which can ultimately lead to death (Holtzman et al., 2011).

The diagnosis of AD in living patients includes neurological and psychometric testing such as the clinical dementia rating and the Mini Mental State Examination (Folstein et al., 1975). An accurate neuropathological diagnosis can however only be determined during post-mortem examination of brain to detect lesions of amyloid and tau (Perrin et al., 2009).

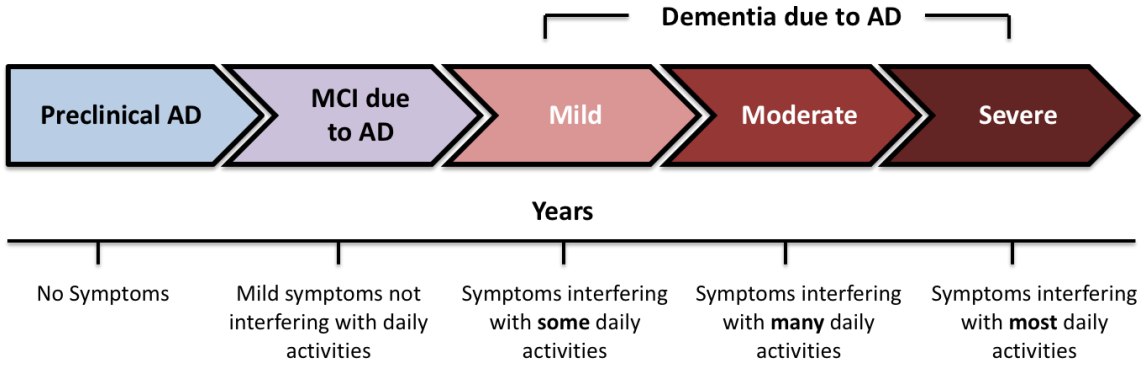

Figure 1.1. Stages of the AD continuum.

AD patients can present with three main stages of the disease which include preclinical AD, MCI due to AD, and dementia due to AD (separated into mild, moderate and severe) which can develop over time (years). Adapted from (2020 Alzheimer's disease facts and figures, 2020).

1.4 Neuropathology of AD

Post-mortem brains from individuals with AD display neuropathological features of the disease compared to a healthy brain (Holtzman et al., 2011). Classical hallmarks include brain atrophy, characteristic neuronal loss, extracellular deposits of Aβ peptide in plaques and intracellular accumulation of hyperphosphorylated tau as NFTs (Fig 1.2) (Holtzman et al., 2011). In addition, there are other common features such as neuropil threads, dystrophic neurites and synaptic loss (DeKosky and Scheff, 1990; Scheff et al., 1990; Masliah et al., 1994; Mandelkow and Mandelkow, 1998; Iqbal and Grundke-Iqbal, 2002) that are accompanied by astrogliosis and microglial reactivity (Beach et al., 1989; Itagaki et al., 1989).

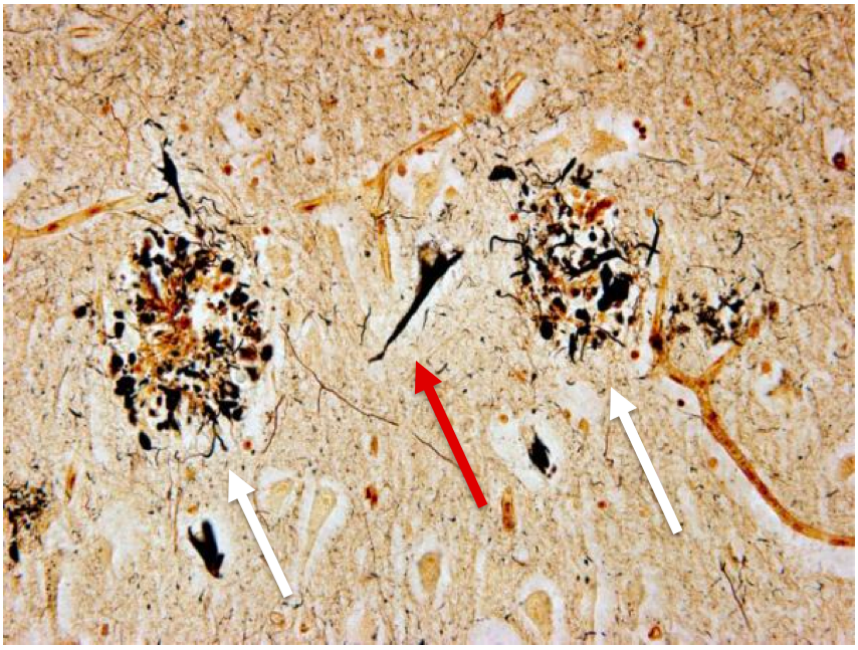

Figure 1.2. Aβ plaques and NFTs from the temporal cortex of human post-mortem AD brain.

Two extracellular Aβ plaques (*white arrows*) and an intracellular neurofibrillary tangle (*red a*rrow) after staining with a modified Bielschowski stain. Magnification at 400x. Figure taken with permission and adapted from (Perl, 2010).

1.4.1 Beta-amyloid (Aβ) Plaques

Aβ plaques are composed primarily of Aβ peptides, fragments of the amyloid precursor protein (APP). These peptides accumulate and are deposited in the extracellular space in AD brain (Yates and McLoughlin, 2008). Parenchymal amyloid plaques can be described as being either diffuse or focal (dense core). Diffuse plaques are large (up to 100 μm in diameter) have ill-defined borders and do not contain any fibrillar Aβ. Examples of diffuse plaques include “lake-like”, “fleecy and “subpial band-like”. Diffuse plaque types can be found in both non-demented individuals as well as in the AD brain (Thal et al., 2015). Dense core plaques on the

other hand are distinguished as “mature”, “classical” and “neuritic” (Serrano-Pozo et al., 2011). These plaque types are characterised by a halo of soluble oligomeric Aβ species, are surrounded by dystrophic neurites and swollen presynaptic dystrophies which contain hyperphosphorylated tau and are associated with toxicity of the surrounding neuropil, synapse loss and glial cell activation (Koffie et al., 2009; Serrano-Pozo et al., 2011; Bouvier et al., 2016; Sadleir et al., 2016). Thal phases describe the abundance of Aβ pathology and distribution (mentioned below) across the AD brain and these assist in neuropathological scoring of disease severity (Fig 1.3) (Thal et al., 2002):

Phase 1. Appearance in the isocortex

Phase 2. The hippocampus and entorhinal cortex

Phase 3. Striatum and diencephalic nuclei

Phase 4. Brainstem nuclei

Phase 5. Finally, the cerebellum and additional brainstem nuclei

1.4.2 Neurofibrillary (Tau) Tangles

NFTs are composed of intracellular accumulations of hyperphosphorylated microtubule-associated protein tau and aggregated as paired helical filaments (PHFs) and straight filaments (Grundke-Iqbal et al., 1986). “Pre-tangles” which contain soluble, hyperphosphorylated and often misfolded tau species are considered to be precursors of NFTs (Uchihara et al., 2001). NFT-containing neurons can take on a characteristic “flame-shaped” appearance and eventually overtime, these NFT-containing neurons die leaving behind neuron remnants and these are known as extracellular “ghost” tangles (Braak et al., 1994). NFT pathology follows a distinct

spatiotemporal pattern of spread throughout the AD brain described as six Braak stages which assist in neuropathological scoring and classification of disease severity (Fig 1.3) (Braak and Braak, 1991, 1995).

Braak I. Presence of NFTs in layer II of the transentorhinal and entorhinal cortices.

Braak II. Subiculum and *Cornu Ammonis* area 1 (CA1) of the hippocampus

Braak III. Limbic system including thalamic nuclei and amygdala

Braak IV. The rest of the hippocampal formation, thalamic nuclei and basal ganglia

Braak V. Most of the association areas of the neocortex are occupied by NFTs and considerable atrophy of temporal and frontal cortices

Braak VI. Isocortex with the exception of the motor cortex and cerebellum which remain relatively unaffected by NFT accumulation.

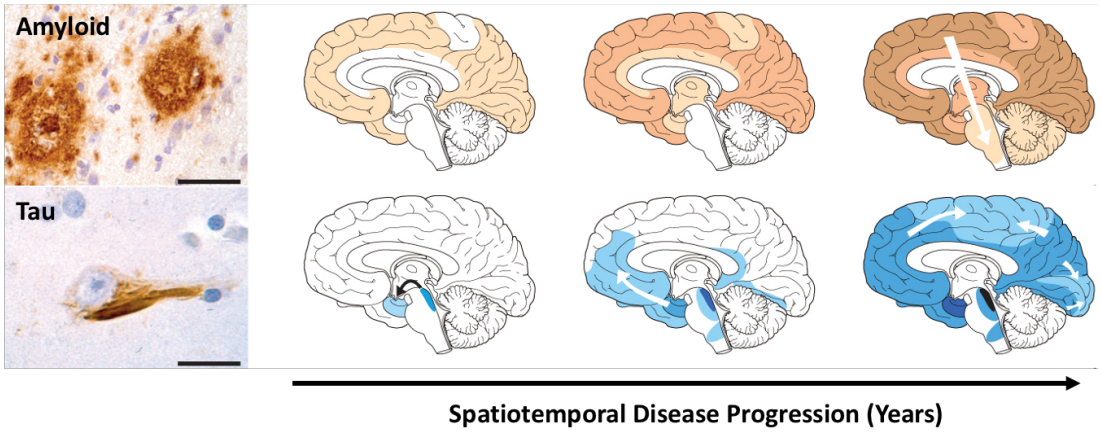

Figure 1.3. Spread of Aβ and tau pathology across AD brain.

Representation of the characteristic pathological disease progression (*years, black arrow*) in terms of the appearance and increasing burden of lesions in AD. These include Aβ (*yellow*) and tau (*blue*) spread (*white arrows*) with darker colouring indicating increased pathological density. Also shown are Aβ deposits and a NFT from the neocortex of an individual with AD. Scale bars for amyloid deposits and NFT are 50 μm and 20 μm, respectively. Figure taken with permission and adapted from (Jucker and Walker, 2013).

1.4.3 Neuropathological Assessment of AD

Recently, new National Institute on Aging-Alzheimer's Association (NIA-AA) guidelines for the neuropathological classification of AD have been proposed (Montine et al., 2012; Jack et al., 2018) that combine Thal Aβ phases, Braak NFT stages and Consortium to Establish a Registry for Alzheimer's Disease (CERAD) scores (Hyman et al., 2012; Montine et al., 2012). The latter are based on the semi-quantitative neuropathological assessment of neuritic plaques (absent, sparse, moderate and frequent) (Mirra et al., 1991). Together, these measures provide an overall "ABC" score (**A**myloid, **B**raak, **C**ERAD) which reflects the amount of 'AD

specific change' on a four-tiered weighting (Not, Low, Intermediate and High) (Montine et al., 2012). This system recognises earlier stages of AD neuropathological change that occur in the background of the disease process.

1.4.4 The Heterogeneity of AD

AD is both aetiologically and clinically heterogenous with various pathological subtypes, making the relationship between clinical presentation and underlying mechanisms much more complex (Schneider et al., 2007, 2009; Kapasi et al., 2017). AD itself presents with distinct clinicopathological subtypes based on NFT distribution and brain atrophy. A study from the Mayo Clinic found that in 889 AD cases, 11% had the presence of hippocampal sparing and 14% had limbic predominant tangle pathology, each presenting with different age of onset, disease duration and rates of cognitive decline (Murray et al., 2011). Other subtypes include typical and minimal atrophy as well as other clinical variants that show distinct regional patterns of tau: nonamnestic, posterior cortical atrophy, corticobasal syndromal, behavioural, primary progressive aphasia and mild dementia variants (Jellinger, 2020).

The new NIA-AA criteria for AD now reflects more recent studies that suggest only a minority of individuals have a purely AD diagnosis; that being defined by Aβ plaque and NFT neuropathology (Boyle et al., 2018). The Florida Department of Elder Affairs at Mayo Clinic found that after examination of 1242 brains, less than half of patients with a primary AD diagnosis were considered "pure AD" (Fig 1.4) (Rabinovici et al., 2017). In fact, brain regions that are vulnerable to AD-associated pathological changes, are also vulnerable to other disease processes which include cerebrovascular lesions (the most common coexisting pathology), α-synucleinopathy and transactive response DNA-binding protein 43 kD (TDP-43) proteinopathy (Boyle et al., 2018). Relatedly, The Religious Orders Study and the Rush Memory and Aging

Project found that 45.8% of individuals with probable AD, had mixed pathologies including macroscopic infarcts and neocortical DLB (Schneider et al., 2009). In a separate study of 349 individuals diagnosed with AD, 43% had detectable Lewy body pathology (Uchikado et al., 2006). Boyle and colleagues (2018) found that after examination of 1079 brains, over 230 different neuropathologic combinations were present, that may in some form contribute to cognitive decline in AD (Boyle et al., 2018). As such toxic effects of neocortical Lewy bodies account for around 41% of the cognitive loss observed in AD-diagnosed patients with their impacts varied at a person-specific level (Bennett et al., 2012a, 2012b). Studies have additionally reported that 50%, 57% and 63% of brains with an AD diagnosis also have TDP-43 pathology identification in the medial temporal lobe (Amador-Ortiz et al., 2007; Hu et al., 2008; Josephs et al., 2014; Thomas et al., 2020). TDP-43 pathology in AD patients' brains can also correlate with faster progression of brain atrophy, cognitive impairment and atypical clinical presentation (Josephs et al., 2008, 2014; Wilson et al., 2013; Matej et al., 2019). Additionally, other common pathologies include eosinophilic Hirano bodies, granulovacuolar degeneration and cerebral amyloid angiopathy (CAA) (Perl, 2010; Serrano-Pozo et al., 2011), the result of which can lead to the loss of synapses and neurons commonly associated with cognitive decline in AD (Boyle et al., 2015; Arvanitakis et al., 2016).

Due to the heterogeneity of AD, complications can arise in the ante-mortem diagnosis, treatment and drug design, which are currently specific for AD-related changes. Hence, a greater understanding of the underlying biological mechanisms that lead to neuropathological comorbidities in AD will provide better targeting, efficacy and stratification of populations with more homogeneous signatures of complex diseases.

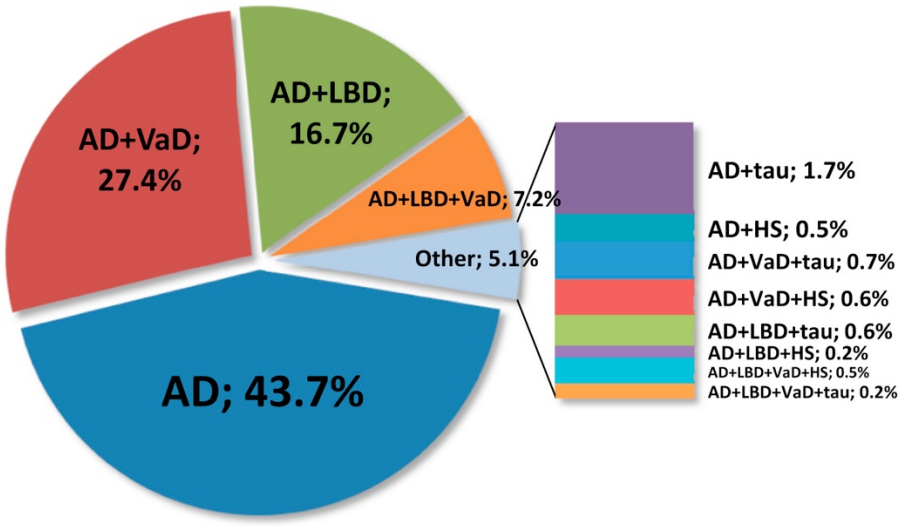

Figure 1.4. Co-morbid pathologies in AD diagnosed patients.

A study in 2014 examining 1242 brains (Braak IV/ Thal phase 3 or greater) of which only 43.7% of brains were diagnosed with 'pure AD', and the majority having a co-pathological diagnosis. Tau refers to agyrophilic grains disease, a medial temporal tauopathy associated with age. Alzheimer's disease (AD); vascular dementia (VaD); Lewy body diseases (LBD); hippocampal sclerosis (HS). Figure taken with permission from (Rabinovici et al., 2017).

1.5 APP and Aβ

1.5.1 Amyloid Precursor Protein (APP)

APP belongs to a family of highly conserved type I single-pass transmembrane glycoproteins which include amyloid precursor like-proteins 1 and 2 found in mammals (Kang et al., 1987; Wasco et al., 1993). APP has a highly conserved extracellular amino-terminal (N-terminal) domain and a short cytoplasmic tail (Kang et al., 1987). Alternative splicing of the *APP* gene encodes for a number of different

isoforms with the three major APP encoded proteins being the 695 amino acid form (APP_{695}) which is enriched in brain tissue, and the 751 (APP_{751}) or 770 (APP_{770}) amino acid forms expressed predominantly in other tissue types (O'Brien and Wong, 2011). APP is particularly enriched in regions of the cerebral cortex and hippocampus, areas severely affected in AD (Bahmanyar et al., 1987; Arai et al., 1991).

APP was first identified as a cell surface receptor-like protein (Kang et al., 1987). Since then, APP has been shown to be essential for embryogenesis, neuronal migration (Young-Pearse et al., 2007) and brain maturation (Löffler and Huber, 1992). APP is highly enriched within synapses, where it is implicated in synaptic maintenance (Kamenetz et al., 2003), spine and synapse formation (Lee et al., 2010; Choi et al., 2013) and, synaptic plasticity including long-term potentiation (LTP), a mechanism thought to underlie memory storage (Dawson et al., 1999; Taylor et al., 2008; Lisman, 2017).

1.5.2 APP Processing

APP is continually synthesised and rapidly metabolised within neurons (Bateman et al., 2006; Moghekar et al., 2011). APP is sorted in the endoplasmic reticulum (ER) and golgi apparatus and trafficked along axons to synaptic terminals (Koo et al., 1996; Selkoe et al., 1996), a process regulated by trafficking factors (Jiang et al., 2014). Only a part of APP processing is reported to occur at the cell surface (Groemer et al., 2011; Choy et al., 2012), where it is then internalised by clathrin-mediated endocytosis to endosomes either to be metabolised into Aβ or trafficked from the endosome to the lysosomal compartment for degradation (Haass et al., 1992; Wang et al., 2017a; Van Acker et al., 2019).

The proteolysis of APP occurs via two major pathways; amyloidogenic which causes the generation of Aβ peptides, or non-amyloidogenic which occurs predominately in physiological conditions and prevents Aβ peptide formation, the fate of which is determined by the interaction of certain proteins and secretases (Fig 1.5) (Zhang et al., 2011; Jiang et al., 2014).

In the non-amyloidogenic secretory pathway, APP is initially cleaved by α-secretase enzymes such as a disintegrin and metalloproteinase (ADAM) (including ADAM9, ADAM10 and ADAM17) at $Lysine_{16}$ (Lys) and $Leucine_{17}$ (Leu) in the Aβ peptide sequence, thereby precluding Aβ formation and instead releasing a soluble APP-α fragment known as sAPPα (Jorissen et al., 2010; Kuhn et al., 2010; Rivera et al., 2010; Paschkowsky et al., 2019). Following this, the resultant C-terminal fragment α (CTFα) which remains in the membrane is cleaved by γ-secretase enzymes and forms a P3 fragment and an APP intracellular domain (AICD) that translocates to the nucleus where it has roles in modulating gene expression pathways (Haass and Selkoe, 1993; Thinakaran and Koo, 2008; Sheng et al., 2012). AICD can also affect actin dynamics and alter mitochondrial morphology (Ward et al., 2010; Lopez Sanchez et al., 2019).

In the amyloidogenic pathway, β-secretase enzymes also known as β-site APP cleaving enzymes (BACE), cleaves APP at sites Met_{671} and Asp_{672} and releases soluble APP-β fragments (sAPPβ) (Vassar et al., 1999; Kimura et al., 2016). BACE cleavage of APP produces a C-terminal fragment of 99 amino acids (C99) (Morishima-Kawashima, 2014) which remains tethered to the membrane. This can be further cleaved using the initial endopeptidase-like ε-cleavage which forms a 48-49 residue length Aβ polypeptide still bound to the membrane and AICD (Chow et al., 2010; Zhang et al., 2011; Haass et al., 2012; Sanders, 2016). γ-secretases then

undergo carboxypeptidase-like cleavages, shortening the Aβ polypeptide to 38-43 residue length Aβ which is then liberated from the membrane (Sanders, 2016; Yuksel and Tacal, 2019; Arber et al., 2020). γ-secretases are formed of multiprotein complexes which include proteases such as presenilin-1 (PS1), found widespread in the cell, or its homolog presenilin-2 (PS2), which can direct the γ-secretase complex to late-endosomes (LE) or lysosomes (Sannerud et al., 2016). γ-secretases have however weak specificity for the Aβ peptide which results in varying lengths of Aβ peptide (38-43 residues in length) (Selkoe and Wolfe, 2007; Fernandez et al., 2016). Interestingly, destabilisation of γ-secretase-APP interactions can lead to the production of longer Aβ peptides (Chévez-Gutiérrez et al., 2012; Veugelen et al., 2016; Szaruga et al., 2017).

Among the different sized Aβ species, $A\beta_{40}$ and $A\beta_{42}$ are the two most common in the human brain (Zhao et al., 2020). Physiologically, the ratio composition is approximately 90% of $A\beta_{40}$ and 10% of $A\beta_{42}$ are formed, where $A\beta_{42}$ is reported to be the more toxic species of the two (LaFerla et al., 2007). In AD however, the $A\beta_{42}$: $A\beta_{40}$ ratio is increased, due to increased production of $A\beta_{42}$ peptides which have a high propensity to form toxic oligomeric Aβ (Sengupta et al., 2016). More recently, BACE-1 is reported to cleave $A\beta_{40}$ or $A\beta_{42}$ peptides forming a Carboxy-terminal (C-terminal $A\beta_{34}$ peptide), which is possibly involved in the clearance of Aβ in AD (Liebsch et al., 2019). Aβ peptides are released from the cell into the extracellular space via exosomes and deposit as oligomeric Aβ, fibrillar Aβ and Aβ plaques (Rajendran et al., 2006). A schematic diagram describing amyloidogenic and nonamyloidogenic processing of APP is shown below (Fig. 1.4).

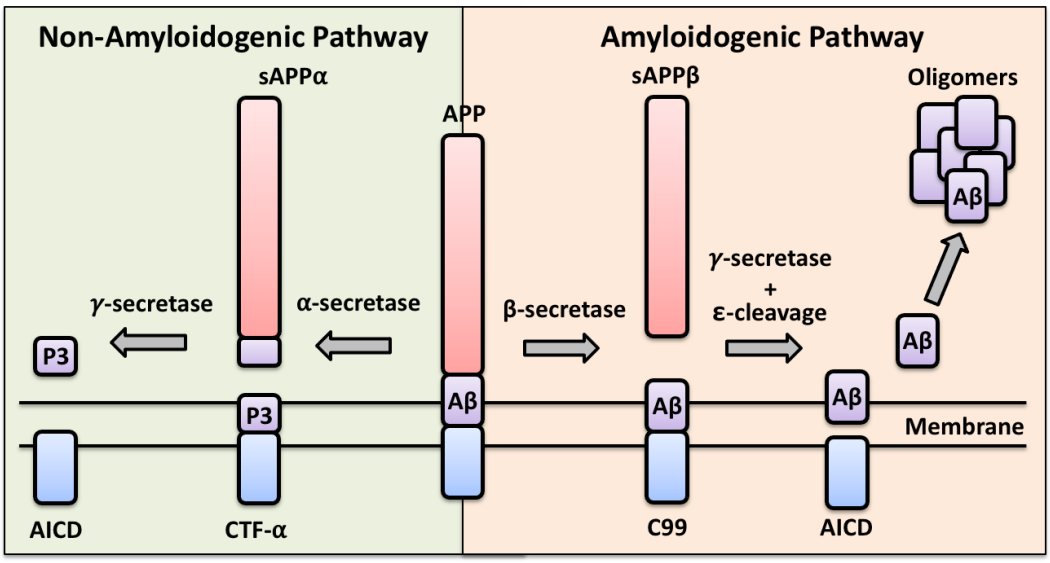

Figure 1.5. APP processing and Aβ peptide production.

APP can undergo sequential proteolytic processing in two mutually exclusive pathways; non-amyloidogenic and amyloidogenic. In the non-amyloidogenic pathway (green box, Left), α-secretase cleaves APP within the Aβ sequence producing sAPPα and CTF-α which are non-toxic products. CTF-α can then be further cleaved by γ-secretase to produce an AICD and a P3 peptide. In the amyloidogenic pathway, β-secretase cleaves APP to produce sAPPβ and C99 fragments. C99 is then subsequently cleaved by γ-secretase ε-cleavage producing a 48-49 length Aβ polypeptide which is subsequently cleaved by γ-secretases releasing shortened Aβ peptides of 38-43 amino acids in length, although these can be longer. In AD, this fragment can oligomerise and form toxic aggregates. Adapted from (Zhao et al., 2020).

Recently, a novel APP-cleavage has been discovered, producing additional APP fragments which occur by δ-pathway, η-pathway and meprin pathways (Müller et al., 2017). These pathways were first identified using genetic knockout (KO) of these enzymes in rodent brain extracts, confirming the physiological basis of these pathways (Jefferson et al., 2011; Willem et al., 2015; Zhang et al., 2015). As such, some of these APP fragments which include Aη-α and Aη-β may be implicated in AD pathogenesis (Andrew et al., 2016). These fragments are reported to be present in dystrophic neurons, where they attenuate neuronal activity as shown in hippocampal slices (Willem et al., 2015).

1.6 Tau

Tau is a microtubule associated protein encoded by the microtubule-associated protein tau (*MAPT)* gene located on chromosome 17q21.3 and contains sixteen exons (Neve et al., 1986; Andreadis et al., 1992). Tau can be alternatively spliced into six isoforms in the adult central nervous system either by including or excluding exons 2, 3 and 10. Exons 2 and 3 at the N-terminal region can be spliced to produce tau proteins with 0, 1 or 2 N-terminal inserts (0N, 1N, or 2N) (Goedert et al., 1989b). Alternative splicing of exon 10 gives rise to the formation of tau isoforms with either three (exon 10 excluded; “3R”) or four (exon 10 included: “4R”) microtubule binding repeat (R) domains at the C-terminal end, the ratio of which is approximately equal in the healthy adult brain (Goedert et al., 1989a; Himmler et al., 1989; Andreadis et al., 1992; Hasegawa et al., 2014). A larger variant of tau, “big tau” is also present in the peripheral nervous system (Goedert et al., 1992b).

1.6.1 Tau Phosphorylation

Phosphorylation is the most common post-translational modification of tau, which contains 85 serine (Ser), threonine (Thr) and tyrosine amino acids that can be phsophorylated (Noble et al., 2013). The majority of phosphorylation of tau occurs at clusters located in a proline-rich domain which flanks the microtubule-binding domain (Noble et al., 2013; Guo et al., 2017). The phosphorylation state of tau, which regulates microtubule binding properties, is controlled by protein kinases which adds phosphate groups onto tau and phosphatases that catalyses the removal of phosphate groups. Kinases that are directed to clustered proline-rich domain of tau include glycogen synthase kinase 3 (GSK3), cyclin-dependent protein kinase 5 and mitogen activated protein kinase (MAPK) (Hanger et al., 1992, 2009; Baumann et al., 1993; Lovestone et al., 1994, 1996; Cruz et al., 2003; Noble et al., 2003; Martin et al., 2013). Tau can also be phosphorylated by non-proline directed kinases such as calmodulin-dependent kinase II (CaMKII) (Ghosh and Giese, 2015), and cyclic adenosine monophosphate (cAMP)-dependent protein kinase A (PKA) (Hanger et al., 2009; Martin et al., 2013) as well as by non-receptor tyrosine kinases such as fyn and Abl (Lee et al., 2004; Derkinderen et al., 2005). Phosphatases that act to dephosphorylate tau include protein phosphatase 1, 2A (PP2A), and 5 (Liu et al., 2005).

Phosphorylation of tau is developmentally regulated. Relatively high levels of phosphorylation allow for a dynamic cytoskeleton that is important for cell polarity, neurite growth and remodelling during early embryonic development (Biernat and Mandelkow, 1999). However, an imbalance in tau kinase and phosphatase activity results in the hyperphosphorylation of tau in diseases such as AD and other tauopathies, which include progressive supranuclear palsy (PSP), corticobasal degeneration (CBD), Pick's disease (PiD) and frontotemporal lobar dementia (FLTD)

(Noble et al., 2013). It has been reported that roughly 20% of tau epitopes are phosphorylated in the healthy adult brain unlike in AD brain in which over 50% of sites are found to be abnormally or hyper-phosphorylated (Hanger and Noble, 2011; Noble et al., 2013). It however remains to be established whether increased tau phosphorylation in general or phosphorylation at specific sites is responsible for contributing to disease pathogenesis.

1.6.2 Tau Function in Health and Disease

The main function of tau, first discovered in *vitro*, is to promote tubulin polymerisation to form a stable assembly of microtubules via interactions of tubulin with the C-terminal microtubule-binding domains of tau in a phosphorylation-dependent manner (Weingarten et al., 1975; Cleveland et al., 1977; Mitchison and Kirschner, 1984; Drubin and Kirschner, 1986). Tau is widely found in the axon of neurons where it interacts with microtubules and is critically involved in regulating efficient axonal transport of cellular cargos (Spittaels et al., 1999; Mandelkow et al., 2003; Dixit et al., 2008). In disease, hyperphosphorylation of tau reduces the affinity of tau for microtubules and can cause microtubule disassembly and dysfunctional axonal transport. For example, mimicking decreased or increased phosphorylation of tau at Ser and Thr residues alters axonal transport in fly, rodent and human neuronal models (Utton et al., 1997; Mudher et al., 2004; Rodríguez-Martín et al., 2013). In AD, microtubule binding is reduced leading to structural abnormalities and breakdown of axonal transport mechanisms which can further drive neurotoxicity (Fath et al., 2002). This can impair the movement of protein cargo and mitochondria including reduced clearance of aggregated forms of tau which in turn can “clog” microtubules and consequently disrupt axonal transport further along the axon (Ebneth et al., 1998; Stamer et al., 2002; Mandelkow et al., 2003).

More recently, it has become evident that tau has a much more diverse range of neuronal functions compared with its more known physiological role in polymerisation and stabilisation of microtubules (Wang and Mandelkow, 2016). It has been reported that tau associates with plasma membranes (Brandt et al., 2005; Pooler and Hanger, 2010; Pooler et al., 2012). Tau that is associated with plasma membranes is dephosphorylated at certain epitopes which are in fact abnormally phosphorylated in AD brain (Arrasate et al., 2000; Ekinci and Shea, 2000; Maas et al., 2000; Pooler and Hanger, 2010). The interaction of tau with membranes is thought to be regulated by the tau N-terminal domain (Brandt et al., 2005; Pooler et al., 2012). This interaction suggests that tau may also play a critical function in signal transduction that is regulated by phosphorylation (Reynolds et al., 2008; Pooler et al., 2012). Tau also associates with synapses in disease, with its binding to tyrosine kinases such as fyn, directing tau and fyn to dendritic spines where fyn phosphorylates NMDA receptor subunit 2B (NR2B) to mediate Aβ toxicity at the synapse (Ittner et al., 2010). Tau has also been reported to interact with synaptic vesicles by its N-terminal domain via the transmembrane vesicle protein, synaptogyrin-3 (Zhou et al., 2017; McInnes et al., 2018). This also implicates tau in having a detrimental role at synapses and suggests that tau may mediate synaptotoxicity in pathological states (discussed further below in section 1.10.2). Finally, tau is also said to be implicated in deoxyribonucleic acid (DNA) protection from oxidative stress and heat damage identified in the cellular nuclei (Sultan et al., 2011). Nuclear tau is largely dephosphorylated and so in disease when phosphorylation is increased, this may disrupt the protective effects of dephosphorylated tau in nuclei (Sultan et al., 2011).

1.6.3 Tau Oligomerisation and Aggregation

Tau is a largely soluble protein in neurons, however in diseases such as AD and other tauopathies, it becomes insoluble and aggregates (Schweers et al., 1994). For tau to aggregate, it undergoes conformational changes due to post translational modifications and as such dissociates from microtubules (Grundke-Iqbal et al., 1986; Binder et al., 2005; Hanger and Wray, 2010; Wang et al., 2014). Such changes can lead to the formation of tau dimers and oligomers (Friedhoff et al., 1998). Significant evidence suggests that tau oligomers are the more toxic species of tau. Tau oligomer formation precedes its aggregation, and is associated with neurodegeneration (Berger et al., 2007; Lasagna-Reeves et al., 2011). Tau oligomers can be soluble and insoluble and both forms have been identified in AD and FTD brains (Berger et al., 2007). Similarly, transgenic mice such as the regulatable transgenic (Tg) 4510 (rTg4510) model which conditionally expresses a mutant (P301L) form of human tau that causes FTD, show high molecular weight tau oligomers which develop prior to NFTs, and that correlate strongly with cognitive impairment (Berger et al., 2007). All six tau isoforms can be abnormally phosphorylated and incorporated into NFTs (Goedert et al., 1992a). GSK-3-mediated tau phosphorylation can promote the formation of insoluble oligomeric full length and truncated tau species (Chun et al., 2007). Additionally, increased tau phosphorylation at the AT100 site is evident in PP2A activity-deficient transgenic mice which also show activation of GSK-3 (Kins et al., 2001; Louis et al., 2011). As such, phosphorylation of tau at the AT100 epitope has been reported to underpin NFT formation suggesting that abnormal tau phosphorylation precedes tau aggregation (Götz et al., 2001). However, the relationship between tau phosphorylation and subsequent tau aggregation still remains unclear since some phosphorylation of tau at specific residues is vital for tau function, and phosphorylation at some sites that mediate the detachment of tau from microtubules may prevent tau aggregation (Schneider et al., 1999).

Tau can also be proteolytically cleaved at several sites and this cleavage may also be critical for mediating the formation of pathological tau aggregates, as tau fragments are found in insoluble tau preparations from PSP, CBD and FTD (Wray et al., 2008; Hanger and Wray, 2010). A number of enzymes are implicated in tau cleavage, including caspase-3. Caspase-3-cleaved tau has a higher propensity to aggregate compared to full-length tau and is thought to form aggregation seeds that sequester full length tau and enhances its aggregation, supporting its role of tau cleavage in NFT formation (Gamblin et al., 2003; Rissman et al., 2004).

It not yet clear as to the extent to which aggregated tau species are toxic, neuroprotective or inert, yet they have recently been reported to be involved in the spread and propagation of tau pathology in AD, as discussed further in Section 1.6.4.

1.6.4 Tau Seeding and Propagation

Recent studies have reported that tau released from neurons into the extracellular space can spread or propagate across the diseased brain in a “prion-like” way (De Calignon et al., 2012; Jucker and Walker, 2013; Sanders et al., 2014). When pathological forms of human tau extracted from either tau mutant mice or post-mortem human AD brain were injected into mice expressing wild-type (WT) human tau, the seeded brain material is taken up by neurons and spreads from the site of injection to other neurons along anatomically connected pathways (Clavaguera et al., 2009; Harris et al., 2012; Liu et al., 2012; Guo et al., 2016; Gibbons et al., 2017; Narasimhan et al., 2017). This seeded material, the conformation of which is also important, can recruit endogenous tau once internalised (Clavaguera et al., 2013, 2014; Ahmed et al., 2014; Iba et al., 2015). Similarly, groups have reported that extracts immunodepleted of tau, where no pathology is detected, confirm that tau is

the driver of seedings mechanisms (Yanamandra et al., 2013; Nobuhara et al., 2017; Vandermeeren et al., 2018).

The mechanisms by which monomeric or small tau oligomers are released from neurons into the extracellular space are however still unclear (Chai et al., 2012; De Calignon et al., 2012; Pooler et al., 2014; Yamada, 2017), but are thought to include unconventional secretory pathways (Chai et al., 2012; Fontaine et al., 2016; Merezhko et al., 2020), exosome release (Saman et al., 2012; Baker et al., 2016; Polanco et al., 2016; Deng et al., 2017; Wang et al., 2017b), release of larger extracellular vesicles (ectosomes) (Dujardin et al., 2014), tunnelling nanotubes (membranous bridges) (Rustom et al., 2004; Tardivel et al., 2016) or “free” tau movement (Chai et al., 2012; Pooler et al., 2013b). Support for these mechanisms have been reported in both experimental models and AD patients, where seed-competent tau species have been detected as either localised in vesicles or “free” tau in CSF, interstitial fluid and blood (Yamada et al., 2011; Saman et al., 2012; Fiandaca et al., 2015; Barthélemy et al., 2016; Takeda et al., 2016; Winston et al., 2016; Blennow and Zetterberg, 2018; Guix et al., 2018). These mechanisms of tau transmissibility are thought to mainly occur at or near synaptic terminals, resulting in the spread of tau between synaptically connected neurons (Liu et al., 2012) as opposed to spread to neurons in close proximity (Ahmed et al., 2014; Furman et al., 2017; DeVos et al., 2018; Henderson et al., 2020). Endogenous tau is secreted from rat primary neurons as a physiological process stimulated by neuronal activity (Pooler et al., 2013a), suggesting that extracellular tau may in fact play a role in signalling between neurons (Medina and Avila, 2014; Fuster-Matanzo et al., 2018; Jadhav et al., 2019). This may involve tau interactions with post-synaptic receptors (Pooler et al., 2014) and signalling complexes or the destabilisation of dendritic spines (Koleske, 2013). Tau spread has been further supported by evidence demonstrating that oligomeric tau species and not tau monomers are taken up by human neurons leading

to full-length tau oligomerisation and further tau release and spread (Frost et al., 2009; Guo and Lee, 2011; Kfoury et al., 2012; Wu et al., 2013). Likewise, oligomeric tau can be taken up by cultured neuronal cells by endocytosis (Wu et al., 2013), a process that may be controlled by low-density lipoprotein receptor-related protein 1 (Wu et al., 2013; Rauch et al., 2020). The propagation of extracellular tau may also be mediated by microglial phagocytosis of tau aggregates leading to tau secretion from microglia via exosomes (Asai et al., 2015). Interestingly, the presence of Aβ has also shown to accelerate tau propagation (Pooler et al., 2015).

The precise relationship between tau modifications and tau release and spread require further elucidation to determine how these mechanisms are involved in the physiological and pathological roles of tau, all of which will be important for the development of AD therapies and associated tauopathies in preventing tau spread or even disease progression.

1.7 Genetics of AD

AD can be divided into two main subtypes based on the age of onset: early-onset AD (EOAD) and late-onset AD (LOAD). EOAD (30-65 years) is mostly due to autosomal dominant mutations, but accounts only for a small percentage (1-2%) of all AD cases. LOAD (>65 years) on the other hand is the most common form of AD, which is mostly due to sporadic occurrence from a combination of genetic and environmental factors and is very rarely due to single gene mutation (Tanzi, 2012; Khanahmadi et al., 2015).

1.7.1 Early-Onset AD (EOAD)

The first known genetic link to AD was discovered in patients with Down syndrome (DS) which results from having three copies of chromosome 21 (trisomy). Most DS patients have AD-like symptoms and exhibit neuropathological hallmarks of AD in

post-mortem analysis (Lemere et al., 1996; Head et al., 2015). The *APP* gene was mapped to chromosome 21, with these patients carrying three copies of APP, suggesting that having an excess of APP can lead to AD (St. George-Hyslop et al., 1987; Goate et al., 1991; Murrell et al., 1991; Lemere et al., 1996).

EOAD is caused by mutations in one of the following three genes encoding APP itself or presenilins 1 and 2 (PS1, PS2) which are proteins involved in APP processing and Aβ generation; *APP* (Goate et al., 1991), *PSEN1* (Levy-Lahad et al., 1995) and *PSEN2* (Sherrington et al., 1995).

Most of the mutations in the *APP* gene cluster around sites of proteolytic *APP* processing by the β- and γ-secretase enzymes (Fig 1.5), particularly close to the Aβ peptide sequence which is the major component of amyloid plaques. These mutations can alter Aβ production, increasing the levels of the pathogenic $A\beta_{42}$ peptide and making them more likely to aggregate, decreasing levels of the non-toxic $A\beta_{40}$ peptide, or increasing $A\beta_{42}$ (Suzuki et al., 1994; Scheuner et al., 1996; Tanzi, 2012). Prevailing evidence now suggests that there is however more to Aβ than just $A\beta_{40/42}$, but that other lengths are important, including $A\beta_{43}$, $A\beta_{38}$, and shorter fragments of Aβ (Arber et al., 2020). *APP* mutations account for 10-15% of EOAD cases (Bekris et al., 2010). Examples of causal *APP* mutations that lead to increased Aβ production include the missense *APP* “Swedish” mutations (*APP*K670N, and M671L) (Mullan et al., 1992), the “Florida” mutation (I716V) (Eckman et al., 1997) and the “London” mutation (*APP*V717I) (Goate et al., 1991; Mullan et al., 1992). Interestingly, a rare *APP* mutation (A673T) was discovered in a small Icelandic population which was found to be protective against cognitive decline and AD (Jonsson et al., 2012). This was further supported by A673T in *vitro* studies that found a 40% reduction in Aβ production when A673T mutant APP was expressed in comparison to WT APP (Jonsson et al., 2012).

The other forms of mutations which are the most common form of EOAD are in the *PSEN1* (chromosome 14) and *PSEN2* (chromosome 1) genes which encode for PS1 and PS2 proteins, respectively (Clark et al., 1995; Levy-Lahad et al., 1995; Sherrington et al., 1995). PS1 and PS2 along with Aph-1, pen-2 and nicastrin proteins form a part of the γ-secretase enzyme complex which has a major role in APP cleavage and production of Aβ peptides (De Strooper and Annaert, 2000, 2010; Haass et al., 2012; Rajendran and Annaert, 2012; Selkoe and Hardy, 2016). PS1 and PS2 act by increasing the $A\beta_{42}$: $A\beta_{40}$ ratio by influencing γ-secretase activity (Tanzi, 2012), reduce the production of $A\beta_{40}$ and increase the production and deposition of $A\beta_{42}$ (Duff et al., 1996; Scheuner et al., 1996; Citron et al., 1997). However, it is suggested that *PSEN2* mutations may be less efficient at producing Aβ fragments than *PSEN1* (Bentahir et al., 2006). The functional consequence and importance of presenilin mutations and their splice variants are however still unclear, but differential expression of these isoforms can regulate APP proteolytic processing (Bergström et al., 2016). As such, *PSEN2* lacking exon 5 can lead to an increase in Aβ peptide production (Sato et al., 2001), yet isoforms without exons 3 and 4 and/or without exon 8 do not affect Aβ peptide production (Grünberg et al., 1998). However, whether presenilin's cause a loss of function or alterations in the production of Aβ remains under debate (Shen and Kelleher, 2007; Chévez-Gutiérrez et al., 2012).

1.7.2 Late-Onset AD (LOAD)

Unlike EOAD which is bound by genetics in an autosomal dominant fashion, LOAD or sporadic AD, accounts for more than 95% of AD cases. These cases are much more complex in that genetic risk factors are believed to coincide with environmental and lifestyle factors to determine a lifetime risk of AD.

Apolipoprotein E (ApoE) is a specialised protein important for metabolism and transport of cholesterol, including triglycerides, in the human body (Mahley et al., 2006). The *ApoE* gene is found on chromosome 19 and has three major isoforms: ε2, ε3 and ε4, of which the ε4-allele is abundant in ~40% of patients with AD and is a major risk factor for LOAD (Corder et al., 1993; Farrer, 1997; Kim et al., 2009; Hannon et al., 2020). Individuals harbouring one or two copies of the ε4 allele show an increased risk of developing sporadic AD of approximately four- and ten-fold, respectively. Comparatively, possession of the ε2 allele, recognised as the longevity gene, is reported to provide neuroprotection against AD and decreases the risk of LOAD (Corder et al., 1993; Li et al., 2020).

In the brain, the ε4 isoform can enhance Aβ production by affecting γ-secretase activity (Lane-Donovan et al., 2016). ApoE ε4 further contributes to reduced Aβ clearance by impairment of lysosomal degradation and breaking down the blood-brain barrier which affects Aβ transportation (Montagne et al., 2020). Moreover, neprisylin-dependent proteolytic degradation of Aβ is impaired by ApoE ε4 (Jiang et al., 2008). ApoE ε4 also promotes Aβ accumulation and oligomeric Aβ much more compared to the ε3 allele (Ye et al., 2005; Kim et al., 2009; Castellano et al., 2011; Hashimoto et al., 2012; Tai et al., 2013; Huynh et al., 2017). Interestingly, ApoE KO mice present Aβ-induced synaptic dysfunction which is heightened compared to WT littermates (Keller et al., 2000). ApoE is deposited alongside Aβ and cholesterol in plaques (Burns et al., 2003). ApoE has also been shown to bind to Aβ, the inhibition of which ameliorates its pathological effects (Pankiewicz et al., 2014; Liu et al., 2017). This, along with evidence showing that ε4 isoform carriers have greater amyloid and tangle pathology (Benzing and Mufson, 1995; Nagy et al., 1995) supports the idea that ApoE is a risk factor for LOAD. However, the underlying mechanisms of ApoE toxicity in the brain are not known and the presence of ε4 isoform alone does not always lead to the development of AD.

Genome-wide association studies have identified more than 20 genetic risk factors associated with AD, that can broadly be grouped into genes that encode proteins with roles in Aβ processing, tau binding, lipid metabolism, protein trafficking and inflammation (Schellenberg and Montine, 2012; Lambert et al., 2013; Karch and Goate, 2015). These include bridging integrator 1 (BIN-1) (Chapuis et al., 2013; Lambert et al., 2013), sortilin related receptor 1 (Rogaeva et al., 2007; Vardarajan et al., 2015), phosphatidylinositol binding clathrin assembly protein, clusterin (Seshadri et al., 2010) and triggering receptor expressed on myeloid cells 2 (Guerreiro et al., 2013; Jonsson et al., 2013). More recently, 5 new rare variant risk genes for LOAD have been identified which include *IQCK*, *ACE*, *ADAM10*, *ADAMTS1,* and *WWOX* (Kunkle et al., 2019). These genetics variants although only offer a small contribution to the genetic component of disease, they are however important for the understanding of disease mechanisms and offer insight as a potential therapeutic target.

1.8 Animal models of Aβ Production or Mutant Tau

Mouse models are widely used to study mechanistic aspects of disease. Mice have a highly conserved genome with much similarity to humans, are flexible for genetic modifications, can be tested for behaviour, and have a relatively short lifespan that allows for time specific monitoring of disease progression (Waterston et al., 2002). Several AD-like models have been developed including those expressing WT and mutant human APP, PS1, or tau, or multigenic mice that express several AD-related genes and show accelerated disease progression compared to mice expressing only one disease transgene.

- Mice expressing human APP and/or PS1/PS2 mutations show varying degrees of Aβ over-production and deposition, some aspects of neurodegeneration and subtle tau changes. Examples are the Tg2576 mouse over-expressing the “Swedish” mutation which gives rise to increased levels of APP, $A\beta_{42}$ and show cognitive deficits from approximately 6 months of age (Hsiao et al., 1996; Holcomb et al., 1998; Westerman et al., 2002), or 5xFAD mice expressing APP with the Swedish, Florida and London mutations as well as two PS1 mutations (Section 1.8.1) (Oakley et al., 2006). Recently APP knock-in mouse models have been developed, for example, “Swedish” and Iberian (I716F) mutations have been introduced into mice which maintain APP expression at endogenous levels. These mice show Aβ accumulation from 6 months of age, elevated $A\beta_{42}$ relative to $A\beta_{40}$ and cognitive impairments (Saito et al., 2014).
- Mice overexpressing mutations in the human *MAPT* gene which encodes tau allow for the study of tauopathies and AD-related tau changes. For example, some mouse models express WT human tau (Andorfer et al., 2003), or human tau with a mutation that occurs in FTD, such as P301L (Lewis et al., 2000; Allen et al., 2002).
- Multigenic AD-like models include multiple transgenes such as APP or APP with PS1/2 and/or MAPT (typically P301L-mutated tau) all of which can lead to plaque deposition, increased tau phosphorylation and NFT formation, as shown in the 3xTg-AD line (Oddo et al., 2003).

These mice have all provided some mechanistic insights into events underlying disease progression in AD. However, better models are still required to more faithfully recapitulate aspects of AD progression and allow the development of novel therapeutic approaches that can be translated for clinical use. For this PhD study, the 5xFAD mouse model was used (Oakley et al., 2006).

1.8.1 The 5xFAD Mouse Model

Most transgenic models take ~6 to 12 months for amyloid plaque development (Spires and Hyman, 2005). In order to accelerate amyloid deposition, multiple FAD mutations can be co-expressed in transgenic mice. Previous studies have reported an increase in Aβ production in mice co-expressing FAD-causing mutations in human APP and PS1 (Citron et al., 1997; Holcomb et al., 1998).

The 5xFAD transgenic mouse model was established by Oakley and colleagues (2006) and overexpresses five human AD-causing mutations in human APP and PS1. The *APP* transgene harbours the Swedish (K670N, M671L), Florida (I716V), and London (V717I) FAD mutations and the *PS1* transgene contains the M146L and L286V mutations (Fig 1.6) (Oakley et al., 2006). The rationale behind this approach was that the Swedish mutation leads to an increase in total Aβ production whereas the Florida and London APP mutations, and the M146L and L286V PS1 mutations lead to the increased production of $A\beta_{42}$, recognised to be a toxic Aβ peptide. This approach will drive Aβ deposition, formation of amyloid plaques and AD-associated neurodegeneration (Eckman et al., 1997; Citron et al., 1998). 5xFAD mice were generated by co-injection of independent APP695 and PS1 transgenes, both using the neuron-specific mouse Thy1 promoter (Moechars et al., 1996). Both transgenes were incorporated equally into the genome of C57/B6XSJL hybrid embryos (Oakley et al., 2006).

The 5xFAD transgenic model shows accelerated amyloid deposition and gross neuropathological abnormalities. At ~1.5 months of age, the mice show substantial amounts of cerebral $A\beta_{42}$, an elevated ratio $A\beta_{42}$: $A\beta_{40}$, and accumulation of intraneuronal $A\beta_{42}$ prior to thioflavin S (Thio-S)-positive cerebral plaque formation (Oakley et al., 2006). By 2 months of age, the deposition of extracellular amyloid is

evident in regions of layer V cortex and the subiculum and their numbers rapidly increase with age. Mice also display characteristics of neuroinflammation at this age with astro- and micro-gliosis apparent in proximity to amyloid deposition (Oakley et al., 2006). By 6 months of age, amyloid plaques are apparent across the hippocampus and cortex and also in regions of the brainstem, thalamus and olfactory bulb but they are minimal in the cerebellum, which is largely protected from AD pathology (Oakley et al., 2006). Along with amyloid plaques, NFTs consisting of hyperphosphorylated tau are characteristic in AD brain (Lee et al., 1991). However, no evidence of NFTs is found in 5xFAD mice. However, some increases in tau phosphorylation at Ser396 are apparent from 2-6 months of age, when compared to WT controls (Kanno et al., 2014). Evidence of synapse degeneration was reported in the 5xFAD mice; whole-brain levels of the presynaptic maker synaptophysin and syntaxin, and postsynaptic density 95 (PSD-95) declined between 4-9 months (Oakley et al., 2006). Interestingly, ultrastructural studies of 5xFAD brain show evidence of progressive, age-related synaptic loss and brain atrophy with ~50% loss of synapses compared to age-matched WTs (Neuman et al., 2015). Neuronal death is apparent in many regions, particularly areas with severe amyloid pathology from ~6 months of age (Oakley et al., 2006; Eimer and Vassar, 2013). These mice also show loss of cholinergic neurons by 6 months of age (Devi and Ohno, 2010), reduction in parvalbumin-positive inhibitory interneurons at 14 months of age (Flanigan et al., 2014), changes in myelination ~6-7 months of age (Chu et al., 2017) and deterioration of synaptic transmission and LTP in area CA1 of the hippocampus at 6 months of age (Kimura and Ohno, 2009).

Along with several pathological features relevant to disease, 5xFAD mice show age-dependent impairments in cognition. For example, these mice display spatial working memory impairments in a Y-maze task at 4-5 months of age (Oakley et al., 2006; Devi and Ohno, 2010), and have deficits in spatial reference memory formation, as assessed using the Morris water maze beginning at 6-months of age (Flanigan et al., 2014; Xiao et al., 2015; O'Leary et al., 2018). At 12 months of age, 5xFAD mice also have abnormal social interactions and impaired social recognition memory (Flanigan et al., 2014).

It is recognised that the 5xFAD mouse model does not fully recapitulate the full extent of AD morphological and behavioural changes, but it models the exacerbated production of Aβ, and its deposition into amyloid plaques and the neurodegenerative events caused by Aβ. The model, therefore, allows investigations of important Aβ-related mechanisms that are relevant to AD.

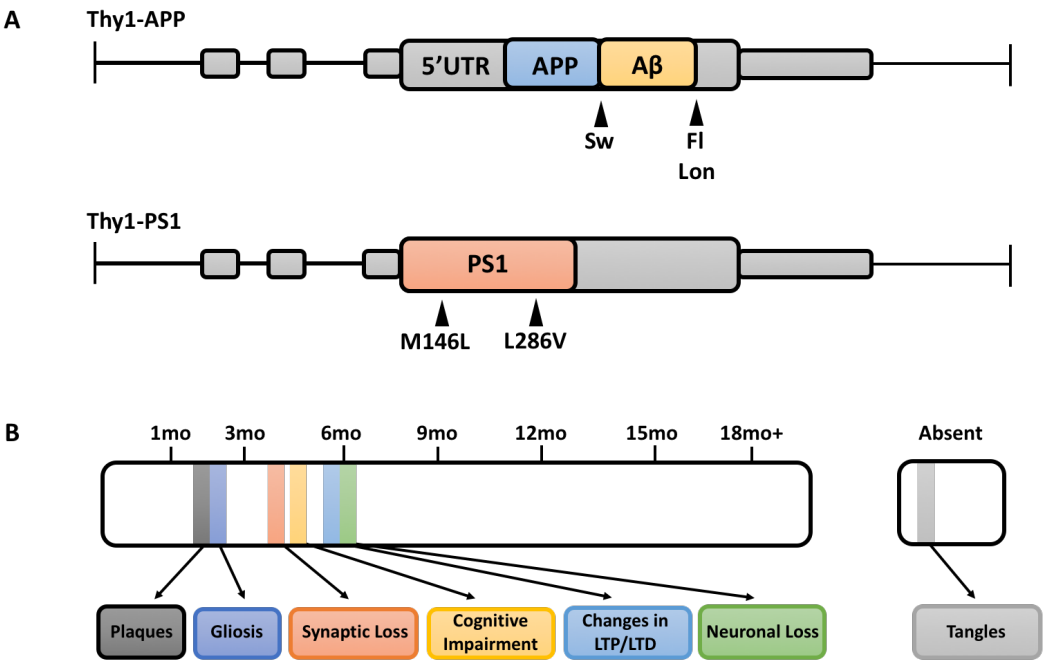

Figure 1.6. Diagram of 5xFAD APP and PS1 mutant transgenes and temporal pathological hallmarks.

a) Swedish (Sw), Florida (Fl) and London (Lon) mutations and M146L and L286V PS1 mutations were introduced into the thy1-APP and PS1 transgenes, respectively (Black arrow heads). Small grey boxes indicate Thy1 exons and larger coloured boxes represent coding regions inserted into Thy1 exon 2 of the mouse Thy1 transgene expression cassette. The APP transgene also has a 5′ untranslated region (5′UTR), which contains an interleukin-1β translational enhancer element. Adapted from (Rogers et al., 1999). **b)** Timeline of pathological changes in the 5xFAD model.

1.9 The Amyloid Cascade Hypothesis

The original amyloid cascade hypothesis is based on the notion that excessive amounts of pathological Aβ, more specifically the neurotoxic $A\beta_{42}$ peptide, lead to amyloid plaque formation and triggers further AD-related neuropathology including NFTs, inflammation, synapse loss and ultimately neuronal loss and inflammation (Hardy and Higgins, 1992). This assertion was mainly based on the evidence that EOAD mutations increase Aβ production and are sufficient to cause AD. This hypothesis has been revised over the years to account for emerging evidence in the field (Hardy and Selkoe, 2002; Selkoe and Hardy, 2016). Firstly, as described above, not all AD-related mutations in APP and PS1/PS2 lead to $A\beta_{42}$ overproduction, some prevent Aβ production and may be neuroprotective (Shen and Kelleher, 2007). Additionally, evidence from in *vitro* and in *vivo* models suggest that the Aβ neurotoxicity is also contingent with the expression of human tau (Rapoport et al., 2002; Jin et al., 2011). There is no significant correlation between the progression of amyloid plaque density and dementia, unlike NFT progression which correlates better to cognitive decline in the disease (Fig 1.3) (Arriagada et al., 1992; Bancher et al., 1993; Gómez-Isla et al., 1997; Giannakopoulos et al., 2003; Lowe et al., 2018; Mattsson-Carlgren et al., 2020). Moreover, treatments targeting Aβ, either by active or passive immunisation or that aim to inhibit the action of β- and γ-secretases have been largely unsuccessful (Honig et al., 2018; Schneider, 2020). Therapies have shown limited success due to their lack of efficacy in clearing Aβ, an ineffectiveness at reducing tau pathology and/or lack of efficacy in improving cognitive deficits even when Aβ is efficiently cleared, all of which suggest that removal of Aβ alone is not enough to treat AD (Hardy, 2009; Nicoll et al., 2019). However, it is important to note that there have been limitations in the study design such as clinical trials being conducted in those with advanced disease, and not in early disease when they are likely to be most effective. Lastly, translation of findings in mouse models of disease

to human trials remains problematic. Mouse models in which $A\beta_{42}$ is overexpressed, are unable to recapitulate all aspects of the human condition (Benilova et al., 2012). In addition, mouse models in general have a short lifespan, and are generally used to examine the effect of treatments in conditions of divergent genetic profiles, and co-morbidities that are common in clinical trial cohorts.

An updated version of this cascade hypothesis postulates that rather than plaques themselves it is the more soluble, oligomeric form of Aβ, that constitute the more toxic Aβ species and correlates more strongly with AD pathogenesis (Lue et al., 1999; McLean et al., 1999; Wang et al., 1999; Haass and Selkoe, 2007). However, it is still unclear whether it is solely oligomeric Aβ that represents the main toxic element in AD, whether amyloid plaques are harmful or inert, or whether they act in concert. It has been suggested that insoluble amyloid plaques act as inactive "reservoirs" which either release or attract soluble oligomeric Aβ that can mediate synaptotoxic and neurotoxic effects. In support of this, synapse loss occurs in close proximity to amyloid plaques and reduces with increased distance from plaques (Spires et al., 2005; Koffie et al., 2009).

1.10 The Synapse and AD

Synaptic dysfunction is one of the earliest features of AD that occurs prior to neuronal loss and underlies the clinical symptoms of the disease (Arendt, 2009; Spires-Jones and Hyman, 2014). Synapse loss in AD was first described in the 1990s by Dekosky and Scheff (1990) as well as Terry et al. (1991) and Masliah et al. (1994) who investigated synapses at the ultrastructural level using electron microscopy and molecular techniques, respectively. They observed extensive synapse loss across several regions of post-mortem AD brain and reported this to be the best anatomical

correlate of cognitive impairment in human AD, more so than the burden of plaques or NFTs (DeKosky and Scheff, 1990; Scheff et al., 1990; Terry et al., 1991; Masliah et al., 1994, 2001; DeKosky et al., 1996).

In the early stages of AD, presynaptic terminals were shown to sprout and expand possibly as a compensatory mechanism to emerging neuron damage, and this was followed by a 15%–25% loss of synaptic density in the frontal cortex and limbic system relative to age-matched control brain (Masliah et al., 1994; Scheff et al., 2006, 2013; Wishart et al., 2006). In line with this, a 25% reduction in the expression of the synaptic protein marker synaptophysin in the dentate gyrus and frontal cortex was evident in AD brain compared to brain from age-matched healthy individuals. Synaptophysin levels, were however, largely preserved in the neocortex (Sharma et al., 2012b; De Wilde et al., 2016). In more severe stages of AD, a loss of up to 40% of synapses in the neocortex and limbic system has been reported (De Wilde et al., 2016). These observations are supported by proteomic analysis of AD hippocampus (Begcevic et al., 2013) and frontal cortex (Yao et al., 2003) which also indicate alterations in genes that encode or influence functional synaptic proteins.

Synapses are a heterogenous group of structures, with varying sub-types, phenotypes, functional demands and molecular composition and so the mechanisms underlying synaptic loss in AD are still unclear. However, they are likely a part of a spectrum of pathogenic molecular cascades which begin with disruption to synaptic vesicle machinery, receptor trafficking, mitochondrial deficits, axonal transport disruption and lack of neurotrophic support from glia (Overk and Masliah, 2014). Evidence also suggests direct toxic roles for Aβ and tau at synapses. A better understanding of synaptic damage and/or loss in AD is hence required since this may provide a novel therapeutic outlook for the disease.

1.10.1 Synaptic effects of Aβ

Aβ production and its release from neurons into the extracellular space are closely associated with the activity of synapses, both at glutamatergic and gamma aminobutyric acid (GABA)ergic synapses. Low concentrations of Aβ have been shown to be critical for synapse structure and plasticity required for learning and memory. For example, APP and BACE-1 KO mice show impairments in LTP and memory formation (Dawson et al., 1999; Laird et al., 2005). Aβ can contribute to enhanced inhibitory function mediated by GABAergic receptors that can further interfere with LTP mechanisms (Palop et al., 2007). Low concentrations of monomeric Aβ also play a role in trophic processes which enhance neuronal survival and have neuroprotective actions (Whitson et al., 1989). Evidence suggests that $A\beta_{40}$ and $A\beta_{42}$ monomers are necessary for neuronal survival and memory for example by increasing neuronal cell viability by protecting against N-methyl-D-aspartate (NMDA)-induced toxicity and modulating neurotransmission by enhancing activity-dependent synaptic vesicle release (Abramov et al., 2009). These studies provide convincing evidence that physiological levels of mainly monomeric Aβ play a vital role in maintaining synaptic function.

However, the accumulation of Aβ, particularly of soluble oligomeric species, is closely linked with the disruption of normal synaptic processes, synaptic dysfunction and synaptotoxicity in AD in experimental models, evidence that appears to be supported in post-mortem human tissue (Walsh et al., 2002; Cleary et al., 2005; Shankar et al., 2007; Li et al., 2009; Spires-Jones et al., 2009; Mucke and Selkoe, 2012; Klein, 2013; Wang et al., 2017c; Jackson et al., 2019b). It was initially assumed that Aβ toxicity was mediated by the insoluble fibrillar form, which is present in amyloid plaques, however it is has been now widely believed that it is the soluble non-fibrillar oligomeric forms of Aβ that accumulate in AD, that leads to synapse failure and eventual loss

(Lambert et al., 1998; Selkoe, 2002; Cleary et al., 2005; Piccini et al., 2005; Haass and Selkoe, 2007; Shankar et al., 2007; Tu et al., 2014; Ding et al., 2019; He et al., 2019). Oligomeric Aβ has been shown to specifically bind to hippocampal synapses and lead to collapse of dendritic spines compared to fibrillar and monomeric forms of Aβ (Hsieh et al., 2006; Calabrese et al., 2007; Lacor et al., 2007; Shankar et al., 2007; Wei et al., 2010; Arbel-Ornath et al., 2017). This is correlated with increased intraneuronal and extracellular Aβ accumulations (Koffie et al., 2009; Tampellini et al., 2009; Harwell and Coleman, 2016) as well as increased intraneuronal APP (Zou et al., 2015). Soluble oligomeric Aβ disrupts synaptic transmission and inhibits LTP whilst increasing long-term depression (LTD) in brain slices (Li et al., 2011). Accordingly, these assemblies of Aβ also impair learning and memory when injected into rodent hippocampus (Shankar et al., 2007, 2008; Barry et al., 2011; Borlikova et al., 2013; Hu et al., 2014; Wang et al., 2017c; Yang et al., 2017). Dendritic spine loss can be rescued, and synaptic marker levels recovered, after the removal of soluble Aβ using a topical antibody (Spires-Jones et al., 2009) further supporting a role for the synaptotoxic effects of Aβ oligomers.

Studies by Spires-Jones and colleagues report an inverse relationship between oligomeric Aβ and synapse numbers (Spires-Jones and Hyman, 2014; Spires-Jones et al., 2017). With the use of array tomography, oligomeric Aβ is found localised in proximity to amyloid plaques (Pickett et al., 2016). Synapses closest to plaques (<10 μm) show higher intensity of oligomeric Aβ and synapse loss is greater when compared to areas distal from the plaque edge (>45 μm), which are more reflective of normal synaptic levels in healthy individuals (Koffie et al., 2009; Pickett et al., 2016). The synapses with accumulating oligomeric Aβ also colocalised with clusterin, an abundant apolipoprotein, levels of which are elevated in ApoE ε4 carriers (Jackson et al., 2019b). These papers also describe using human AD and mouse models of

AD-like changes, the presence of oligomeric Aβ at both pre- and post-synaptic sites, with these synapses being much smaller in size in comparison to Aβ deficient synapses, further suggesting that Aβ contributes to synaptic shrinkage, collapse and dendritic spine loss (Koffie et al., 2009, 2012). Oligomeric Aβ can also affect post synaptic processes, first described by Lacor and colleagues (2007) with evidence that oligomers localised to dendritic spines in hippocampal neurons, affect their shape and density (Lacor et al., 2007). Furthermore, oligomeric Aβ may have a specific effect on excitatory synapses, as a decline to glutamate signalling pathways have been reported (Pickett et al., 2019).

1.10.2 Tau at the Synapse

Tau is a microtubule binding protein, that stabilises microtubules in a phosphorylation-dependent manner (Mandelkow et al., 1995). As such, tau is found primarily enriched within neuronal axons (Binder et al., 1985). However, some tau, particularly in disease, is found in dendritic spines (Ittner et al., 2010). Tau regulates several neuronal processes which include organelle trafficking and transportation of proteins and cargos along axons (Brandt and Lee, 1994; Dixit et al., 2008). Tau can regulate synaptic functions by modulating antero and retro -grade transport of synaptic vesicles and organelles between the synaptic compartments and soma (Mandelkow et al., 2003; Reynolds et al., 2008). Tau-deficient neurons show a 60% reduction in synaptic bouton size and shortening of dendrites and axons, recognising the importance of tau for the maintenance of synapses (Dawson et al., 2001). Numerous studies have now suggested that tau may be involved in synaptic dysfunction in AD. For example, presynaptic protein loss correlates with the presence of hyperphosphorylated tau and tau tangles (Coleman and Yao, 2003; Hoover et al., 2010; Kopeikina et al., 2012; Crimins et al., 2013; Menkes-Caspi et al., 2015; Zhou et al., 2017; Busche et al., 2019).

Tau has been identified in both presynaptic and postsynaptic components (Henkins et al., 2012; Tai et al., 2012, 2014; Pooler et al., 2014; Zhou et al., 2017). Interestingly, synaptoneurosomes from human AD brain containing both pre- and post-synaptic ends, revealed that the amount of tau within synaptoneurosomes is roughly equivalent in control and AD brain (Tai et al., 2012). Intriguingly however, only synapses in the AD brain contained tau phosphorylated at Ser396/404 (PHF1 epitope) which was found to be highly enriched at postsynaptic sites compared to presynaptic terminals (Tai et al., 2012). Others have shown that PHF-1 positive tau only accumulates in the presynapse (Harris et al., 2012). Tau redistribution from axons to somatodendritic compartments, is a characteristic feature of AD (Haass and Mandelkow, 2010; Kurbatskaya et al., 2016; Croft et al., 2017; Glennon et al., 2020). Cultured rat neurons treated with oligomeric Aβ also display mislocalisation of tau to dendrites alongside increases in tau phosphorylation at specific sites (Zempel et al., 2010). Similar data were reported in *vivo* using array tomography to analyse tau content at synaptic sites (Kopeikina et al., 2013). Experiments in fly and rat neurons provide further evidence showing tau localisation at the pre-synapse which disrupts synaptic vesicle release via interactions with the presynaptic protein, synaptogyrin-3 (Zhou et al., 2017; McInnes et al., 2018). Notably, the mislocalisation of phosphorylated and oligomeric tau from the cytoplasm to synapses correlates closely with dementia in AD (Perez-Nievas et al., 2013). Furthermore, phosphorylated oligomeric tau is found in synapses of the frontal cortex in AD, unlike tau aggregates which may be more inert and have less toxicity than tau oligomers (Henkins et al., 2012; Cowan and Mudher, 2013). Taken together, these studies provide convincing evidence that tau mislocalisation and accumulation of phosphorylated tau oligomers at synapses in disease is detrimental.

1.10.3 Mechanisms of Synaptic Dysfunction in AD

The molecular mechanisms that lead to synaptic dysfunction and death in AD are not yet fully understood, however some candidate pathways have been suggested to play a role in this process (Fig 1.7) (Dinamarca et al., 2012).

Aβ oligomers have been known to bind to both 3-hydroxy-5-methyl-4-isoxazolepropionic acid (AMPA) and NMDA receptor subunits leading to excitotoxicity that causes synaptic depression and spine loss (Wei et al., 2010; Rönicke et al., 2011; Paula-Lima et al., 2013). Aβ has also been shown to bind to glutamate transporters at glutamatergic synapses (Li et al., 2009), metabotropic glutamate receptor type 5 (mGluR5) receptors (Renner et al., 2010), α7-nicotinic acetylcholine receptors (Wang et al., 2000a), all of which are important for Aβ induced NMDA receptor internalization (Snyder et al., 2005). Ephrin type-B receptor 2 (EphB2), a receptor tyrosine kinase, has also been implicated as being a receptor for Aβ which can regulate NMDA receptors and has been found reduced in both the Tg2576 AD-like mouse model and in human brain (Cissé et al., 2011). Accumulation of Aβ can also cause increases in calcium influx mediated by NMDA receptors in early AD as shown in primary cortical neuronal cultures (Parameshwaran et al., 2008; Ferreira et al., 2012). This elevation in calcium influx is associated with excitotoxicity, stress-related signalling cascades, increased oxidative stress and reactive oxidative species, impairment of energy metabolism and defective calcium homeostasis which led to altered calcium compartmentalisation, synaptic destabilization and eventual dendritic spine loss (Fig 1.7) (Mattson et al., 1992; Kuchibhotla et al., 2008; Zempel et al., 2010; Demuro et al., 2011). Calcium activation and influx can also mediate degeneration of synapses via calcineurin, a calcium-dependent protein phosphatase which can mediate pathways by oligomeric Aβ causing the internalisation of NMDA and AMPA receptors and also necessary for LTD (Snyder et al., 2005; Hsieh et al., 2006; Wu et al., 2010a;

Koffie et al., 2011). Aβ induced neurotoxic calcium dyshomeostasis, along with destabilisation of anchoring synaptic receptors can interfere in cytoskeletal processes and trigger dendritic spine collapse (Roh et al., 2013). Oligomeric Aβ-EphB2 binding can further lead to its proteasomal degradation (Cissé et al., 2011). Aβ has also been shown to bind to prion protein and with mGluR5 can activate an eukaryotic Initiation Factor 2 phosphorylation pathway that ultimately leads to dendritic spine loss (Um et al., 2013). Activation of mGluR5 by Aβ also increases local protein synthesis and leads to an elevation of synaptic APP synthesis, promoting its abnormal cleavage producing more toxic Aβ (Westmark, 2013). Additionally, Aβ can lead to elevation of Dickkopf-related protein 1, an agonist of the wnt pathway, leading to activation of non-canonical signalling to cause synapse dysfunction (Purro et al., 2012). Aβ can further stimulate activation of mitochondrial apoptotic pathways by activation of caspase-3 leading to synaptic depression and loss (Park et al., 2020).

Tau has been shown to localise with pre- and post-synaptic compartments, as described above. When phosphorylated, tau can bind to fyn (Bhaskar et al., 2005) and both are mislocalised to dendrites. Fyn phosphorylates NR2B to regulate its interaction with PSD-95 and the effects on NMDA receptor enhances excitotoxicity in the presence of Aβ (Ittner et al., 2010). A study by Hoover and colleagues (2010) reported in cultured neurons from P301L tau overexpressing mice that abnormal tau phosphorylation can affect glutamate receptor subunit 1, 2/3 and NMDA receptor subtype 1 postsynaptic trafficking and anchoring to the post synaptic density and can lead to dendritic spine collapse and loss (Fig 1.7) (Hoover et al., 2010; Kopeikina et al., 2013). Pathological tau may also confer toxicity to the presynaptic terminal as shown by microinjection of human tau into the presynaptic terminal of the squid axon which eradicated synaptic transmission, possibly due to dysfunctional synaptic vesicle docking (Moreno et al., 2011). Abnormal tau may also disrupt trafficking of mitochondria to pre- and post-synaptic terminals, normally essential for synaptic

function, local energy production, non-apoptotic caspase activation and synaptic calcium homeostasis (Mandelkow et al., 2003; Hoover et al., 2010; Li et al., 2010; Kopeikina et al., 2011; Reddy, 2011; Eckert et al., 2014). This is supported by ultrastructural analyses from post-mortem human tissues where atypical mitochondria were colocalised to synapses in AD compared to controls (Pickett et al., 2018). Furthermore, mislocalised tau, shown in neurons expressing the P301L mutation increase abnormal AMPA receptor clustering (Miller et al., 2014) which can lead to deficits in synaptic transmission. Taken together, these evidences support the notion that pathologically abnormal tau can be synaptotoxic by impairing cellular transport and receptor targeting of specific synaptic sub-types which can lead to eventual synapse loss.

Due to the overlap between Aβ and tau mechanisms involved in synaptic toxicity, it is likely that they cooperate to drive the disruption in these processes (Pickett et al., 2019). Synaptosomes from human AD brains show co-localisation between phosphorylated tau and Aβ (Fein et al., 2008). Wu and colleagues (2018) have reported that synaptic proteins along with tau are phosphorylated in the presence of Aβ (Wu et al., 2018). Oligomeric Aβ has been reported to be involved in the mis-localisation of tau from axons to dendritic compartments whilst increasing abnormal tau phosphorylation (Zempel et al., 2010). Furthermore, Tiwari and colleagues reported that transcriptional APP processing and hence Aβ can cause changes in tau hyperphosphorylation by modulating CaMKIIα expression at the synapse that is linked to spatial memory impairments (Tiwari et al., 2016; Ghosh et al., 2020). As such, Amar and colleagues showed using the Tg2576 mouse model, that once activated by Aβ oligomers, CaMKIIα increases tau phosphorylation at epitopes Ser202/Ser416 and mis sorting into spines (Amar et al., 2017). Likewise, tau phosphorylation and translocation may mediate Aβ induced toxicity at the synapse (Mairet-Coello et al., 2013; Miller et al., 2014). Moreover, Aβ and tau have been linked

to dysregulation of calcium levels and activation of calcineurin that can lead to synaptic dysfunction (Mattson et al., 1992; Kuchibhotla et al., 2008; Wu et al., 2010a; Zempel et al., 2010; Hudry et al., 2012; Yin et al., 2016). Furthermore, APP/PS1 mice, which have increased Aβ production and express human tau show depressed neuronal hyperactivity (Busche et al., 2019) confirming that both Aβ and tau are required for the impairment of synaptic integrity. More recently, it has been suggested that Aβ and tau may confer indirect effects on synaptic integrity by inducing neuroinflammatory processes which include complement-cascade dependent increase in microglial activation (Heneka et al., 2015). As such, the recruitment of microglia to Aβ primed synapses and vulnerable to tau-mediated changes undergo synaptic engulfment and pruning by microglia (Hong et al., 2016; Shi et al., 2017a; Dejanovic et al., 2018; Litvinchuk et al., 2018; Pickett et al., 2018; Rajendran and Paolicelli, 2018; Henstridge et al., 2019). Together, these findings suggest the interaction between tau and Aβ may mediate toxicity to synapses which lead to eventual synaptic loss and neurodegeneration in AD. This relationship between Aβ and tau at the synapse in AD requires further investigation to identify suitable molecular targets for therapeutic intervention and to slow cognitive decline.

Overall, investigating the molecular mechanisms implicated in the dysfunction of synapses is important for understanding early disease events. In this project, cysteine string protein (CSP) alpha, has been studied. CSPalpha is a pre-synaptic protein, previously found to be dysregulated in AD (Tiwari et al., 2015) and that may play a crucial role in synaptic degeneration.

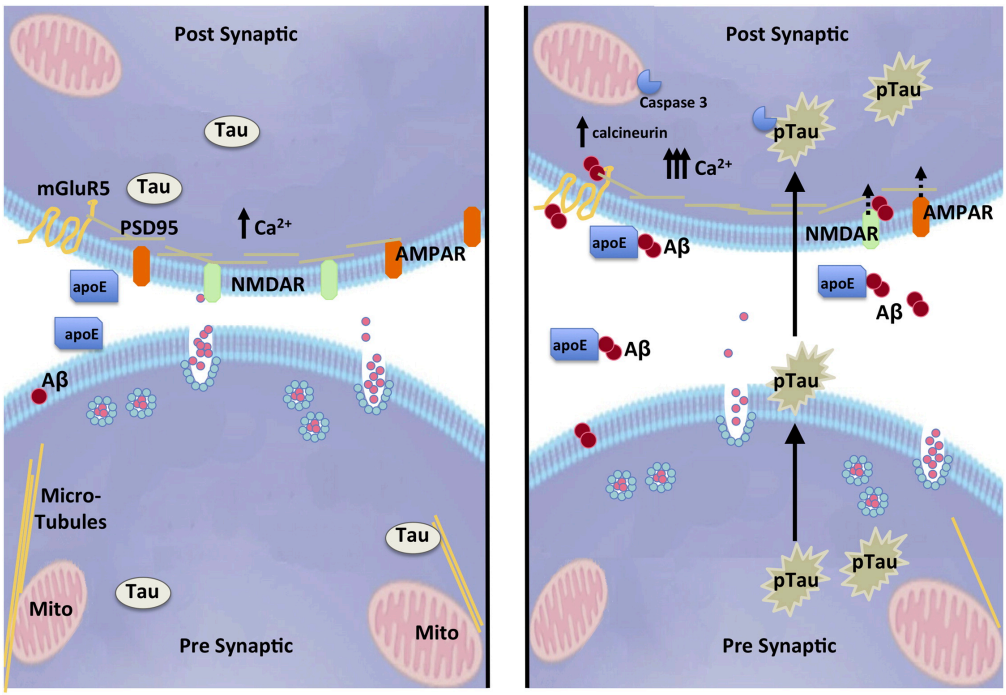

Figure 1.7. Aβ and tau effects at the synapse.

Illustration summarising some of the main Aβ and tau effects. In comparison to the healthy synapse (*left*), in AD (*right*), oligomeric Aβ, initiates a cascade of events once trafficked and binds to post-synaptic receptors. This includes elevating calcium concentrations, calcineurin and caspase-3 activation as well as synaptic NMDA and AMPA receptor internalisation. Phosphorylated tau is shown to mislocalise to the synapse downstream of Aβ where it has been demonstrated to be transported transynaptically. Tau synergistically operates to further drive toxicity initiated by Aβ and subsequently alters synaptic transmission, eventually leading to the dysfunction of synapses and synaptic integrity. The interplay between Aβ and tau in health and disease, however, still remains unclear. Figure taken with permission from (Spires-Jones and Hyman, 2014).

1.11 CSPalpha

CSPalpha is a 34 kilodalton (kDa) molecular co-chaperone protein localized at presynaptic vesicles (Koutras and Braun, 2014; Burgoyne and Morgan, 2015). It is encoded by the *DNAJC5* gene (chromosome 20q13.33) and belongs to the CSP family, of which CSPalpha is the only isoform expressed in the brain. It contains a J domain and hence belongs to the DnaJ family of chaperones and has 11-14 cysteine residues which undergo palmitoylation allowing CSPalpha to attach onto synaptic vesicles (Braun and Scheller, 1995; Ohyama et al., 2007). CSPalpha has multifunctional roles involved in modulating regulated exo- and endocytosis as well as in protein refolding mechanisms. The importance of CSPalpha for synaptic survival has been demonstrated by analysis of Drosophila *melanogaster* null mutants and mouse KOs which exhibit impaired neurotransmission, neurodegeneration and premature death (Zinsmaier et al., 1994; Fernández-Chacón et al., 2004).

1.11.1 Discovery of CSPalpha

CSP was first discovered in Drosophila *melanogaster* by Zinsmaier and colleagues (1990) using a neuronal-specific monoclonal antibody - mAb ab49. Immunohistochemical staining using this monoclonal antibody localised exclusively to synaptic terminals suggesting that the encoded proteins may contribute to synaptic function. As such, cloning of antigen complementary DNA revealed that the antibody detected three splice variants of a novel gene. The sequences were distinguished by a consecutive string of eleven cysteine residues which led to the name “cysteine-string protein” (Zinsmaier et al., 1990).

The first CSP protein vertebrate homolog with ~70 % similarity to the fly protein emerged during an attempt to identify subunits of presynaptic calcium channels in Torpedo californica (Gundersen and Umbach, 1992). Since then, CSPs have been

characterised in many organisms including mammalian species (Mastrogiacomo and Gundersen, 1995; Chamberlain and Burgoyne, 1996; Coppola and Gundersen, 1996), Xenopus. (Mastrogiacomo et al., 1998) and Caenorhabditis *Elegans* (C-*elegans*) (also known as dnaj-14) (Kashyap et al., 2014), however they were not found in unicellular eukaryotes, like yeast (Buchner and Gundersen, 1997).

Sequencing of CSP showed that mammals express three CSP proteins - CSPalpha, CSPbeta and CSPgamma encoded by the *DNAJC5 a*, *b* and *g* genes, unlike vertebrates such as Drosophila *melanogaster* and C-*elegans* that have a single CSP-encoding gene (*Csp* and *dnj-14*, respectively) (Zinsmaier et al., 1994). The sequences of CSPalpha and CSPbeta share a high degree of sequence similarity unlike CSPgamma which is more distantly related (Burgoyne and Morgan, 2015). Different mammalian species of CSP are 98-100% similar (Fig 1.8b) compared to 50-60% homology in Drosphila and ~35% in C-elegans (Chamberlain and Burgoyne, 2000). CSPalpha is expressed in most cell types and virtually all neurons. In contrast, mammalian CSPgamma is only expressed in testis, whereas CSPbeta is also expressed in auditory hair cell neurons (Gorleku and Chamberlain, 2010; Burgoyne and Morgan, 2015). The functional roles of CSPbeta and CSPgamma are however not fully understood (Fernández-Chacón et al., 2004; Schmitz et al., 2006).

1.11.2 CSPalpha Structure

CSPalpha has a highly evolutionarily conserved structure (Fig 1.8b). CSPalpha protein has five main domains: i) N terminal domain, ii) a “J” domain, iii) a linker domain (between 83 and 136), iv) a cysteine string-rich domain (CSD) and v) a C-terminal domain (Fig 1.8a).

The N-terminal domain of CSPalpha includes a serine as the 10th amino acid which can undergo phosphorylation by PKA and/or protein kinase B (Evans et al., 2001; Evans and Morgan, 2005). Phosphorylation at this site can inhibit CSPalpha interactions with other presynaptic proteins including syntaxin (Evans et al., 2001) and synaptotagmin (Evans and Morgan, 2002). Interestingly, phosphomimetic mutations at Ser10 of CSPalpha was shown to alter the kinetics of exocytosis in PC12 cells compared to WT and a phosphodeficient mutant (Chiang et al., 2014). As such, Ser10 phosphorylation of CSPalpha can lead to major conformational changes in its overall structure, which can impact heavily on CSPalpha interactions, such as the interaction between phosphorylated Ser10 and Lys58 in the J domain, which has the tendency to affect its physiological function (Patel et al., 2016).

The J domain is highly conserved between species and has a high degree of sequence homology with a region of the bacterial chaperone protein DnaJ; a characteristic region also identifiable in the DnaJ/ heat shock protein (Hsp) 40 family of molecular co-chaperones (Chamberlain and Burgoyne, 2000). The J domain contains a highly conserved histidine, proline, and aspartic acid (HPD) motif that is required for interaction with Hsp70 proteins (Chamberlain and Burgoyne, 1997).

The linker domain is also a highly conserved region of ~20 amino acids, between the J domain and the CSD. The exact role of the linker domain is unclear, but it has been shown to be associated with regulated exocytosis (Zhang et al., 1999; Boal et al., 2004; Bronk et al., 2005). The linker domain is however, in combination with other protein domains, important for CSP self-association into CSP-CSP dimers, trimers and oligomers (Braun and Scheller, 1995; Braun et al., 1996; Chamberlain and Burgoyne, 1997; Magga et al., 2000; Swayne et al., 2003, 2006). However, a recent study reported that mutating all 14 cysteines to serines in full length CSPalpha (1-198 amino acids) resulted in a protein that did not oligomerise unlike a CSD deficient

construct (1-112 amino acids only of CSPalpha) which formed visible aggregates (Patel et al., 2016). Although there is much debate about the origins of CSPalpha self-association, these CSPalpha modifications play a significant role in the physiological chaperone function of CSPalpha (Swayne et al., 2003). As such, mutant CSPalpha oligomers can lead to the mislocalization and subsequent loss of synaptic soluble, N-ethylmaleimide-sensitive attachment receptors (SNARE) protein-chaperoning function (Naseri et al., 2020b). Furthermore, amino acids 106-114 which flanked the CSD and include some of the CSD itself, have been shown to mediate membrane binding of CSPalpha (Greaves and Chamberlain, 2006). The CSD contains 11-14 cysteine residues, of which position 4-7 are important for CSPalpha palmitoylation and the others available for further palmitoylation and CSPalpha trafficking (Greaves and Chamberlain, 2006). This relatively stable post-translational modification of CSPalpha can cause an electrophoretic mass shift of ~7 kDa (Gundersen et al., 1994). As such, the 34 kDa form of CSPalpha associates with membranes, whereas the un-palmitoylated 27 kDa species remains soluble and cytoplasmic (Greaves and Chamberlain, 2006; Gundersen, 2020). The hydrophobicity of the CSD is also crucial for initial membrane binding prior to palmitoylation (Greaves and Chamberlain, 2006).

The C-terminal domain is poorly characterised although it appears to be required for efficient CSD palmitoylation (Greaves et al., 2008) and contains a recognition site for the palmitoylation enzyme zDHHC17 (Lemonidis et al., 2015; Henderson et al., 2016; Gorenberg et al., 2020).

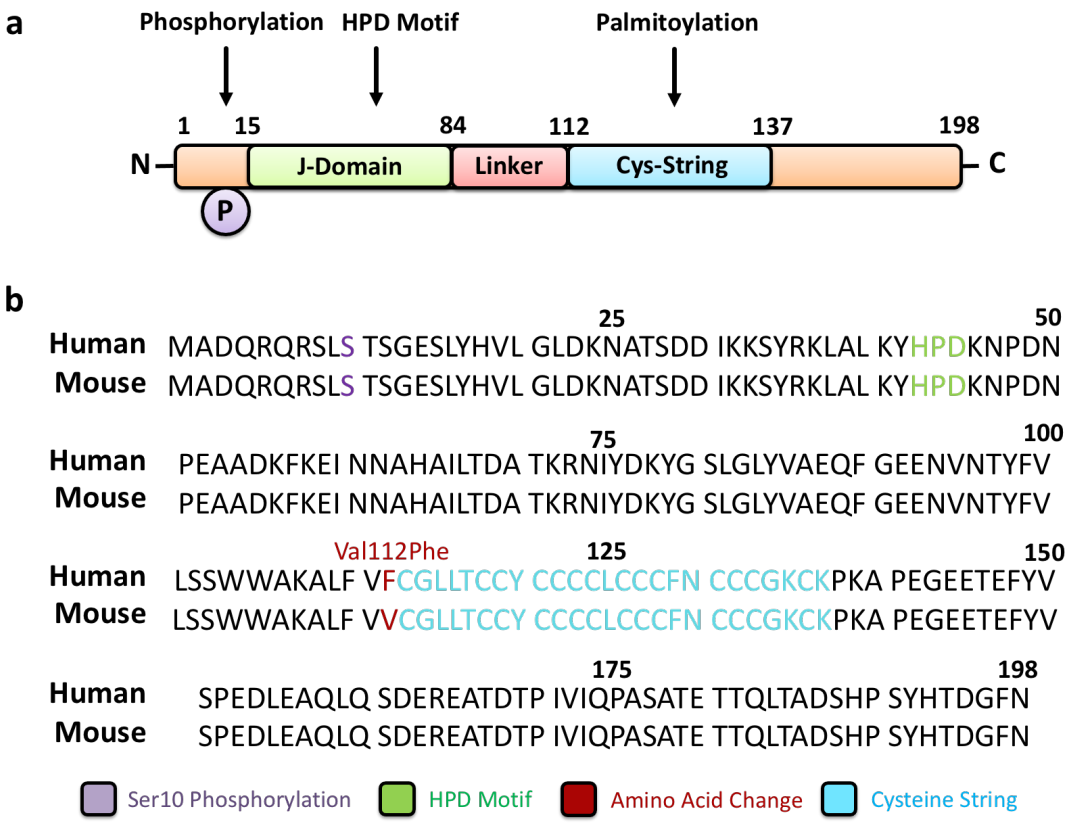

Figure 1.8. Protein structure of CSPalpha.

a) Black arrows show locations of the Ser10 phosphorylation site, the HPD motif in the J domain for constitutively expressed Hsp70 or heat-shock protein cognate 70 (Hsc70) binding, and the 11-14 cysteine-string region of the protein. Numbering is indicative of amino acids flanking each domain based on human CSPalpha. Adapted from (Burgoyne and Morgan, 2015) **b)** Protein sequences of human and mouse CSPalpha aligned to show that CSPalpha is highly conserved amongst mammals with only one single amino acid difference at site 112 from valine to phenylalanine found at the beginning of the CSD (highlight in blue, sites 112-137). Ser10 phosphorylation (highlight in purple, site 10) and HPD motif (highlight in green, sites 43-45) also shown. Adapted from (Zhang and Chandra, 2014).

1.11.3 Cellular and Subcellular Expression of CSPalpha

CSPalpha immunoreactivity was originally documented as being localised to the synaptic neuropil and neuromuscular junctions of Drosophila *melanogaster* (Zinsmaier et al., 1990). CSPalpha is tethered to synaptic vesicles and constitutes about ~1% of total synaptic protein content. On average eight CSP monomers are present per vesicle (Fig 1.9) (Mastrogiacomo et al., 1994; Chamberlain and Burgoyne, 2000; Takamori et al., 2006; Fornasiero et al., 2018). Labelling of CSPalpha in presynaptic terminals has been reported at both excitatory and inhibitory synapses (García-Junco-Clemente et al., 2010). CSPalpha has been well characterised within axosomatic synapses in the brain, with staining detected in mossy fiber terminals in the *Cornu Ammonis* area 3 (CA3) region of the hippocampus (Kohan et al., 1995). CSPalpha is also strongly expressed in the plexiform layers of the rat retina (Kohan et al., 1995) and Drosophila *melanogaster* photoreceptor terminals (Hamanaka and Meinertzhagen, 2010). Additionally, CSPalpha is localised to synaptic vesicles of ribbon synapses found at inner ear hair cells of rats and guinea pigs (Eybalin et al., 2002). CSPalpha further exhibits a punctate appearance in neuronal axons and synaptic boutons in Neuro-2a cells and primary neuronal cultures, which correlate to its vesicular localisation (Benitez and Sands, 2017). As such, CSPalpha has been used as a suitable marker for presynaptic terminals and synapses in several studies (Amorim et al., 2015; Bate and Williams, 2018; McInnes et al., 2018; Selvaraj et al., 2019).

Although CSPalpha is enriched in neurons, the Human Protein Atlas reports a widespread immunoreactivity of CSPalpha in several other human tissues (www.proteinatlas.org). As such, CSPalpha is reported as being highly expressed in various non-neuronal cell types (Kohan et al., 1995; Chamberlain and Burgoyne, 1996; Coppola and Gundersen, 1996; Eberle et al., 1998), and in association with

secretory vesicles including those from the pancreas (Braun and Scheller, 1995; Weng et al., 2009), stomach (Zhao et al., 1997), adrenal glands, (Kohan et al., 1995; Chamberlain and Burgoyne, 1996), liver (Brown et al., 1998; Zhang et al., 2002) and lungs (Park et al., 2008; Raiford et al., 2011). However, CSPalpha has not been reported to have any non-neuronal expression in the brain.

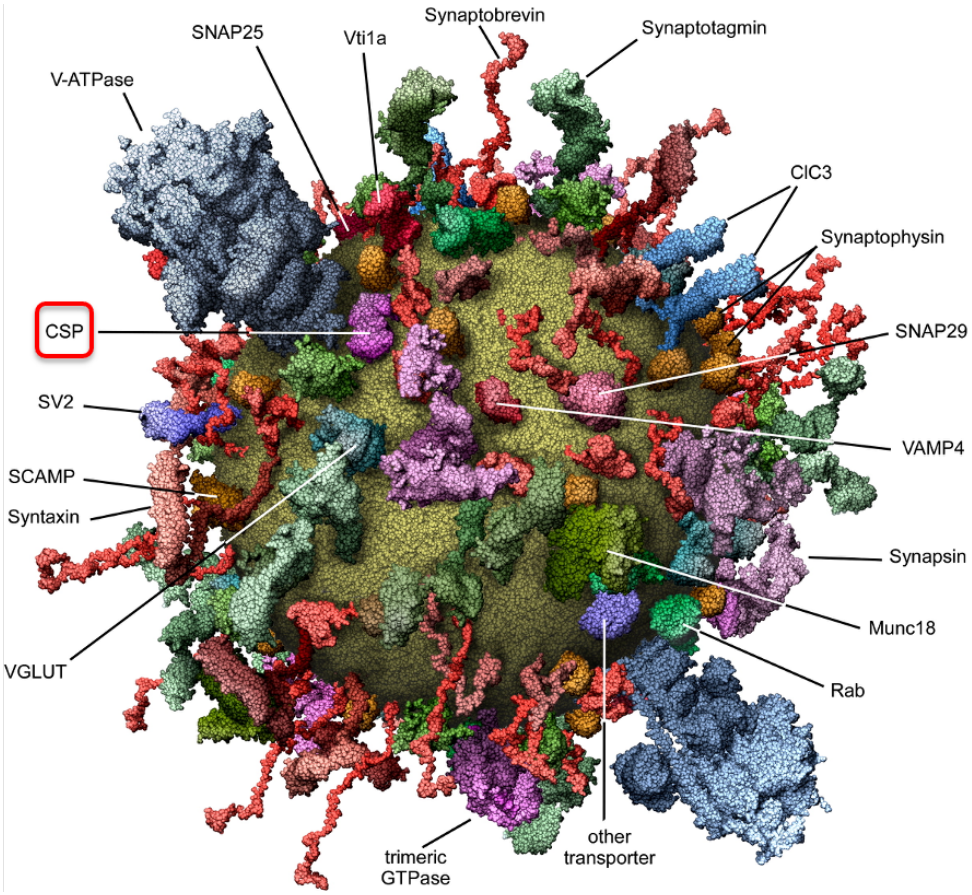

Figure 1.9. A model of synaptic vesicle associated proteins.

CSPalpha is a presynaptic vesicle protein highlighted (*red box*) alongside several other synaptic vesicle associated proteins. Figure taken with permission and adapted from (Takamori et al., 2006).

1.11.4 Cellular Function of CSPalpha

CSPalpha was first proposed to be an integral calcium channel subunit after Gunderson and Umbach (1992) found that CSP anti-sense messenger ribonucleic acid (mRNA) inhibited the activity of voltage dependent N-type calcium channels expressed in Xenopus oocytes (Gundersen and Umbach, 1992). Subsequent findings identified CSPs as being localised to synaptic vesicle proteins arguing against the possibility of CSPs being a subunit of N-type calcium channels (Mastrogiacomo et al., 1994; Chamberlain and Burgoyne, 2000). At the same time, analysis of CSP null mutant Drosophila *melanogaster* confirmed that CSP was vital for normal synchronous neurotransmission and synaptic vesicle release (Zinsmaier et al., 1994). It was suggested that vesicular CSPs might instead regulate calcium channels nearby sites of vesicle docking at presynaptic membranes (Mastrogiacomo et al., 1994). CSP interactions with the recombinant loop of P/Q-type calcium channels were shown in *vitro*, however no direct association of CSP and N-type calcium channels were observed, questioning CSPs role in calcium regulation (Leveque et al., 1998). Furthermore, expression patterns of CSP across tissues suggest that CSP plays a major role in exocytosis and not to regulate calcium channel activity as many CSP enriched regions do not contain cells with voltage gated calcium channels (Chamberlain and Burgoyne, 1996; Coppola and Gundersen, 1996; Eberle et al., 1998).

Evidence has since accumulated showing CSPs role independent of calcium channels in regulated exocytosis and which instead reflect the similarity between CSPalpha, and other proteins involved in exocytotic mechanisms. Several proteins have been identified that are important for CSPalpha exocytotic mechanisms. Firstly, the J domain of CSPalpha, interacts via a HPD motif with Hsc70 chaperone proteins (Braun et al., 1996; Chamberlain and Burgoyne, 1997). Biochemical analysis

confirmed that this interaction can stimulate the ATPase activity of Hsc70 and its role in regulating refolding, disaggregation and/or assembly of client proteins and protein complexes (Chamberlain and Burgoyne, 1997). Furthermore, CSPalpha can form a trimeric chaperone complex (CSPalpha - Hsc70 - small glutamine-rich tetratricopeptide repeat-containing protein (SGT) complex) that is able to regulate the interaction of CSPs with synaptic proteins (Fig 1.10) (Stahl et al., 1999; Tobaben et al., 2001). Although CSPalpha can bind to SGT, the physiological significance of this interaction still remains unclear. The only evidence of which stems from a CSP-SGT interaction defined with recombinant proteins in *vitro*, however, this could not be replicated in *vivo* (Tobaben et al., 2003). In fact, a recent study reported at least 42 proteins expressed at synapses that are CSPalpha clients many of which are membrane-associated or membrane domain-containing proteins (Trepte et al., 2018). These interacting proteins include SNARE proteins, which are required to traffic synaptic vesicles in proximity to or directly with plasma membranes, such as synaptosome- associated protein of 25 kDa (SNAP25), syntaxin, vesicle associated membrane protein (VAMP) and synaptotagmin, all of which are involved in mediating vesicular exocytosis (Sharma et al., 2011).

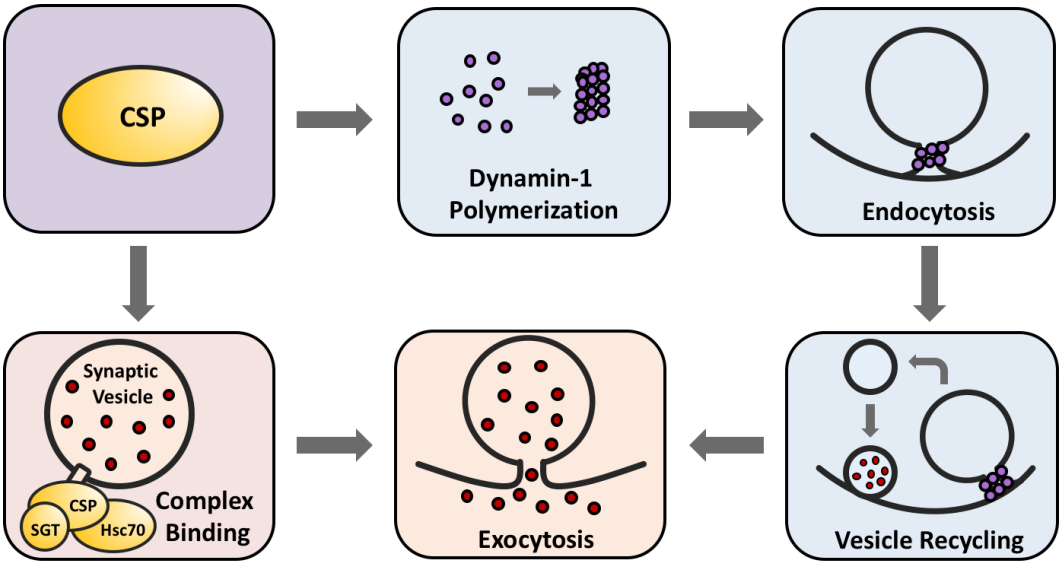

Figure 1.10. Synaptic vesicle recycling is regulated by CSPalpha.

CSPalpha binds to the vesicle fission protein dynamin-1 (*purple*) to facilitate its polymerization which results in vesicular endocytosis. The CSPalpha-Hsc70-SGT trimeric complex interacts with SNARE proteins via its J-domain to mediate exocytosis of neurotransmitters and misfolded proteins (*red*). Adapted from (Sheng and Wu, 2012).

The ability of CSPalpha to interact with its client proteins syntaxin or synaptotagmin in *vitro* was found to be modulated by CSPalpha phosphorylation on Ser10 (Evans et al., 2001; Evans and Morgan, 2002). CSPapha also regulates vesicular endocytosis and recycling through interactions with dynamin-1 (Fig 1.10) (Rozas et al., 2012; Sheng and Wu, 2012; Zhang et al., 2012). Furthermore, CSPalpha can control the density of large-conductance calcium-activated potassium (BK) channels to impact on excitability at synapses (Kyle et al., 2013; Ahrendt et al., 2014). As such, CSPalpha has been proposed to have a significant role in the long-term maintenance of synaptic homoeostasis (Lopez-Ortega et al., 2017). CSPalpha has also been implicated in

regulating proteasomal degradation of cystic fibrosis transmembrane conductance regulator (CFTR) protein suggesting a role at the level of the endoplasmic reticulum (Zhang et al., 2002; Schmidt et al., 2009) and has more recently been reported to have a direct or indirect function with the mammalian target of rapamycin pathway which leads to a depletion of neural stem cells in the hippocampus (Nieto-González et al., 2019).

A more novel role of CSPalpha has also been proposed, whereby CSPalpha forms an essential component of an unconventional protein secretion pathway used to export neurotoxic misfolded proteins either by an exosome dependent and/ or exosome-independent release process (Deng et al., 2017; Lee et al., 2018; Pink et al., 2018). CSPalpha regulates physiological tau, alpha synuclein and TDP-43 release from neurons, via a non-canonical pathway that is dependent on Hsc70 and SNAP-23 (Fontaine et al., 2016; Merezhko et al., 2020). Interestingly, it has been proposed that CSPalpha and Hsc70 together also play an important function in misfolding-associated protein secretion (MAPS) by the deubiquitylation of misfolded proteins (Fig 1.11) (Kim et al., 2018; Lee et al., 2018; Xu et al., 2018; Ye, 2018; Hu et al., 2020). Cargos released within the MAPS pathway are not however bound to vesicles (Lee et al., 2016). Comparatively, extracellular vesicles such as exosomes exported by neurons have been suggested to contain CSPalpha, hence CSPalpha may cause its own release into the extracellular space (Deng et al., 2017). Together, these observations indicate the importance of CSPalpha at the synapse, for the regulation of synaptic transmission, important for the maintenance of healthy synapses, and for protein release, the function of which is not clearly understood but might be linked to pathological prion-like propagation and disease progression.

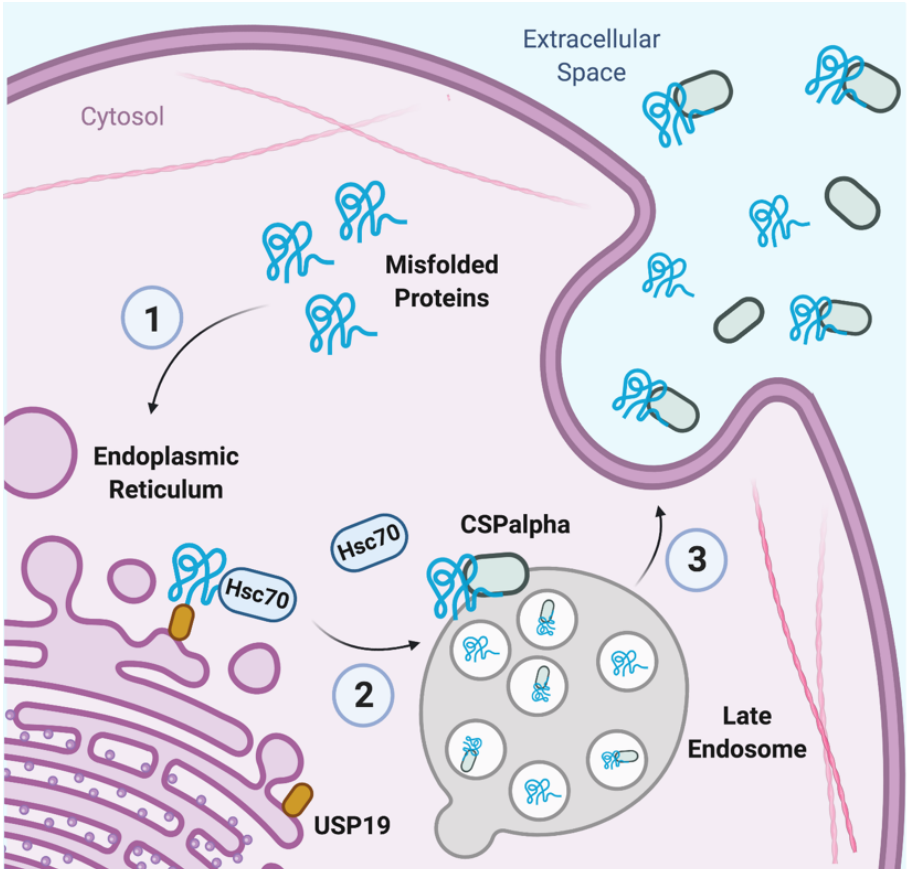

Figure 1.11. A potential unconventional pathway of CSPalpha-mediated misfolded protein secretion.

1) Misfolded proteins are recruited to ER surface and bind the ubiquitin-specific protease 19 (USP19) receptor and assisted by Hsc70 chaperone. **2)** Misfolded proteins are trafficked to CSPalpha that is associated with the late endosome (LE) membranes and lysosomes. **3)** The CSPalpha and misfolded protein complex are transported to the lumen of LEs via translocation channels. LEs fuse with the plasma membrane releasing misfolded proteins including CSPalpha into the extracellular space. Adapted from (Xu et al., 2018). Created with Biorender.com.

1.11.5 CSPalpha and Neurodegeneration

Studies have highlighted the neuroprotective role of CSPalpha at the synapse and its implications in SNARE complex assembly (Burgoyne and Morgan, 2015). In multiple experimental models, deletion of CSPalpha has led to neurodegenerative phenotypes. Expression of loss of function CSPalpha mutants in Drosophila *melanogaster* leads to uncoordinated movements, temperature-sensitive paralysis and eventual synaptic degeneration (Zinsmaier et al., 1994; Burgoyne and Morgan, 2015). Similarly, in CSPalpha null mutant C-*elegans*, show fulminant neurodegeneration and a reduced lifespan (Kashyap et al., 2014). Moreover, phenotypic changes of homozygous CSPalpha KO mice include the impairment of activity-dependent synaptic vesicle release that can lead to progressive age-dependent synaptic degeneration and strikingly mice die prematurely before the age of three months (Fernández-Chacón et al., 2004).

These phenotypes are consistent with perturbations to vesicular recycling machinery that normally regulate endo- and exocytotic processes and ultimately affect activity-dependent synaptic transmission. This may further support observations in CSPalpha KO mice whereby SNARE complex proteins such as SNAP-23 and SNAP-25, vital for exocytosis, are reduced (Chandra et al., 2005; Sharma et al., 2011), Furthermore, investigation into CSPalpha interactions in KO mice indicate that SNAP-25 is a major client protein, and its defective function can lead to a deficit and failure of SNARE complex assembly and increased ubiquitination and proteasomal degradation (Sharma et al., 2011, 2012a). As such, impaired assembly of the SNARE complex, a hallmark of CSPalpha KO mouse brain (Chandra et al., 2005; Sharma et al., 2011), has also been identified in post-mortem AD and Parkinson's disease (PD) brain (Sharma et al., 2012b). Interestingly, the neurodegeneration and increased mortality observed in CSPalpha KO mice was reversed upon overexpression of the PD-

associated protein alpha-synuclein which co-operates with CSPalpha to promote the formation of SNARE complexes with VAMP2/synaptobrevin binding (Chandra et al., 2005; Burré et al., 2010; Greten-Harrison et al., 2010). However, reductions of SNAP-25 expression were not affected by the overexpression of alpha-synuclein (Chandra et al., 2005). Finally, increases in CSPalpha dimerization as a result of the drug quercitin were shown to impair synapse formation and synaptic transmission in snail neurons (Xu et al., 2010), suggesting that dimerization of CSPalpha disrupts its normal function.

The mechanistic consequences of a dysregulation in CSPalpha leading to synaptic dysfunction are not completely understood, however a disruption or absence of CSPalpha has undesirable consequences on synaptic functional and structural integrity, though challenging questions remain regarding mechanisms underlying CSPalpha and neuroprotection, especially in neurodegenerative diseases.

1.11.6 Evidence for a role of CSPalpha in Human Neurodegenerative Diseases

In humans, loss of function mutations in the *DNAJC5* gene encoding CSPalpha are the cause of autosomal dominant adult-onset neuronal ceroid lipofuscinosis (ANCL) (also known as Kuf's disease, neuronal ceroid lipofuscinosis 4, CLN4), a neurodegenerative disorder featuring progressive cognitive decline with dementia, alongside symptoms of movement disorders, anxiety and early mortality (Nosková et al., 2011; Cadieux-Dion et al., 2013). The ANCL-causing CSPalpha mutations reside in the CSD and consist of a substitution of leucine at amino acid 115 for arginine (L115R) or the deletion of leucine at amino acid 116 (L116Δ) (Benitez et al., 2011; Nosková et al., 2011; Velinov et al., 2012; Cadieux-Dion et al., 2013). More recently, a thirty-base pair in-frame duplication in exon 4 of the *DNAJC5* gene, resulting in an additional seven cysteine residues in the CSD, has been identified in ANCL

(Jedličková et al., 2020). CSPalpha mutations arise within the CSD, a region important for the structure and function of CSPalpha, particularly for its palmitoylation and anchoring to plasma membranes (Greaves et al., 2008). Post-mortem ANCL brain show decreased expression of CSPalpha at synapses and an accumulation of mutant forms of CSPalpha aggregates within the cell body, alongside lysosomal storage deficits (Nosková et al., 2011; Henderson et al., 2016).

These findings elaborate on the hypothesis that mutations in CSPalpha lead to the mistargeting and additionally the formation of high molecular weight sodium dodecyl sulphate (SDS)-resistant aggregates of CSPalpha. Further findings reported that these aggregates were membrane bound and palmitoylated, and after treatment with hydroxylamine, known to depalmitoylate proteins, caused the mutant CSPalpha aggregates to solubilise both in mammalian cell lines and post-mortem human brain homogenates, suggesting a link between palmitoylation, aggregate formation and eventual neurodegeneration (Greaves et al., 2012). Intriguingly, it was also found that aggregation of CSPalpha inhibits its function as a molecular chaperone (Zhang and Chandra, 2014). This is in line with studies that have recently proposed ANCL pathology to be better associated with lysosomal functions (Benitez et al., 2015; Benitez and Sands, 2017). CSPalpha overexpression in ANCL mutant fibroblasts inhibited the secretion of lysosomal enzymes (Benitez and Sands, 2017). In addition, in Drosophila *melanogaster*, mutant human CSPalpha abnormally accumulated and co-localised with pre-lysosomal markers (Imler et al., 2019). Complementary work by Sambri and colleagues (2017) explored the possibility of lysosomal dysfunction and reduced CSPalpha levels at the presynaptic terminal and found disruptions to SNARE complex formation in lysosomal storage disorders (Sambri et al., 2017). More recently, Naseri and colleagues (2020) discovered that ANCL mutant CSPalpha oligomerisation occurs by the ectopic binding of iron-sulfur clusters, resulting in the

CSPalpha mislocalisation and subsequent dysfunction of its SNARE-chaperoning activity (Naseri et al., 2020a).

ANCL is the only human disease known to be caused directly by genetic mutations in CSPalpha. However, other neurodegenerative diseases have been linked to altered protein levels and/or functional alterations of CSPalpha. As mentioned previously, CSPalpha KO mice, which display severe neurodegeneration, can be rescued by the over expression of alpha-synuclein, a protein that is deposited in hallmark Lewy body formation and pathology in PD (Bridi and Hirth, 2018). Volpicelli-Daley and colleagues (2011), when investigating the consequence of alpha synuclein sequestration from the presynaptic terminal into insoluble aggregates, found reductions in both alpha synuclein and CSPalpha after the addition of exogenous WT alpha synuclein preformed fibrils in primary cortical neurons (Volpicelli-Daley et al., 2011). Shifaruji and colleagues (2018) also reported a potential contribution of CSPalpha in PD, whereby reduced levels of phosphorylated CSPalpha (Ser10 and Ser34) and SNAP-25 were found in the striatum (a major affected region in patients with PD) of protein kinase C γ KO mice (Shirafuji et al., 2018). More recently, Calo and colleagues (2020) reported that alpha synuclein aggregates reduce CSPalpha levels in the striatum of 1-120h alpha synuclein mouse model at 12 months of age compared to WTs (Caló et al., 2020). However, increased CSPalpha by viral delivery in *vivo* in these mice rescued deficits in vesicle recycling caused by synaptic alpha synuclein aggregation, hence making CSPalpha an attractive therapeutic target for early PD (Caló et al., 2020). CSPalpha may also be implicated in AD (Engmann et al., 2011) as shown by Tiwari and colleagues (2015), reporting altered CSPalpha levels within the post-mortem AD hippocampus, a decline that was found not to result from overall synapse loss since equivalent loss of synaptophysin was not apparent (Tiwari et al., 2015). This data suggests that CSPalpha may be an early marker of synaptic degeneration in AD (discussed below in Section 1.11.7) (Tiwari et al., 2015).

Furthermore, CSPalpha has been shown to interact with mutant huntingtin protein, in which there is a polyQ expansion, although it does not interact with the WT protein (Miller et al., 2003), suggesting that sequestration of CSPalpha by mutant huntingtin protein could play a role in Huntington's disease (HD). CSPalpha has also been linked to other lysosomal storage diseases, as shown in a mouse model of mucopolysaccharidosis type IIIA. CSPalpha expression levels, along with CSPalpha palmitoylation were severely reduced, in line with lysosomal impairment that led to an increase in protein destabilisation and proteasomal degradation (Gorenberg and Chandra, 2017; Sambri et al., 2017). CSPalpha has also been suggested to be indirectly involved in amyotrophic lateral sclerosis (ALS) whereby, models of ALS show reduced expression of Hsc70, a major interacting partner of CSPalpha, at synaptic terminals resulting in vesicle recycling defects (Coyne et al., 2017).

1.11.7 CSPalpha and AD

Circumstantial evidence suggests that CSPalpha is critical for the maintenance of healthy synapses (Gorenberg and Chandra, 2017) and the loss of synapses is an early event in neurodegenerative diseases such as AD (Selkoe, 2002). Hence, a reduction in CSPalpha-dependent synaptic maintenance may also play a role in AD.

Zhang and colleagues (2012) were the first to report changes in the expression of CSPalpha in AD brain. Using age-matched human control and AD frontal cortex, they identified a 40% reduction in CSPalpha protein levels in AD (Zhang et al., 2012). This reduction, however, may not be indicative of synapse loss as CSPalpha expression was normalised to actin, which is present in both neuronal and glial cells, and therefore may not account for neuronal loss in AD. Tiwari and colleagues (2015) further characterised CSPalpha protein levels in post-mortem AD hippocampus and cerebellum. They showed that in early and late stage of AD, CSPalpha expression

was significantly reduced in the superior temporal gyrus (STG) and hippocampus relative to the pre-synaptic protein synaptophysin, which allows assessment of CSPalpha amounts in remaining synapses. CSPalpha protein levels were also found to be elevated in AD cerebellum, a region mostly resistant to AD pathology. Increased protein levels of CSPalpha in AD cerebellum was confirmed with immunohistochemistry (Tiwari et al., 2015). This data indicates that CSPalpha expression is reduced in remaining synapses in degenerating tissues and that CSPalpha is upregulated in regions that are spared from extensive neurodegeneration. This suggests that perhaps a loss of CSPalpha may play a role in the early stages of synaptic dysfunction whereas an upregulation of CSPalpha may protect brain regions during AD development.

Experimental models are now being used to understand the molecular changes pertaining to the levels of CSPalpha. It has also been shown that CSPalpha protein levels are elevated in hippocampus and cortex of young, but not old, human tau (htau) mice, a model of AD tau pathology (Tiwari et al., 2015). Thus, a transient upregulation of CSPalpha appears to correlate with a period of apparent neuroprotection in htau mice, that occurs prior to the development of tau pathology and neurodegeneration observed in older mice at which time CSPalpha amounts are reduced (Tiwari et al., 2015). In contrast the forebrain of the Tg2576 mouse, a model for elevated Aβ and amyloid plaque development (Hsiao et al., 1996), did not show any changes in CSPalpha levels at 4 and 12 months of age when compared to WT littermates (Tiwari, 2015). However, frontal cortical brain extracts from AD patients containing soluble oligomeric Aβ applied onto primary neuronal cultures resulted in the dose-dependent loss of CSPalpha and synaptophysin, a result which when extracts were depleted of Aβ did not change protein amounts, suggesting the role of Aβ in CSPalpha decline at the synapse (Bate and Williams, 2018).

Proteomic studies have also indicated that CSPalpha may be altered in AD. This was shown in studies that assessed the middle frontal gyrus of post-mortem AD brain. Sarkosyl-insoluble fractions were analysed using nanoLiquid chromatography-electrospray ionization mass spectrometry and identified a reduction in CSPalpha abundance in AD compared to control (Metaxas et al., 2018). This result was validated using the same techniques in the left-brain hemispheres of the APP/PS1 FAD mouse model. In these experiments, not only was reduced CSPalpha found in APP/PS1 transgenics compared to WT littermates, but also an age-related decline in CSPalpha expression was found only to be evident in transgenic mice (Metaxas et al., 2018). CSPalpha was also found to have ≥33 % impaired turnover in the cortex of 6-month-old $App^{NL\text{-}F/NL\text{-}F}$ knock-in mice, which show increases in misfolded Aβ peptides (Hark et al., 2021). Interestingly, a study looking into the phosphoproteomics dataset in cortical synaptoneurosomes of APP/PS1 mice reported an elevation in the level of CSPalpha phosphorylation at Ser10 (Wu et al., 2018).

These reports shed light on the importance of CSPalpha in health and disease. It can be suggested that an early up-regulation of CSPalpha may be a compensatory mechanism that protects synapses and therefore neurons against degeneration. It is hence important to determine the relationship between CSPalpha and synaptic health in AD and hence requires further investigation.

Aims and Objectives

This PhD thesis aimed to conduct a more detailed characterisation of CSPalpha protein changes in post-mortem AD brain. In doing so, putative CSPalpha aggregates were discovered, which re-directed the original aims of this thesis. The specific objectives that form the basis of the thesis are therefore to:

1. Investigate whether alterations in CSPalpha abundance / and or localisation are a sensitive marker of synaptic protection/ degeneration during AD progression

2. Characterise CSPalpha protein accumulations/aggregates in relation to AD pathology

3. Examine the association of altered or modified CSPalpha with synapses

4. Determine the specificity of CSPalpha aggregates in AD in comparison to other neurodegenerative diseases

Chapter 2. Materials and Methods

2.1 General Molecular Biology Reagents

All reagents used were from Sigma-Aldrich (UK) and ultrapure water (MilliQ H_2O) was used in the preparation of all solutions, unless otherwise stated.

2.2 General Cell Biology Reagents

Protein and Lysis Buffers

Phosphate Buffered Saline (PBS)	0.01 M Phosphate buffer (pH 7.4)
	0.0027 M Potassium chloride (KCL)
	0.137 M Sodium chloride (NaCl)
Tris Buffered Saline (TBS) 1 L	50 mM Tris-hydrochloride (HCl), pH 7.4
	150 mM NaCl
PBS-T	PBS
	0.1 % (v/v) Tween-20
TBS-T	TBS
	0.1 % (v/v) Tween-20

Synaptoneurosome Buffer A	25 mM 4-(2-hydroxyethyl)-1-piperazineethanesulfonic acid pH 7.5
	120 mM NaCl
	5 mM KCl
	1 mM Magnesium Chloride
	2 mM Calcium Chloride
	Protease inhibitor cocktail (PIC) (Roche, UK)
	Phosphatase inhibitor (Roche, UK)
	2 mM Dithiothreitol (DTT)
Synaptoneurosome Buffer B	50 mM Tris pH 7.5
	1.5 % (w/v) SDS
	2 mM DTT
Differential solubility high salt (HS) buffer	50 mM Tris-HCl pH 7.4
	750 mM NaCl
	10 mM Sodium Fluoride

	5 mM Ethylenediaminetetraacetic acid (EDTA)
	PIC
	Phosphatase inhibitor cocktail
Differential solubility HS- triton X-100 Buffer	HS buffer
	10 % (v/v) Triton X-100
Differential solubility HS- sucrose Buffer	HS buffer
	30 % (w/v) sucrose
Differential solubility HS- sarkosyl Buffer	HS buffer
	20 % (v/v) N-Lauroylsarcosine (Sarkosyl)

Sodium dodecyl sulphate-polyacrylamide gel electrophoresis (SDS-PAGE)

Resolving Gel	10 % (w/v) acrylamide (National Diagnostics, UK)

	25 % (v/v) resolving buffer, pH 8.8 (National Diagnostics, UK)
	0.01 % (w/v) ammonium persulphate (APS, National Diagnostics, UK)
	0.1 % (v/v) N,N,N',N' tetramethylethylenediamine (TEMED, National Diagnostics, UK)
Stacking Gel	4 % (w/v) acrylamide
	25 % (v/v) stacking buffer, pH 6.8 (National Diagnostics, UK)
	0.075 % (w/v) APS
	0.15 % (v/v) TEMED
Running Buffer	10 % (v/v) Running Buffer (National Diagnostics)
Protein Molecular weight markers	Precision Plus Protein™ All Blue Standards (Bio-Rad, Hertfordshire, UK) (Protein molecular weight markers kDa- 250, 150, 100, 75, 50, 37, 25, 15, 10

	Full-Range Rainbow™ Enhanced chemiluminescence (ECL)™ Molecular Weight Marker (Amersham™, GE Healthcare, UK) (Protein molecular weight markers kDa - 225, 150, 102, 76, 52, 38, 31, 24, 17, 12)
Transfer Buffer	10 % (v/v) Transfer buffer (National Diagnostics, UK) 20 % (v/v) Methanol
Blocking Buffer	Odyssey Blocking Buffer (927-60001, Licor Biosciences Ltd., UK) diluted 1:1 in TBS 5 % (w/v) Non-fat dried milk powder (Tesco, UK) in TBS

Immunohistochemistry/ Immunofluorescence

Sodium Citrate Buffer	10 mM Sodium Citrate pH 6
Normal goat serum (NGS) Blocking Buffer	10 % (v/v) NGS (Sigma, UK) In TBS

Normal Swine Serum (NSS) Blocking Buffer	10 % (v/v) NSS (Dako Ltd, UK) In PBS
Sudan Black	3.33 % (w/v) Sudan Black 70 % (v/v) Ethanol

Array Tomography

Glycine	50 mM Glycine In TBS
Citric Buffer	10mM Citric Acid pH 6
Blocking Buffer	0.1 % (w/v) Coated fish gelatine 0.05 % (v/v) Tween20 In TBS
4′,6-diamidino-2--phenylindole (DAPI)	0.1 % (w/v) DAPI

Mouse Immunofluorescence

4% Paraformaldehyde (PFA)	4 % (v/v) PFA
	50M Sodium hydroxide
	In PBS
Antifreeze	30 % (w/v) Sucrose
	0.1M Phosphate Buffer
	30 % (v/v) Ethylene Glycol
Blocking Buffer	5% (v/v) NGS
	0.1% Triton X-100
	In PBS
Thioflavin-S (Thio-S)	0.05 (w/v) % Thio-S
	50% (v/v) Ethanol

2.3 Human Post-Mortem Brain Samples

2.3.1 London Neurodegenerative Diseases Brain Bank

Frozen brain tissues and 10% formalin-fixed, paraffin-embedded brain sections were obtained from the London Neurodegenerative Diseases Brain Bank at the Institute of Psychiatry, Psychology and Neuroscience, King's College London (Table 2.1). The first set of samples contained sections from post-mortem human Brodmann Area 9 (BA9) (dorsolateral and medial prefrontal cortices) from neurologically normal individuals (Braak 0-II) [n=6], and severe AD (Braak V-VI) [n=5] (Table 2.1). The second set of samples contained both tissues and sections from post-mortem human BA9 control (Braak 0-II), moderate AD (Braak III-IV) and severe AD (Braak V-VI) [n=10 for each group] (Table 2.2). A third set of tissues contained hippocampal and cerebellar sections from control subjects (Braak 0-II) and subjects with severe AD (Braak VI) [n=3, respectively] (Table 2.3). A fourth set of hippocampal tissues and temporal cortex sections were obtained from control subjects (Braak 0-II) and subjects with either AD (Braak VI), FTLD, mixed dementia, dementia with Lewy bodies (DLB), [n=8 for each group], PSP or PiD [n=2 for each group] (Table 2.5). Cases were randomly selected for either hemispheres (left or right) to be stored as either frozen or fixed tissue. Cases were sex- and age- matched as much as possible. Tissue was assessed for post-mortem delay (PMD) and tissue quality to ensure that these parameters are comparable between the groups as shown in previous studies (Wang et al., 2000b; Engmann et al., 2011; Bayés et al., 2014; Tiwari et al., 2015). All human tissue was handled according to Human Tissue Authority regulations and guidelines set out by the London Neurodegenerative Diseases Brain Bank.

2.3.2 Edinburgh Brain Bank

Tissue sections obtained from the Edinburgh Brain Bank were from post-mortem human BA9 from neurologically normal individuals (Braak 0-II) [n=9] and severe AD (Braak V-VI) [n=10] (Table 2.4). The University of Edinburgh is a charitable body, registered in Scotland, with registration number SC005336.

2.3.3 Oxford Brain Bank

Tissue sections obtained from the Oxford Brain Bank were from post-mortem human BA9 and temporal cortex from a neurologically normal individual (Braak 0-II) and a subject with ANCL (Braak V-VI) [n=1 for each group] (Table 2.6). Acknowledgement of the Oxford Brain Bank, supported by the Medical Research Council (MRC), Brains for Dementia Research (Alzheimer's Society and Alzheimer's Research UK), and the NIHR Oxford Biomedical Research Centre for the tissues. The views expressed are those of the authors and not necessarily those of the NHS, the NIHR or the Department of Health.

Table 2.1 Characteristics of BA9 cases used in this study.

Table shows details of sex, age, PMD, Braak/BNE stage, primary pathological diagnosis and cause of death for cases from which frozen BA9 tissue and sections was obtained.

Case Number	Case ID	Pathological Diagnosis	Cause of Death	Braak/BNE Stage	PMD (hours)	Sex (M/F)	Age at Death (years)
1	BBN_10250	Control case (AD modified Braak II)	-	II	9	F	92
2	BBN_14408	Mild age-related changes (control brain) - AD modified Braak stage with mild focal amyloid angiopathy	Myocardial infarction	0	45	M	90
3	BBN_16236	Control case but with Hypoxic-type changes and amyloid angiopathy (AD BNE modified Braak I-II)	Aortic sclerosis; Infection	I-II	41	F	89
4	BBN_18816	Old infarcts in the right cerebral hemisphere	Colorectal cancer	0	53	M	84
5	BBN_4581	Ageing process, consistent with Braak stage II	-	II	24	M	82
6	BBN_18401	Control case (very early Alzheimer disease pathology - BNE stage I) with focal amyloid angiopathy	Congestive cardiac failure; Aortic stenosis	I	47	M	82

7	BBN_15711	Consistent with ageing	CAA	0	48.25	M	80
8	BBN_16317	Early tau pathology Braak II, no neuritic plaques	Ruptured anterior myocardial infarct	II	47	M	79
9	BBN_22594	Control brain	Kidney cancer	0	21	F	77
10	BBN_22991	Early ageing changes BNE stage 1	Bowel perforation; Primary colonic tumour; Metastatic lung carcinoma pulmonary embolism	I	27	F	73
11	BBN_9924	Alzheimer changes consistent with Braak III and amyloid angiopathy	-	III	12.5	M	81
12	BBN_2931	AD (moderate - limbic stage) Braak III	Bronchopneumonia	III	19.5	F	92
13	BBN002.29410	AD (modified Braak (BNE) stage 4) with moderate amyloid angiopathy	Lower respiratory tract infection, Aspiration pneumonia; Ischaemic heart disease, Adult respiratory distress syndrome; Anorectal sepsis (operated)	IV	86	M	84

14	BBN002.28871	AD (modified Braak (BNE) stage 4) with moderate amyloid angiopathy and moderate to severe cerebrovascular changes and limbic TDP-43 pathology (Joseph stage II)	-	IV	47	F	95
15	BBN002.28694	AD (modified Braak (BNE) stage IV) with mild amyloid angiopathy	Dementia AD; Old age	IV	55.5	F	86
16	BBN002.28693	AD pathology (modified Braak (BNE) stage IV), Thal phase 4 with moderate to severe amyloid angiopathy.	Advanced dementia; Hypertension, rheumatoid arthritis, chronic kidney disease	IV	48	M	91
17	BBN_24549	AD (modified Braak (BNE) stage 4, Mild amyloid angiopathy	Congestive cardiac failure; Chronic obstructive pulmonary disease; Dementia	IV	53	M	98
18	BBN_24400	AD (modified Braak (BNE) stage 3-4	Old age; Dementia in AD	III-IV	79	M	88
19	BBN_15210	AD (modified Braak stage IV) with limbic TDP-43 pathology	-	IV	28	M	82
20	BBN_9887	AD Braak IV	Pneumonia; Multi-infarct dementia; Ischaemic heart disease	IV	29.5	F	92

21	BBN_4197	AD Braak VI	Bronchopneumonia	VI	26.5	F	83
22	BBN_4195	AD BNE modified Braak stage V with extensive amyloid angiopathy	Septicaemia - urinary tract; Type 2 diabetes	V	77	M	83
23	BBN_4180	AD Braak VI BNE 5	-	V-VI	35	M	73
24	BBN_9928	AD Braak VI with marked amyloid angiopathy	-	VI	5.5	M	72
25	BBN002.30168	AD (modifed Braak (BNE) stage VI	Pneumonia; AD; Diabetes, hypertension	VI	43	F	68
26	BBN002.30132	AD (modifed Braak (BNE) stage VI) Thal phase 5	Old age; AD	VI	48	F	95
27	BBN002.30130	AD (modified Braak (BNE) stage VI with skips) Thal phase 5 and moderate degree of cerebrovascular pathology and limbic and early cortical TDP-43 pathology	AD; Fall, osteoartheritis, Prostate cancer	VI	27	M	85
28	BBN002.28762	AD (modified Braak (BNE) stage V) with moderate to severe amyloid angiopathy	AD	V	70	M	86
29	BBN002.28697	AD (modified Braak (BNE) stage VI) with moderate amyloid angiopathy and dementia with Lewy bodies (limbic stage) and limbic TDP-43 pathology	Dementia in AD, atypical mixed type	VI	38.5	F	89

30	BBN_24402	AD (modified Braak (BNE) stage 6	AD	VI	79	F	85

Table 2.2. Case details for post-mortem BA9 tissues used for immunohistochemistry in this study.

Table shows details of sex, age, PMD, Braak stage/ BrainNet Europe (BNE) stage, primary pathological diagnosis and cause of death for cases from which paraffin embedded sections was obtained.

Case Number	Case ID	Pathological Diagnosis	Cause of Death	Braak/BNE Stage	PMD (hours)	Sex (M/F)	Age at Death (years)
1	BBN_15777	Normal Adult Brain	Carcinoma of breast	0	21.5	F	87
2	BBN_15616	Normal Adult Brain	Myocardial infarction	0	6	M	86
3	BBN_1571	Normal Adult Brain	-	0	50	M	59
4	BBN_15790	Normal Adult Brain	Liver, renal and respiratory failure	0	40	M	40
5	BBN_15734	Mild age-related changes	Bladder carcinoma	0	9.5	M	78
6	BBN_16368	Argyrophilic grains low to moderate density and early Alzheimer-type neurofibrillary lesions	-	II	13	F	82
7	BBN_9881	AD Braak stage V Mild amyloid angiopathy	-	V	12.5	F	80

8	BBN_9775	AD Braak stage V Moderate amyloid angiopathy	Cerebrovascular Accident	V	26	M	86
9	BBN_9796	AD Braak stage V	Bronchopneumonia; End stage dementia	V	<24	F	84
10	BBN_9829	AD Braak stage V	Bronchopneumonia	V	12	F	97
11	BBN_9855	AD Braak stage VI Severe amyloid angiopathy	-	VI	41	M	80

Table 2.3. Cases details from Table 2.1 from which cerebellar and hippocampal tissues were obtained.

Case Number	Case ID	Braak/BNE Stage	PMD (hours)	Sex (M/F)	Age at Death (years)
4	BBN_18816	0	53	M	84
5	BBN_4581	II	24	M	82
9	BBN_22594	0	21	F	77
21	BBN_4197	VI	26.5	F	83
24	BBN_9928	VI	5.5	M	72
29	BBN002.28697	VI	38.5	F	89

Table 2.4 Case details for post-mortem BA9 used in Array tomography.

Table shows details of sex, age, PMD, ApoE genotype, pH, Braak/BNE stage, primary pathological diagnosis and cause of death for sections obtained. Details of BA17 case used as a positive control also shown.

Case Number	CASE ID	Brain Region	Pathological Diagnosiss	Cause of Death	Braak/BNE Stage	PMD (hours)	Sex (M/F)	Age at Death (years)	ApoE (Genotype)	pH
1	001.35823	BA9	-	-	-	72	F	40	3/3	6.41
2	001.34215	BA9	No significant abnormalities	Pulmonary thromboembolism	0	49	M	50	-	5.88
3	001.32577	BA9	Thal phase 3 Braak tangle stage II WM pathology, mild Mild non-amyloid small vessel disease (SVD) Microinfarcts, cerebral white matter Mild arteriolar Aβ-CAA	Metastatic lung cancer; Chronic obstructive pulmonary disease	II	74	M	81	3/3	6.07

4	001.30972	BA9	No significant abnormalities	Ischaemic heart disease; Coronary artery atherosclerosis	0	99	M	34	3/4	6.32
5	001.30140	BA9	WM pathology, mild Mild non-amyloid SVD	Haemopericardium; Dissection of thoracic aorta	0	122	M	50	3/4	6.12
6	001.33614	BA9	WM pathology, mild	Haemopericardium; Ruptured acute myocardial infarct; Coronary artery atheroma and thrombosis	0	76	M	46	3/3	6.11
7	001.35529	BA9	No significant abnormalities	Coronary artery atheroma	0	96	M	58	3/3	6.49
8	001.30841	BA9	Mild non-amyloid SVD	Myocardial infarction; Coronary artery abnormalities	-	103	M	40	3/3	5.69
9	001.33636	BA9	Thal Amyloid phase 5 Braak tangle stange VI Mild arteriolar Aβ-	Advanced dementia, AD	VI	43	M	93	3/4	5.92

			CAA WM Pathology, severe Severe non-amyloid SVD Lewy Body Disease, brain stem subtype							
10	001.32929	BA9	Thal amyloid phase 5 Braak tangle stage VI WM pathology, severe Severe non amyloid SVD Severe arteriolar Aβ-CAA	Bronchopneumonia; Urinary tract infection	VI	80	F	85	3/3	6.03
11	001.30973	BA9	Thal amyloid phase 5 Braak tangle stage VI Severe arteriolar Aβ-CAA WM pathology, moderate Moderate non-amyloid SVD Alzheimer's Disease	Vascular dementia; Hypertension; Atrial fibrillation; Ischaemic heart disease; Chronic kidney disease	VI	96	F	89	3/4	6.03

12	001.31499	BA9	Thal phase 5 Braak tangle stage VI WM pathology, moderate Mild non-amyloid SVD Mild arteriolar Aβ-CAA Lewy Body Disease, brain stem subtype Alzheimer's Disease	Bronchopneumonia, AD	VI	78	M	85	3/4	6.12
13	001.35182	BA9	Thal amyloid phase 5 Braak tangle stage VI WM pathology, mild Mild non-amyloid SVD Severe arteriolar Aβ-CAA	AD	VI	49	M	66	3/3	6.12
14	001.31495	BA9	Thal phase 4 Braak tangle stage VI WM pathology, mild Mild non-amyloid SVD Mild arteriolar Aβ-	Stage IV Lung cancer; Type 2 diabetes; Ischaemic heart disease	VI	38	M	81	3/4	5.79

			CAA AD							
15	001.35564	BA9	Thal phase 5 Braak tangle stage VI Moderate arteriolar Aβ-CAA WM pathology, mild Mild non-amyloid SVD Lewy Body Disease, brain stem subtype Alzheimer's Disease	Aspiration pneumonia; VaD	VI	52	F	90	-	5.99
16	001.33698	BA9	Thal amyloid phase 5 Severe arteriolar Aβ-CAA WM pathology, moderate Severe non-amyloid SVD Lewy Body Disease, brain stem subtype AD	-	VI	76	F	90	3/4	6.29
17	001.29695	BA9	Thal phase 5 Braak tangle stage VI WM pathology,	AD	VI	72	M	86	3/4	6.1

			severe Severe non-amyloid SVD Moderate arteriolar Aβ-CAA Lewy Body disease, limbic subtype AD							
18	001.30883	BA9	Thal amyloid phase 5 Braak tangle stage VI Moderate arteriolar CAA WM pathology, severe Moderate non-amyloid SVD AD	Sepsis Advanced dementia	VI	69	F	61	3/4	6.15
19	001.28410	BA17	AD Braak tangle stage VI Thal phase 5 WM pathology, mild Moderate non-amyloid SVD Mild arteriolar Aβ-CAA	Inanation; AD	VI	109	F	62	3/3	6.04

Table 2.5 Case details for post-mortem tissues across several neurodegenerative diseases (Controls, AD, mixed dementia, FTLD, DLB, PSP and PiD) used in this study.

Table shows details of sex, age, PMD, Braak/BNE stage, primary pathological diagnosis and cause of death for cases from which frozen hippocampal tissue and temporal cortex sections was obtained.

Case Number	Case ID	Pathological Diagnosis	Cause of Death	Braak/BNE Stage	PMD (hours)	Sex (M/F)	Age at Death (years)
Control							
1	BBN_14408	Mild age-related changes (control brain) - AD modified Braak stage + with mild focal amyloid angiopathy	-	0	45	M	90
2	BBN_24381	Minimal ageing changes BNE stage +, control	Cancer	0	78	F	66
3	BBN_24371	Tau Braak stage II, control	Metastasized cancer with no primary found.	II	44	F	90
4	BBN_24666	Braak stage II consistent with ageing, control	Hospital acquired pneumonia; Chronic obstructive pulmonary disease; Bilateral lung disease	II	66	F	74

5	BBN_24200	Control brain- very mild AD BNE stage 2	Lung infection; Heart attack	II	62	F	67
6	BBN_20040	Consistent with ageing (Tau Braak stage II), control	Lung cancer	II	22	F	80
7	BBN_22991	Early ageing changes BNE stage 1, control	-	I	27	F	73
8	BBN_10208	Very mild ageing changes, Hyperphosphorylated-tau stage 1	Metastatic prostate cancer	I	25	M	67
Alzheimer's Disease							
9	BBN_23396	AD BNE stage 6	-	VI	71	M	83
10	BBN002.26152	AD (modified Braak (BNE) stage VI)	Aspiration pneumonia; AD	VI	69	M	63
11	BBN_25019	AD (modified Braak (BNE) stage VI), and severe amyloid angiopathy	Bronchopneumonia; Dementia	VI	30	F	73
12	BBN_24382	AD (modified Braak (BNE) stage VI)	Dementia	VI	31	F	79
13	BBN_22220	AD BNE stage 6	-	VI	57	M	85
14	BBN_24558	AD (modified Braak (BNE) stage VI)	End stage AD	VI	27	F	84
15	BBN002.26733	AD BNE stage 6	-	VI	77	M	84
16	BBN_20016	AD BNE stage 6	-	VI	31	F	87
Mixed Dementia							
17	BBN_18814	AD (modified Braak (BNE) stage VI) with extensive amyloid angiopathy	AD and cerebrovascular disease	VI	68	M	91

18	BBN_10196	AD (modified Braak stage VI) with limbic TDP-43 pathology	-	VI	5.25	F	93
19	BBN_4179	AD (modified Braak (BNE) stage V) with widespread and severe amyloid angiopathy	-	V	65	M	87
20	BBN_9974	AD (modified Braak (BNE) stage VI) with widespread severe amyloid angiopathy	-	VI	20	F	83
21	BBN_18794	AD (modified Braak (BNE) stage V-VI) with amyloid angiopathy	-	V-VI	11	M	76
22	BBN_24945	AD (modified Braak (BNE) stage VI (posterior predominant), Thal phase 4 and TDP-43 pathology Joseph's stage IV (type A pattern)	Community acquired pneumonia; Dementia	VI	28	F	96
23	BBN_16299	AD Braak VI BNE 5	-	V-VI	-	F	88
24	BBN_24206	AD BNE stage 6 with severe amyloid angiopathy	-	VI	80	F	81
	Frontotemporal Lobar Dementia						
25	BBN_19697	FTD with TDP-43 positive inclusions (FTD-TDP) subtype A	-	-	72	F	78
26	BBN002.26170	FTD with TDP-43 positive inclusions (FTLD-TDP) (subtype C) with Limbic stage Lewy body pathology (Limbic stage DLB)	-	-	8.5	M	62
27	BBN_24681	FTD with motor neurone disease (FTLD-MND) subtype B	Aspiration pneumonia; Motor neuron disease; Frontal lobe syndrome	V	67	F	71

28	BBN_21004	FTD TDP-43 proteinopathy	Metastatic carcinoma of the bronchus	-	58	F	74
29	BBN_10245	FTLD-TDP (type A) with mild to moderate vascular pathology	-	III	31	M	87
30	BBN002.26654	FTD with TDP-43 pathology (FTLD-TDP), type A, Diffuse Lewy Body Disease, limbic subtype (McKeith).	-	-	48.5	F	91
31	BBN002.28594	FTD with TDP-43 positive inclusions (FTLD-TDP type A)	Pneumonia; Dementia	-	66	M	72
32	BBN_24396	FTD due to TDP-43 proteinopathy (Type A) AD BNE (Braak) stage 4	End stage dementia	IV	34	F	71
	Dementia with Lewy Bodies						
33	BBN_18396	Lewy body disease, consistent with Parkinson's disease dementia (PDD) (diffuse neocortical type); Alzheimer-type tau pathology BNE 3, CERAD plaque score B	-	III	-	F	74
34	BBN_16241	Lewy body disease - limbic/transitional type (PD +/- dementia / DLB)	Aortic sclerosis; Infection	III	-	F	79
35	BBN_16400	Lewy body pathology in brainstem, limbic areas, neocortex	End-stage PD	-	35	M	74
36	BBN_16353	DLB (diffuse neocortical)	End stage PD	-	18	M	74
37	BBN_24626	AD BNE stage 4, mild neocortical diffuse Lewy body disease	-	IV	-	F	87
38	BBN_16313	Severe small & large vessel disease sufficient to cause Vascular dementia and/or Parkinsonism	-	III	-	F	93

39	BBN_16309	Lewy body disease / PD Braak VI; McKeith 'neocortical' AD Braak stage III	Aortic sclerosis; Infection	III	-	M	70
40	BBN_13797	Diffuse Lewy body disease, early neocortical type. Early tau pathology, Hyperphosphorylated-tau stage 2	-	II	40	M	66
	Progressive Supranuclear Palsy						
41	BBN_15712	PSP	Multi-infarct dementia	-	21	M	71
42	BBN_20997	PSP Very early Alzheimer type changes		-	35	F	72
	Pick's Disease						
43	BBN_10248	PiD (FTLD)	Myocardial infarction; Ischaemic heart disease	-	90	F	80
44	BBN_16369	PiD	Brain atrophy aspiration pneumonia	-	62	M	71

Table 2.6 Case details for post-mortem BA9 and temporal cortex brain from an age-matched control and ANCL patient.

Table shows details of sex, age, PMD, Braak/BNE stage, primary pathological diagnosis and cause of death for sections obtained.

Case Number	Case ID	Pathology	Cause of Death	Braak/BNE Stage	PMD (hours)	Sex (M/F)	Age at Death (years)
1	BBN004.30941	Ischaemic heart disease	Myocardial infarction; Ischaemic heart disease	0	18.25	M	55
2	BBN004.26173	Neuronal Ceroid Lipofuscinosis Type 4 (Kuf's disease/ Adult-onset ceroid lipofuscinosis)	-	0	36	M	58

2.4 Protein Extraction and Fractionation

2.4.1 Biochemical Fractionation (Synaptoneurosomes)

Synaptoneurosomes were prepared as previously described (Hollingsworth et al., 1985). Briefly, 150 mg of frozen tissue was homogenized in 10 volumes of cold Buffer A (Chapter 2, Section 2.2), using a Teflon-glass mechanical tissue grinder (25 strokes) and filtered through 2 x 80-mm pore filters. A portion of the filtrate was supplemented with H_20 and 10% SDS, boiled for 5 minutes (min) and centrifuged at 15 000 x *g* (av) for 15 min, and a portion of the supernatant was collected as the total fraction. Next, using 5-mm pore filters, the rest of the supernatant was filtered and centrifuged at 1000 x *g* (av) for 10 min producing a synaptoneurosome pellet. The supernatant was collected as cytosolic fraction, which was further centrifuged at 100 000 x *g* (av) for 30 min. The synaptoneurosome pellet was centrifuged again at 1000 x *g* (av) for 10 min and the pellet was supplemented with 0.2 mL Buffer B (Section 2.2) and further boiled for 5 min. This was then centrifuged at 15 000 x *g* (av) for 15 min and the supernatant was collected as synaptoneurosome fraction. Synaptophysin and PSD-95 were used as synaptic markers to check the purity of each fraction (Chapter 3, Section 3.4.4). Samples were also examined for phosphorylated tau protein and Aβ content to confirm the neuropathological assessment (Chapter 3, Section 3.4.3).

2.4.2 Differential Solubility Extraction

To determine the solubility of CSPalpha isolated from human brain samples, BA9 post-mortem human samples underwent sequential extractions using a method adapted from previous publications (Waxman et al., 2008; Peng et al., 2018). Briefly, 100 mg of frozen tissue was thawed on ice and gray matter was separated from white matter (WM). Tissues were homogenized using an electric homogeniser (Tissue

Master 125, Omni International, UK) in 5 volumes of cold HS buffer (Chapter 2, Section 2.2). Homogenates were kept on ice for 20 min before being centrifuged at 170,000 *g* (av) (Optima Max-XP ultracentrifuge, Beckman Coulter, USA) for 30 min at 4°C. The HS supernatant was saved, and the pellet was resuspended and re-homogenised in HS buffer and centrifuged again at 170,000 *g* (av) for 30 min. The resulting supernatant was stored as the HS soluble fraction. The HS-insoluble pellet was extracted by homogenisation with HS-TX buffer (Chapter 2, Section 2.2) and centrifuged at 170,000 *g* (av) for 30 min at 4°C. The resulting supernatant was collected as the HS-TX soluble fraction. Next, the HS-TX insoluble pellets were extracted in HS-TX-Sucrose and centrifuged at 170,000 *g* (av) for 30 min at 4°C to float the myelin. The resulting pellets were extracted with 20 % (v/v) of the ionic detergent N-lauryl-sarcosine (sarkosyl) (Sigma, UK) in HS buffer. Samples were nutated at room temperature for 1 hour and then centrifuged at 136,000 *g* (av) for 30 min at 4°C. The sarkosyl soluble (SS) supernatant was collected as the SS fraction. Sarkosyl insoluble (SI) pellets were washed in HS-sarkosyl buffer and centrifuged at 136,000 *g* (av) for 10 min at 4°C. The SI supernatant was discarded, and the pellet was resuspended directly in 5 volumes of 2 x sample buffer (National Diagnostics, UK), collected as the SI fraction. 5 µL of each extract was used for western blot analysis. Samples were examined for CSPalpha solubility and total tau protein was used to confirm the neuropathological assessment and as a marker of insolubility in disease (Chapter 3, Section 3.4.12).

2.4.3 Total Homogenate Preparation

Total homogenates were prepared from frozen hippocampal brain tissue was conducted by N. Meeson (Table 2.5). Briefly, proteins were isolated using radioimmunoprecipitation assay lysis buffer (Santa Cruz Biotechnology). Phenylmethane sulfonyl fluoride, protease inhibitor cocktail and sodium

orthovanadate were added to the buffer in a 1:100 ratio (Santa Cruz Biotechnology), and 0.25% (w/v) SDS. Tissue was homogenised on ice using a mechanical homogeniser (15 strokes at 700 rpm). Homogenates were centrifuged at 855 *g* (av) for 10 min, and the supernatants were collected and stored at -20°C until use.

2.5 Bicinchoninic acid (BCA) protein assay

Tissue homogenate protein concentrations were determined using a BCA Protein Assay Kit (Thermo Scientific, Waltham, MA, USA) according to the manufacturer's instructions. Briefly, 25 µL of bovine serum albumin (Thermo Scientific, Waltham, MA, USA) was diluted in MilliQ H_2O and used to create a standard (ranging concentrations from 0 to 2 mg/mL) and 25 µL of sample were diluted in lysis buffer and equal volumes of sample or standard were pipetted induplicate into a 96-well plate (Nunca). BCA Reagent A was mixed with Reagent B in a 1:50 ratio and 100 µl of the solution was added to individual wells. The plate was incubated at 37°C for 30 min and the absorbance at 595 nm was determined. Using the resulting absorbance readings, the protein concentrations were then calculated.

2.6 Western Blotting

Western blotting was used to identify proteins and allow quantification of protein amounts. Briefly, samples were processed and prepared for SDS- polyacrylamide gel electrophoresis (PAGE), used to separate the proteins according to their molecular size. Proteins were then transferred onto a membrane and probed with specific antibodies.

2.6.1 SDS-PAGE

Samples were prepared for SDS-PAGE in a reducing loading buffer containing 0.5 M Tris-HCl (pH 6.8), 4.4% (w/v) SDS, 20% (v/v) glycerol, 2% (v/v) 2-mercaptoethanol, and bromophenol blue (EC-886, National Diagnostics Ltd., UK) in a 1:1 ratio. The samples were boiled at 95 ˚C for 5 min to denature the proteins. Samples were then centrifuged at 10 000 x *g* (av) for 10 seconds (s) to remove cell debris and insoluble material.

Two different methods were used for SDS-PAGE as outlined below:

2.6.1.1 SDS-PAGE Method 1

10 % or 4 – 12 % Bis Tris gradient polyacrylamide 15-well gels were cast in 1.0 mm plastic cassettes (Life Technologies, UK). Gels were inserted into the XCell SureLock™ Mini-Cell electrophoresis system (Life Technologies, UK), and chambers were filled with running buffer (National Diagnostics) (Section 2.2). The prepared samples (Table 2.1) were then loaded onto the gel at a known protein concentration and were separated by electrophoresis at 100 volts (V) for 2.5 hours until the bromophenol blue dye front ran to the bottom of the gel. Protein molecular weight markers (Precision Plus Protein™, Biorad) were loaded in the first lane of gels to allow for determination of protein size. Following SDS-PAGE, proteins were transferred onto 0.45 µm nitrocellulose membranes (GE Healthcare, UK) in Biorad tanks filled with transfer buffer (National Diagnostics). Proteins were transferred at 100 V for 1 hour on ice. To expose Aβ epitopes, membranes were boiled for 2 x 1 min in TBS (800 watt microwave). Membranes were incubated for 1 hour at room temperature in either 5% milk blocking solution or in Odyssey® Blocking Buffer (Li-cor Biosciences Ltd., UK), depending on primary antibody, to prevent non-specific binding. Primary antibodies (Table 2.7) were prepared in appropriate blocking

solution with TBS and were added to membranes, which were then incubated overnight at 4 ˚C. The next day, primary antibody solution was removed, and membranes were washed 3 x 10 min in TBS-T (0.2% (v/v) Tween20, Sigma (UK)). The appropriate infra-red dye secondary antibodies (Table 2.8) were diluted in either 2% milk blocking solution or Odyssey® Blocking Buffer with TBS, and then incubated with the membranes for 1 hour at room temperature. Secondary antibodies were then removed, and membranes were washed two times in TBS-T and once with TBS for 10 min each.

Membranes were scanned for fluorescence emission at 700 nm and 800 nm wavelength on an Odyssey® infrared scanning system (Li-cor Biosciences Ltd., UK). Scanning intensity of membranes was optimized according to the strength of the background and antigen signals to allow for quantification of integrated signal intensity within a linear range. Only protein bands of expected molecular weight were quantified using Odyssey® analysis software V3.0 (Li-cor Biosciences Ltd., UK), and background signal was subtracted automatically.

2.6.1.2 SDS-PAGE Method 2

30 µg samples were loaded equally in a volume of 20 µL into each well of a 4–15% Criterion™ TGX™ precast gels (containing 18 or 26 wells) (Bio-Rad) alongside with a molecular weight rainbow marker (RN800E). Gradient gels have an increasing acrylamide concentration allowing proteins of several molecular weights to be separated efficiently. Samples were separated using SDS-PAGE at 100 V for 2 hours in running buffer (National Diagnostics, UK). Following SDS-PAGE, gels were placed in transfer buffer (National Diagnostics, UK) prior to wet transfer. Wet transfer materials were arranged in a sandwich using filter papers, pads, and the methanol-

activated polyvinylidene fluoride 0.2 µm membrane were soaked in transfer buffer. Proteins were transferred onto membranes in a transfer tank (Bio-Rad) at 100 V for 1 hour. Membranes were blocked in TBS-T (0.2 % (v/v) containing 5 % (w/v) non-fat dry milk powder (Tesco, UK) at room temperature for 1 hour to prevent non-specific binding. Following overnight incubation with primary antibodies (Table 2.7) in the same blocking buffer, membranes were washed with TBS-T for 3 x 10 min and then incubated in 2% blocking buffer with horseradish peroxidase conjugated secondary antibodies (P0447/8, DAKO) at room temperature for 1 hour. After further washing for 3 x 10 min in TBS-T, membranes were incubated with ECL reagent (Thermo Scientific) for 5 min at room temperature. Bound antibody was detected linearly after exposure to X-ray films (Amersham). Bound antibodies were dissociated from membranes by the addition of stripping buffer (Santa Cruz Biotechnology) for 1 hour at room temperature, followed by washing in TBS-T for 3 x 10 min, blocking and re-probing with other primary antibodies.

Semi-quantitative densitometry analysis was performed on western blots performed using the ECL method by plug-in ImageJ software (NIH). Outliers were excluded if the signals obtained were greater than 2 x standard deviation from the mean.

Table 2.7. Primary antibodies used for western blotting in this study.

Antibody	Epitope and Specificity	Host Species/ Type	Dilution	Predicted Molecular Weight (kDa)	Source/ Reference
6E10	Anti-β-amyloid Amino acids 1-16 of human Aβ sequence	Mouse	1/500	APP – 110 Aβ Monomers – 4	803001, Biolegend, UK
Beta Actin	Amino acids 1-100 of Human beta Actin	Mouse	1/5000	42	ab8226, Abcam, UK
CSPalpha	Raised against recombinant rat CSP with deletion of cysteine string	Rabbit	1/50000	~ 29-34	AB1576, Merck Millipore Ltd., UK
Hsc70	Amino acids 583-601 at C-terminus of human Hsc70	Mouse	1/1000	70	sc-7298, Santa Cruz, UK
NR2B	Amino acids 1437-1482 of NR2B subunit of NMDA receptor	Rabbit	1/500	170	06-600, Merck Millipore Ltd., UK
NSE	NSE purified from human brain	Mouse	1/10000	46	Dako, Ltd., UK
NSE	Synthetic peptide from of human NSE	Rabbit	1/10000	46	AB951, Merck Millipore Ltd., UK
Phosphorylated CSPalpha	CSPalpha phosphorylated at Ser10	Rabbit	1/1000	~ 29-34	Kind gift from Prof Alan Morgan (University of Liverpool, UK)
PHF-1	Tau phosphorylated at ser396/ 404	Mouse	1/1000	~ 50-64	Kind gift from Prof Peter Davies
PSD-95	Amino acids 50-150 of mouse PSD-95	Rabbit	1/1000	95	ab18525, Abcam, UK
Synaptophysin	Amino acids 221-313 of synaptophysin of human origin	Mouse	1/1000	38	sc-17750, Santa Cruz, UK

Synaptophysin	Residues surrounding 250-300 (C Terminal) of human synaptophysin	Rabbit	1/100000	38	ab32127, Abcam, UK
Synaptophysin	Residues surrounding Alanine230 of human synaptophysin	Rabbit	1/1000	38	4329, Cell Signalling Technology, UK
Total Tau	Purified from human brain	Mouse	1/10000	50	A0024, Dako, Ltd., UK

Table 2.8. Secondary antibodies used for western blotting in this study (Section 2.7.1 – Method 1).

Secondary Antibody	Wavelength	Dilution	Source
IR Dye Goat anti Mouse	680	1/10000	926-68070, LI-COR Biosciences, UK
IR Dye Goat anti Rabbit	680	1/10000	926-68071, LI-COR Biosciences UK
IR Dye Goat anti Mouse	800	1/10000	926-32210, LI-COR Biosciences, UK
IR Dye Goat anti Rabbit	800	1/10000	926-32211, LI-COR Biosciences UK

2.8 Human Post-Mortem Immunostaining

2.8.1 Tissue Preparation for Immunostaining

Brain tissue samples were obtained as 7 µm 10% formalin-fixed, paraffin-embedded tissue sections from the London Neurodegenerative Diseases Brain Bank (King's College London, UK).

2.8.2 Immunohistochemistry

Immunohistochemistry was performed as described (Tiwari et al., 2015). Sections were deparaffinised in xylene for 2 x 2 min and rehydrated in a range of ethanol concentrations (2 x 99 % (v/v) and 1 x 95 % (v/v) for 2 min each). Activity of endogenous peroxidases was blocked by incubating sections in 3% hydrogen peroxide for 30 min at room temperature. To enhance antigen retrieval, sections underwent citrate buffer pre-treatment for 16 min in a microwave (6 min medium high, 2 x 5 min low (800 watt)). Sections were washed 2 x 5 min in TBS and a hydrophobic barrier was drawn around sections using wax. Sections were blocked in 10% (v/v) NSS (X0901, DAKO) for 1 hour and then a primary antibody against CSPalpha (1:500 AB1576, Merk Millipore) in TBS was applied overnight at 4°C. Next, sections were washed 2 x 5 min in TBS and incubated with a biotinylated secondary antibody (1:100, Swine anti-rabbit immunoglobulin/biotinylated, E0353, DAKO Ltd) for 45 min. After further 2 x 5 min washes in TBS, sections were incubated with avidin:biotin enzyme complex (Vectastain Elite ABC kit, Vector Laboratories, UK). Sections were washed 2 x 5 min and were developed in 0.5 mg/ml 3,3′-diaminobenzidine chromogen (DAB) (Sigma-Aldrich Company Ltd, Dorset UK) in TBS (pH 7.6) containing 0.05% H_2O_2 for 5 min. Sections were rinsed in MilliQ H_2O and dehydrated 95% and 2 x 99% ethanol and 2 x 2 min in xylene. Samples were mounted onto slides using DPX (VWR). Slides were qualitatively analysed by neuropathologists Drs Claire Troakes, Istvan Bodi and

Tibor Hortobagyi. Brightfield images were taken using an Olympus Slide scanner (VS120) and analysed using Olympus Viewer software (VS120).

2.8.3 Immunofluorescence

Sections underwent deparaffinisation in xylene (100% (v/v)) and were rehydrated in graded concentrations of ethanol (2 x 99% (v/v) and 1 x 95% (v/v) ethanol for 2 min each). Sections were rinsed in MilliQ H_2O for 5 min and exposed to citrate buffer pre-treatment for 16 min in a microwave (6 min medium high, 2 x 5 min low, 800 watt) to enhance antigen retrieval. Sections were washed 2 x 5 min in TBS-Tween20 (0.01% Tween20, Sigma) and a hydrophobic barrier was drawn using a PAP pen. Sections were blocked for 1 hour in 10% (v/v) NGS (Sigma) in TBS before incubation with primary antibodies (Table 2.9) in 1% (v/v) NGS and 1 x TBS at 37 °C for 1 hour. Following rinsing and 2 x 5 min washes in TBS-T (0.01% Tween20), sections were incubated with fluorescently tagged secondary antibodies (Table 2.10) diluted in TBS for 45 min at room temperature. Following further washing in TBS-T, sections were then exposed to 10 min of sudan black (Sigma, UK) treatment to reduce autofluorescence. Sections were washed 8 x 3 min in TBS-T and coverslips were mounted using vectashield mounting medium containing DAPI (H-1200, Vectashield).

Table 2.9. Primary antibodies used for immunohistochemistry and immunofluorescence.

Antibody	Epitope and Specificity	Species	Dilution	Source
6E10	Anti-β-amyloid Amino acids 1-16 of human Aβ sequence	Mouse	1/500	803001, Biolegend, UK
AT8	Tau phosphorylated at Ser202/Thr205	Mouse	1/250	MN1020, Thermoscientific, UK
CSPalpha	Raised against recombinant rat CSP with deletion of cysteine string	Rabbit	1/250	AB1576, Merck Millipore Ltd., UK
GFAP	Glial fibrillary acidic protein (GFAP)	Mouse	1/250	VP-G805, Vector Laboratories
Phosphorylated CSPalpha	CSPalpha Phosphorylated at Ser10	Rabbit	1/50	Kind gift from Prof Alan Morgan (University of Liverpool, UK)
Synaptophysin	Amino acids 221-313 of synaptophysin of human origin	Mouse	1/250	sc-17750, Santa Cruz, UK
Hsc70	Amino acids 583-601 at C-terminus of human Hsc70	Mouse	1/1000	sc-7298, Santa Cruz, UK
IBA-1	Peptide corresponding to 20 amino acids from N-terminal region of human Iba1/AIF1	Mouse	1/200	MABN92, Merck Millipore Ltd., UK
SMI312	Homogenised hypothalamic recovered from Fischer 344 rats	Mouse	1/500	Kind gift from Prof Chris Miller (King's College London, UK)
LAMP1	Residues surrounding Ser140 of human LAMP1	Rabbit	1/250	C54H11, Cell Signalling, UK
SNAP-25	Raised against post-mortem human brain	Mouse	1/250	sc-20038, Santa Cruz, UK

Table 2.10. Secondary antibodies used for immunofluorescence.

Secondary Antibody	Wavelength	Dilution	Source
Alexa Fluor Goat anti Rabbit	488	1/250	A11034, Thermofisher Scientific, UK
Alexa Fluor Goat anti Mouse	568	1/250	A11004, Thermofisher Scientific, UK

2.9 Human Post-Mortem Imaging

2.9.1 Epifluorescence Imaging

Images were captured using a Leica DM5000B fluorescence microscope and CTR5000 camera (Leica Microsystems, Germany) and a Nikon Ti-E Live Cell Three Camera microscope, using the 20x and 40x objective lens. All parameters including lamp intensity, video camera setup and calibration were constant during image capture and images were stored as TIFF files.

2.9.2 Spinning Disk Confocal Microscopy

Tissue sections were examined using a Nikon Eclipse Ti inverted spinning disk confocal microscope (Nikon Instruments, UK) with a Yokogawa CSU-1 disk head and Andor iXon EMCCD camera and either a 20x, 40x or 60x oil objective lens (Nikon Instruments, UK). Parameters including laser settings, camera setup and calibration were kept constant during image capture. Image 'Z' stacks were acquired covering a total 'Z' depth of 12 µm. A maximum intensity and volume projection were produced from collapsing the Z stacks in NIS-Elements AR software (Nikon Instruments, UK). Using 3-dimensional (3D) volumetric measurement, images were thresholded with a minimum value of 8 μ^3 size. Images were stored as TIFF files.

2.9.3 Super Resolution Microscopy

Human tissue images were captured using an iSIM Super Resolution microscope with Vt-iSIM scan head with Hamamatsu Flash4.0 sCMOS camera with a 100X/1.49NA oil objective. Image 'Z' stacks were acquired covering a total 'Z' depth of 12 µm. Volume projection images were produced in NIS-Elements AR software (Nikon Instruments, UK).

2.10 Array Tomography

2.10.1 Tissue Preparation for Array Tomography

Fresh post-mortem human brain tissue from BA9 was embedded as previously outlined (Kay et al., 2013) by Dr Jamie Rose (University of Edinburgh). In brief, samples were collected at autopsy, cut into small cortical blocks (1 mm × 1 mm × 5 mm) and fixed in 4% paraformaldehyde for 2–3 hours. Samples were then dehydrated in ascending graded ethanol concentrations and incubated in LR white resin overnight. Cortical blocks were then baked in LR white resin which was polymerized at 56 °C for 24 hours and stored at room temperature until required. Resin embedded tissue blocks were cut into array ribbons of 70 nm serial sections using an ultracut microtome (Leica) with a Jumbo Histo Diamond Knife (Diatome, Hatfield, PA) and collected onto gelatin coated coverslips.

2.10.2 Array Tomography Immunostaining

For array tomography, a hydrophobic barrier was drawn around each ribbon and left to dry for 30 min. Ribbons were rehydrated in 50 mM glycine for 5 min and exposed to EDTA (pH 8.0) treatment using a pressure cooker for 1 min. Ribbons were also rehydrated in 50 mM glycine for 5 min. Array ribbons were blocked for 30 min with fish gelatine. Ribbons were then incubated with primary antibodies (Table 2.11) overnight at 4^{o}C. Ribbons were continuously washed 3 times in TBS and appropriate Alexa fluor conjugated secondary antibodies were applied for 30 min. Following this, ribbons were continuously washed 3 more times in TBS. Sections were counterstained with 0.01 mg/mL DAPI for 5 min, washed in TBS and mounted onto coverslips using immunomount (DAKO). A ‘no primary’ negative control was included for each experimental day, and a short ribbon was used using as positive control for Aβ plaques.

Images were acquired with a Zeiss Axio Imager Z2 upright epifluorescent microscope equipped with a CoolSnap digital camera using a high-resolution 63x oil 1.4NA Plan Apochromat objective and AxioImager software with array tomography macros (Carl Zeiss, Ltd, Cambridge UK). Images were manually acquired from the area of interest on each serial section of the ribbon using either Aβ plaques or DAPI stained nuclei as a reference marker. Image stacks were created and aligned for regions of interest in the neuropil using Image J and the MultiStackReg custom plugin (Micheva et al., 2010) . Binarized image stacks were combined using different thresholding algorithms in Image J. For synaptic image stacks this allowed the detection both high and low intensity synapses in an automated method. Using custom MATLAB scripts, images were manually thresholded to detect synaptic puncta and for CSPalpha accumulations present around Aβ plaques. Synaptic density was calculated using thresholded images to remove background noise (only objects present in 2 or more stacks were retained) and to further calculate the colocalization of Aβ with both CSPalpha and synaptophysin (presynaptic terminals). The relative colocalization was calculated as a 10% minimum overlap of the number of colocalization puncta or deposits of/sum total puncta for each protein of interest. Additionally, MATLAB scripts were used to measure the density of presynaptic accumulations (both CSPalpha and synaptophysin) from the centre of the Aβ plaque core (plaque distance) using bin sizes 0-10 μm, 10-20 μm, 20-30 μm and 30-40 μm.

Table 2.11. Primary antibodies used for array tomography.

Antibody	Epitope and Specificity	Species	Dilution	Source
6E10	Anti-β-amyloid Amino acids 1-16 of human Aβ sequence	Mouse	1/200	803001, Biolegend, UK
CSPalpha	Raised against recombinant rat CSP with deletion of cysteine string	Rabbit	1/100	AB1576, Merck Millipore Ltd., UK
Synaptophysin	*E. coli*-derived recombinant human synaptophysin	Goat	1/50	AF5555, R&D Systems, UK

2.11 5xFAD Mouse Model

5xFAD mice (n=3) and WT mice (n=4) were obtained from Professor Po Wah So (King's College London). A colony of breeding mice was established at the Institute of Psychology, Psychiatry and Neuroscience. 5xFAD mice generated on a C57/B6 x SJL background strain express AD-linked mutant human *APP* (Swedish (K670N/M671L), Florida (I716V), and London (V717I)) and *PSEN1* (M146L and L286V) transgenes.

5xFAD mice (Oakley et al., 2006) were generated by two independent transgenes encoding mutant human amyloid beta precursor protein (APP) complementary DNA sequence (altered to include the APP mutations) and mutant human *PSEN1* complementary DNA sequence (altered to include the PSEN1 mutations) both inserted into exon 2 of the mouse Thy1 gene. Both transgenes were equally co-injected into the pronuclei of C57/B6 x SJL hybrid embryos.

Mice were group housed under standard laboratory conditions with food and water ad libitum. All procedures carried out were in accordance with the UK Animals Scientific Procedures Act 1986 and was approved by Animal facility of the Institute of Psychology, Psychiatry and Neuroscience, King's College London.

2.11.1 Mouse Genotyping

Genotyping of human mutant APP and PS1 expression in 5x FAD mice was carried out by M. Aljuhani in the group of Professor Po Wah So (King's College London). Briefly, to confirm the presence of mutant transgenics, DNA was extracted from ear clips, followed by polymerase chain reaction (PCR), agarose gel electrophoresis and eventually visualisation of DNA fragments under ultraviolet light illumination. As

anticipated, mutant human PS1 and APP were detected in 5xFAD mice, but not in WT littermates (Fig 2.1)

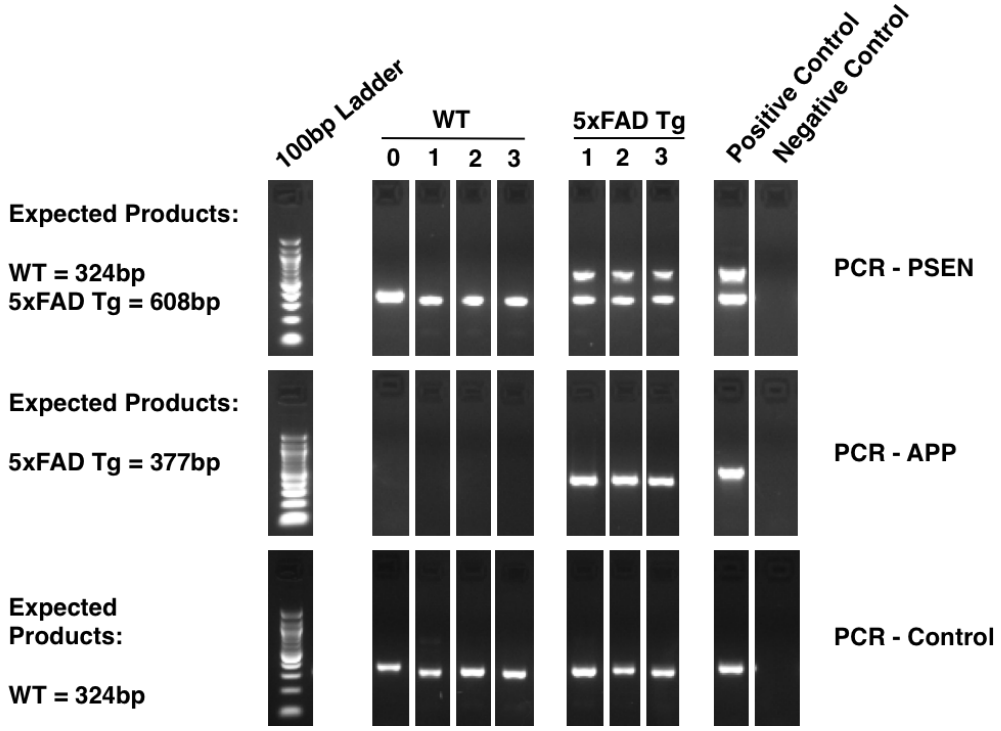

Figure 2.1. Human mutant PS1 and APP expression in 5xFAD mice.

DNA from WT and 5xFAD mice were extracted, amplified by PCR and visualized on agarose gels. Human PS1 detected at 608 base pairs (bp) and APP detected at 377 bp were only evident in 5xFAD mice and not in WT. Endogenous mouse PS1 was detected at 324 bp in WTs. A 100 bp ladder molecular marker was electrophoresed next to the samples.

2.11.2 Mouse Tissue Preparation

5xFAD mice were sacrificed by terminal anesthesia using 0.1 ml pentobarbitone (Euthatal, Merial Animal Health Ltd, UK) into the chest and transcardially perfused with PBS followed by 4% (w/v) PFA in PBS. Brains were post-fixed in 4 % (w/v) PFA overnight and were then cryoprotected for 24 hours in 30% (w/v) sucrose in PBS to prevent fracturing of the tissue during sectioning. Once the brains had sunk in sucrose solution, they were frozen for 30 s in isopentane and chilled to -90 °C with dry ice. Frozen brains were stored at -80°C until required.

Whole brains were sectioned used a Leica CM1860 cryostat (Leica Microsystems, Germany). Samples were mounted onto a specimen disk using OCT mounting medium (Bright Instruments) on dry ice and sectioned coronally at 30 µm. Sections were collected and stored free floating in PBS and were then transferred to antifreeze (Chapter 2, Section 2.2) in a 24-well plate. Sections were stored at -20 °C prior to histological staining.

2.11.3 Mouse Immunofluorescence

A one in 4 series of sections from WT and 5xFAD mice was immunohistochemically labelled with antibodies against CSPalpha, synaptophysin, SNAP-25 and Aβ using a previously published methodology (Aziz et al., 2019). Briefly, 30 µm sections were washed in PBS for 5, 8 and 10 min respectively prior to incubation in PBS blocking buffer containing 5% (v/v) NGS in 0.1% (v/v) Triton X-100 for 1 hour at room temperature to block non-specific antibody binding. Sections were then incubated overnight with shaking at 4°C in PBS containing 0.1% (v/v) Triton X-100 and primary antibodies: CSPalpha (1/2000, AB1576, Merck Millipore), Aβ (1/2000, 803001, Biolegend), synaptophysin (1/1000, sc-17750, Santa Cruz) and SNAP-25 (1/1000, sc-20038, Santa Cruz). Unbound primary antibody was removed by washing 3 x 10

min with PBS at room temperature. Sections were then incubated in PBS containing 0.1% (v/v) Triton X-100 and secondary antibody (1/500 each) (Table 2.10) for 2 hours shaking at room temperature. Unbound secondary antibody was removed by washing 3 x 10 min in PBS. Sections were placed onto Poly-l-lysine slides (VWR, DE), air dried for 1 hour and coverslips were mounted using vectashield mounting medium containing DAPI (H-1200, Vectashield). Additional sections were stained with Thio-S treatment by placing into Thio-S solution for 8 min. Sections were then rinsed for 2 x 1 min in 50% ethanol and then 5 min in TBS before further air drying and mounting.

2.11.4 Mouse Tissue Imaging

Fluorescence images were captured using an Olympus whole slide scanner VS120 with 2/3" CCD camera, motorised XY stage with automatic control. An image overview of the sections was taken using a 2x objective. High resolution images at 60x magnification were also captured using spinning disk confocal microscopy as described above (Chapter 2, Section 2.9.2).

2.12 Statistical Analysis

Data from western blots was analysed using a student's t-test, one-way analysis of variance (ANOVA) followed by Tukey's multiple comparison test or two-way ANOVA with repeated measures and post hoc Sidak multiple comparisons test for parametric tests. For non-parametric data, either Mann Whitney U test or Kruskal–Wallis test was used. Tests for normality which included D'Agostino and Pearson and Shapiro Wilk's test were conducted and values ± 2 x standard deviation from the mean were considered outliers and excluded from analyses. Data are expressed as mean ± standard error of the mean (SEM) unless otherwise stated. This analysis was conducted using Graphpad Prism 8 (Graphpad) software.

Data from array tomography was conducted using analysed image stacks from MATLAB (version R2019a, Mathworks inc. US) and Image J. If required, data were transformed using either Tukey transformation or Box-Cox transformation (log-likelihood or Guerro methods) and Shapiro Wilk's test was used to test for normality. Data was statistically analysed using linear mixed effects modelling with type I-III ANOVA with Satterthwaite's degrees of freedom method. Outliers were included in the data set. Data in bar graphs are presented as either mean ± S.E.M or median with box plots for interquartile ranges. This analysis was conducted using RStudio.

Chapter 3: CSPalpha in Alzheimer's Disease

3.1 Introduction

CSPalpha is a molecular co-chaperone protein localized to presynaptic vesicles in neurons (Burgoyne and Morgan, 2015). CSPalpha has multifunctional roles at both glutamatergic and GABAergic synapses including maintaining proteostasis; refolding and degrading misfolded proteins via adenosine triphosphate (ATP) activation of Hsc70/Hsp70 in order to preserve synaptic function (Braun et al., 1996; García-Junco-Clemente et al., 2010; Deng et al., 2017). CSPalpha also facilitates synaptic transmission by interacting with SNARE proteins such as SNAP-25 to mediate vesicular exocytosis (Sharma et al., 2011). In addition, CSPalpha regulates vesicular endocytosis through interactions with dynamin-1 (Rozas et al., 2012; Sheng and Wu, 2012). Thus, CSPalpha has an important function in maintaining the synaptic network. Of interest to this project, CSPalpha has been reported to prevent presynaptic neurodegeneration (Fernández-Chacón et al., 2004).

Synaptic degeneration is a common early feature in many neurodegenerative diseases and precedes neuron loss (Henstridge et al., 2016). In AD, the presence and abundance of hallmark neuropathological lesions; extracellular neuritic plaques, composed of Aβ peptides, and intracellular NFTs, formed of hyperphosphorylated tau protein aggregates (Selkoe, 2001), are linked with synapse and neuronal loss, and the resulting cognitive impairments observed in AD (Koffie et al., 2009; Spires-Jones and Hyman, 2014). The mechanisms that lead to synapse loss in regions prone to neurodegeneration in AD are not fully known. Circumstantial evidence suggests that CSPalpha is important for these processes (Tiwari et al., 2015; Fontaine et al., 2016). In post-mortem AD forebrain, CSPalpha expression is reduced in regions that

undergo synaptic loss and neurodegeneration and that display extensive tau pathology (Zhang et al., 2012; Tiwari et al., 2015). In contrast, CSPalpha is elevated in the cerebellum, which is resistant to such pathologies in AD (Tiwari et al., 2015). This suggests that CSPalpha loss may promote or allow neurodegeneration whilst its upregulation may have a neuroprotective function in AD. However, the mechanisms underlying these events are not well understood.

BA9 is a region of the dorsolateral and prefrontal cortex involved in the integration of sensory stimuli and higher order executive functions normally associated with cognition (Fuster, 2001). As such, lesions within this area lead to features including altered working memory, failure to anticipate, lack of attention, apathy and cognitive deficits (Szczepanski and Knight, 2014). As such, BA9 has been documented to be an important region in the study of AD that is correlated with synaptic loss and cognitive decline, more so affected late in disease progression (Hof et al., 1990; Arnold et al., 1991; Braak and Braak, 1991; Bussière et al., 2003; Kashani et al., 2008).

Dekosky and Scheff (1990) were the first group to investigate the role of synapses in BA9 AD brain. They revealed that synapse numbers in layer III in BA9 AD brain were reduced compared to controls. Interestingly, they discovered a significant enlargement of synaptic size which correlated with a decline in synapse density, suggesting a possible compensatory mechanism to allow the synaptic contact area to remain stable, although this eventually declined by end stage of disease (DeKosky and Scheff, 1990; Masliah et al., 1994; Mukaetova-Ladinska et al., 2000). Further studies into the synaptoproteome in the BA9 region of AD brain, have suggested that changes at the synaptic protein level are either less pronounced within this region or only mostly evident in cortical gray matter at end stage in severe AD brains (Honer, 2003; Counts et al., 2006; Kashani et al., 2008; Poirel et al., 2018). This was

evidenced by expression levels of synaptophysin, the most wide-spread presynaptic protein, which was reduced by a minimal change of ~12% in the most severe AD brains (Poirel et al., 2018). As such, it was shown that the majority of synaptic markers in BA9 did not correlate with cognitive status. Berezcki and colleagues (2016) identified reduced synaptic SNAP-25 protein levels by enzyme-linked immunosorbent assay (ELISA) analysis within BA9 AD brain which negatively correlated with rapid cognitive decline, however no differences in SNAP-25 were observed in an older study by immunostaining (Clinton et al., 1994; Bereczki et al., 2016). These studies suggest that BA9 is a particular area of interest for investigating synaptic pathology in AD.

As another key synaptic protein, investigations of CSPalpha in human AD have been limited. As such, research into the expression of CSPalpha, as a suitable marker for synaptic dysfunction compared to traditional synaptic proteins, may offer a better mechanistic insight into the temporal progression of disease. Hence it can be hypothesised that:

- Levels of CSPalpha may be increased as a compensatory mechanism in early stages of BA9 AD in comparison to other synaptic proteins but will show reduced levels in severe stages of AD and may be a suitable marker of early presynaptic dysfunction.

Recently, the Giese group have obtained preliminary results in BA9 where putative CSPalpha protein accumulations have been discovered. These deposits associate with diffuse and neuritic cored plaques. These structures and their association with Aβ plaques and synapses are a main focus of this PhD project.

3.2 Aims

The primary objective of the studies presented in this chapter was to characterise CSPalpha protein as a novel pathological marker of AD using post-mortem human tissues. The specific aims of this chapter were to:

1. Investigate the relevance of CSPalpha protein expression, modified and/or distribution as a synaptic marker within different stages of AD post-mortem human tissues, with a focus on the BA9 region.
2. Use biochemical and histological techniques to examine and characterise the discovery of abnormal CSPalpha structures in AD brain.
3. Determine using the 5xFAD mouse model that aggressively develops Aβ deposition, whether CSPalpha accumulations are a consequence of Aβ deposition by comparing CSPalpha in 5xFAD mice to WT littermates.

The results from this work will contribute to studies of synaptic content and neuronal health in AD and may distinguish CSPalpha protein as a better pathological marker of synapses in AD.

3.3 Methods

The materials and methods conducted in this study have been fully described in Chapter 2, Sections 2.4.1 and 2.6.1.2. Briefly, post-mortem human tissue sections from the BA9 region were obtained from the London Neurodegenerative diseases Brain Bank in three different groups: control (mild age associated neuropathological changes) (Braak 0-II) [n=10], moderate AD (Braak III-IV) [n=10] and severe AD (Braak V-VI) [n=10]. Tissues were homogenised to enrich for synaptoneurosomes which were electrophoresed on 10% SDS gels for western blotting and were probed for antibodies against a housekeeping neuronal protein marker, neuron specific

enolase (NSE), and synaptophysin, a synaptic protein marker, to normalise against neuron and synapse content, respectively. Data from immunoblots were analysed using D'Agostino and Pearson and Shapiro Wilk's test for normality distribution and data was statistically analysed using a One-Way ANOVA with post hoc Tukey multiple comparisons test. Outliers, calculated as two standard deviations away from the mean, were excluded from the data set. Data in bar graphs are presented as mean ± S.E.M.

Using a subset of the same post-mortem human brain BA9 tissues from control (Braak 0-II) and severe AD brains (Braak VI) [n=6 per group], proteins from homogenates were extracted on the basis of their differential solubility in buffers containing high salt, triton X-100 and sarkosyl. Enriched fractions were immunoblotted using the same 10% gels. Blots were probed for antibodies against CSPalpha, PHF-1 and total tau along with a total protein stain to allow normalisation to total protein amounts.

For immunohistochemistry, post-mortem human tissue sections were acquired from BA9 for control (Braak 0-II) [n=6] and severe AD (Braak V-VI) [n=5]. Briefly, 7 µm thick tissue sections were immunolabelled using an antibody against CSPalpha and haemotoxylin was used to stain for neuronal nuclei. Slides were imaged using the Olympus Slide Scanner VS120 (Olympus, UK).

Similarly, tissue sections from a subset of cases used in immunoblotting experiments - control/ early AD (Braak 0-II) [n=5], moderate AD (Braak III-IV) [n=5] and severe AD (Braak VI) [n=5] along with further brain sections acquired from the hippocampus and cerebellum [n=3]. These tissues underwent immunofluorescence staining using antibodies against CSPalpha, Aβ, hyperphosphorylated tau, neurofilament changes, glial markers, synaptic proteins such as synaptophysin and SNAP-25 and interacting

proteins which include Hsc70. DAPI was used to stain neuronal nuclei. Slides were imaged using Nikon Eclipse Ti-E 3 camera inverted microscope with a Two camera system using Andor Neo sCMOS camera, Nikon Eclipse Ti Inverted Spinning Disk Confocal microscope with Yokogawa CSU-1 disk head and Andor iXon EMCCD camera and iSIM super resolution microscope with V t-iSIM scan head and Hamamatsu Flash4.0 sCMOS camera to provide imaging data for this thesis.

Array tomography analysis was conducted on post-mortem human tissue sections, from BA9 control (Braak 0-II) [n=8] and severe AD (Braak VI) [n=10]. As described previously, 70 nm thin brain sections underwent an immunofluorescence staining protocol, being probed for antibodies against CSPalpha, synaptophysin and Aβ, and imaged using a Zeiss axioimager microscope (Zeiss, UK). Images underwent post-processing, stack alignment and analysis for synaptic density, plaque distance and colocalization. Data from image stacks were analysed using MATLAB (version R2019a, Mathworks inc. US), Fiji and RStudio. Shapiro Wilk's test was used to test for normality and data was statistically analysed using linear mixed effects modelling with type I-III ANOVA with Satterthwaite's degrees of freedom method. Outliers were included in the data set. Data in bar graphs are presented as either mean ± S.E.M or median with box plots for interquartile ranges.

Lastly, 5xFAD mice were obtained from Dr Po Wah Soh (King's College London). These mice were maintained and then culled at ~6-7 months of age. Female 5xFAD [n=3] and WT mice [n=4] were perfused and brains removed with the assistance of Dr Keiko Mizuno (King's College London). Mouse brains were sectioned and immunolabelled using antibodies against synaptic proteins including CSPalpha, synaptophysin and SNAP-25 along with Aβ. Slides were imaged using an Olympus Slide Scanner VS120 (Olympus, UK), and a Nikon spinning disk confocal microscope was used for qualitative analysis.

3.3.1 Demographical Characteristics of Post-Mortem Human Tissue Samples

CSPalpha loss has been shown to precede synaptic degeneration in AD (Tiwari et al., 2015). To investigate this further, CSPalpha protein expression changes affected by the temporal progression of disease were explored. As shown previously by Tiwari and colleagues (2015), CSPalpha expression is altered in both the hippocampus, where levels were severely reduced early on in disease development, and the cerebellum where CSPalpha levels were increased, more in-line with end stage of disease progression (Tiwari et al., 2015). This study investigates changes in the prefrontal cortex BA9, a region that is affected only in the later stages of AD and displays enlarged synapses when synaptic degeneration first begins to occur (DeKosky and Scheff, 1990; Masliah et al., 1994; Mukaetova-Ladinska et al., 2000; Reddy et al., 2005; Serrano-Pozo et al., 2011; Poirel et al., 2018). Hence, understanding changes of BA9 over different Braak stages may provide a more in depth understanding into the progression of synaptic changes of CSPalpha with respect to synaptic decline in the progression of AD.

In order to investigate this, human tissue brains from BA9 were obtained from the MRC London Neurodegenerative Diseases Brain Bank that were neuropathologically diagnosed as several Braak stages (0-VI) [Braak stage 0-II; n=10, Braak stage III-IV; n=10, Braak stage V-VI; n=10] (Chapter 2, Section 2.3 Table 2.1).

Age, sex and PMD were assessed to determine whether they might have an effect on the data generated in this study (Table 3.1). Following D'Agostino & Pearson testing, data was analysed using one-way ANOVA analysis which showed no statistically significant differences between Braak 0-II, Braak III-IV and Braak V-VI groups for both age ($F(2, 27) = 3.139$, $p=0.06$) and PMD ($F(2, 27) = 0.6113$, $p=0.55$). Chi-squared testing showed no statistically significant sex differences between the

groups (χ^2 = 0.272, p=0.873). These parameters are therefore not likely to influence the results observed in this study.

Table 3.1. Summary of BA9 cases and controls used in the BA9 study.

Table shows the number of cases of each Braak stage group, the percentage of cases that were female, the average age at death and PMD (mean ± SEM).

Braak Stage	Number of Cases	Female (%)	Age (Years) Mean ± SEM	PMD (Hours) Mean ± SEM
0-II	10	40	82.8 ± 1.9	36.2 ± 4.7
III-IV	10	40	88.9 ± 1.8	45.8 ± 7.6
V-VI	10	50	81.9 ± 2.6	45.0 ± 7.6

3.4 Results

3.4.1 CSPalpha antibody validation

In this thesis, a previously published commercially available anti-CSPalpha antibody (AB1576) was used for investigating the expression and localisation of CSPalpha at the presynaptic terminal (Kohan et al., 1995; Mastrogiacomo and Gundersen, 1995; Boal et al., 2004; Rüttiger et al., 2004; Benitez et al., 2015; Tiwari et al., 2015; Henderson et al., 2016; Shirafuji et al., 2018; Naseri et al., 2020a). This CSPalpha antibody was developed from recombinant rat CSP with the cysteine-string deleted and recognises the alpha isoform of CSP (Kohan et al., 1995; Mastrogiacomo and Gundersen, 1995). To confirm the specificity of this CSPalpha antibody for use in this PhD study, western blot analysis was performed on forebrain and cerebellum regions of WT and CSPalpha KO mouse tissue, a kind gift from Dr Fernandez-Chacon (IBiS, Seville, Spain) (Fernández-Chacón et al., 2004). These homozygous mutant KO mice lack CSPalpha protein, and so the antibody should not detect any CSPalpha protein within these brains. Immunoblot analysis showed no detection of CSPalpha bands in the KO compared to the WT mouse brains lysates in which clear bands appeared at the predicted molecular weight of CSPalpha (29-35 kDa) (Fig 3.1). CSPalpha appeared as a smear and/ or doublet in the WT mouse brain, likely due to post-translational modifications of CSPalpha protein.

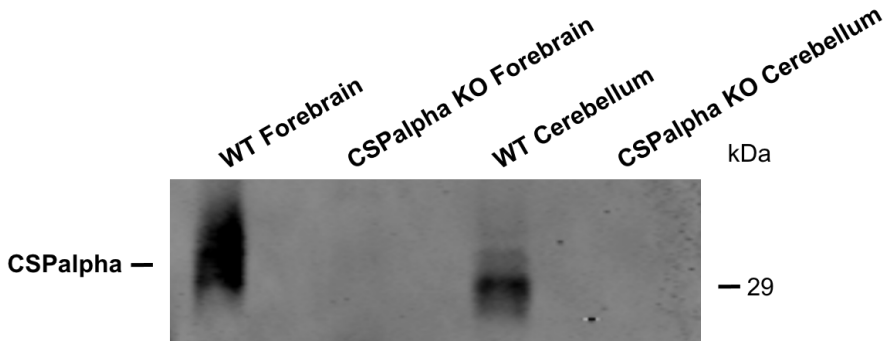

Figure 3.1 Specificity of anti-CSPalpha antibody.

Detection of total monomeric CSPalpha (~ 29 kDa) in WT but not CSPalpha KO, forebrain and cerebellum mouse lysates confirming specific binding of antibody to CSPalpha [n=1 mouse per group].

3.4.2 Assessment of Protein Degradation and Tissue Quality

To first determine the quality and protein levels in human brain tissue samples, total homogenates were extracted using a buffer containing 1.5% SDS (Chapter 2, Section 2.4.1) and analysed using SDS-PAGE. Protein degradation was assessed to compare between groups, as described in previous studies (Wang et al., 2000b; Engmann et al., 2011; Bayés et al., 2014; Tiwari et al., 2015; Kurbatskaya et al., 2016; Jackson et al., 2019b). These lysates were electrophoresed on western blots and membranes were probed with an antibody against the C-terminal region of the NR2B post-synaptic ionotropic glutamate receptor known to be proteolyzed rapidly after death. This antibody recognises full-length protein NR2B (170 kDa) and degradation products presented as two or three distinct bands at approximately 150 kDa (Fig 3.2a). The degradation products are evident only in post-mortem tissues making NR2B a useful marker assessing post-mortem synaptic protein integrity (Bayés et al.,

2014). The human post-mortem synapse proteome integrity ratio for NR2B degradation (NR2B ratio) was defined as the ratio of the intensity of the highest molecular weight band relative to the lower bands. There were no statistically significant differences in NR2B ratio amongst the different Braak stage groups (0-II, III-IV and V-VI) ($F(2,27) = 0.01542$, $p=0.9847$) (Fig 3.2b), suggesting that levels of synaptic integrity are maintained (Bayes et al., 2014) and are equivalent in tissues from these groups.

It has been suggested that longer PMD times correlate with greater degradation of products (Wang et al., 2000b; Ferrer et al., 2008). To determine whether there was any correlation between the NR2B ratio and PMD in the AD samples, non-parametric Spearman correlation analysis was used to generate correlation co-efficients (r values) and their significance. No statistically significant correlations between the NR2B ratio and PMD in any of the Braak stage groups, although Braak III-IV group did appear to show a trend for negative correlation between NR2B degradation and PMD ($r = -0.5581$, $p = 0.0936$) (Fig 3.2c).

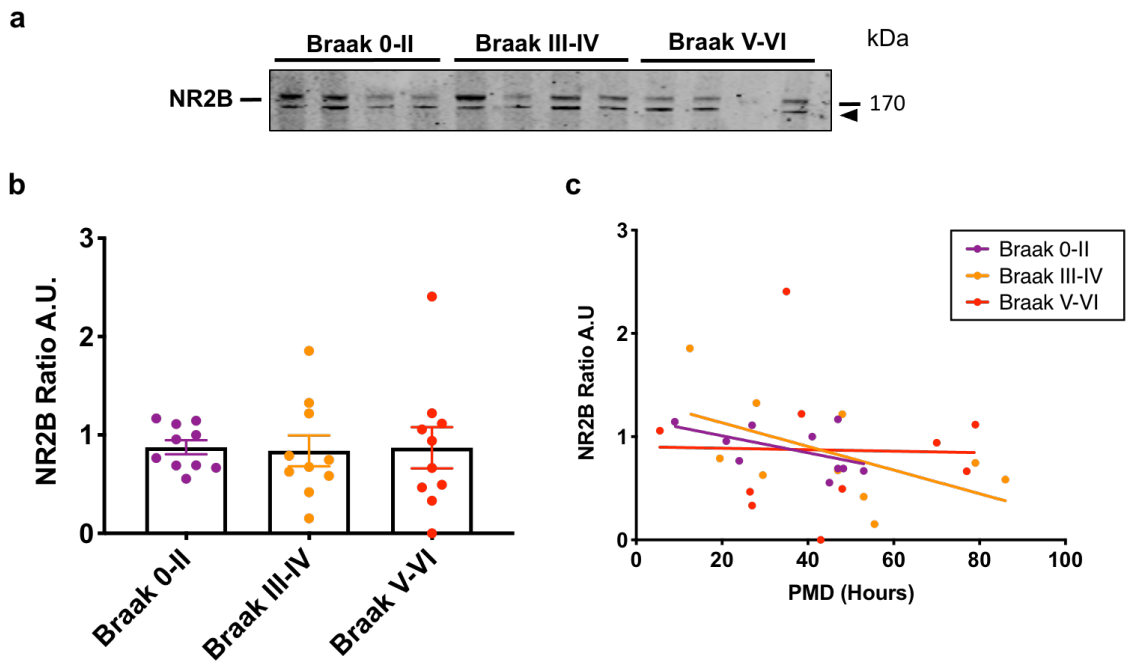

Figure 3.2. NR2B proteolysis in post-mortem human brain samples.

a) Representative western blots of BA9 post-mortem human lysates probed with an anti-NR2B antibody showing two distinct high molecular weight bands in Braak 0-II, Braak III-IV and Braak V-V groups. The upper band (170 kDa) corresponds to the full-length protein and lower band to degradation products (~150 kDa) (*Black arrowhead*). **b)** Bar charts showing no changes in the ratio of full length to cleaved NR2B, as an indication of synapse degradation. Following Shapiro Wilk's normality testing, data was analysed using One-Way ANOVA. Data shown are mean ± SEM. **c)** Scatter plots showing correlation of the NR2B ratio relative to PMD for all Braak stage groups [n=10 cases per group].

3.4.3 Confirmation of neuropathological diagnosis in post-mortem BA9 Brain

Having confirmed the tissues were age-matched and with the shortest possible PMD, neuropathological diagnosis of the tissues was next assessed using temporal development of tau pathology with increasing Braak stage. As the abnormal processing of tau is closely associated with neuronal dysfunction in AD (Crimins et al., 2013), total homogenate fractions from BA9 frontal cortex were immunoblotted for tau phosphorylated at Ser396/404 epitopes, detected by the anti-PHF1 antibody (expected band size, approximately ~50-68 kDa). The house keeping neuronal protein, neuronal specific enolase (NSE) (band size 46 kDa) was used to confirm protein present in each of the samples (Fig 3.3).

Interestingly, various tau bands were observed which reflect the tau isoforms, which can be differentially modified by truncation, phosphorylation of tau and formation of higher molecular weight oligomers and aggregates (Watanabe et al., 1999; Kurbatskaya et al., 2016) (Fig 3.3). There was some variability amongst the groups where tau phosphorylation at this site was not detected, however this may be down to factors such as cause of death, brain hemisphere examined, prescribed medications, PMD and adjustments of brain changes after death, pH of tissues, pathological comorbidities or phosphorylation at other sites of interest not identified with the anti-PHF1 antibody (Hanger et al., 2009). These results, however, support previous findings that tau is abnormally phosphorylated in AD and increased in degenerating regions of AD brain (Khatoon et al., 1994), and confirms the Braak staging of these tissues.

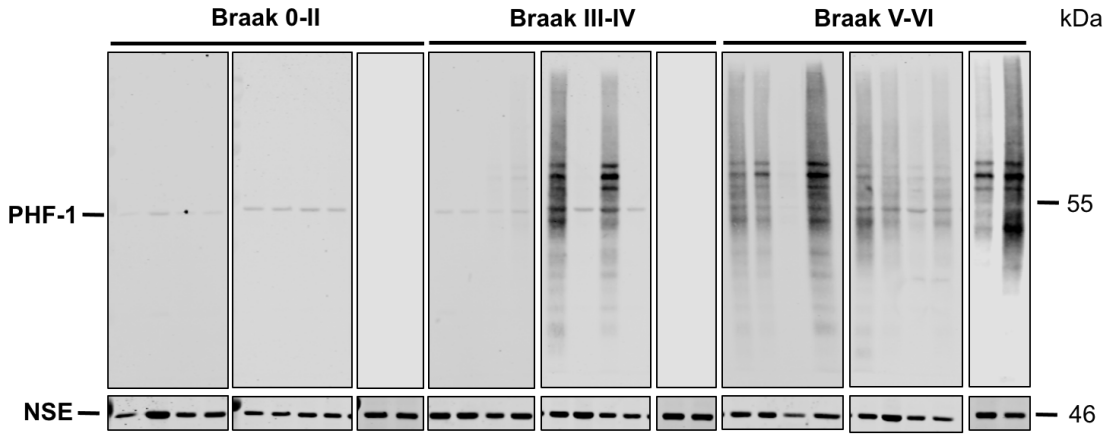

Figure 3.3. Neuropathological assessment of tau phosphorylated at Ser396/404.

a) Full-length western blots of post-mortem BA9 cortex total homogenates probed with an antibody against the PHF-1 epitope to detect phosphorylated tau (~50-68 kDa) and NSE as a loading control (46 kDa) in Braak 0-II, Braak III-IV and Braak V-V groups. As expected, smears of tau bands were identified in moderate and severe AD stages. [n=10 cases per group].

Post-mortem BA9 tissues were next examined for a Aβ content. APP is the precursor transmembrane glycoprotein that, when cleaved by β- and γ- secretases gives rise to Aβ (Dawkins and Small, 2014). Total amounts of APP protein were assessed by SDS-PAGE where immunoblots were probed with an antibody against the N-terminus of APP (6E10). Three characteristic bands for APP were observed at approximately 106, 113 and 130 kDa, depicting the three main isoforms of APP (695, 751, 770) in human brain (Nordstedt et al., 1991) (Fig. 3.4a). Quantification of total APP immunoreactivity (sum of the three APP species) from Braak 0-II, III-IV and V-VI BA9 brain were normalised to NSE where no statistically significant differences between any of the groups were found ($H(3) = 1.901$, $p=0.3866$) (Fig 3.4b). This is in line with

a previous report from cerebral cortex tissues showing no differences in total APP amounts between non-demented controls and end stage AD (Nordstedt et al., 1991).

Monomeric levels of Aβ (band size 4 kDa) were examined, however Aβ monomers were only evident for a subset of tissue samples and could not be quantified due to the difficulty in detecting these small protein fragments, presumably due to rapid postmortem degeneration or other technical issues (Fig 3.4a). Along with examining Aβ monomer expression, it would also be interesting to examine the abundance $A\beta_{40}$ and $A\beta_{42}$ in post-mortem control and AD brain using more specific antibodies. Also, use of ELISA or related quantitative methods may provide greater sensitivity to determine possible alterations in Aβ between groups and individual brains.

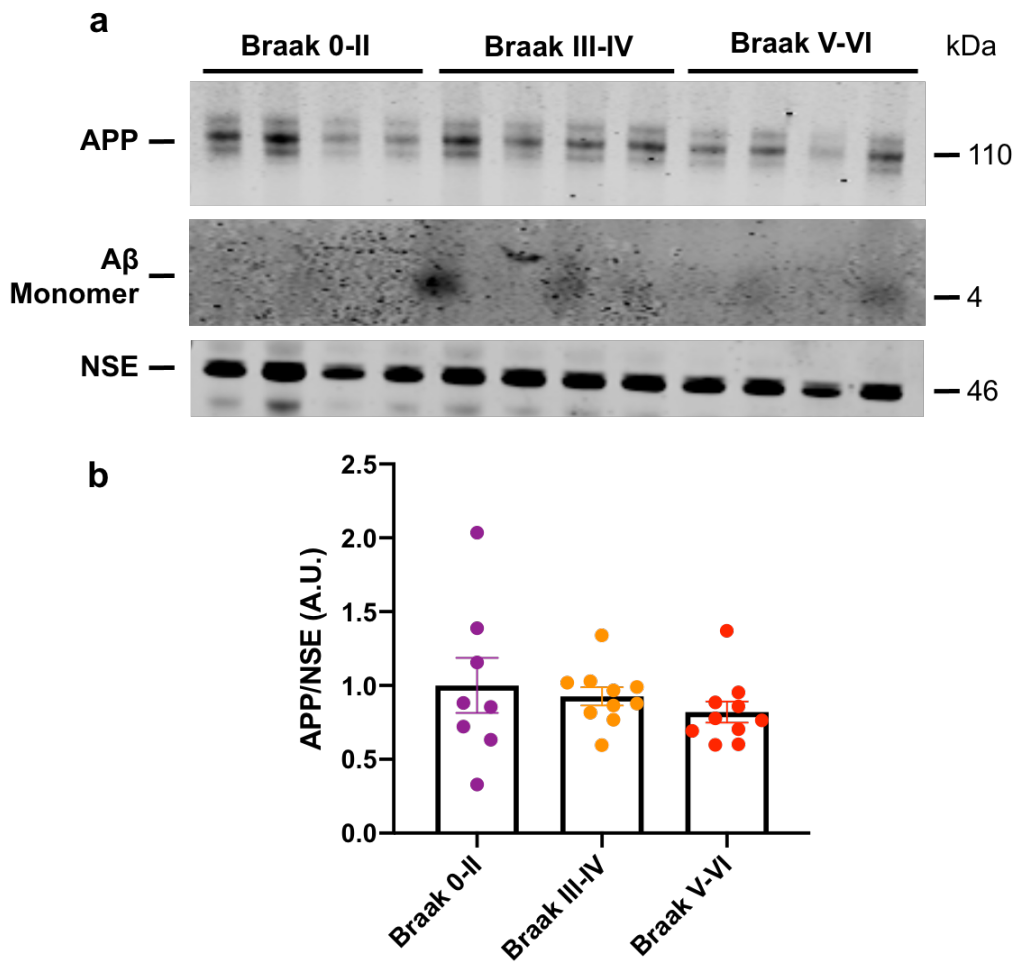

Figure 3.4. Measurement of APP amounts and identification of monomeric Aβ.

Representative western blots probed with the 6E10 antibody to detect full-length APP isoforms (~110 kDa) and monomeric Aβ (4 kDa) in post-mortem BA9 of Braak stages 0-II, III-IV and V-VI. APP was normalised to NSE, used here as a loading control (46 kDa). **b)** Bar charts show quantification of APP amounts in BA9 brain in Braak stages when normalised to NSE protein in the same samples. Following D'Agostino and Pearson normality testing, data were analysed using non-parametric Kruskal–Wallis test. Data shown are mean ± SEM expressed as a fold average of control. [n=10 cases per group].

3.4.4 Synaptic enrichment of BA9 fractions

Having confirmed the neuropathological diagnosis of the samples, CSPalpha protein levels were next examined to determine if this is specifically affected the synaptic compartment during AD progression. The study of synaptic proteins has provided valuable information about the underlying molecular mechanisms of neuronal activity (Cohen et al., 1977; Kennedy et al., 1983) and disease pathogenesis (Unger et al., 2005). The isolation of synapses consisting of pre- and post-synapses is a useful technique to understand the subcellular localisation of proteins and their molecular composition at synapses (Hebb and Whittaker, 1958). The term synaptoneurosome was hence suggested referring to the presynaptic sac (synaptosome) and its attachment to a resealed postsynaptic sac (neurosome) (Hollingsworth et al., 1985; Quinlan et al., 1999). This preparation enriches remaining brain synapses unlike examination of total homogenates to examine synaptic protein specific changes without the confound of synapse loss (Tai et al., 2012). As such, this technique has shown to capture pathways involved in glutamatergic and GABAergic synaptic signalling, changes in long term potentiation and depression as well as cyclic adenosine monophosphate response element-binding protein signalling (Tai et al., 2012; Hesse et al spires jones 2019). BA9 tissues were fractionated into total, cytosolic and synaptic fractions, as reported previously (Arendt, 2009; Tai et al., 2012), since this allows sensitive measurement of the abundance of proteins in the synaptic compartment.

Fractions were assessed for synaptic content by immunoblotting with antibodies against the presynaptic proteins CSPalpha, synaptophysin and SNAP-25 and the postsynaptic protein, PSD-95 which were present in both total and synaptic fractions (Fig 3.5). This not only confirmed the presence of pre- and post-synaptic terminals in the synaptoneurosome preparation but also as there was higher signal intensity

compared to global total fractions, this suggested greater enrichment of synaptic proteins within the synaptoneurosome fraction (Fig 3.5). As expected, synaptic proteins were not detected in the cytosolic fraction. NSE, a neuronally expressed enzyme, used here as a suitable housekeeping protein, was present in all three fractions. Hsc70, a chaperone protein known to interact with CSPalpha was found in all fractions, particularly in the cytosolic compartments (Fig 3.5). A further step, to ensure purity and no contamination of fractions would however have been to probe for histone H3, to ensure exclusion of a nuclear marker, as previously as described (Jackson et al., 2019b) and differentiation of synapse sub-types using specific glutamatergic (Vesicular glutamate transporter 1 (VGLUT-1)) and GABAergic (Glutamic acid decarboxylase (GAD) 65/ GAD67) markers. Although not the scope of the study, exclusion of glial and oligodendrocyte markers would be necessary as this could add a cell-type specific confound between samples. Overall, however, the differential detection of the proteins examined confirmed the fractionation of these samples into crude total lysates, cytosolic and synaptoneurosome fractions.

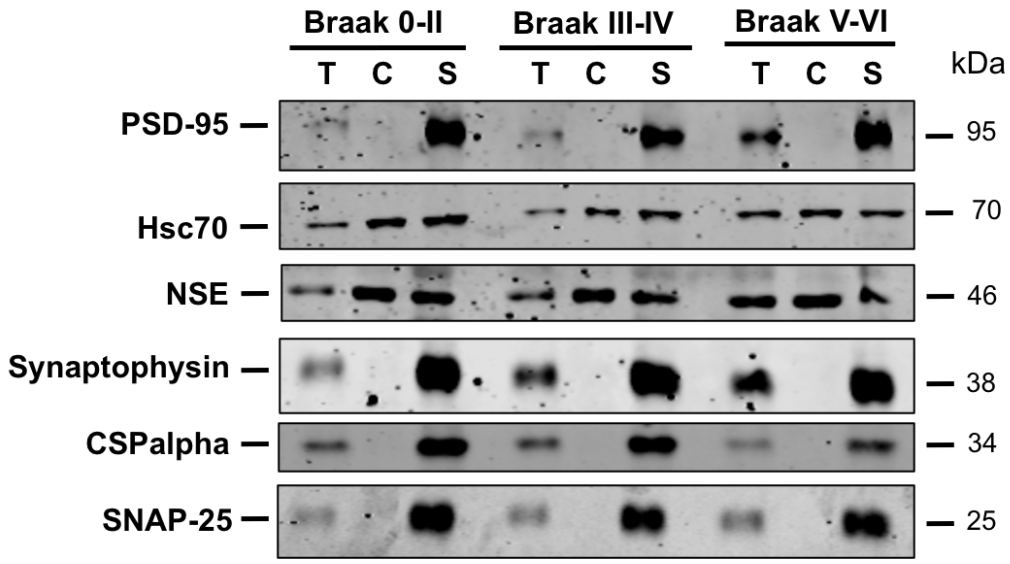

Figure 3.5. Characterisation of fractions yielded from synaptoneurosome preparations.

Western blots of total (T), cystosolic (C) and synaptoneurosome (S) fractions from Braak stages 0-II, III-IV and V-VI BA9 samples were probed with antibodies against presynaptic (synaptophysin, CSPalpha, SNAP-25) and postsynaptic (PSD-95) markers. Synaptic proteins were only detected in total and synaptoneurosome fractions and not in cytosolic fractions. The neuronal marker, NSE and cytosolic protein Hsc70 were detected in all three fractions. Molecular weights of proteins are shown on the right-hand side.

3.4.5 CSPalpha expression is reduced in end-stage AD BA9

Having confirmed synaptic protein enrichment in synaptoneurosomes and shown that CSPalpha is detected within the synaptic fraction, it was hypothesised that CSPalpha levels would be transiently upregulated as a compensatory mechanism for early synapse loss in early-mid stages of AD in the BA9 region due to an enlargement of synaptic size found in this region (DeKosky and Scheff, 1990), which is then reduced upon synaptic loss in later disease stages. Since CSPalpha is a synaptically localised co-chaperone, a loss of synapses will affect its expression and to account for this, the amounts of CSPalpha protein were calculated relative to those of synaptophysin, a marker of pre-synaptic terminals, as used previously in several studies (Honer, 2003). This allows assessment of CSPalpha amounts in remaining synapses that is distinct from a general effect of synapse change (Weiler et al., 1990; Vawter et al., 1999).

A Braak I-II case was loaded on all western blots as a reference sample to enable quantification. Western blots were probed for antibodies against presynaptic CSPalpha and synaptophysin and clear bands were present at their corresponding molecular weights (Fig 3.6a). In total lysates, despite an apparent reduction in CSPalpha amounts, no statistically significant differences were found in CSPalpha amounts between Braak I-II, III-IV and V-VI groups ($H(3) = 0.5531$, $p=0.7584$) (Fig 3.6b). This suggests that global CSPalpha amounts are relatively stable in BA9 during AD progression. This is in marked difference to the hippocampus, where CSPalpha levels are reduced as AD progresses (Tiwari et al., 2015). There was high variability in the severe AD group and the lack of significance might have been the result of an anomalous sample, that did not meet criteria for being removed as an outlier. As reported previously (Fig 3.4), CSPalpha protein is not enriched in the cytosolic fractions and so immunoblotting was not conducted for these samples.

CSPalpha protein amounts were then examined along with synaptophysin in synaptoneurosome fractions of post-mortem BA9 (Fig 3.6c). When normalised to synaptophysin, there was a trend towards differences between the groups ($F(2, 26) = 3.165$, $p = 0.059$). The biggest difference was apparent in synaptoneurosomes from severe AD brains (Braak V-VI) which showed reduced CSPalpha expression compared to moderate AD samples (Braak III-IV) (Fig 3.6d). To determine whether this result was powered in this study, an independent two-tailed t-test between Braak III-IV and Braak V-VI samples was calculated which obtained 62.7% power (G*Power 3.1). It appears that this result is underpowered (<80%) even though the effect size for this analysis ($d = 1.11$) suggests this is a large biological effect (G*Power 3.1). A sample size estimate of at least 23 cases per group would be required to reach a conclusive result. Determination of power can however be limiting as it may not be generalisable to the population based on a pilot study, in addition to the limited tissue availability.

However, as previously described for other presynaptic proteins, this overall result possibly indicates that synaptic proteins are conserved during early AD within this region (as shown by a slight elevation between Braak 0-II and III-IV), followed by a decline at end stage AD when synapses become dysfunctional and degenerate (Mukaetova-Ladinska et al., 2000; Vallortigara et al., 2014; Kurbatskaya et al., 2016). In summary, using BA9 as an additional brain region to monitor disease progression, these findings suggest that CSPalpha may be a suitable marker of synaptic changes in AD. However, it is now important to understand the possible mechanisms that may drive a reduction in CSPalpha at the synapse. As a synaptic protein, CSPalpha should be enriched within the synaptic compartment, allowing more subtle differences in CSPalpha expression to be identified.

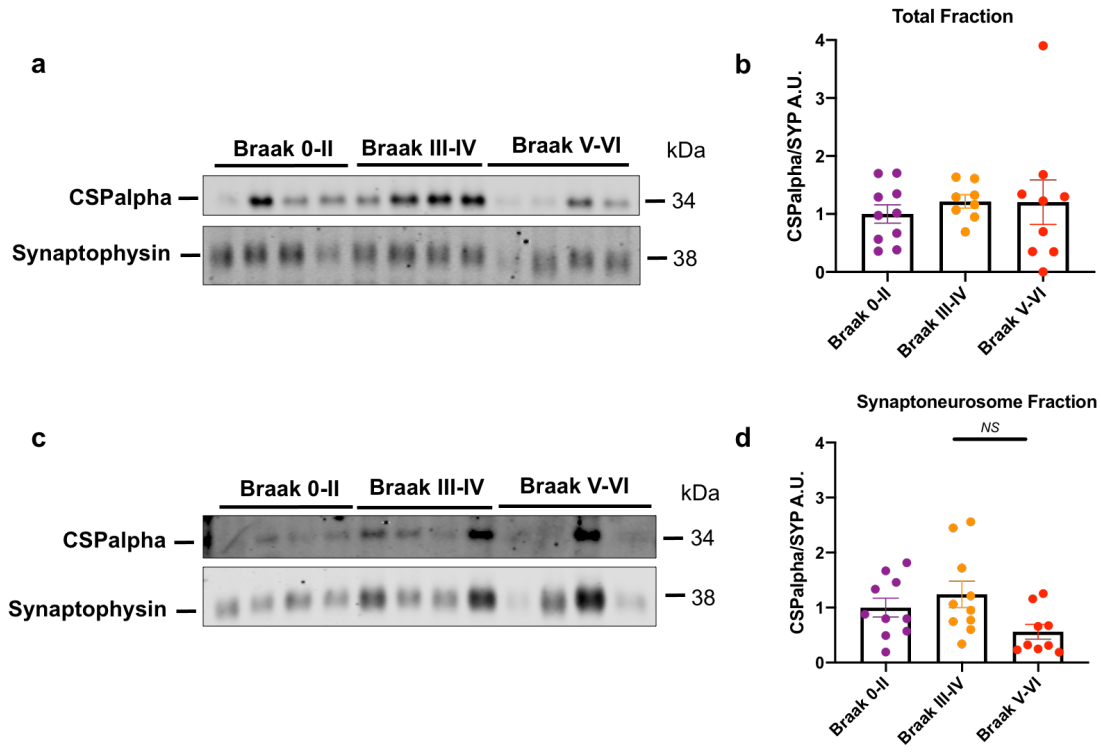

Figure 3.6. CSPalpha and synaptophysin protein levels in AD BA9.

a) Representative western blots of total homogenates from Braak stages 0-II, III-IV and V-VI post-mortem BA9 cortex showing bands for CSPalpha and synaptophysin as a presynaptic loading control. **b)** Bar charts show quantification of CSPalpha amounts in these samples relative to synaptophysin amounts in the same sample. Following D'Agostino and Pearson normality testing, data were analysed using non-parametric Kruskal–Wallis test. **c)** Representative western blots of synaptoneurosomes probed for CSPalpha and synaptophysin. **d)** Bar charts show quantification of CSPalpha amounts in BA9 synaptoneurosome when controlled for synaptic content by normalising to synaptophysin levels. Following D'Agostino and Pearson normality testing, data were analysed using a one-way ANOVA. Data shown are mean ± SEM expressed as fold average control. *NS* = Not statistically significant. [n = 10 cases per group].

3.4.6 Novel CSPalpha aggregate-like accumulations identified in AD

Although western blots allow measurement of protein abundance, they do not provide detailed information about synapse loss, specific changes in synapses or the colocalization of multiple synaptic proteins. Tiwari and colleagues (2015) previously reported, using an optimised anti-CSPalpha antibody for immunohistochemistry, reduced CSPalpha immunoreactivity in the hippocampal granule cell layer and in STG of AD brain compared to healthy controls, concomitant with their immunoblotting results (Tiwari et al., 2015). Furthermore, they showed an increase in CSPalpha staining in the neuropil of AD cerebellar cortex compared to control. The immunoblotting analysis shown in section 3.4.5 suggests that CSPalpha expression could be altered in the BA9 region of AD brain. Hence, to examine this further, the distribution and localisation of CSPalpha was next studied in BA9.

Paraffin-embedded sections of BA9 from five neuropathologically diagnosed severe AD (Braak V-VI) and six control (Braak 0-II) brains (Chapter 2, Section 2.3, Table 2.2) were immunolabelled with an antibody against CSPalpha. Strikingly, in these sections immunolabelled for CSPalpha and counterstained with haematoxylin to identify cellular nuclei, a previously unreported aggregate-like accumulation of abnormal CSPalpha staining was observed (Fig 3.7a-c). These accumulations had a round/oval profile and were distinct from the much smaller punctate staining in the neuropil which corresponds to typical synaptic staining patterns for presynaptic CSPalpha. Few to moderate abnormal deposits of CSPalpha were identified in 3/6 Braak stage 0-II cases (Fig 3.7a) and were more frequently observed in all five Braak V-VI AD brains (Fig 3.7b). Interestingly, only 1/3 Braak stage 0-II cases with CSPalpha deposits showed a neuropathological diagnosis of mild age-related alterations, unlike the other two cases which had no prior brain changes. It was not possible, however, to qualitatively visualise a change in CSPalpha protein levels even after replication due

to the varied DAB staining intensity. Additionally, background staining was only evident within the gray matter with reduced CSPalpha immunoreactivity in WM tracts, where fewer synaptic terminals are found, yet some ‘aggregate-like’ deposits of CSPalpha were also evident in the WM regions of BA9 brain (Fig 3.7c). No CSPalpha positivity was observed in a negative control section where no primary antibody was applied (Fig 3.7d).

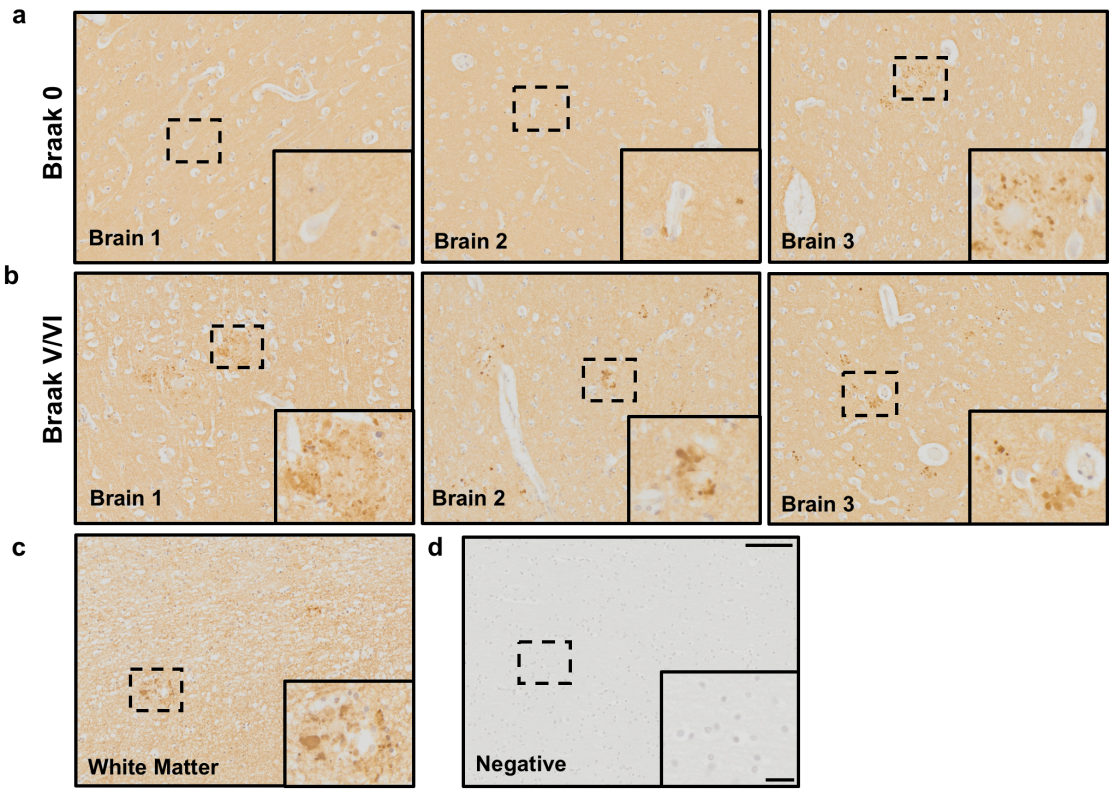

Figure 3.7. Accumulations of CSPalpha protein in BA9 AD brain.

Representative images from fixed post-mortem human BA9 sections from age-matched **a)** Braak 0-II [n=6] and **b)** severe AD (Braak V-VI) [n=5] cases probed with an anti-CSPalpha antibody. Lower magnification images (10x) and higher magnification (40x) insets from the same field of view (*dashed box*). Aberrant labelling of CSPalpha deposits is shown alongside a background of punctate synaptic CSPalpha labelling using the CSPalpha antibody (AB1576) (*brown*). Nuclei were counterstained using haematoxylin (*blue*). **c)** Representative image of WM from an AD Braak VI brain which showed less prominent CSPalpha labelling. **d)** Negative control incubated with no primary antibody confirms the specificity of labelling. Scale bars are 100 μm (low magnification image) and 20 μm (high magnification inset).

Dr. Istvan Bodi (King's College London), a neuropathologist blind to the disease state of the tissue, performed a qualitative comparison of CSPalpha signal in these cases. The neuropathology of AD brain sections was confirmed with the presence of halo-like structures that depicted the possible presence of Aβ plaques in proximity to the CSPalpha accumulations (Table 3.2). A qualitative comparison between Braak stage V-VI and Braak stage 0-II brains yielded three main patterns of CSPalpha positivity. Firstly, CSPalpha positivity was found in what appears to be swollen dystrophic dendrites encircling neuritic Aβ plaques, a prominent pathological feature of AD (Benzing et al., 1993; Vickers et al., 2016). in which the amyloid core was not stained by CSPalpha, (Fig 3.7b). Secondly, CSPalpha positivity was found in possible scattered swollen WM axons, particularly in the presence of WM atrophy and thirdly, round granular positivity in the deep cortex, suggestive of degenerating axons. The latter two forms of positivity were most likely not disease specific, unlike the first type of CSPalpha positivity amongst possible neuritic Aβ plaques. This result confirms the presence of abnormal CSPalpha labelling in Braak V-VI AD brain with a possible association with Aβ plaque pathology.

Table 3.2. Qualitative neuropathological characterisation of post-mortme human tissues.

Comparisons between Aβ disease diagnosis and Braak staging with the presence of possible Aβ plaques and CSPalpha deposits in non-demented Braak 0-II [n=6] and end-stage AD Braak V-VI [n=5]. Numbers in parentheses refer to cases from Chapter 2, Section 2.3, Table 2.2.

No.	Braak Stage	Qualitative Neuropathological Assessment	
		Neuritic Plaques Present Yes/No	CSPalpha deposits present Yes/No
1	0	No	No
2	0	No	No
3	0	No	No
4	0	No	No
5	0	Yes	Yes
6	II	No	No
7	V	Yes	Yes
8	V	Yes	Yes
9	V	Yes	Yes
10	V	Yes	Yes
11	VI	Yes	Yes

Immunofluorescence was next used to further visualise amorphous globular deposits of CSPalpha and to confirm the specificity of the antibody for colocalisation studies. A subset of AD brain sections, from the same cases used for immunoblotting, were used; Braak stage 0-II, Braak stage III-IV and Braak stage V-VI [n=5 cases per group] (Chapter 2, Section 2.3, Table 2.1). A specific alexa fluor 488 conjugated secondary antibody was used to detect bound anti-CSPalpha (AB1576) antibody. No or sparse CSPalpha accumulations were identified in Braak 0-II tissue, with frequently diffuse or clustered deposits observed in Braak stages III-IV and V-VI cases (Fig 3.8a, b). This is the first study of its kind to visualise CSPalpha expression in AD using immunofluorescence and this work replicated the novel finding of CSPalpha accumulations observed using DAB staining. These results suggest the possibility that CSPalpha deposition may increase as Braak stage severity increases, although quantitative stereological analysis along with greater sample numbers would be required to confirm this.

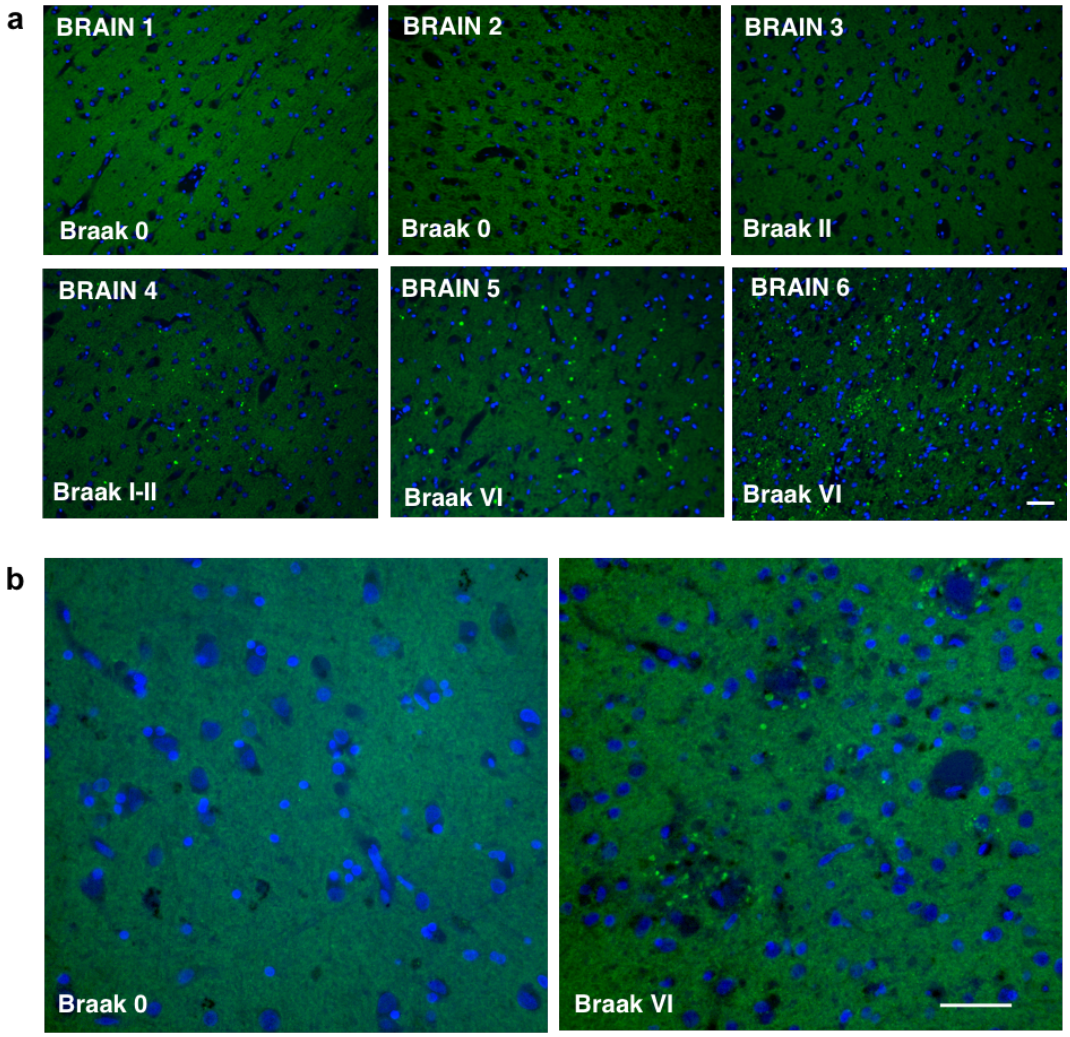

Figure 3.8. Amorphous CSPalpha accumulations increase with AD severity.

a) Representative epi-fluorescent images of 7 µm thick post-mortem human BA9 brain sections from Braak stages 0-VI immunolabelled using an antibody against CSPalpha (*green*) and DAPI (*blue*). [n=5 cases per group]. Magnification 20x. Scale bar 50 µm **b)** Representative images taken using the Nikon Eclipse Ti-E 3 camera inverted microscope of a brain section from Braak stage 0 and VI immunolabelled using an antibody against CSPalpha (*green*) and DAPI (*blue*). Magnification 40x. Scale bar 50 µm. Fluorescent spots of CSPalpha immunoreactivity reveal novel CSPalpha accumulations within the gray matter. Background intensity is indicative of synaptic staining.

Having identified novel CSPalpha deposits in BA9 AD brain, it was important to establish if these previously unreported bulbous CSPalpha accumulations were also present in other regions, such as the hippocampus, a region primarily and severely affected in AD (Braak and Braak, 1991) and the cerebellum, a region which is resistant to such pathologies (Larner, 1997). Tiwari and colleagues (2015) who have previously investigated the expression pattern of CSPalpha within these regions, did not find any evidence of these amorphous CSPalpha structures (Tiwari et al., 2015).

Hippocampus and cerebellum from Braak stage 0-II cases with no prior neuropathological diagnosis and severe AD Braak stage VI cases that showed frequent deposits of CSPalpha in BA9 were used for this regional comparison [n=3 for each group]. Immunolabelling with the anti-CSPalpha antibody showed a similar pattern of CSPalpha staining in the grey matter neuropil across each region (Fig 3.9). Abnormal accumulations of CSPalpha were found in all three brain areas in AD Braak VI brains compared to only presynaptically localised CSPalpha protein found in Braak 0-II brains (Fig 3.9). Sparsely populated and clusters of CSPalpha-positive deposits were apparent in BA9, hippocampal and cerebellar brain regions. Furthermore, CSPalpha clusters had a negatively stained internal core (Fig 3.9, Hippocampus, Brain 3), further suggesting the possibility that these spaces may contain the core of a fibrillar amyloid plaque. Comparatively, in the cerebellum, CSPalpha structures were fewer, more densely clustered and covered a larger spatial area, suggesting the existence of more diffuse amyloid deposits, more commonly found within this region (Joachim et al., 1989). Background CSPalpha staining intensity varied amongst the regions, however this may be reflected by tissue quality, preservation and imaging plane.

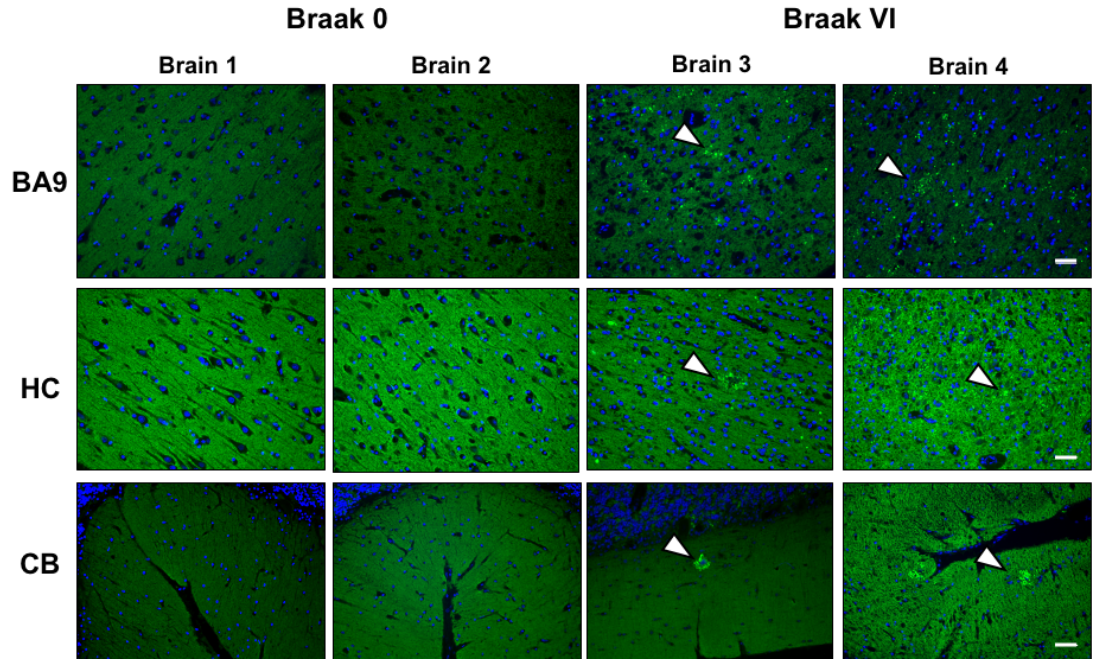

Figure 3.9. Globular CSPalpha positive structures identified in several regions in AD brain.

Representative images of post-mortem human BA9, hippocampus (HC) and cerebellum (CB) from AD (Brains 3 and 4, Braak stage VI) and Braak 0-II (control) brain sections (Brains 1 and 2) immunolabelled using an antibody against CSPalpha (*green*). DAPI was used to stain nuclei (*blue*). *White arrow heads* are indicative of CSPalpha accumulations. Magnification 20x. Scale bar 50 μm. [n=3 for each group].

3.4.7 Aberrant localisation of CSPalpha in proximity to amyloid deposits in AD brain

As previously described by neuropathological examination and immunofluorescence characterisation, the pattern of immunolabelling was indicative of abnormal CSPalpha deposits surrounding and physically associated with possible Aβ plaque pathology. To confirm this idea, co-immunofluorescence labelling was performed with antibodies against CSPalpha and β-amyloid (6E10). A halo of immunoreactivity of CSPalpha accumulations was identified surrounding 6E10-positive Aβ deposits which did not infiltrate the plaque core (Fig 3.10a). To look at these undefined aggregates more closely in relation to Aβ pathology, spinning disk confocal microscopy was used. From initial observations, and compared to normal background CSPalpha synaptic puncta staining, these deposits were found to be relatively large in size as observed using maximum intensity projection images (Fig 3.10a). The association of CSPalpha with Aβ plaques suggests that changes in CSPalpha localisation in AD brain may be linked to the progressive accumulation of Aβ pathology and its toxicity to surrounding synapses.

It was next important to determine if CSPalpha also associates with abnormal tau changes in AD. CSPalpha is involved in physiological tau release mechanisms and can indirectly bind to tau via Hsc70 as shown in primary rat cortical neurons (Fontaine et al., 2016; Deng et al., 2017). Consecutive sections from Braak VI and Braak 0-II brain were immunolabelled for CSPalpha and hyperphosphorylated tau (AT8 phospho-Ser202/Thr205). A large abundance of AT8-positive labelling was observed in late-stage AD brains in the form of neuropil threads, pre-tangles, NFTs and neuritic dystrophies (Fig 3.10b). However, most bulbous CSPalpha accumulations were distant from tau pathology with only a few AT8-postive dystrophic neurites infrequently colocalising with CSPalpha immunoreactivity (Fig 3.10b). This suggests

that there is a limited extent of CSPalpha association with hyperphosphorylated tau in severe, late-stage AD brain.

Studies in both humans and transgenic mouse models have reported the presence of dystrophic axonal swellings in proximity to amyloid plaques in AD, which may explain the abnormal localisation of CSPalpha deposits (Knowles et al., 1999; Le et al., 2001; D'Amore et al., 2003; Spires et al., 2005; Adalbert et al., 2009; Coma et al., 2010; DaRocha-Souto et al., 2012; Perez-Nievas et al., 2013). Hence, co-immunofluorescence was performed using the anti-neurofilament marker, SMI312, specific for highly phosphorylated axonal epitopes on neurofilaments. It can also distinctly visualise aberrantly sprouting axons with their apparent bulb-like swellings and curved axonal features in the surrounding areas of neuritic plaques. Characteristic CSPalpha protein structures were observed around Aβ deposits that rarely overlapped with SMI312-positive immunoreactive interaxonal enlargements enclosed within the same area (Fig 3.10c). This preliminary result suggests that only some CSPalpha accumulations may localise within dysfunctional axonal structures encircling Aβ deposits in AD brain.

Neuroinflammation is another characteristic feature of AD with the presence of astrogliosis and activated microglia found surrounding Aβ deposits (Mandybur and Chuirazzi, 1990; Sofroniew and Vinters, 2010). To determine if CSPalpha deposits may be glial in origin, AD brain was co-labelled with antibodies against CSPalpha and either glial cell fibrillary acidic protein (GFAP), a marker of activated astrocytes or ionised calcium binding adapter molecule 1 (Iba-1), a microglial marker. Numerous GFAP-positive astrocytes and some Iba-1-positive microglia were identified surrounding sites of amyloid deposition (Fig 3.10d, e). However, hypertrophic astrocytes did not associate with the majority of CSPalpha accumulations (Fig 3.10e). Similarly, immunoreactive microglia, whose processes suggest a phagocytic

morphology, were found adjacent to some CSPalpha deposits and encapsulated around amyloid plaques but there was little evidence to suggest that CSPalpha deposits were microglial in origin (Fig 3.10d). Thus, the accrual of CSPalpha may be associated with some but not all neuroinflammatory changes induced by either astrocytic or microglial activity.

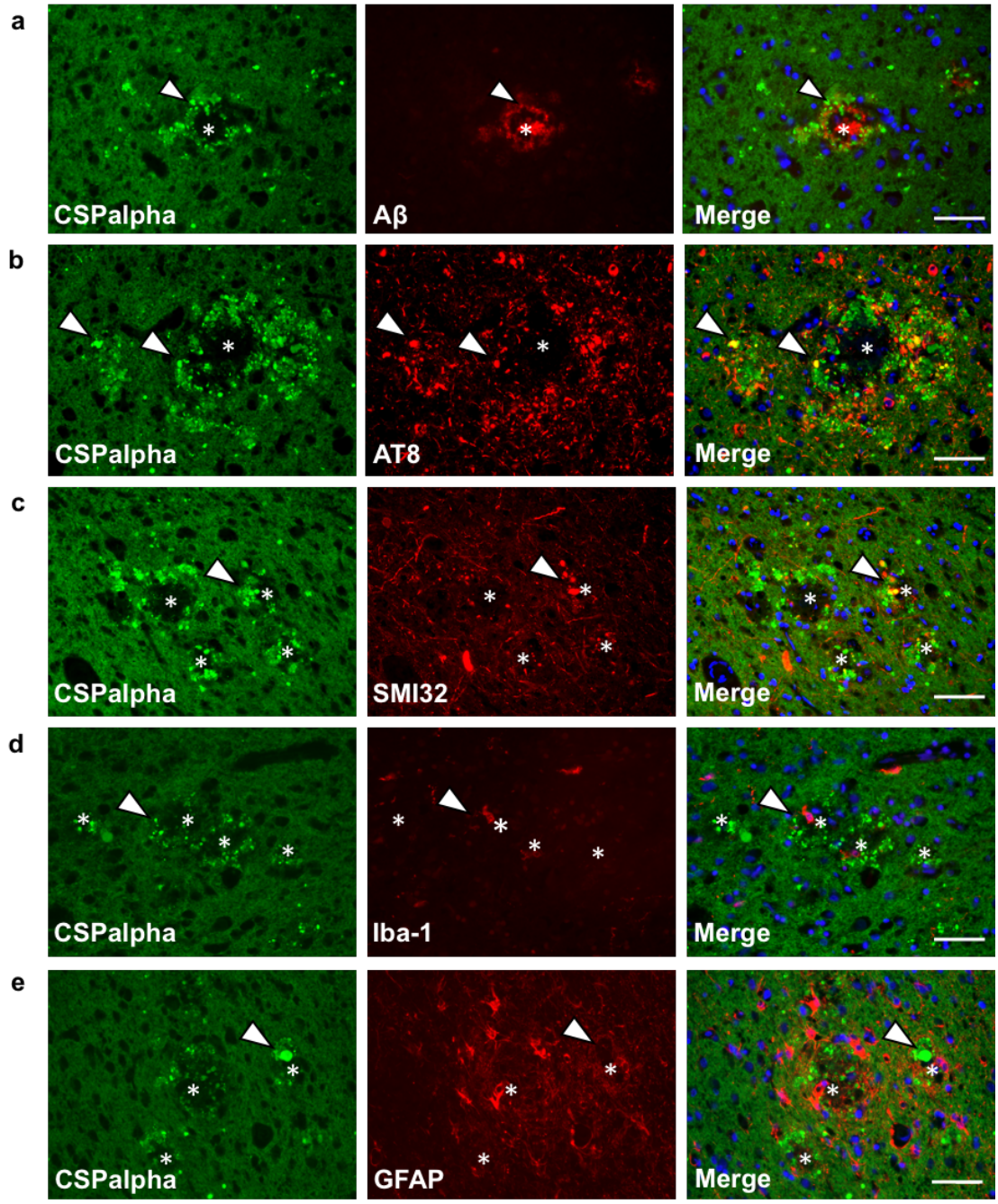
a
CSPalpha
Aβ
Merge
b
CSPalpha
AT8
Merge
c
CSPalpha
SMI32
Merge
d
CSPalpha
Iba-1
Merge
e
CSPalpha
GFAP
Merge

Figure 3.10. CSPalpha accumulations associate with Aβ plaques but do not fully colocalize with other AD associated pathology.

Representative images of sections from a Braak VI post-mortem human BA9 AD brain, with consecutive sections co-labelled with antibodies against CSPalpha (*green*) and **a)** Aβ (6E10, *red*), **b)** AT8 [tau phosphorylated at Ser202/Thr205] (*red*), **c)** SMI312 [neurofilament/ dystrophic neurites] (*red*), **d)** Iba-1 [microglia] (*red*) and **e)** GFAP [activated astrocytes] (*red*). Merge of images shown together with DAPI staining (*blue*). CSPalpha immunoreactivity is localised in proximity to amyloid deposits and overlaps with some but not all dystrophic neurites, AT8-positive tau and glial cell positivity (*white arrowheads*). *Asterisks* indicative of plaque core. Consistent patterns of presynaptic CSPalpha puncta are observed as background staining. Magnification 40x. Scale bar 50 μm. [n=3 Braak VI brains].

3.4.8 Characterisation of CSPalpha accumulations in proximity to Aβ deposits

To better visualise the close spatial relationship of irregular CSPalpha accumulations in proximity to both diffuse and neuritic cored Aβ deposits, sections from five BA9 Braak VI AD cases were examined using high resolution spinning disk confocal imaging (Fig 3.11a, b). Qualitative analysis revealed a number of Aβ deposits associated with CSPalpha (Fig 3.11a, b). No accumulations were found in areas distant from Aβ plaques, and not every plaque had an accumulation of CSPalpha. CSPalpha accumulations were associated with both diffuse (low staining intensity and diffuse spread of Aβ deposition) and neuritic cored plaques (consisting of a higher staining intensity and a neuritic core). CSPalpha accumulations around neuritic cored plaques were more clustered and annulus compared to the sparse accumulation around diffuse plaques, which often lack neuritic components (Dickson, 1997). These

deposits were giant-sized in comparison to neuronal processes in the adjacent neuropil areas.

Quantitative volumetric measurement of CSPalpha accumulations were conducted and showed that out of a total 681 CSPalpha accumulations measured, the predominant size of these structures ranged between 10 and 50 μm^3 (56.4%, mean size 24.8 ± 0.57 μm^3), followed by those in the region of 50 to 100 μm^3 (22.6%, mean size 71.2 ± 1.16 μm^3). Only 14.8% (mean size 164 ± 5.94 μm^3) were over 100 μm^3. CSPalpha accumulations appeared to vary across both neuritic cored [n= 440 objects, n= 101 plaques, maximum object volume 328 μm^3, median object volume 30.9 μm^3] and diffuse plaques [n= 241 objects n= 54 plaques, maximum object volume 346 μm^3, median object volume 39.4 μm^3] (Fig 3.11c). These results are in-line with similar findings reported by Sachez-Varo and colleagues (2012), where they found comparable sizes of dystrophic neurites using transmission electron microscopy in 4-5-month-old APP/PS1 mouse model (Sanchez-Varo et al., 2012). They also found that non-dystrophic neurites have an average size of 1.42 ± 0.77 μm^2 and only 1% of dystrophic neurites were under 5 μm^2. Previous reports have suggested that the appropriate cut off for dystrophic neurites as >2.5 μm in diameter (Spires et al., 2005; Sanchez-Varo et al., 2012; Jackson et al., 2016; Serrano-Pozo et al., 2016) and so this was used as the threshold for the current analysis. 3D equatorial diameter (diameter of sphere with same volume as measured object) was measured using the following equation (Nikon Elements, Nikon), from which the volume was determined as a minimum threshold of 8 μm^3:

$$Equatorial\ Diameter_{3D} = \left(\frac{6\ x\ Volume}{\pi}\right)^{\frac{1}{3}}$$

To further map the localisation of CSPalpha at a greater depth and with better optical sectioning within the context of Aβ deposits, images were also obtained from an iSIM microscope (Fig. 3.12) where granular and/or globular CSPalpha immunoreactivity appeared surrounding larger amyloid deposits (Fig 3.12 a-c). It would also be interesting to see whether the size of Aβ plaques correlates to the size and/or number of CSPalpha deposits, but this would require a larger sample size.

a Neuritic Cored Plaque

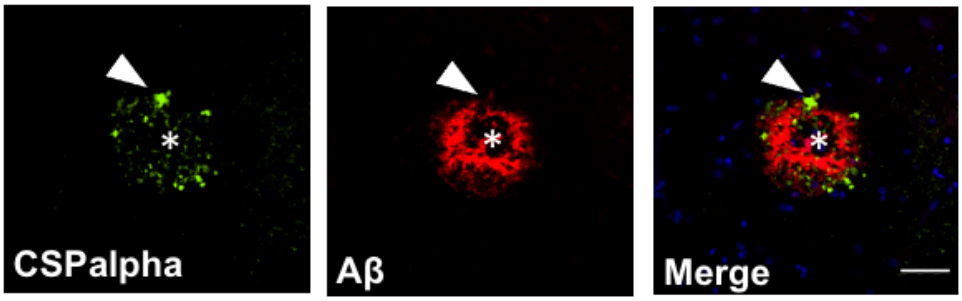

b Diffuse Plaque

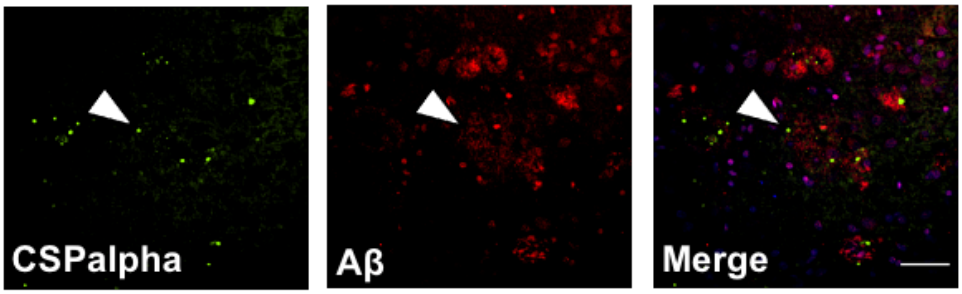

c

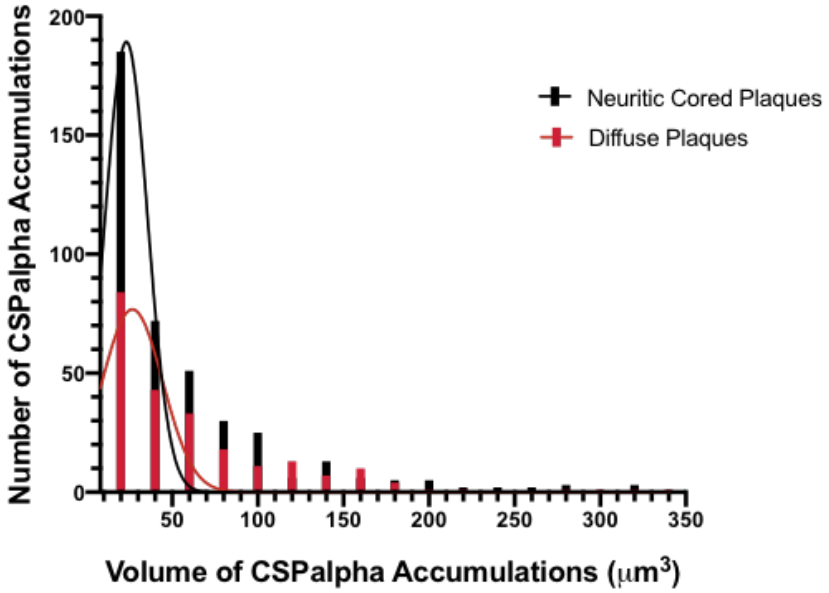

Figure 3.11. CSPalpha accumulations are found in association with both neuritic cored and diffuse Aβ plaques.

Representative spinning disk confocal images (projection of a stack of 10 optical sections) reveal CSPalpha accumulations (*green*) in Braak VI post-mortem BA9 human AD brain that are localised within or surrounding Aβ-positive **a)** neuritic cored and **b)** diffuse plaques (*red*). Nuclei are stained with DAPI (*blue*). Synaptic neuropil staining was subtracted from measurements. Magnification 20x. Scale bar 25 μm. *White arrow heads*– CSPalpha accumulations and *asterisks* - plaque core. **c)** Histogram showing quantification of the number of CSPalpha accumulations and their volumetric measurement plotted as data from individual plaques for both neuritic cored [n = 101] and diffuse plaques [n = 54]. [n=5 brains].

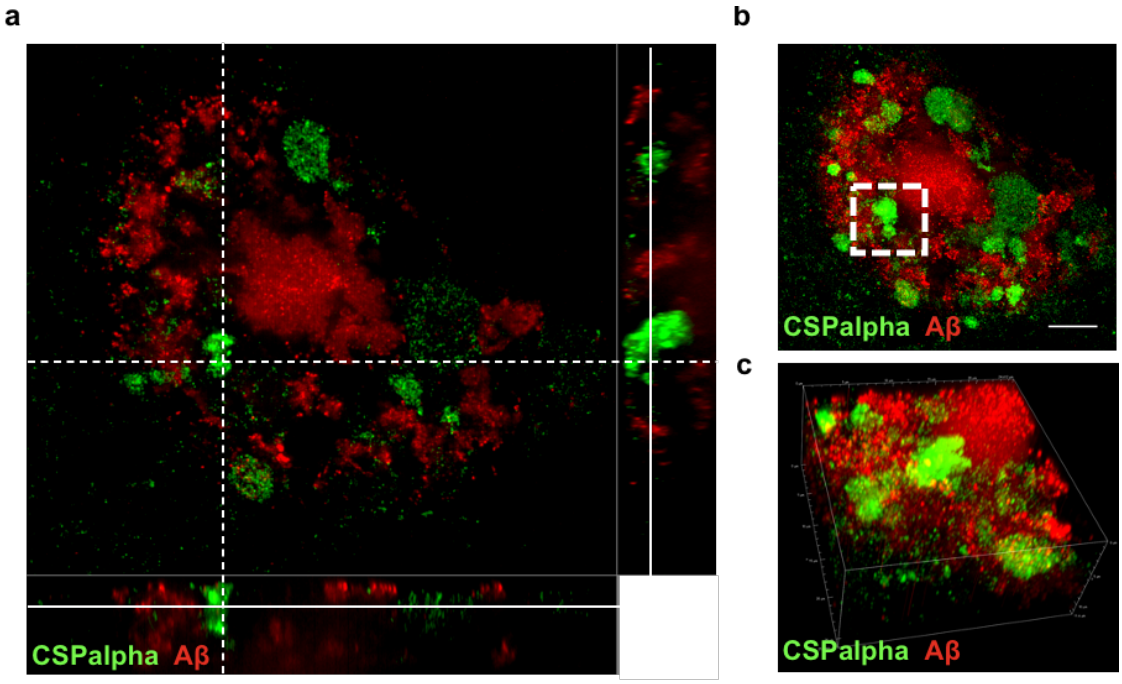

Figure 3.12. Super resolution microscopy showing Aβ plaque-associated CSPalpha accumulations.

a) Representative 25 x 26 µm iSIM image section showing zoomed-in and orthogonal views of the CSPalpha aggregates in association with a large neuritic cored Aβ plaque. White segmented line intersects a CSPalpha aggregate. **b)** Maximum intensity projection of 58 optical sections of the same orthogonal field of view. White segmented box shows the same CSPalpha aggregate. Scale bar 10 µm. **c)** Volumetric 3D maximum intensity projection images of the field with zoomed view of an isolated CSPalpha aggregate. Magnification 100x. Volume of box: 25 µm x 26 µm x 11 µm.

3.4.9 CSPalpha accumulations localise with synaptic markers in proximity to amyloid plaques

Previous studies have reported the disruption and disorganisation of synapses in AD whereby presynaptic proteins have been found to accumulate within degenerating and dystrophic presynaptic terminals, termed 'presynaptic dystrophies' which are incorporated at the earliest stages of Aβ plaque formation (Brion et al., 1991; Masliah et al., 1991, 1993; Clinton et al., 1994; Bittner et al., 2010; Sanchez-Varo et al., 2012; Kandalepas et al., 2013; Hadley et al., 2015; Gomez-Arboledas et al., 2018). These presynaptic structures are similar in shape and size to the plaque associated CSPalpha deposits found here. As such, it was important to explore the possibility that CSPalpha, like other synaptic markers accumulate in the same locality.

Synaptophysin, a presynaptic protein, is present on CSPalpha-bound synaptic vesicles (Takamori et al., 2006; Wilhelm et al., 2014) and so it is possible that these proteins co-localise within the presynaptic terminal. CSPalpha and synaptophysin were immunolabelled in Braak VI BA9 post-mortem brain sections and showed colocalization of presynaptic neuropil immunoreactive for both proteins. In AD brains, reduced labelling intensity of CSPalpha and synaptophysin were found within and around the central core of Aβ plaques, as previously reported (Fig 3.13a) (Koffie et al., 2012). Clustered deposits of CSPalpha were evident in a halo-like shape, suggesting the presence of a neuritic cored plaque (Fig 3.13a). Similarly, to previously published findings, a characteristic punctate lobular profile of synaptophysin was observed that decorated the periphery of a central hollowed core, which was absent in control brains (Kandalepas et al., 2013; Hadley et al., 2015; Sadleir et al., 2016; Ye et al., 2017; Gomez-Arboledas et al., 2018; Ovsepian et al., 2019). Most synaptophysin-positive accumulations appeared to be closer to the plaque centre, unlike CSPalpha which appeared to cover a larger spatial area around the periphery.

Interestingly, only a small number of CSPalpha accumulations appeared to colocalise with synaptophysin deposits within BA9 AD brain (3.13a).

Brain sections were next co-labelled using antibodies against CSPalpha and SNAP-25, a SNARE protein known to be a downstream interacting partner of CSPalpha. Interestingly, SNAP-25 has been shown to accumulate, like CSPalpha within the AD brain (Clinton et al., 1994; Hadley et al., 2015). SNAP-25, like CSPalpha labelled the presynaptic neuropil as previously reported (Bereczki et al., 2016). SNAP-25 was also found to accumulate, of which only some associated with CSPalpha deposits surrounding an immuno-positive Aβ halo, similar to the observations for synaptophysin (3.13b).

Hsc70, a cytosolic chaperone protein, has also been shown to interact with CSPalpha as reported previously in the literature (Zhang et al., 2012), and so it was hypothesised that accumulations of CSPalpha may show some immunoreactivity with Hsc70. Co-labelling with antibodies for both target proteins showed some overlap between CSPalpha accumulations and Hsc70 (Fig 3.13c). This is interesting as immunoblotting data suggests that Hsc70 is elevated in end-stage AD compared to early Braak stages (0-II, III-IV) (Chapter 6, Fig 6.1). This elevation in Hsc70 expression has also been shown in post-mortem human AD temporal gyrus compared to controls, 3xTg and 5xFAD mice and Aβ treated neurons (Sharma et al., 2012b; Zhang et al., 2012; Piedrahita et al., 2016; Yang and Tohda, 2018). Although Hsc70 and CSPalpha are localised to separate neuronal compartments, Hsc70 may be mislocalised, forming a complex with CSPalpha accumulations. However, it is still unknown whether their interaction at the molecular level remains intact in AD.

Taken together, this data confirms the localisation of CSPalpha accumulations in the vicinity of Aβ plaques with only few localised with presynaptic proteins and putative interacting proteins. This suggests that there may be a distinct population of amorphopus CSPalpha lesions in AD that may form their own presynaptic dystrophies and that do not contain known synaptic or interacting proteins or could be extracellular to the presynaptic terminal and do not resemble a dystrophic neurite. This also implies that the mechanisms by which CSPalpha accumulates or where this deposition may occur is different from that of other synaptic proteins that accumulate in AD.

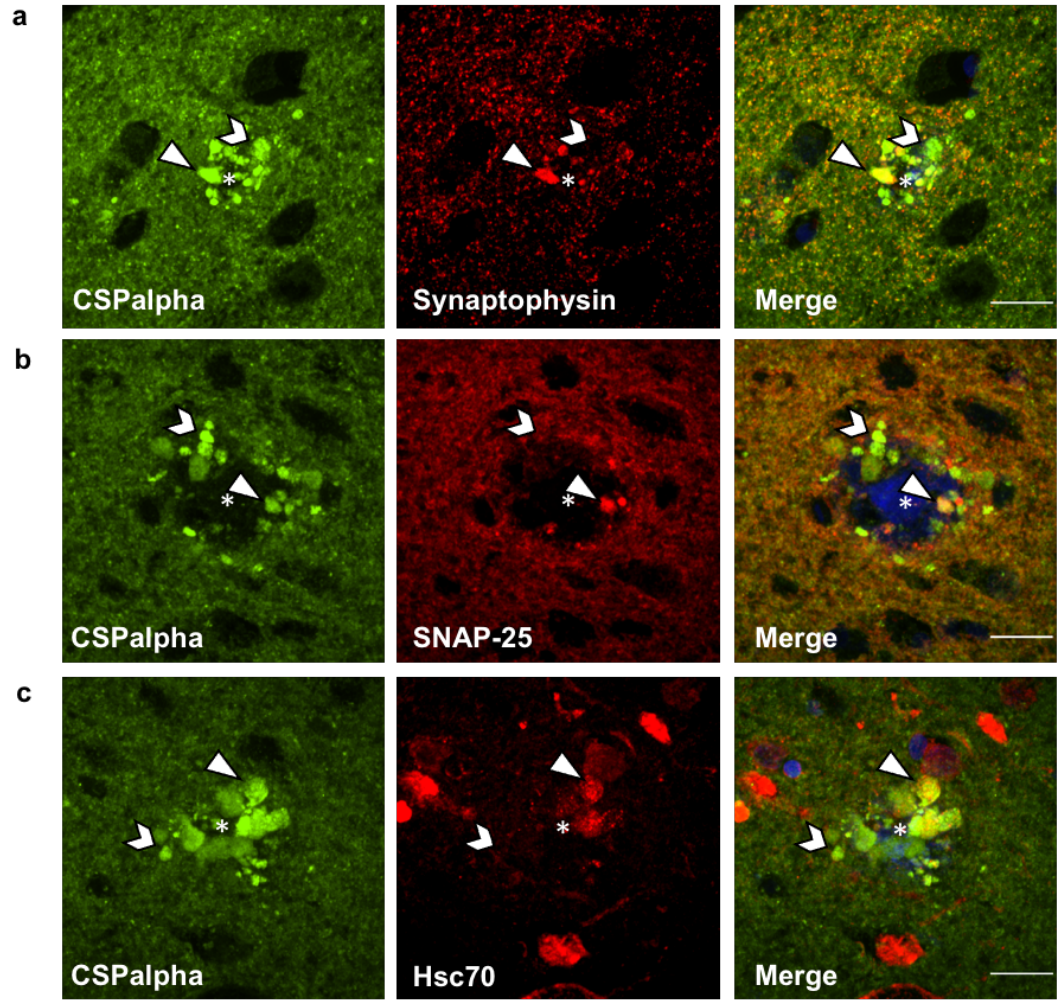

Figure 3.13. Few CSPalpha accumulations colocalize with presynaptic terminal structures in proximity to amyloid plaques.

Representative images of sections from BA9 brain sections of Braak stage VI human AD brains co-labelled with antibodies against **a)** CSPalpha (*green*) and synaptophysin (*red*), or **b)** SNAP-25 (*red*), **c)** Hsc-70 (*red*). DAPI (*blue*) was used to stain nuclei. CSPalpha immunoreactivity displays a plaque-like staining pattern that overlaps with some synaptophysin-positive presynaptic structures, likely dystrophic terminals, as well as SNAP-25, and Hsc-70. *White arrowheads*– CSPalpha accumulations and *asterisks* - plaque core. Magnification 60x. Scale bar 20 µm.

3.4.10 Few CSPalpha accumulations colocalize with presynaptic terminal structures in proximity to Aβ plaques using Array Tomography

While traditional imaging techniques which include confocal and multiphoton light microscopy have been used to study synaptic structures, the drawback is that synapses are too small to be imaged effectively, especially with poor z-resolution (~1000 nm). Array tomography (AT) is a high-resolution technique (Micheva et al., 2010), that overcomes the difficulties of axial, or z-resolution by imaging ribbons of 70 nm thin serial brain sections, providing not only better optical sectioning but greater visualisation of the inaccessible synaptic architecture. AT has been optimized for use in post-mortem human tissue (Koffie et al., 2012; Kay et al., 2013), and previous reports have shown that there is a loss of synapses in AD compared to controls, a loss that is intensified in regions closest to the plaque halo <35 μm (Koffie et al., 2009, 2012; Jackson et al., 2019b). However, accumulations of synaptic proteins, in particular have never before been studied using this technique.

AT was used here to investigate the presynaptic localisation of CSPalpha protein in late-stage AD and to determine whether presynaptic alterations can result in the accumulation of CSPalpha in proximity to Aβ plaques. Blocks of post-mortem human BA9 was obtained from non-demented controls Braak 0-II [n=8] and from severe late-stage AD Braak VI [n=10] from the Edinburgh Brain Brank.

Age, PMD and sex were examined to determine whether they might have an effect on the data generated in this study (Table 3.3). For age, following D'Agostino & Pearson normality testing, data was analysed using non-parametric two-tailed Mann Whitney U test which showed a statistically significant difference between control and AD groups ($U = 2.5$, $p=0.0002$). For PMD following D'Agostino & Pearson normality testing, data was analysed using parametric two-tailed t-test which showed a statistically significant difference between control and AD groups ($t = 2.149$, $p=0.047$).

There was also a marked underrepresentation of samples from females in the Braak stage 0-II group which after Chi-squared testing showed a nonsignificant trend towards sex differences between the groups ($\chi^2 = 2.813$, p=0.094). These variations may have an overall effect on the outcome of the results (Table 3.3).

Table 3.3. Summary of AD and controls brains used in the AT study.

Table shows the number of cases of each Braak stage group, the percentage of cases that were female, the average age at death and PMD (mean ± SEM).

Braak Stage	Number of Cases	Female (%)	Age (Years) Mean ± SEM	PMD (Hours) Mean ± SEM
0-II	8	12.5	49.9 ± 5.2	86.4 ± 8.1
VI	10	50	82.6 ± 3.4	65.3 ± 5.9

Briefly, as described previously in Chapter 2, Section 2.10, brain sections were probed with anti-CSPalpha, anti-synaptophysin and anti-Aβ antibodies in a two-day protocol. Array images were taken from consecutive serial sections and reconstructed to produce 3D volume images of tissue. Stacked images were segmented to include structures that were present in two or more images within each stack and only within the neuropil areas (Fig 3.14a, b). Images were then thresholded into two groups: 1) smaller presynaptic puncta (object size 3-400/500) and 2) larger presynaptic protein accumulations (object size 400/500+) before analysis. Labelling on different days were normalised using a positive control for the presence of Aβ plaques.

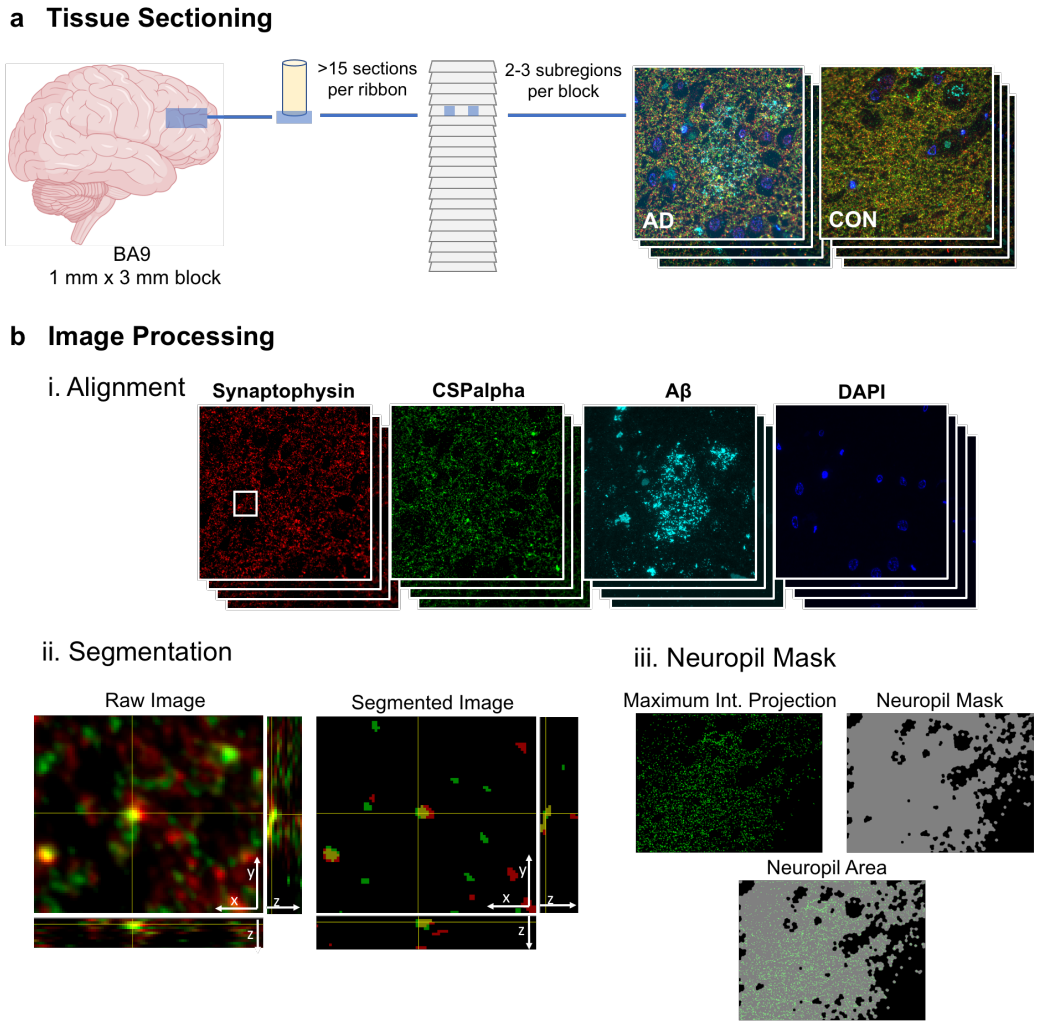

Figure 3.14. Array tomography study design.

a) Sections from control [n=8] and severe BA9 AD brains [n=10] were processed and embedded within LR white resin blocks. From each block, a ribbon consisting of >15 70nm thin sections were cut. 2-3 subregions were imaged from each ribbon using antibodies probed against CSPalpha (*green*), synaptophysin (*red*) and Aβ (*cyan*). Nuclei were labelled with DAPI (*blue*). Created with Biorender.com **b)** Images were processed by firstly combining consecutive images of each channel into stacks. **i)** Synaptophysin was used as a reference channel for alignment of consecutive sections which were applied across all other channels (*white square*). **ii)** Images were then segmented using an algorithm removing single objects and retaining connected

components between two or more sections, producing 3D objects that can be filtered by size. Representative orthogonal views of raw (*left*) and segmented (*right*) 70nm thin section shown. **iii)** Finally, a maximum intensity projection of synaptic localisation was used to calculate the neuropil area. Representative image of 70 nm thin section for CSPalpha as a maximum intensity projection, neuropil mask and area. Adapted from (Colom-Cadena et al., 2017).

The results show diffuse CSPalpha protein immunoreactivity detected in both control and AD sections (Fig 3.15a, b). On some occasions, non-specific immunoreactivity was identified in the same channel as CSPalpha in cell nuclei. A consistent density of presynapses (number of synaptophysin puncta/mm^3) was found in BA9 Braak VI ($7.4x10^8 \pm 6.4x10^7$) sections compared to controls ($7.3x10^8 \pm 4.2x10^7$), suggesting that the global synaptic level remained the same within this region (Fig 3.16a). Similar differences were found for CSPalpha protein (Braak VI, $8.1x10^8 \pm 8.3x10^7$ and controls, $7.5x10^8 \pm 7.6x10^7$), suggesting that the amount of CSPalpha protein relates to the measurement of synaptic content (Fig 3.16b). Unlike previous reports that show an increasing synapse loss in proximity to Aβ plaques (Koffie et al., 2012), a statistically significant characteristic reduction of CSPalpha protein was not found. This result is probably due to fact that both neuritic cored and diffuse plaques were included within these measurements, in which diffuse plaques do not accentuate synapse loss within their vicinity unlike neuritic cored plaques that have greater toxicity (Masliah et al., 1990).

AT showed that CSPalpha overlaps with synaptophysin positive puncta staining, indicative of presynaptic terminals within the neuropil. There was no statistically significant difference in CSPalpha protein colocalization with presynapses in AD brains (21.6% ± 2.3) compared to controls (25.5% ± 4.3) ($p=0.158$) (Fig 3.16c). This result was also confirmed with synaptophysin positive puncta colocalising with

CSPalpha puncta in Braak VI (28.1% ± 1.5) and controls (33% ± 2.6) which show similar values (Data not shown). Although CSPalpha is a presynaptic protein, complete synaptic colocalization was not observed. This may be a technical limitation due to the experimental protocol whereby double labelling of both proteins may not be as efficient as single labelling for the same presynaptic terminal. Additionally, this is a limit of detection of AT whereby not enough synapses are captured due to resin fixation and only synapses with a large abundance of CSPalpha are visualised. Better labelling of tissues may hence provide tighter values and reduced inter-patient variability. However, these synapses have been thresholded and so within individual synapses, CSPalpha levels in general may well be lower.

It has previously been shown that synapses co-localise with Aβ, most likely the oligomeric forms, near Aβ plaques (Koffie et al., 2012; Pickett et al., 2016; Jackson et al., 2019b). Presynapses containing CSPalpha that also colocalised with Aβ together at the synapse were investigated. A statistically significant effect was found for the percentage of synaptophysin-positive synapses overlapping with CSPalpha and Aβ in AD (0.2% ± 0.08) and controls (0.02% ± 0.02) due to Aβ plaque status and not disease type ($t=2.396$, $p=0.02$) (Fig 3.16d). This suggests in brains where Aβ plaques are present, Aβ is found within CSPalpha containing presynapses and may have a role in the mechanisms that ultimately lead to the dysfunction and eventual loss of the presynaptic compartment.

In the same cohort of tissues, several accumulations of CSPalpha were observed in proximity to Aβ plaques (Fig 3.15a-c, g) in late-stage AD brains ($2.6x10^8 \pm 8.1x10^7$) compared to control ($7.3x10^7 \pm 4.1x10^7$) (Fig 3.17b). Interestingly, there was evidence of accumulations of synaptophysin, possibly linked to presynaptic dystrophies or degenerating synapses, density levels of which were found to be higher due to Aβ plaque status in AD and control brains (Braak VI, $8.3x10^7 \pm 8.6x10^6$ and controls,

$6.9x10^{7}$ ± $1.8x10^{7}$) (t=2.842, p=0.0046) (Fig 3.17a). This is consistent with previous immunohistochemical findings of both abnormal CSPalpha and synaptophysin-positive accumulations in post-mortem human tissue. Globular CSPalpha structures were found associated with both neuritic cored and diffuse Aβ plaques (Fig 3.15c, g). Of the CSPalpha structures analysed, 12.2% ± 4.0 colocalised with presynaptic dystrophies in AD compared to control (2.6% ± 1.7) (Plaque status effect; t=5.362, p=0.0004) (Fig 3.17c). This suggests that dystrophies located in proximity to Aβ plaques can be CSPalpha positive and/or synaptophysin negative but this does not exclude the possibility of extracellular accumulation of CSPalpha (Fig 3.15d, e, h and i). Interestingly, CSPalpha deposits with synaptophysin-positive structures also colocalised with Aβ in AD and control brains (Braak VI, 3.7% ± 1.9 and controls, 0.3% ± 0.3) (Plaque status effect; t=2.053, p=0.0472) (Fig 3.17d, 3.15f, j).

The distance of these accumulations from the Aβ plaque centre was next measured. Distances were referenced to the 30-40 μm bin, furthest away from the plaque where it would not be expected for deposits to be present (representative of a non-plaque area). The 40-50 μm bin was removed from analysis due to focal issues when imaging at the field edge. Greater amounts of CSPalpha accumulations were found to be highly localised <10 μm distance (t=2.701, p=0.009) and between 10-20 μm (t=3.24, p=0.002) from the Aβ plaque core (Fig 3.18a), unlike synaptophysin-positive presynaptic dystrophies found only <10 μm from the plaque core (t=4.152, p=0.0001) (Fig 3.18b). This confirms that CSPalpha accumulations are found at a further distance from the plaque core in comparison to synaptophysin-positive presynaptic dystrophies. The localisation of both structures aligns with the gradual decline of Aβ peptide from the Aβ plaque as distance increases. Significantly, most Aβ was found in areas <10 μm distance (t=12.713, $p<2x10^{-16}$) and between 10-20 μm (t=7.597, $p=3.49x10^{-10}$) from the plaque core (Fig 3.18c). There was also a statistically significant effect due to age (t=4.016, p=0.006) and an effect due to PMD as shown

by a statistical trend (t=-2.202, p=0.07) within the AD cohort. This further suggests that the density of Aβ is highest in the region closest to the plaque centre, where increased amounts of both CSPalpha and synaptophysin positive accumulations are found. However, as the density of Aβ declines further than the 10 μm bin, only CSPalpha accumulations are present. This alludes to the possibility for different mechanisms by which abnormal synaptic structures can become deposited in proximity to the Aβ plaque.

The limitation in this analysis however was determining a manual threshold for synaptic puncta and synaptic accumulations. There was a cut off between obtaining the maximum number of synaptic puncta and selecting a threshold that would only capture single accumulations of proteins. There is a possibility that at lower thresholds, accumulations became fragmented into smaller puncta which were in fact used for puncta analysis and so may have affected the overall result. To resolve this, a better automated method would be required to select for single synaptic puncta sizes and determine the cut off for whole presynaptic accumulations. Furthermore, there is a potential sampling bias, due to the low sample numbers of cases and hence limited number of areas within which plaques were located for analysis across each section. To improve this, further sections would be required to power this analysis and reduce the limitation of plaque burden.

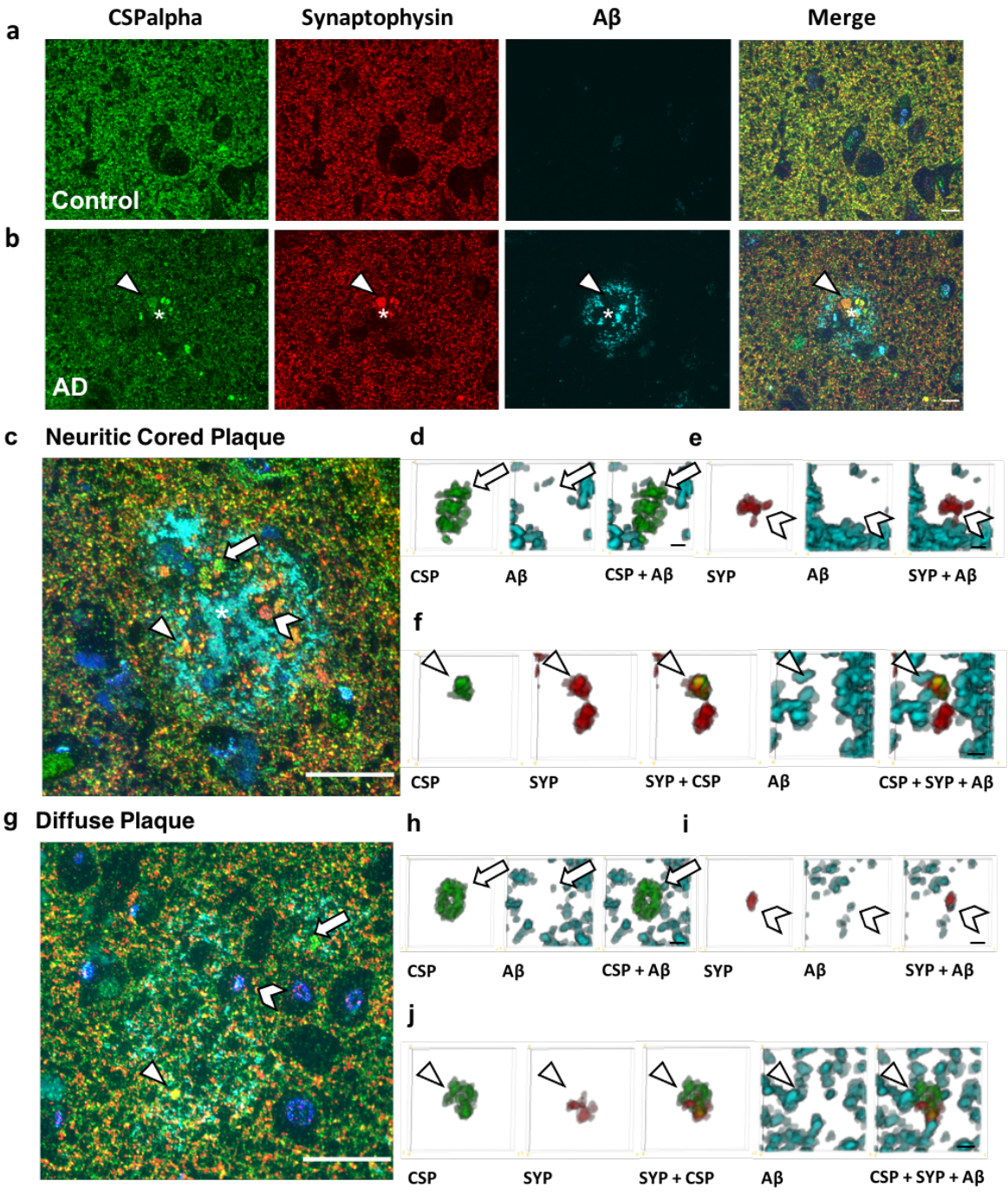
a
CSPalpha
Synaptophysin
Aβ
Merge
Control
b
AD
c
Neuritic Cored Plaque
d
e
CSP
Aβ
CSP + Aβ
SYP
Aβ
SYP + Aβ
f
CSP
SYP
SYP + CSP
Aβ
CSP + SYP + Aβ
g
Diffuse Plaque
h
i
CSP
Aβ
CSP + Aβ
SYP
Aβ
SYP + Aβ
j
CSP
SYP
SYP + CSP
Aβ
CSP + SYP + Aβ

Figure 3.15. CSPalpha accumulations associate with synaptophysin-positive presynaptic dystrophies at both neuritic cored and diffuse plaques.

Representative array tomography images of human BA9 **a)** control [n=8] and **b)** Braak stage VI AD sections [n=10] co-labelled with antibodies against CSPalpha (*green*), synaptophysin (*red*) and Aβ (*cyan*). Nuclei are stained with DAPI (*blue*). Triangular arrow heads - CSPalpha accumulations. Asterisk' – Aβ plaque core. Magnification 60x. Scale bar 10 µm. **c)** Large representative image of a neuritic cored and **g)** diffuse Aβ plaque with labelling of CSPalpha, synaptophysin, Aβ. Nuclei are stained with DAPI. Magnification 60x. Scale bar 20 µm. *Asterisk'* – Aβ plaque core. **d, h)** Representative 3D reconstructions using Image J volume viewer of a singular amorphous CSPalpha (CSP) deposit alone, Aβ alone and CSP with Aβ (*rectangular arrow heads*), **e, i)** synaptophysin (SYP)-positive presynaptic dystrophy alone, Aβ alone and SYP with Aβ (*chevron arrow heads*) and, **f, j)** colocalization between CSPalpha, SYP-positive presynaptic dystrophy and Aβ (*triangular arrow heads*). **d-f)** 3D volume images consist of 14 stacks and **h-j)** consists of 15 stacks. Magnification 60x. Scale bar 1 µm.

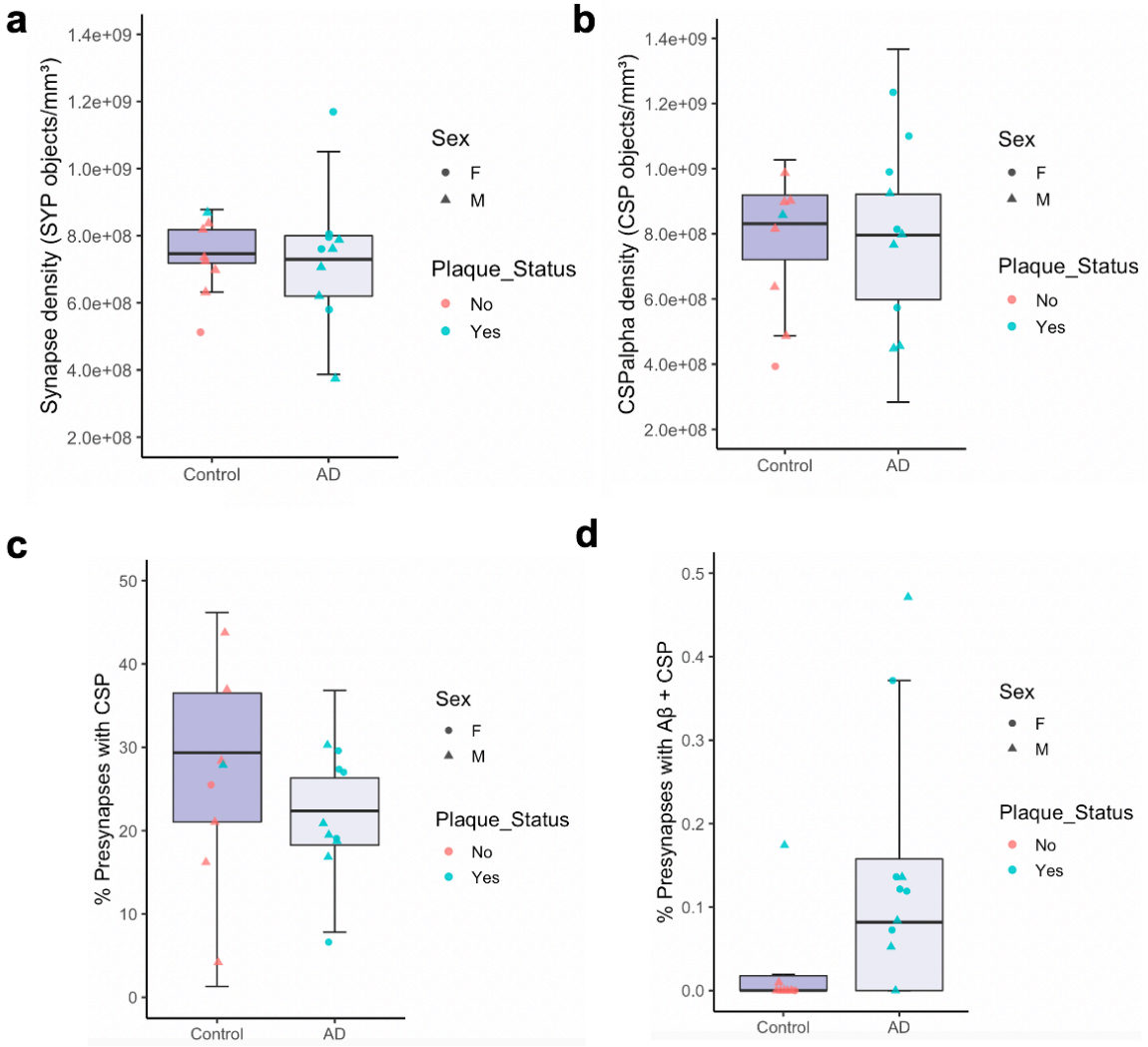
a
Synapse density (SYP objects/mm³)
1.4e+09
1.2e+09
1.0e+09
8.0e+08
6.0e+08
4.0e+08
2.0e+08
Control
AD
Sex
F
M
Plaque_Status
No
Yes
b
CSPalpha density (CSP objects/mm³)
1.4e+09
1.2e+09
1.0e+09
8.0e+08
6.0e+08
4.0e+08
2.0e+08
Control
AD
Sex
F
M
Plaque_Status
No
Yes
c
% Presynapses with CSP
50
40
30
20
10
0
Control
AD
Sex
F
M
Plaque_Status
No
Yes
d
% Presynapses with Aβ + CSP
0.5
0.4
0.3
0.2
0.1
0.0
Control
AD
Sex
F
M
Plaque_Status
No
Yes

Figure 3.16. Density and colocalization analysis of synaptic proteins using array tomography.

Quantification of immunoreactivity in control [n=8] and AD Braak VI [n=10] BA9 brain sections using AT analysis. **a)** No differences were detected in the density of synapses (number of synaptophysin (SYP)-positive objects/mm³) (Data was transformed using the Boxcox method) and **b)** density of CSPalpha (CSP), objects/mm³ are shown for each group. Data shown are mean data points per case with boxplots showing median for every data point with error bars showing inter-quartile ranges. **c)** Analysis of the percentage of presynapses colocalised with CSPalpha objects and **d)** the percentage of presynapses colocalising with both Aβ and CSPalpha. Data shown are median data points per case with boxplots showing median for every data point with error bars showing inter-quartile ranges. All data underwent Shapiro-Wilk's normality testing and was analysed using a parametric linear mixed effects model. Symbol representations; *Circle* – Female (F), *Triangle* – Male (M). Colour representations; *Orange* – No Aβ plaques present, *Blue* – Aβ plaques present.

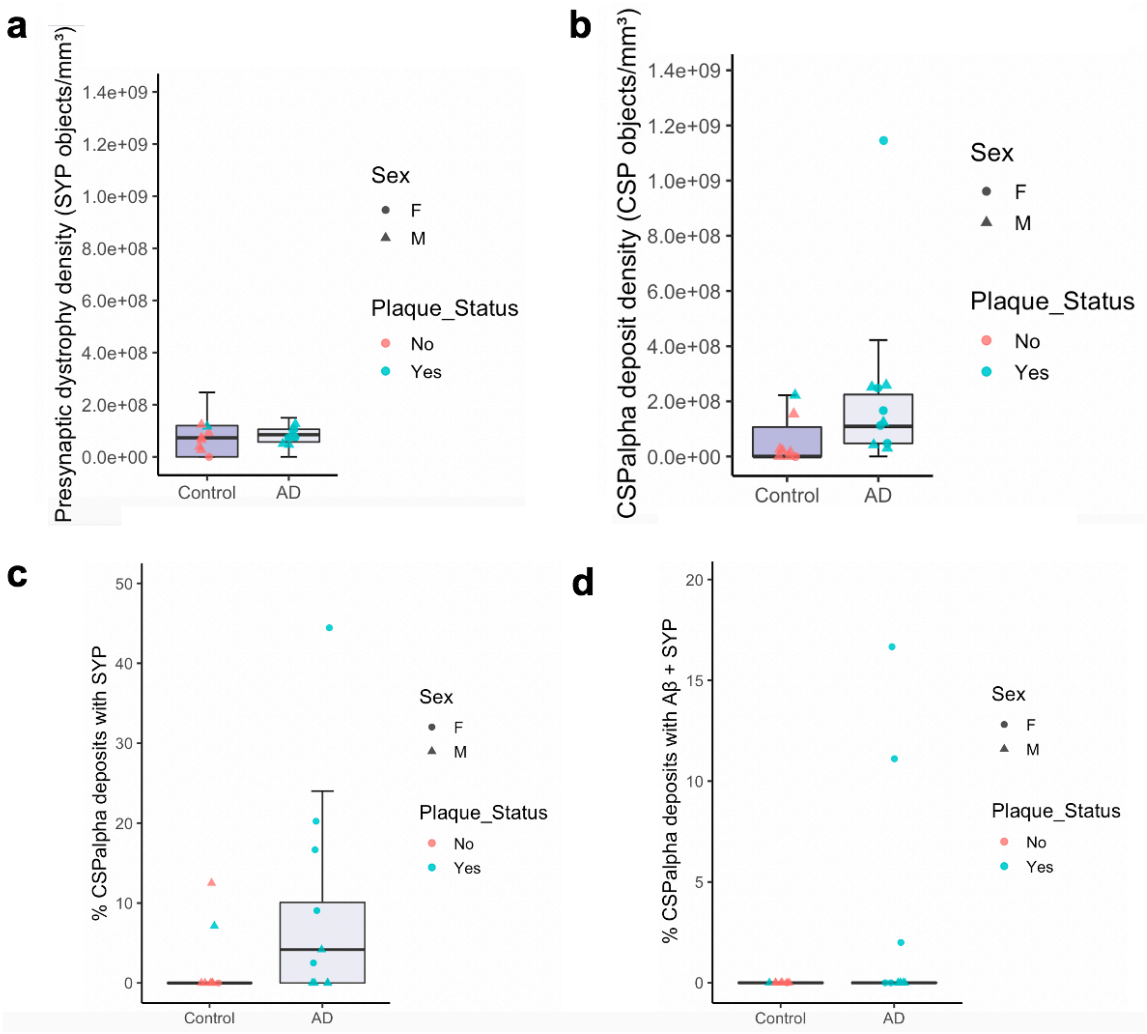
a
Presynaptic dystrophy density (SYP objects/mm³)
1.4e+09
1.2e+09
1.0e+09
8.0e+08
6.0e+08
4.0e+08
2.0e+08
0.0e+00
Control
AD
Sex
F
M
Plaque_Status
No
Yes
b
CSPalpha deposit density (CSP objects/mm³)
1.4e+09
1.2e+09
1.0e+09
8.0e+08
6.0e+08
4.0e+08
2.0e+08
0.0e+00
Control
AD
Sex
F
M
Plaque_Status
No
Yes
c
% CSPalpha deposits with SYP
50
40
30
20
10
0
Control
AD
Sex
F
M
Plaque_Status
No
Yes
d
% CSPalpha deposits with Aβ + SYP
20
15
10
5
0
Control
AD
Sex
F
M
Plaque_Status
No
Yes

Figure 3.17 Density and colocalization analysis of synaptic accumulations using array tomography.

Quantification of immunolabelled control [n=8] and AD Braak VI [n=10] BA9 brain sections using array tomography analysis. **a)** Differences were detected in the density of presynaptic dystrophies (number of synaptophysin (SYP)-positive objects/mm^3) **b)** but not in the density of CSPalpha (CSP) deposits per mm^3 shown for each group. **c)** Analysis of the percentage of CSPalpha deposits that colocalised with SYP-positive presynaptic dystrophies (Data was transformed using the Boxcox method) and **d)** the percentage of CSPalpha deposits colocalising with both Aβ and SYP. Data shown are median data points per case with boxplots showing median for every data point with error bars showing inter-quartile ranges. All data underwent Shapiro-Wilk's normality testing and analysed using a parametric linear mixed effects model. Symbol representations; *Circle* – Female (F), *Triangle* – Male (M). Colour representations; *Orange* – No Aβ plaques present, *Blue* – Aβ plaques present.

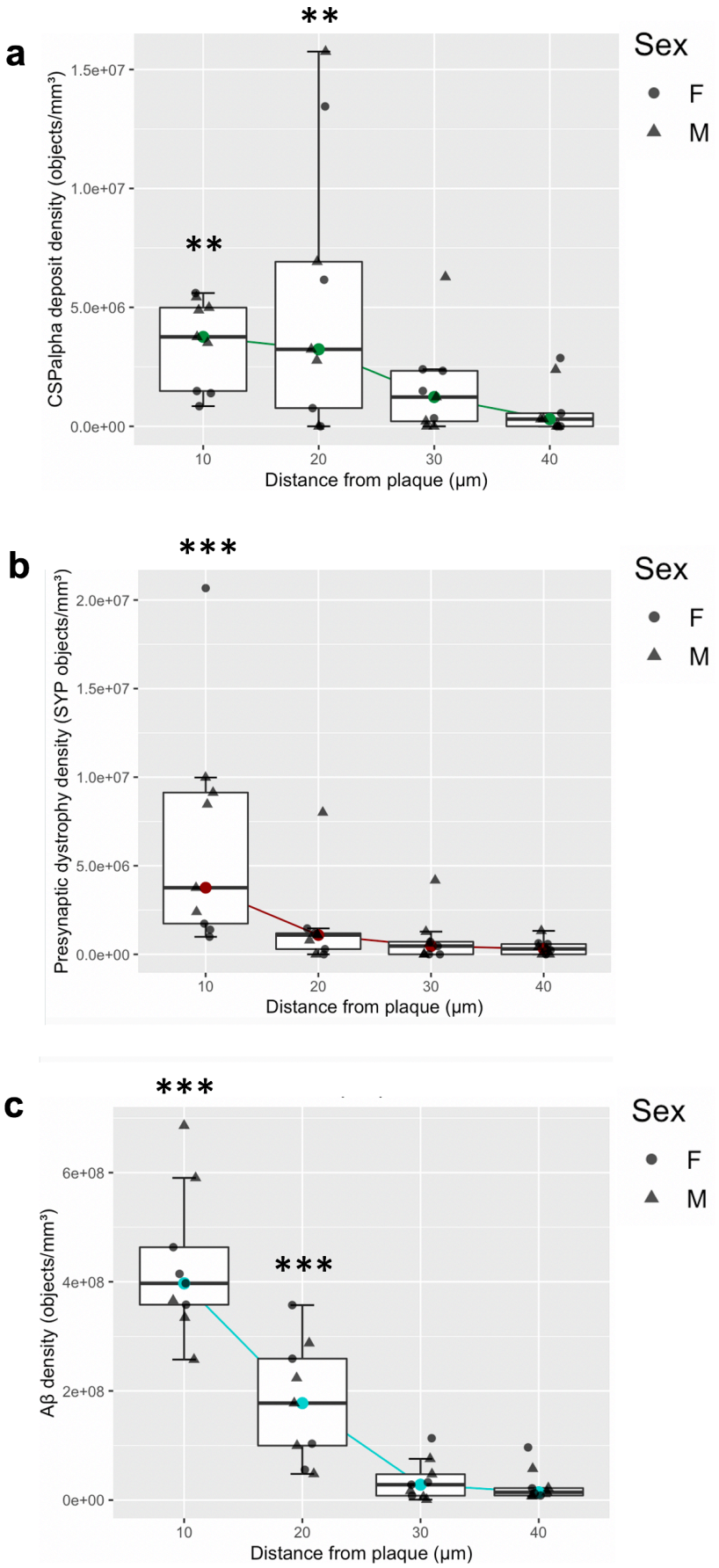
a
**
**
CSPalpha deposit density (objects/mm³)
1.5e+07
1.0e+07
5.0e+06
0.0e+00
10
20
30
40
Distance from plaque (µm)
Sex
F
M
b
***
Presynaptic dystrophy density (SYP objects/mm³)
2.0e+07
1.5e+07
1.0e+07
5.0e+06
0.0e+00
10
20
30
40
Distance from plaque (µm)
Sex
F
M
c
***
***
Aβ density (objects/mm³)
6e+08
4e+08
2e+08
0e+00
10
20
30
40
Distance from plaque (µm)
Sex
F
M

Figure 3.18. Greater density of presynaptic accumulations in areas closest to the Aβ plaque centre.

Array tomography images were analysed to yield density of synaptic accumulations at a distance of 0-10 µm (10 µm), 10-20 µm (20 µm), 20-30 µm (30 µm) and 30-40 µm (40 µm) from the Aβ plaque core. **a)** Quantification of median CSPalpha deposit density in Braak VI brains reveals a statistically significant gain of abnormal structures approaching Aβ plaques <10 µm and 10-20 µm distance from the plaque core **b)** and a statistically significant amount of synaptophysin-positive presynaptic dystrophies were localised <10 µm distance from the plaque core. **c)** There was a gradual decline in Aβ levels with most statistically significant densities <10 µm and 10-20 µm from the plaque centre. This effect was also statistically significant for age and PMD. Data shown are median data points per case with boxplots showing median for every data point with error bars showing inter-quartile ranges. All data underwent Shapiro-Wilk's normality testing, transformed using a Tukey transformation and analysed using a parametric linear mixed effects model with t-tests using Satterthwaite's method. Symbol representations; *Circle* – Female (F), *Triangle* – Male (M). ** $p<0.001$, *** $p<0.0001$.

3.4.11 CSPalpha accumulations are phosphorylated at Ser10.

Phosphorylation of proteins, especially at the synaptic level, is vital for synaptic functions such as vesicle release which regulates synaptic strength and plasticity (Evans and Morgan, 2003). It has been previously shown that CSPalpha has a functional role within exocytotic mechanisms, a process regulated by cAMP dependent PKA (Weisskopf et al., 1994; Linden and Ahn, 1999; Evans et al., 2001). Interestingly, it has been reported in Drosophila *melanogaster,* C-*elegans*, mice, rats and in humans tissue studies that CSPalpha can be phosphorylated by kinases at

several sites, however it is principally phosphorylated by PKA at Ser10, suggesting this post-translational site is an evolutionarily conserved regulatory mechanism (Evans et al., 2001; Evans and Morgan, 2002). CSPalpha phosphorylation at Ser10 has been reported to be important for the modulation of vesicle fusion and release kinetics, by causing structural destabilisation of CSPalpha at its N-terminus, weakening its interaction with synaptotagmin and syntaxin presynaptic proteins (Evans and Morgan, 2002; Patel et al., 2016). On the other hand, PKC γ phosphorylation of CSPalpha at Ser10 and Ser43, promotes its interaction with Hsp70/Hsc70 enhancing its chaperone activity for synaptic maintenance (Evans et al., 2001; Shirafuji et al., 2018; Velasco et al., 2019). Ser10 phosphorylation of CSPalpha has also been suggested to assist in fusion pore expansion that can modulate the rate of exocytosis (Prescott et al., 2008; Chiang et al., 2014; Patel et al., 2016). Although the implication of such a post-translational modification is still not fully understood, it may play a role in the functional integrity of the synapse which is a major target across several neurodegenerative diseases.

To explore the possibility of altered CSPalpha phosphorylation in AD tissues and whether CSPalpha accumulations may also be phosphorylated, rabbit antiserum specific for CSPalpha phosphorylated at Ser10 was kindly gifted by Prof. Alan Morgan (University of Liverpool). This antiserum corresponded to the phosphorylated CSPalpha peptide sequence containing amino acid residues 4-14 (QRQRSLSTSGE) (MWG Biotech, Milton Keynes, UK) (Fig 3.19a) (Evans and Morgan, 2005). The resultant antiserum was produced by affinity-purification using the phosphorylated CSPalpha peptide coupled to an immobilised resin (Evans and Morgan, 2005).

To test whether the CSPalpha pSer10 antiserum could detect CSPalpha phosphorylation at Ser10, WT and CSPalpha KO mouse homogenates were immunoblotted (Fig 3.19a). A positive band for CSPalpha phosphorylation at Ser10

was present at ~29-34 kDa, the molecular weight of CSPalpha, in forebrain homogenates from WT but not KO tissues. This confirmed antiserum binding and in addition showed CSPalpha phosphorylation within endogenous mouse tissues. (Fig 3.19b). Next, to validate the specificity of the antisera to CSPalpha phosphorylated at Ser10, antisera was used to probe electrophoresed purified recombinant CSPalpha protein (either PKA- phosphorylated or non-phosphorylated) (Evans and Morgan, 2005) in comparison to a rabbit polyclonal total CSPalpha antibody (AB1576). The CSPalpha pSer10 antibody detected only a single band at ~29kDa in the PKA-phosphorylated recombinant protein sample, unlike the total CSPalpha antibody which detected bands in both the phosphorylated and non-phosphorylated peptide samples. These bands were at lower molecular weight compared to physiological CSPalpha, as the recombinant protein does not contain posttranslational modifications. This result demonstrated that the pSer10 antiserum only detects CSPalpha phosphorylated at Ser10. Furthermore, CSPalpha pSer10 antiserum along with the total CSPalpha antibody was used to probe homogenates from post-mortem human control hippocampus. Bands were detected at ~29-34 kDa confirming the presence of post-translationally modified CSPalpha protein in human brain tissue. Beta-actin was used as a loading control for these blots and showed a band present in human tissue samples but was undetected in purified recombinant protein samples.

Having validated the specificity of the CSPalpha pSer10 antiserum and its expression in human control tissue, this CSPalpha modification was then examined in post-mortem AD brain to determine whether CSPalpha is also phosphorylated in disease. Using immunofluorescence and the CSPalpha pSer10 antibody, positive background staining similar to results for total CSPalpha was observed in the gray matter neuropil in both early and late-stage AD groups, and also identified immunoreactivity of CSPalpha accumulations in AD brain (Fig 3.20a, b). These deposits of CSPalpha phosphorylated at Ser10 were localised in the vicinity of diffuse and neuritic cored Aβ

plaques in severe AD (Fig 3.20b). This suggests that CSPalpha deposits are phosphorylated in AD, however the functional consequences of this modification are not fully understood.

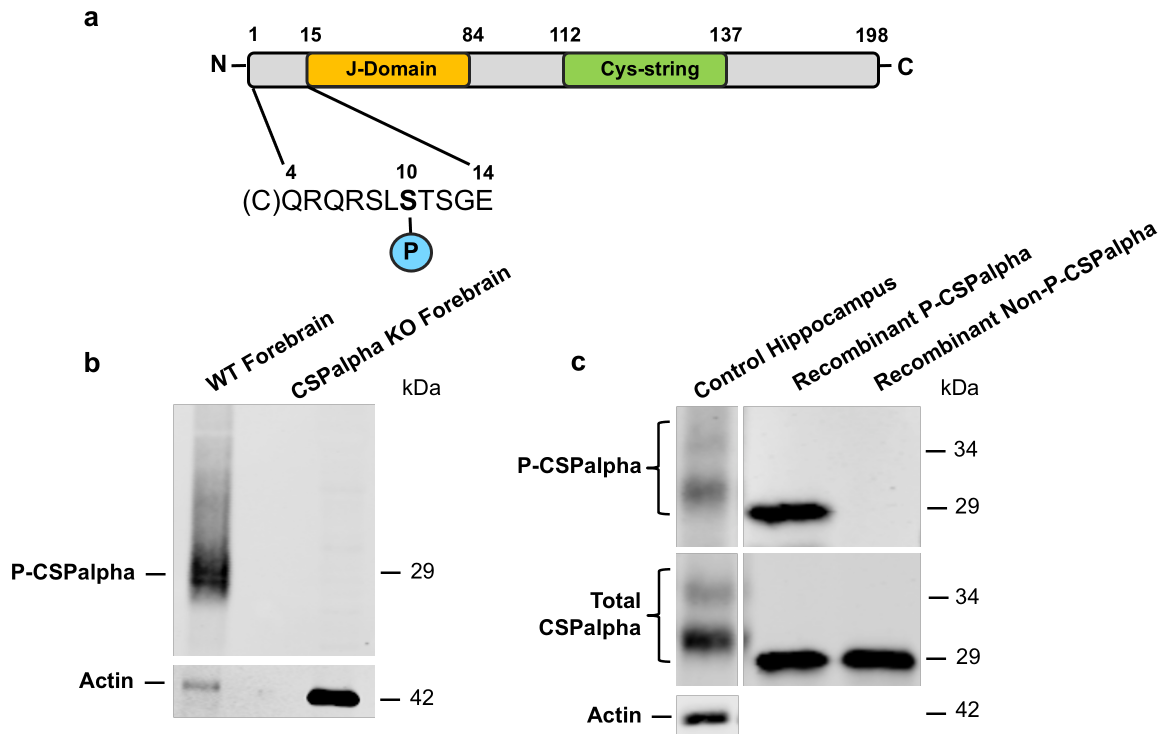

Figure 3.19. An antibody against CSPalpha phosphorylated at Ser10 specifically detects phosphorylated CSPalpha.

a) Schematic representation of CSPalpha indicating the J-domain, cysteine string and the location of the PKA Ser10 phosphorylation site including the peptide sequence. Phospho-CSPalpha (4–14) was used to raise the antibody, with an additional N-terminal cysteine to facilitate coupling. Adapted from (Evans and Morgan, 2005). Representative western blots showing **b)** detection of CSPalpha pSer10 (P-CSPalpha) in WT, but not CSPalpha KO forebrain. Beta-actin was used as a loading control. **c)** Representative western blots showing detection of only phosphorylated, but not non-phosphorylated recombinant CSPalpha peptides by the phospho-CSPalpha antibody. CSPalpha pSer10 was also detected in human hippocampus. Due to the lack of posttranslational modifications, recombinant protein appears to be of lower molecular weight than CSPalpha from tissue.

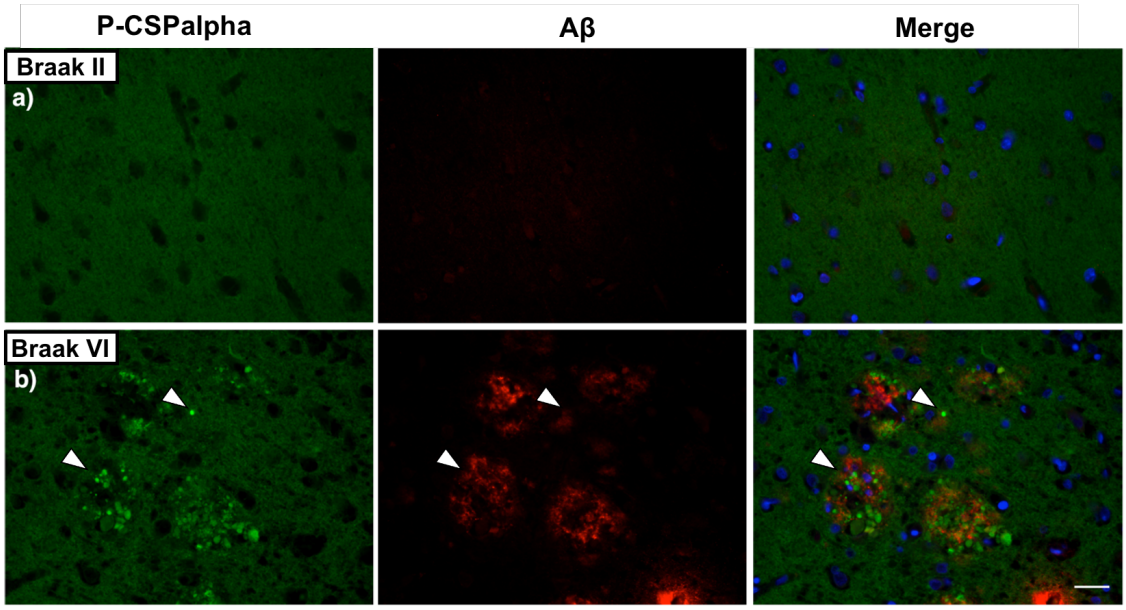

Figure 3.20. Phosphorylated CSPalpha protein deposits identified proximal to Aβ plaques.

Representative images of sections from post-mortem human BA9 **a)** control (Braak stage II) and **b)** AD (Braak stage VI) brain immunolabelled with antibodies against CSPalpha pSer10 (*green*) and Aβ (*red*). Nuclei are stained with DAPI (*blue*). *White arrow heads* indicative of CSPalpha accumulations. Magnification 40x. Scale bar 30 µm. [n=1 per group].

3.4.12 Monomeric CSPalpha protein solubility is altered in AD

AD, along with other neurodegenerative diseases, are classed as proteinopathies, which show a gradual accumulation of detergent-insoluble protein aggregates in the brain that play a central role in pathophysiology of disease and lead to cognitive decline (Ross and Poirier, 2004). When proteins aggregate as a result of alterations to their native conformation, their solubility changes with their size, making them more insoluble. For example, Aβ fibrils consist of repeating units of misfolded protein which

exhibit a cross-β structure (Hamley, 2012). These protein aggregates however are highly resistant to thermal denaturation and solubilisation and so traditional biochemical techniques prove difficult to purify Aβ for further analysis (Ross and Poirier, 2004; Gozal et al., 2009; Seyfried et al., 2012; Hales et al., 2016).

To fully understand the nature of CSPalpha accumulations, tissue samples were extracted with increasing strength of harsh detergents. Briefly, as described in Chapter 2, Section 2.4.2, fractions of post-mortem human Braak stage 0-II and V-VI AD BA9 tissues [n=6 cases per group] were homogenised in detergents of increasing strength and sedimented by ultracentrifugation. Buffers included high salt (disrupts membranes and protein solubility (Bass et al., 2017)), triton X-100 (permeabalises membranes and solubilises non-polar proteins (Bass et al., 2017)) and sarkosyl (solubilises natively folded proteins without solubilizing misfolded protein aggregates (Hasegawa et al., 2002; Neumann et al., 2006; Gozal et al., 2009; Bai et al., 2013; Diner et al., 2014, 2017). Sarkosyl is known to be less stringent compared to the ubiquitous anionic detergent SDS and preserves less robust oligomeric misfolded protein aggregates that cannot withstand SDS treatment (Nizhnikov et al., 2014). Immunoblotting membranes were probed with anti-CSPalpha, anti-PHF-1 and anti-total tau antibodies along with a total protein stain to detect the total amount of protein present within each homogenate fraction that was loaded onto the gels.

Most soluble proteins were found to be extracted by HS after total protein stain (Licor, UK), with consecutively reduced protein amounts detected in the more stringent fractions (Fig 3.21a). The lowest signal intensity was observed in the sarkosyl-insoluble (SI) fraction, where only the most insoluble proteins are partitioned. Interestingly, signal intensity was observed in SI fraction of control tissues, suggesting some insoluble proteins are also present in healthy control brain, possibly due to

some unknown underlying aggregated proteins. Alternatively, the fractionation may not have been a complete success. There is however a compromise between protein enrichment and obtaining greater purity to reduce protein loss of low abundance proteins within these multiple steps.

Monomeric CSPalpha (34 kDa) was present in all fractions of Braak 0-II and Braak V-VI AD tissues. As expected, most CSPalpha protein was enriched in the HS-TX fraction with the strongest signal intensity as CSPalpha is known to be found on hydrophobic presynaptic membranes (Fig 3.21a). All fractions from both groups were normalised to the HS-TX fraction for quantification of relative CSPalpha amounts in each fraction. In Braak 0-II tissues, CSPalpha amounts were found mostly enriched within the HS fraction compared to the sarkosyl-soluble (SS) and SI fractions. However, in Braak V-VI tissues, most CSPalpha amounts were enriched in the SS fraction compared to HS and SI fractions. The SI fraction is where most insoluble proteins would be expected to be present. Since limited CSPalpha was detected in this fraction, this may suggest that most CSPalpha accumulations may not be sarkosyl insoluble or that the deposits are rapidly denatured (Fig 3.21a). A statistically significant difference in CSPalpha solubility was detected between Braak 0-II and Braak V-VI groups ($F(1,10)=8.6$, $p=0.015$), specifically between the SS fractions ($p=0.011$) where Braak V-VI tissues had more CSPalpha enrichment compared to Braak 0-II tissues (Fig 3.21b).

Differences between each of the fractions as well as an interaction between fractions and Braak stages had a significant effect on the variation between samples. This suggests that in Braak 0-II tissues, most CSPalpha protein is solubilised, however in AD, less CSPalpha is solubilised, suggesting that the native structure of CSPalpha may be altered and there may be a conformation change in the monomeric form of this protein, possibly as more insoluble complexes of CSPalpha are formed. This

infers the possibility of two confirmations of CSPalpha, the monomeric form of CSPalpha found at the presynaptic terminal, and the complexed accumulation of CSPalpha found as proteinaceous deposits that line Aβ plaques.

Hyperphosphorylation of tau protein is a classical hallmark of AD and forms the building block of insoluble NFTs (Alonso et al., 2018). In order to confirm the neuropathological diagnosis of tissue samples between healthy controls and AD, membranes were probed with an antibody that detects total tau, both phosphorylated and non-phosphorylated forms. Insoluble tau is normally depicted on full length western blots of AD samples as smears. Using a PHF-1 antibody to detect tau phosphorylated at Ser396/404 and total tau (DAKO) for global tau changes, the results showed increasing insolubility of tau in AD samples, as high molecular weight bands together with smearing through the lanes (Fig 3.21c). As expected in Braak V-VI brains, most prominent protein enrichment was found within the SI fraction, with very little tau remaining in the SS fraction (Fig 3.21c, d). This confirms that most tau in AD has oligomerised or the native structure of tau has been altered, characteristic of tau in AD brain. This is in line with previous reports showing that pathological aggregates such as NFTs are insoluble in sarkosyl, while their natively folded counterparts are soluble (Gozal et al., 2009; Guo et al., 2016; Hales et al., 2016). The converse was observed in the Braak 0-II sections where the majority of total tau remained within the SS fractions and was not evident in the SI pellet (Fig 3.21c, d). These data show that the detergent fractionation was successful.

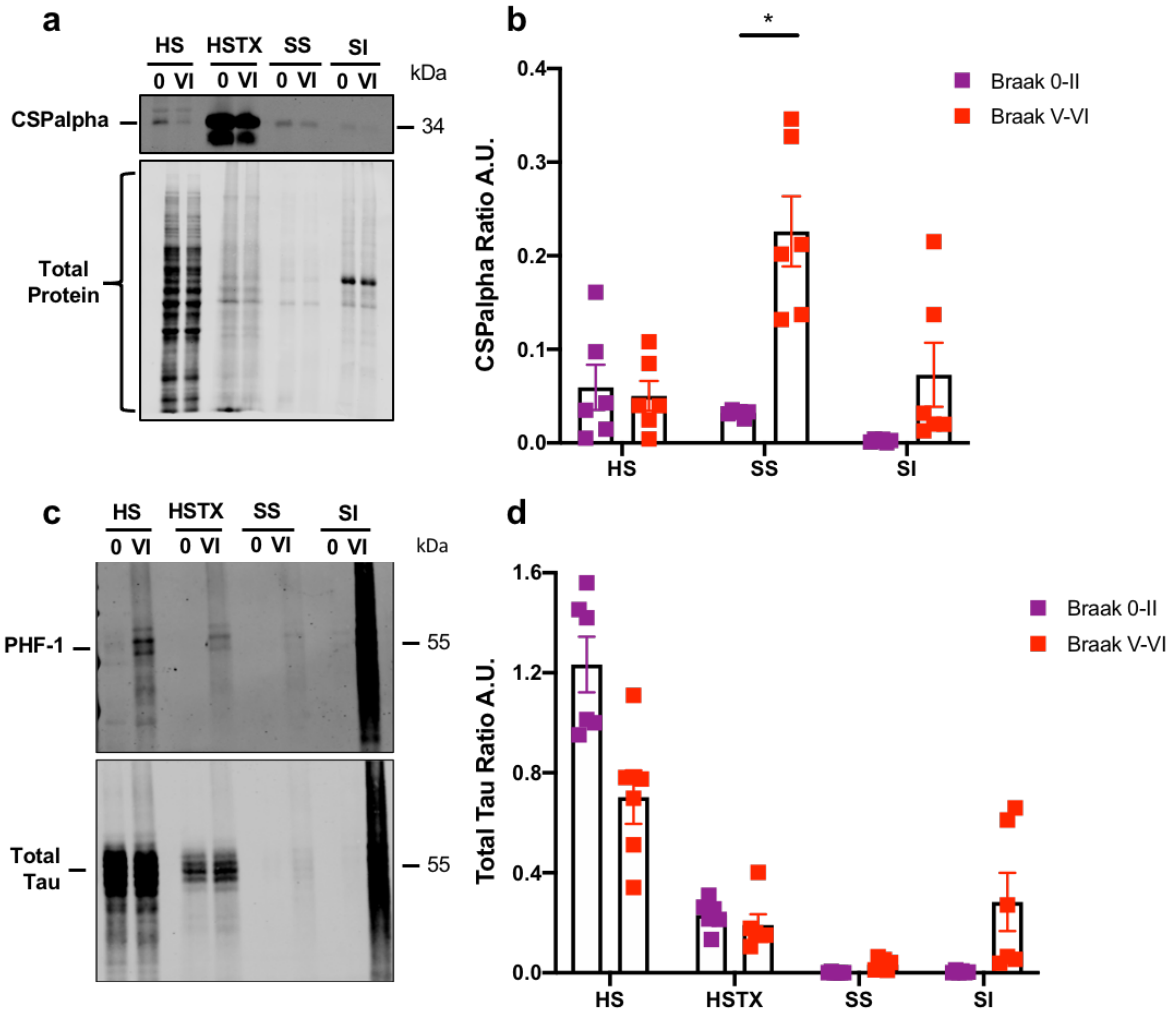
a
HS
HSTX
SS
SI
0 VI
kDa
CSPalpha
34
Total Protein
b
*
Braak 0-II
Braak V-VI
CSPalpha Ratio A.U.
0.4
0.3
0.2
0.1
0.0
HS
SS
SI
c
PHF-1
55
Total Tau
d
Total Tau Ratio A.U.
1.6
1.2
0.8
0.4
0.0
HSTX

Figure 3.21. Solubility of CSPalpha and tau is altered in AD.

a) Representative western blots of post-mortem BA9 Braak 0 and Braak VI brains samples extracted in buffers containing HS, HSTX, SS and SI showing bands for monomeric CSPalpha (~34kDa) and a total protein stain. **b)** Bar charts shows quantification of CSPalpha in each fraction normalised to the HSTX fraction, with a statistically significant difference in SS fractions between control and AD samples. Following Shapiro-Wilk's testing, data was analysed using parametric two-way ANOVA with repeated measures and with Sidak's multiple comparison test. Data shown are mean ± SEM. [n=6 cases per group]. * $p<0.05$. **c)** Representative western blots of the same Braak 0 and VI brains probed with the PHF-1 and total tau antibodies (full length monomer is ~50-68 kDa). **d)** Bar chart shows quantification of tau in each fraction. Tau accumulates in the SI fraction in AD but not in control [n=6 cases per group].

3.4.13 Plaque associated CSPalpha accumulations in 5xFAD transgenic mouse brains

To investigate whether amorphic CSPalpha accumulations are specific to amyloid deposits, 5xFAD mice were used. The 5xFAD mouse model harbours FAD-causing mutations in human *APP* and *PSEN1* genes and progressively develops prominent pathological features which include Aβ plaque formation from as early as 3 months of age, a sharp elevation of Aβ levels until 4-6 months of age, increased neuroinflammation, synaptic loss and dysfunction, neuronal loss and cognitive decline (Oakley et al., 2006). The concomitant features of human AD make the 5xFAD model attractive for studying the mechanisms underlying disease progression and more specifically to shed light on synaptic level changes that occur due to the exclusive development of Aβ pathology.

The methods used for mouse work are described in detail in Chapter 2, Section 2.11. Briefly, expression of mutant transgenes in the mouse colony were detected using DNA extraction, PCR amplification and agarose gel visualisation (Chapter 2, Section 2.11.1). Once genotyping was confirmed, mouse brains were collected from female WT and 5xFAD mice at ~ 6 months of age. 30 µm thick sections were taken from cortical and hippocampal regions and were processed for immunofluorescence and spinning disk confocal microscopy.

After co-labelling with CSPalpha and Aβ antibodies, sections from both WT and 5xFAD mice were found to exhibit increased neuropil labelling of presynaptic CSPalpha within the dentate gyrus hillus, infrapyramidal bundle, stratum lucidum and subiculum of the hippocampus (Figure 3.22a, b). Prominent labelling was apparent with the Aβ antibody marking interneuronal APP, abnormal Aβ conformations and Aβ pathological structures in 5xFAD brain which were absent in the hippocampus of WT mice (Figure 3.22a, b). Additionally, Aβ plaque deposits were evident from as early as 3 months in 5xFAD brain which were associated with abnormal CSPalpha-positive structures, suggesting that these CSPalpha accumulations form during the early development of plaques and before synapse loss first occurs in 5xFAD mice (Oakley et al., 2006) (Chapter 6, Fig 6.2). The subiculum region showed the highest density of Aβ deposits at this time point, with virtually all the 6E10-positive Aβ deposits decorated with clusters of aberrant CSPalpha structures. Spinning disk confocal microscopy, using a 60x objective lens and 0.9um Z-stack revealed CSPalpha accumulations at 6 months of age which encircled Aβ deposits in all three mouse brains, coinciding with morphological similarities to those found in human AD brain (Figure 3.22c, 3.24a). No CSPalpha accumulations were found in areas remote from Aβ plaques. Visual analysis of different areas in tissue sections from mice aged 3, 9 and 12 months suggested that the number of deposits per plaque may increase with age and in parallel to the size of plaques, although this data could not be quantified

as the number of mice were limited to only one per group and regions were not always comparable (Chapter 6, Fig 2). These findings indicate similarities to a previously reported study in APP/PS1 mice that showed the presence of morphologically defined presynaptic dystrophies that correlate to the size of Aβ plaques and not to age of mice, yet to be confirmed in human tissue (Sanchez-Varo et al., 2012).

Synaptic dysfunction and loss, characteristic features of human AD, have also been reported in the 5xFAD mouse model (Oakley et al., 2006). To understand whether synapse health is affected in the 5xFAD colony, hippocampal sections were co-labelled with antibodies against CSPalpha and the presynaptic marker proteins synaptophysin and SNAP-25, which closely reflect the number of functional synapses and whose loss is an indication of early AD changes (Masliah et al., 2001). Importantly, 5xFAD hippocampal sections co-labelled with synaptophysin, revealed synaptic neuropil staining, which colocalised with CSPalpha confirming CSPalpha's presynaptic localisation in mouse tissue. Here, in line with the results from post-mortem human tissues, CSPalpha was found to accumulate in proximity to the halo of Aβ plaques (3.22b-e). Additionally, similar to observations with CSPalpha deposits, synaptophysin-positive accumulations were also found and were localised to Aβ plaques (Fig 3.22d, 3.24b), a result which has been confirmed in 5xFAD mice in previously published reports as a marker of synaptic remnants and presynaptic dystrophies (Kandalepas et al., 2013; Li et al., 2013; Gowrishankar et al., 2015; Sadleir et al., 2016; De Rossi et al., 2019; Smith et al., 2019). Synaptophysin-positive accumulations however did not localise to all CSPalpha clusters in 5xFAD mice (Fig 3.22d, 3.24b). Interestingly, similar to previous findings from immunohistochemistry and AT of human tissue, synaptophysin accumulations were observed closer to the Aβ plaque centre than CSPalpha which was found more distal from the core. To confirm the localisation of synaptophysin deposits to Aβ plaques, positive staining

was confirmed after co-labelling with Thio-S, a marker for fibrillar Aβ (Fig 3.23a), which did not show positivity in a negative control (Fig 3.23b).

Similarly, co-labelling of CSPalpha with SNAP-25, which has been shown to be a downstream interacting partner, also showed colocalization within the neuropil confirming the presynaptic localisation of both proteins. Intriguingly, 'grape-like' deposits of SNAP-25 also were also found in close proximity to what appears to be Aβ deposits in the 5xFAD mice, yet only some of these accumulations colocalised with deposits of CSPalpha (Fig 3.22c, 3.24c). Negative controls did not show immunoreactivity for either proteins of interest (Fig 3.24d). This suggests there may be an altered physiological interaction and structural conformation between CSPalpha and other synaptic proteins that occurs within the presynaptic terminal, and accumulations of synaptic proteins found in disease. However, the mechanisms that lead to such accumulations of synaptic proteins to be deposited in proximity to Aβ plaques are still unclear. Yet these findings do corroborate that the association of CSPalpha with amyloid deposits is neither a terminal feature of the pathology nor specific for early stages of pathogenesis, but this leads to speculation of the involvement of mechanisms of APP dysfunction that result in Aβ plaque formation.

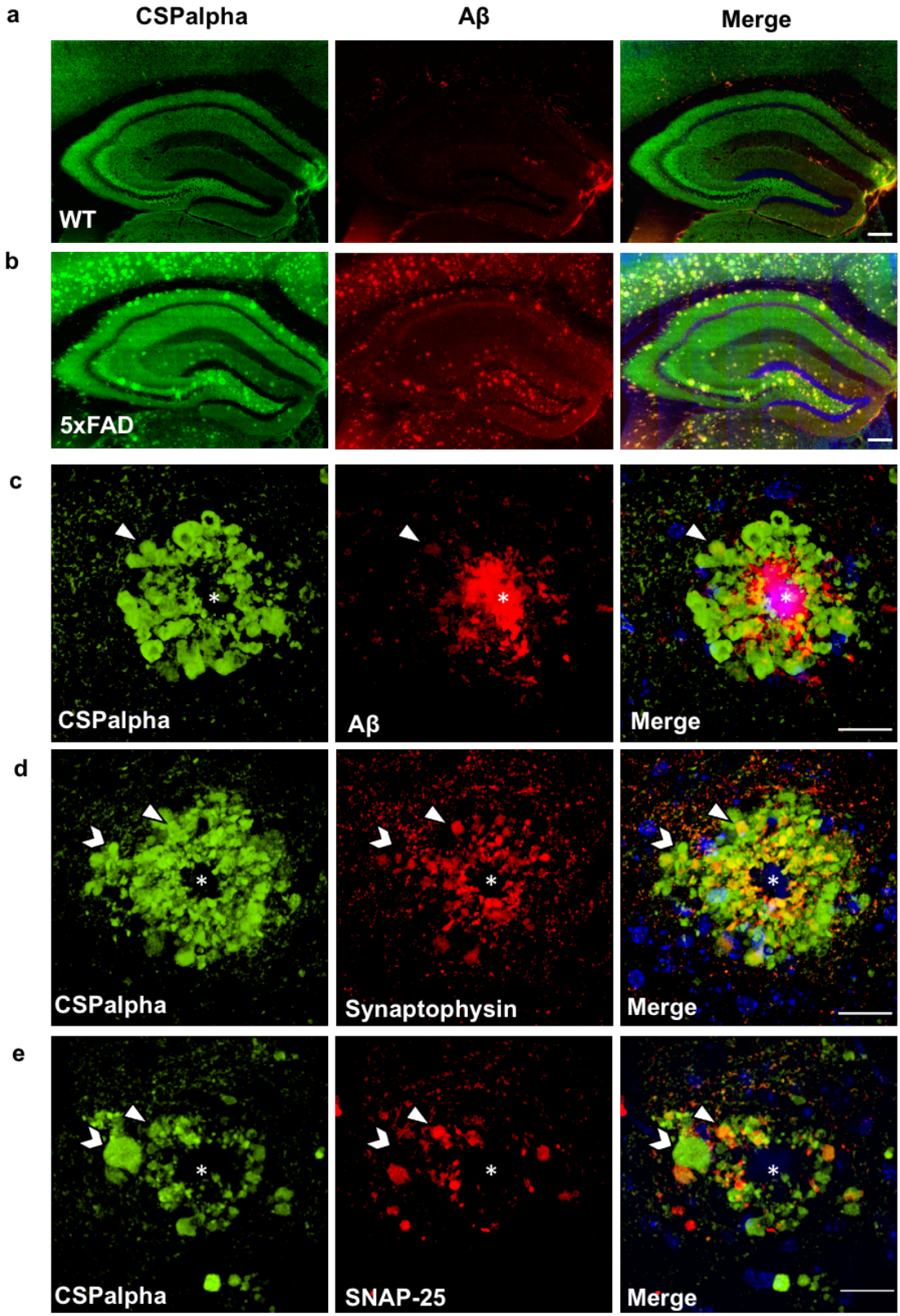
a
CSPalpha
Aβ
Merge
WT
b
5xFAD
c
CSPalpha
Aβ
Merge
d
CSPalpha
Synaptophysin
Merge
e
CSPalpha
SNAP-25
Merge

Figure 3.22. Aβ plaque-associated CSPalpha accumulates with some presynaptic deposits in 5xFAD mice.

a) Representative low magnification images of hippocampal mossy fibers from female WT [n=4] and **b)** 5xFAD transgenic mouse [n=3] brains (~6 months old) co-labelled with CSPalpha (*green*) and Aβ (*red*) antibodies. DAPI (*blue*) was used to stain nuclei. Magnification 2x. Scale bar 200 μm. **c)** Representative higher magnification images of CSPalpha immunoreactivity in proximity to Aβ plaques in 5xFAD mouse sections. **d)** Representative higher magnification images of some but not all CSPalpha accumulations (*green*) co-labelling with presynaptic markers synaptophysin (*red*) and **e)** SNAP-25 (*red*) which surround possible Aβ plaque cores in 5xFAD brain. *Triangular arrows* – Overlapping CSPalpha accumulations, *Chevron arrows*– Non-overlapping CSPalpha accumulations and *asterisks* - plaque core. Magnification 60x. Scale bar 20 μm.

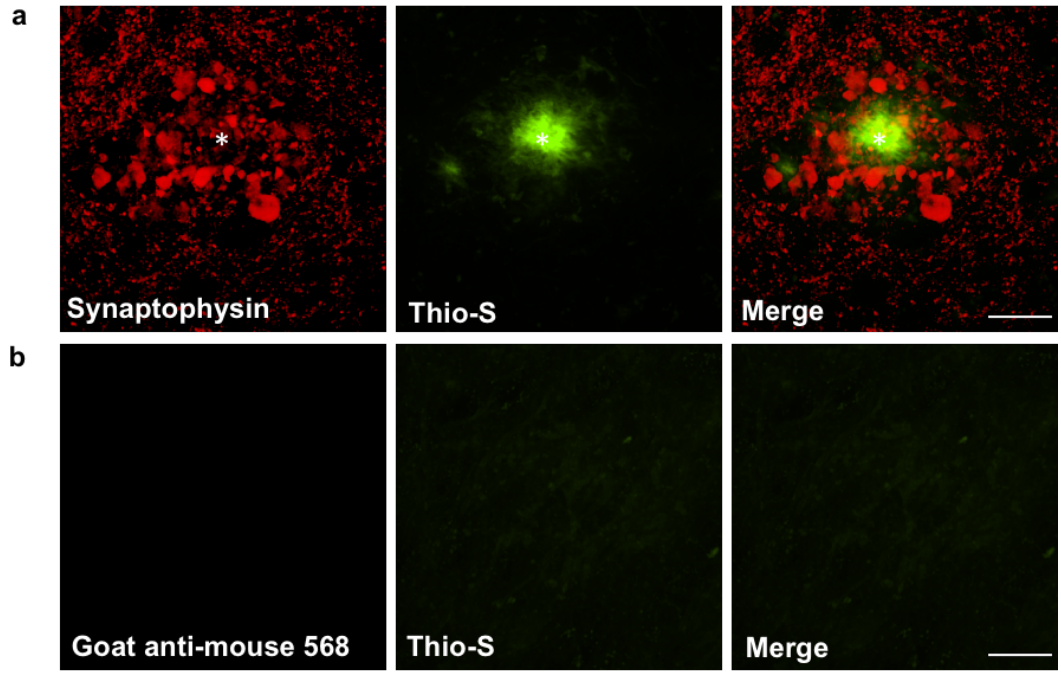

Figure 3.23. Synaptophysin accumulations are localised to fibrillar Aβ deposits in 5xFAD mice.

Representative images of a hippocampal section from 5xFAD mice, co-labelled for presynaptic dystrophies using an antibody against synaptophysin (*red*) which accumulates and surrounds the Aβ plaque cores stained with Thio-S (*green*). **b)** Representative images of negative control of a WT hippocampal mouse brain section probed only with secondary antibodies for alexa-fluor 568 (red), where no background staining or Thio-S staining is visible. *Asterisks' indicative of* plaque core. Magnification 60x. Scale bar 20 μm.

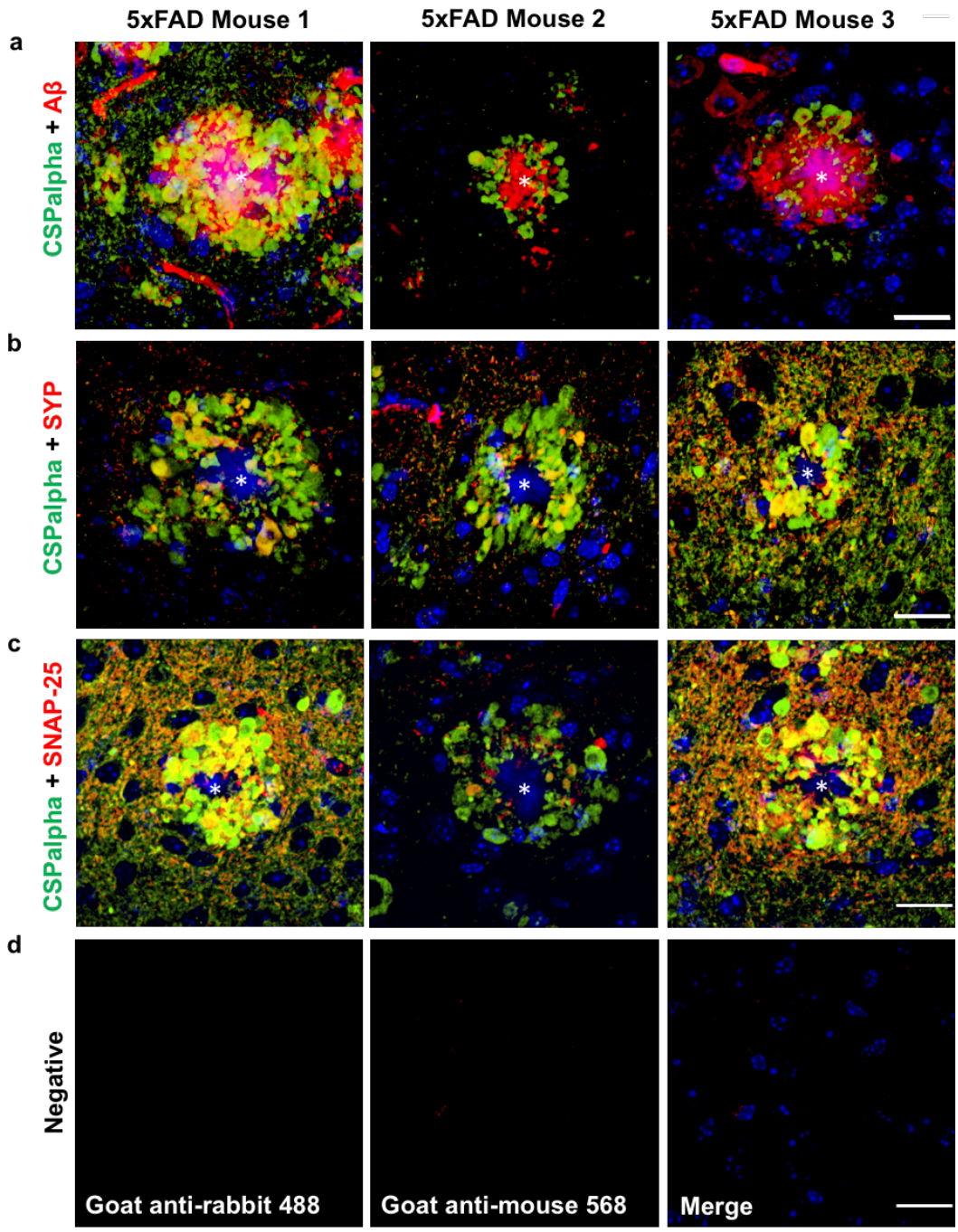
5xFAD Mouse 1
5xFAD Mouse 2
5xFAD Mouse 3
a
CSPalpha + Aβ
b
CSPalpha + SYP
c
CSPalpha + SNAP-25
d
Negative
Goat anti-rabbit 488
Goat anti-mouse 568
Merge

Figure 3.24. Aβ plaque-associated CSPalpha accumulates with some presynaptic protein deposits in each 5xFAD mouse.

Representative higher magnification images of hippocampal sections taken from three 5xFAD ~6-month-old female mice. **a)** Images show CSPalpha immunoreactivity (*green*) in proximity to individual 6E10-positive Aβ plaques (*red*) which shows some colocalisation. DAPI stain (*blue*) was used for nuclei. **b)** Representative high magnification images of some but not all CSPalpha accumulations (*green*) co-labelling with presynaptic markers synaptophysin (SYP) (*red*) and **c)** SNAP-25 (*red*) in each of the 5xFAD mice. DAPI stain (*blue*) was used to identify nuclei. Blue autofluorescence also detected the Aβ plaque core. **d)** Representative images of negative control of a WT hippocampal mouse brain sections probed only with secondary antibodies for alexa-fluor 488 (*green*) and alexa-fluor 568 (*red*), where no background staining is visible. *Asterisks'* indicative of plaque core. Magnification 60x. Scale bar 20 μm.

3.5 Discussion

The aim of this chapter was to investigate the presynaptic co-chaperone protein, CSPalpha as a novel pathological marker of presynaptic dysfunction in AD. CSPalpha was examined by immunoblotting and immunohistochemistry of post-mortem human BA9 tissue samples. The main findings of this study are that 1) there is a statistical trend towards reduction of CSPalpha in BA9 at end-stage AD compared to early AD where levels are protected within remaining synapses, 2) the discovery of novel abnormal structures of CSPalpha associated with hallmark Aβ plaque pathology and some presynaptic dystrophies and 3) verification of amorphous deposits of CSPalpha within the 5xFAD mouse, a model of early Aβ deposition.

In AD, it has previously been hypothesised that a downregulation of CSPalpha protein in the hippocampus and STG may contribute to early-stage synaptic degeneration (Tiwari et al., 2015). This is in agreement with mass spectroscopy data suggesting a reduction in CSPalpha abundance in AD compared to controls (Metaxas et al., 2018). Due to the crucial role of CSPalpha in synaptic survival (Fernández-Chacón et al., 2004), it can be suggested that when CSPalpha is reduced at the synapse, these synapses become vulnerable to synaptotoxic influences. It has been proposed that the loss of synapses within the frontal cortex provides the best correlate for cognitive decline in AD (DeKosky and Scheff, 1990; Terry et al., 1991). Additionally, it is important to understand the temporal progression of disease and as such BA9 frontal cortex provides a brain region that is both preserved early on in disease and severely affected in late stages. Previously published reports of CSPalpha in AD have shown a change in global levels of CSPalpha in total homogenate fractions (Zhang et al., 2012; Tiwari et al., 2015) and normalising immunoblotting data with an actin house-keeping protein (Zhang et al., 2012). This does not however take into account synaptic or neuronal loss, which is important since CSPalpha is a presynaptically

localised protein. Here, the aim was to investigate CSPalpha expression by normalising immunoblotting data to the traditional synaptic marker, synaptophysin (as shown in (Tiwari et al., 2015)) along with synaptoneurosome fractions to examine changes that occur within the presynaptic compartment. Interestingly, the results show that in BA9 AD, CSPalpha is slightly elevated between Braak 0-II and Braak III-IV and is then reduced in Braak V-VI groups when synaptic degeneration is greatest (DeKosky and Scheff, 1990; Masliah et al., 1994; Mukaetova-Ladinska et al., 2000). Similar findings have been reported within this brain region for many other synaptic proteins including synaptophysin, syntaxin, SNAP-25 and alpha synuclein (Mukaetova-Ladinska et al., 2000; Head et al., 2009; Schnaider et al., 2012; Sharma et al., 2012b; Robinson et al., 2014; Kurbatskaya et al., 2016) which could be due to possible neuritic sprouting and increase in size of presynaptic boutons as a possible compensatory mechanism in early presynaptic dysfunction within the frontal cortex (Masliah et al., 1994). The mechanism responsible for the slight transient increase, shown in many synaptic proteins along with CSPalpha and eventual loss at end stages is still not fully known. We have however determined that CSPalpha is lost prior to remaining synapses. This provides greater evidence of CSPalpha being implicated in the mechanisms leading to presynaptic dysfunction and loss.

The increase in synaptic proteins in moderate Braak stages correlates with an increase in tau mis-localisation to synapses and the presence of Aβ, both of which are known to be synapto-toxic (Bussière et al., 2003; Giannakopoulos et al., 2003; Spires-Jones and Hyman, 2014; Guerrero-Muñoz et al., 2015). A possible elevation in CSPalpha however is not as definitive as other synaptic proteins (Kurbatskaya et al., 2016). This may be due to grouping of samples from different Braak stages within this study which may reduce the overall effect, unlike other studies which look at changes within individual Braak stages (Kurbatskaya et al., 2016). Furthermore, this

study did not take into account a specific cortical layer analysis where subtle laminar changes can affect synaptic protein levels (Poirel et al., 2018). Even so, the possible consequence of elevated CSPalpha, may be a compensatory mechanism to protect synapses and to remove unwanted material from the presynaptic terminal. This is in line with previous reports of CSPalpha indirectly interacting with misfolded pathogenic proteins such as tau and being involved in the release of misfolded proteins from the synapse (Fontaine et al., 2016; Deng et al., 2017). Interestingly, CSPalpha along with other synaptic proteins, synaptophysin and synapsin-1 were lost from cortical neurons after treatment with Aβ containing frontal cortex AD brain extracts, a result that was confirmed when no effect was detected using Aβ-depleted brain extracts (Bate and Williams, 2018). It is hence plausible that increasing amounts of CSPalpha may well be indicative of synaptic survival to eradicate the earliest forms of toxicity, after which the burden of misfolded aggregates overwhelms the synaptic machinery and hence CSPalpha is lost. This is further supported by the fact that Aβ plaques and NFT burden is increased after Braak stage IV, and so increases in synaptic proteins precede the build-up of toxic aggregates (Mukaetova-Ladinska et al., 2000). Not only does this make CSPalpha an attractive target of interest when investigating the synapse, it opens the possibility of whether CSPalpha may in fact be a better marker of synaptic degeneration compared to traditional markers. Not only this, it is yet to be elucidated as to whether remaining synapses and the type of synapse (glutamatergic or GABAergic) are a clear representation of functionally viable cells. Further investigation is required to examine the relationship between CSPalpha, tau and Aβ as CSPalpha is elevated in the cerebellum, a region where minimal AD pathology is present (Sjöbeck and Englund, 2001; Tiwari et al., 2015).

It is however important to note the interpatient-variability observed in CSPalpha protein levels as well as normalisation to synaptophysin used as loading controls that

may have confounded the overall results. This may be due to individual differences in synaptophysin protein expression, possible comorbidities in pathological differences between brains contributing to overall synaptic changes, differential expression of synaptophysin expressed in BA9 and protein degradation due to PMD. Loading of samples was not considered to have an impact as any discrepancy was overcome by using a BCA assay to determine protein concentration. However, in order to improve single protein loading control differences, the preferred method would require normalisation using total protein analysis as an alternative, highly sensitive and accurate technique. This further highlights the importance of careful and consistent tissue sampling and analysis using quantitative immunoblotting of post-mortem human tissues. Further discrepancies may have occurred due to contamination and/or capture of different amounts of pre- and post- synaptic compartments in the synaptoneurosome preparation, which can be overcome by alternatively preparing synaptosomes, a method that captures the presynaptic terminal and is largely depleted of functional neuronal and glial cell body elements (Jhou and Tai, 2017).

The next aim was to understand the distribution and localisation of CSPalpha in BA9, which has not previously been investigated in the AD brain. The results yielded a novel finding of aggregate-like accumulations of CSPalpha in AD. These CSPalpha protein deposits are localised either intra- or extracellular in proximity to neuritic cored and diffuse Aβ plaques, and some synaptic tau and SMI312 positive accumulations surrounding plaques (Shankar et al., 2008; Spires-Jones and Hyman, 2014; Sadleir et al., 2016). These putative aggregates are evident in different regions of AD brain including BA9, the hippocampus and cerebellum and are phosphorylated at Ser10. Interestingly, some of these accumulations are localised with synaptophysin and SNAP-25-positive presynaptic dystrophies that are found <10 μm from the Aβ plaque

core unlike CSPalpha only accumulations found further between 10-20 μm as shown by AT.

There are still several unanswered questions that require further investigation such as how these accumulations of CSPalpha form, what are their functional consequences and whether this is an AD specific phenomenon. CSPalpha has been known to intrinsically self-associate as shown in *vitro* using purified CSPalpha (Swayne et al., 2003). It is yet unknown whether CSPalpha behaves in a similar way in *vivo*. CSPalpha aggregation has been identified in a rare neurodegenerative disease*,* ANCL, caused by missense mutations in the *DNAJC5* gene. In ANCL, mutant CSPalpha proteins accumulate and mislocalise intracellularly compared to WT proteins (Nosková et al., 2011). Mutations may lead to a mistargeting of CSPalpha and cause the formation of high molecular weight SDS-resistant aggregates. Additionally, CSPalpha is also reportedly lost from synaptosomes in the CLN5 form of the disease (Amorim et al., 2015). Mutated CSPalpha aggregates are found to be membrane-bound and palmitoylated in post-mortem patient tissue suggesting a possible link between palmitoylation and aggregate formation (Greaves et al., 2012). In comparison to these findings, sarkosyl-soluble monomeric CSPalpha protein was identified, suggesting an altered solubility in AD brain compared to controls. Unlike previous reports, high molecular weight species of CSPalpha were not found, possibly due to different experimental conditions which resulted in proteins lost in pellets deposited by ultracentrifugation, use of only SDS soluble fractions whereby high molecular weight CSPalpha protein may have been retained in the insoluble or pellet fractions, use of SDS gels instead of native immunoblotting gels that would aim to retain full-length CSPalpha but also that CSPalpha in ANCL may have a different conformational change in comparison to AD, where there is no known genetic link. Interestingly, CSPalpha accumulations have been identified within a neuronal model of HD (pathogenic polyQ-Huntingtin mutation (HTT128Q)), which

reported CSPalpha blockages containing Rab4 and Huntingtin protein causing axonal transport disruption and synaptic defects in *vivo* (White et al., 2020).

To understand why co-chaperones like CSPalpha might aggregate especially in disease, several groups have studied the behaviour of similar chaperone proteins in the context of pathological insults. Extracellular chaperones such as small Hsps which include Hsp27 and alpha crystallin B (Jimenez-Sanchez et al., 2015) have been reported to become sequestered within larger aggregates of toxic proteins and may confer a defensive response to prevent amyloid aggregation or deposition and synaptotoxicity (Shinohara et al., 1993). Similarly, Hsp40 and Hsp70, interacting proteins of CSPalpha, have been shown to inhibit the self-assembly of poly-glutamine proteins into amyloid like fibrils in *vitro*, and can bind to APP which can reduce Aβ secretions (Muchowski et al., 2000; Evans et al., 2006; Mannini and Chiti, 2017). DNAJB6, a chaperone part of the DNAJ protein family efficiently inhibits amyloid formation in *vitro,* and even more so the $A\beta_{42}$ toxic peptide implicated in AD (Månsson et al., 2014). Similar to possible neuroprotective effects of CSPalpha at the synapse (Fernández-Chacón et al., 2004), Hsp70 treatment in 5xFAD mice was found to reduce Aβ plaque accumulation and presented with a reduced loss of spatial memory (Bobkova et al., 2014). These data support the notion that molecular chaperones can inhibit the toxicity of proteinaceous aggregates both intra- and extracellularly (Takeuchi et al., 2015; Lazarev et al., 2017). Therefore, it is reasonable to speculate that CSPalpha accumulation may be a previously uncharacterised protective mechanism that acts to prevent further damage to synapses in AD, both intra- and/or extracellularly.

Recently, published evidence has implicated chaperones including CSPalpha in the export of misfolded proteins. The accumulation of misfolded toxic proteins is detrimental to synaptic function in several neurodegenerative diseases, including AD

(Kim et al., 2013). Fontaine and colleagues (2016) demonstrated that increasing CSPalpha expression promoted the secretion of misfolded proteins such as SNAP-23-dependent tau release from endo-lysosomes into the extracellular space from cultured rodent cortical neurons and brain slices (Fontaine et al., 2016). It is possible that some presynaptic CSPalpha deposits colocalise with hyperphosphorylated tau as shown by the human tissue findings, however most CSPalpha protein may be structurally modified and so does not fully associate with tau. This is supported by previously analysis in htau mutant mice whereby CSPalpha is upregulated when no neuronal loss is observed (Tiwari et al., 2015). Other neurodegenerative disease associated proteins such as TDP-43 and alpha-synuclein are similarly released by CSPalpha-dependent mechanisms (Fontaine et al., 2016). Surprisingly, it has been shown that CSPalpha can also be co-secreted along with these misfolded proteins via an unconventional protein secretion pathway that can also include other endogenous chaperones such as DnaJB1, DnaJB11 and DnaJA1 (Deng et al., 2017; Lee et al., 2018; Pink et al., 2018; Xu et al., 2018; Ye, 2018) These mechanisms although operating physiologically, may be exacerbated in disease states, and understanding the mechanisms that lead to CSPalpha release, may elude to the possible formation of extracellular CSPalpha structures, important for elucidating the early stages of synaptic dysfunction.

The final aim investigated the mechanistic underpinnings of the formation of CSPalpha accumulations using the 5xFAD mouse model of Aβ plaque development (Oakley et al., 2006). Here, CSPalpha accumulations were identified in proximity to Aβ plaques which increased in size and number from 3 to 12 months of age and colocalised with other presynaptic proteins. Overall, these mouse model findings show for the first time, supported by human post-mortem AD data that CSPalpha deposits are present in a portion of dying swollen presynaptic terminals,

and possibly the accumulation of vesicle bodies or extracellular synaptic remnants that surround newly forming Aβ plaques. Greater numbers of CSPalpha accumulations were observed, which do not fully colocalise with other presynaptic terminal dystrophy markers such as synaptophysin and SNAP-25, making CSPalpha a better neuropathological marker for examining synaptic dysfunction and loss in diseases in which APP is misprocessed.

It must still be noted that although these experiments provide convincing evidence of similar findings to the human condition, the 5xFAD mouse model is an aggressive system which shows only local Aβ toxicity on synapses without any contribution of NFTs and so does not truly reflect the development and progression of AD in humans. As it was not possible to acquire mice earlier than 3 months of age, or when Aβ plaque deposition first commences, it is difficult to determine the complete sequence of events that ultimately lead to the accumulation of CSPalpha. Additionally, unlike more sporadic forms of AD, the 5xFAD model is based on EOAD due to genetic mutations which only account for a small proportion of human AD cases and may not reflect the global population. Additionally, sex is a possible biological variable as all 5xFAD mice used in this study were females which develop a harsher phenotype and so the results may not be fully representative of 5xFAD mice as a whole (Jankowsky and Zheng, 2017). A better more 'humanised' model is the use of APP knock-in mice generated by a three amino acid change (G676R, F681Y, and H684R) and introduction of two FAD mutations (KM670/671NL and I716F) into the endogenous mouse *App* gene (Saito et al., 2014). This model is advantageous compared to the 5xFAD as it demonstrates elevated Aβ and cortical Aβ deposition in the context of WT levels of APP (Saito et al., 2014). Interestingly, 6-month-old *App* knock-in mice ($App^{NL\text{-}F/NL\text{-}F}$) present with impaired cortical CSPalpha protein turnover, suggesting

that CSPalpha protein alterations are already observable within this mouse model (Hark et al., 2021).

These findings do however corroborate that the association of CSPalpha with Aβ deposits is neither a terminal feature of the disease nor specific for early stages of pathogenesis but may be involved in the mechanisms of APP dysfunction that cause Aβ plaque formation. However, the mechanisms by which CSPalpha is deposited, either within presynaptic dystrophies, vesicular bodies or extracellular to the synapse remains to be elucidated.

What is most interesting is that not only CSPalpha accumulates, but other synaptic proteins also form clusters in disease tissue. The cellular and molecular mechanisms that lead to these presynaptic proteins accumulating at different distances in the periphery of amyloid deposits are however still unclear, a phenomenon that was confirmed in findings using multiple techniques to study both post-mortem human tissue and 5xFAD mice. These abnormal, irregularly shaped structures are reported to be dystrophic neurites which consist of common synaptic proteins (synaptophysin, SNAP-25, syntaxin, VGLUT-1, vesicular inhibitory amino acid transporter and now CSPalpha) and APP, yet lack in dendritic proteins, microtubule-associated protein 2 and β-tubulin immunoreactivity (Boutajangout et al., 2004; Sanchez-Varo et al., 2012; Kandalepas et al., 2013; Trujillo-Estrada et al., 2014; Sadleir et al., 2016; Ovsepian et al., 2019) which strongly suggests the presynaptic nature of these pathological structures. This suggests that at least some of the swollen structures that are classically in close contact with Aβ plaques in AD tissue and are likely to be morphologically disrupted presynaptic terminals. Similarly, CSPalpha accumulation positivity was also identified in scattered swollen WM axons identified in BA9 human tissue. It has been noted that not only presynaptic proteins but also cytosolic proteins such as BIN-1, Hsp70/90, Dynamin-1, clathrin heavy chain 1, phosphoglycerate

kinase 1, and 14–3-3 protein and lysosomal proteins such as lysosomal-associated membrane protein 1 (LAMP-1) (Chapter 6, Fig 6.3) and cathepsin D accumulate either within Aβ plaques or in adjacent dystrophic neurites (Liao et al., 2004; Condello et al., 2011; Gowrishankar et al., 2015; Sadleir et al., 2016; De Rossi et al., 2019). These dystrophic neurites form by disruption to anterograde axonal transport mechanisms by Aβ and tau, leading to organelle accumulation, cytoskeletal disruption, synaptic protein accumulation and eventual 'dying back' of axon degeneration (Adalbert et al., 2009; De Rossi et al., 2019; Hark et al., 2021).

Liao and colleagues (2004) investigated two AD brains by laser capture microdissection and reported 26 proteins enriched in Aβ plaques, yet CSPalpha protein was not identified (Liao et al., 2004). Consistent with other published reports, these terminals are remnants of damaged and dysfunctional synapses that become encompassed within vesicular membranes (Brion et al., 1991; Masliah et al., 1991, 1993; Zhao et al., 2007; Sanchez-Varo et al., 2012). Interestingly, CSPalpha protein has been shown to co-localise with lysosomal proteins, suggesting a mislocalisation into endosomal compartments such as vesicular bodies of axonal dystrophies where these proteins can form multiprotein molecular complexes (Benitez et al., 2015; Benitez and Sands, 2017; Sambri et al., 2017; Lee et al., 2018; Xu et al., 2018; Imler et al., 2019; Mukherjee et al., 2019). Further identification of complexed proteins is required to corroborate this possible mechanism as to whether or not Aβ deposition is a prerequisite for the development of such membranous structures or a by-product of a consequence of neuronal degeneration.

A limitation to these set of results from both post-mortem human and 5xFAD tissues however is the use of relevant markers to detect presynaptic dystrophies. Synaptophysin and SNAP-25 have been well characterised in their presence within

dystrophic neurites, but may not be sensitive enough, and certainly not captured within each dystrophy. APP and BACE1 have been reported to be localised within dystrophic neurites and axons that surround Aβ plaques, observed at the earliest stages of plaque formation making them more relevant markers of axonal dystrophy and may provide more information on the levels of Aβ production and abnormal processing (Kandalepas et al., 2013; Gowrishankar et al., 2015). Furthermore, it is widely known that there is no single synaptotoxic species of Aβ, but instead multiple conformers may play a more significant role, including the more toxic oligomeric Aβ (Pickett et al., 2016). It is however unclear from the present findings as to the species of Aβ associated with presynaptic terminals and localised with CSPalpha accumulations. The 6E10 clone antibody used in this study recognises 1-16 amino acids of the Aβ peptide along with APP which may not provide enough information on Aβ species, toxicity or biophysical structure. Use of Aβ antibodies that recognise different confirmations such as monomeric, fibrillar and oligomeric Aβ may be of more value. These can include use of monomeric $A\beta_{40}$ and $A\beta_{42}$ antibodies, targeting the more relevant amyloidogenic structure of the Aβ peptide (McDonald et al., 2012), NAB-61 which recognizes oligomeric and fibrillar Aβ (Lee et al., 2006) and OC, a conformation-specific antibody that can detect oligomeric Aβ arranged in parallel β sheets (Kayed et al., 2007; Wu et al., 2010b).

To the current knowledge, this is believed to be the first discovery of possible aggregates of CSPalpha, a potential novel pathological hallmark in AD. Taken together, these data suggest that CSPalpha is not only a more sensitive marker for synaptic loss and/or early presynaptic dysfunction compared to traditional synaptic markers in AD, but may be used as a pathological marker for early abnormal synaptic changes. This research has contributed a novel concept into the mechanistic changes underlying synaptic degeneration in AD and so it is plausible that CSPalpha, a co-chaperone with known protective functions, may be useful as a biomarker to provide

novel insights in synapse health and disease. Not only this, it would now be interesting to investigate whether this change is AD specific or is common to the neurodegenerative disease spectrum.

Chapter 4: CSPalpha in Other Neurodegenerative Diseases

4.1 Introduction

The role of synaptic proteins, especially the effects of their progressive loss, has been the subject of increasing interest since the relationship between synaptic loss in AD was first established (Davies et al., 1987). Synaptic dysfunction is a common feature across several neurodegenerative diseases, and contributes to, as opposed to a downstream effect, of neuronal loss (Wishart et al., 2006). However, little attention has been devoted to the role of synapse loss in other forms of dementia which have overlapping pathology, clinical diagnosis and symptoms. It has been suggested the early event of synaptic loss that occurs across several neurodegenerative diseases may well have a common molecular mechanism of pathogenesis directed at the synapse (Wishart et al., 2006). Despite the clinical and pathological differences between different dementias, distinguishing between them remains a significant challenge. There is currently no suitable biomarker with sufficient sensitivity to either stratify or differentiate patients across the dementia spectrum. Hence, investigations into the explanations of synaptic decline across the neurodegenerative disease spectrum may offer an insight into a universal mechanism in the pathogenesis of these diseases.

In line with this, this PhD study has focussed its research to explore the expression changes of CSPalpha protein, a vital presynaptic protein involved in the modulation of presynaptic terminal stability and/or severe degeneration (Fernández-Chacón et al., 2004; Wishart et al., 2012; Gillingwater and Wishart, 2013; Amorim et al., 2015) A mechanistic understanding of the role of CSPalpha protein has only been explored in some neurodegenerative diseases, namely AD, HD, PD, ANCL and spino-

cerebellar ataxia (Miller et al., 2003; Nosková et al., 2011; Wishart et al., 2012; Tiwari et al., 2015; Shirafuji et al., 2018; Caló et al., 2020). However, to the current date, there have been no known studies investigating the expression profile of CSPalpha protein across different dementias, where synapse loss may contribute to the pathogenesis of disease. Hence, it is important to understand the role CSPalpha may have across diseases in comparison to previous findings in AD.

4.1.1 Mixed Dementia

AD is a heterogenous disease with various pathological subtypes that can influence the clinical presentation and underlying biological mechanisms. Cerebrovascular pathologies are known to increase risk of AD and other dementias, suggesting that the pathological mechanisms of vascular disturbances can contribute to disease progression (Snyder et al., 2015). Cerebral amyloid angiopathy (CAA) is highly associated with Aβ peptide accumulation and other amyloid species, not only deposited as plaques in brain parenchyma but also in cerebral blood vessels, and is one of the most prevalent pathologies associated with AD, affecting an estimated 70-97% of individuals (Attems, 2005; Cisternas et al., 2019). CAA amyloid deposits are enriched in $A\beta_{40}$ (in comparison to parenchymal deposits enriched in $A\beta_{42}$) and can impair blood flow and produce small infarcts that can affect arteries, arterioles and capillaries of the cerebral cortices and leptomeningeal vessels (Perl, 2010; Serrano-Pozo et al., 2011). Non-Aβ CAA types also exist which include Familial British dementia (FBD) and Familial Danish dementia (FDD), identifiable by mutation of integral membrane protein 2B (BRI2) which can lead to the accumulation of ABri or ADan amyloid, respectively (Garringer et al., 2010). The risk of such cardiovascular changes is also evident in, VaD, which results from temporally and topographically dispersed ischaemic brain injuries, and is the second most common cause of dementia after AD, accounting for approximately 20% of dementia cases (O'Brien et al., 2003; Jellinger, 2007; Clare et al., 2010; Iadecola, 2010; O'Brien and Thomas,

2015; Wolters and Arfan Ikram, 2019). Synapse loss, the best biological correlate of dementia in AD, has been little studied in cases of mixed dementia with CAA and VaD. A loss of synaptic proteins has been reported in the temporal region of VaD brain (Clare et al., 2010; Sinclair et al., 2015). Furthermore, two studies on various subsets of VaD have found a similar reduction in the presynaptic marker protein synaptophysin compared to that found in AD (Zhan et al., 1993, 1994). More aligned with CAA pathology, genes related to GABAergic synapse pathways are enriched in CAA brains compared to healthy controls (Cisternas et al., 2020). In addition, colocalization between GABAergic synaptic markers and vascular amyloid was shown in a case of Aβ–CAA (Vidal et al., 2000; Cisternas et al., 2020). This makes amyloid angiopathy an important vascular contributor to AD and cognitive decline and hence requires further investigation into its contribution at the molecular level to synaptic changes.

4.1.2 Frontotemporal Lobar Dementia

Fronto-temporal lobar dementia (FTLD) is a heterogeneous disease which affects over 47.5 million people worldwide (Young et al., 2018). FTLD is neuropathologically characterised by conditions that can affect the temporal, frontal cortical and also cerebellar regions of the brain (Al-Sarraj et al., 2011; Tiwari et al., 2015; Johnen and Bertoux, 2019). There are three clinical types of FTLD which include behavioural variant FTD, progressive non-fluent aphasia and semantic variant primary progressive aphasia (Johnen and Bertoux, 2019). These variants of FTLD can also clinically overlap with amyotrophic lateral sclerosis (Lomen-Hoerth et al., 2002). FTLD can be classified according to the type of abnormal neuronal and glial proteinaceous inclusions present and their distribution across the brain (Broe et al., 2003; Josephs et al., 2011) The three main types of proteins associated with FTLD include: tau positive inclusions also known as FTLD-TAU, fused in sarcoma protein (FUS) in FTLD-FUS (Hutton et al., 1998; Neumann et al., 2006) and insoluble inclusions of

TDP-43 in FTLD-TDP (Forman et al., 2006) which represents ~ 50 % of cases (Arai et al., 2006; Neumann et al., 2006; Kwong et al., 2007; Bahia et al., 2013). Cortical TDP-43 pathology is morphologically classified to types A, B, C, and D (Mackenzie et al., 2011). It is currently very difficult to diagnose patients with FTLD without use of a correct clinical criterion. There have been only a few studies in FTLD brains that display a specific pattern of synaptic loss (Liu and Brum, 1996; Mackenzie et al., 2009). This was first reported by Brun and colleagues (1995) who found reduced synaptic density in the frontal lobe of FTLD brains (Brun et al., 1995). They later found a significant loss of synapses in the prefrontal cortex compared to healthy controls and similar expression levels comparable to those found in AD (Liu and Brum, 1996; Liu et al., 1999). This loss however is not apparent in other regions such as the parietal, inferior temporal and posterior cingulate regions (Liu and Brum, 1996). This has been supported by the reduction of several functional synaptic proteins which include Rab3A (vesicle recycling), synaptotagmin (calcium sensor), synapsin-I (vesicle docking and recycling), SNAP-25 (vesicle docking), syntaxin-I (vesicle docking) in the upper layers of FTLD frontal cortex and VGLUT- 1 (glutamate transporter) in caudate head and putamen (Ferrer, 1999; Clare et al., 2010; Riku et al., 2017).

4.1.3 Dementia with Lewy Bodies

Dementia with Lewy bodies (DLB) is the third most common form of dementia which affects over 7.5% of dementia sufferers (Walker et al., 2015). DLB occurs prior to Parkinsonism motor symptoms with pathologies that include intracellular accumulations of Lewy bodies that are misfolded deposits of alpha synuclein, a presynaptic chaperone protein (Braak et al., 2003). Core characteristics of DLB include progressive cognitive impairment, visual hallucinations, loss of executive function and Parkinson's-like extrapyramidal motor features which occur much later during disease progression (Outeiro et al., 2019). Lewy bodies are mainly localised

to the temporal lobe, cerebral cortex and substantia nigra brain regions (Outeiro et al., 2019). DLB pathology is commonly found with additional pathologies such as AD related NFTs and Aβ plaques as well as FTLD associated TDP-43 (Jellinger and Attems, 2007; Jellinger et al., 2007; Nakashima-Yasuda et al., 2007; Kovacs et al., 2008, 2013; Arai et al., 2009; Dugger et al., 2014; Howlett et al., 2015; McAleese et al., 2017). Interestingly, much less in known about the synaptic pathology in DLB, due to conflicting results in the literature. Synaptic density in DLB brains has been reported to be unchanged in comparison to levels in healthy controls (Samuel et al., 1997). Another study suggested that small alpha synuclein aggregates may affect dendritic spines, and showed a 50% marked reduction of the presynaptic markers alpha synuclein and syntaxin (Kramer and Schulz-Schaeffer, 2007; Revuelta et al., 2008). Similarly, presynaptic markers SNAP-25 and Rab3A were also altered in DLB cases correlating to the rate of cognitive decline (Bereczki et al., 2016; Henstridge et al., 2016). However, a study by Revuelta and colleagues (2008) found no association between Lewy body density and synaptophysin loss in DLB hippocampus (Revuelta et al., 2008).

Using CSPalpha as a primary outcome measure, it can be hypothesised that:

- A loss of CSPalpha expression results in synaptic dysfunction in other dementias, where synaptic dysfunction is also evident.

- Having discovered novel plaque-associated accumulation of CSPalpha in AD, these deposits may be present in other neurodegenerative diseases that are pathologically diagnosed with mixed AD pathologies, including Aβ deposition.

4.2 Aims

To investigate these hypotheses, the following objectives were formulated:

1) To examine post-mortem brain tissues of other dementias which include AD, mixed dementia, FTLD and DLB by performing a case-control study to analyse CSPalpha amounts within these neurodegenerative dementias.

2) To investigate whether CSPalpha accumulations are specific to amyloid deposition in AD or whether this is a more generalised phenomenon present in other neurodegenerative diseases.

3) Investigate the localisation of CSPalpha in ANCL, a lysosomal storage order linked to dementia that is directly caused by mutations in the *DNAJC5* gene.

4.3 Methods

The methods and materials used in this chapter are described fully in Chapter 2, Sections 2.4.3 and 2.6.1.2. Briefly, human brain tissue was homogenised by N. Meeson according to the protocol as described. Homogenates were run on 4-15% precast gels for western blotting and were immunoblotted with antibodies against housekeeping proteins NSE and synaptophysin to allow normalisation of sample concentrations according to neuronal and synaptic proteins, respectively. Five separate groups of post-mortem hippocampal brain samples were obtained from the London Neurodegenerative Diseases Brain bank for these studies which include: 1) Control (Braak 0-II) [n=8], 2) AD Braak stage VI [n=8], 3) mixed dementia Braak stage VI [n=8], 4) FTLD (TDP-43 Type A-C) [n=8] and 5) DLB [n=8] (Chapter 2, Section 2.3, Table 2.5). Tissues from the hippocampus were chosen for this study as this region has reduced synaptic proteins in AD and has been shown to be affected in other

dementias, either early or in late stages. Western blot data was tested for normality using Shapiro Wilks test, and statistically analysed using two-tailed independent t-tests. All data points have been presented with the exclusion of outliers calculated as outside two standard deviations away from the mean. Bar graphs show mean ± S.E.M.

From the same brains, a subset of cases [n=5] from the temporal cortex were obtained from the MRC London Neurodegenerative Diseases Brain Bank. It was not possible to obtain hippocampal sections from all samples due to the relative scarcity of these tissues. Where possible, the hippocampal tissues and temporal cortex sections were obtained from the same case. A further group of brain sections from the temporal cortex were obtained which include: PiD [n=2] and PSP [n=2] (Chapter 2, Section 2.3, Table 2.5). Briefly, 7 µm thick paraffin-embedded tissue sections were immunolabelled with antibodies against CSPalpha and either Aβ and/ or hyperphosphorylated tau to detect neuropathological hallmarks. Additionally, tissue sections from a patient with ANCL were obtained from the Oxford Brain bank and immunolabelled using the same techniques (Chapter 2, Section 2.3, Table 2.6). Slides were imaged using a Nikon Eclipse Ti-E 3 inverted microscope.

4.3.1 Demographical characteristics of post-mortem human tissue samples

Age, sex and PMD were quantified to determine whether they might have an effect on the data generated in this part of the study (Table 4.1). Following D'Agostino & Pearson testing, data was analysed using Kruskal–Wallis test which showed a nonsignificant trend towards a difference between control and other dementia groups for age ($H(5) = 8.305$, $p = 0.0810$) and no significant differences for PMD ($H(5) = 1.939$, $p = 0.747$). It should be noted however, that for some cases, PMD case details were not available and excluded from analysis which may have affected different

groups and overall differences observed. Chi-squared testing showed no statistically significant sex differences between the groups (χ^2 = 1.458, p = 0.834). These parameters are therefore not likely to influence the results observed in this study. Variations in age may have an overall effect on the outcome of the results.

Table 4.1. Summary of other neurodegenerative disease cases and controls used in the BA9 study.

Table shows the number of cases of each disease group, the % of female cases, average age at death and PMD (mean ± SEM). *Some PMD details were missing from disease type.

Disease Type	Number of Cases	Female (%)	Age (Years) Mean ± SEM	PMD (Hours) Mean ± SEM
Control	8	75	75.9 ± 3.5	46.1 ± 7.4
AD	8	50	79.8 ± 2.8	49.1 ± 7.6
Mixed Dementia	8	62.5	86.9 ± 2.3	39.6 ± 11.6*
FTD	8	62.5	75.8 ± 3.3	48.1 ± 7.8
DLB	8	50	77.1 ± 3.2	31.0 ± 6.7*

4.4 Results

4.4.1 CSPalpha expression is downregulated in AD hippocampus

The hippocampal brain region is primarily and severely affected in AD (Braak and Braak, 1991) and is characterised by synaptic loss which precedes neuronal loss. Tiwari and colleagues (2015) have previously shown that in mild-stage and severe-stage AD, CSPalpha expression is significantly reduced in forebrain areas including the hippocampus (Tiwari et al., 2015). To independently replicate these findings, the levels of CSPalpha were compared in a distinct set of hippocampal lysates prepared from post-mortem severe AD (Braak stage VI) and controls by western blot analysis. Brains were age-matched and obtained with the lowest possible PMD from the London Neurodegenerative Diseases brain bank.

CSPalpha protein was identified at ~35 kDa and amounts of CSPalpha were normalised to that of the neuronal housekeeping marker, NSE (47 kDa) (Fig 4.1a). NSE is an enzyme constitutively expressed in neurons and can be used to control for neuron loss in AD (Haque et al., 2018). CSPalpha protein expression was also compared to that of the presynaptic vesicle-specific protein synaptophysin (38 kDa), a commonly used marker for synaptic content (Wiedenmann and Franke, 1985), to allow quantification of CSPalpha amounts as a proportion of remaining synapses (Fig. 4.1a). A doublet of bands was observed for CSPalpha, which likely reflects posttranslational modifications of CSPalpha such as palmitoylation (Greaves et al., 2008) and so total CSPalpha amounts (upper and lower bands) were used in the analysis.

Quantification of immunoblot data showed a statistically significant reduction in CSPalpha amounts in the hippocampus of severe AD brains (0.19 ± 0.04) compared to controls (1.00 ± 0.21) when normalised to NSE (t=3.818, p=0.0019 (Fig 4.1b)) and a significant reduction of CSPalpha relative to synaptophysin in AD (0.19 ± 0.06) compared to controls (1.00 ± 0.16) (t=3.843, p=0.0018 (Fig 4.1c)). Synaptophysin levels were found to be reduced in AD brain when normalised to NSE (AD (0.55 ± 0.03) and control (1.00 ± 0.19) (t=4.521, p=0.0005 (Fig 4.1d)). This suggests that synapses are lost in remaining neurons in AD, as previously shown (Tiwari et al., 2015). These findings of CSPalpha protein level reductions in AD brain confirms that CSPalpha loss is not only due to neuronal or synapse loss, hence making it a suitable neuropathological marker for early changes in synaptic dysfunction that precede synapse loss in AD.

The upper band of CSPalpha is postulated to represent a palmitoylated form of the protein with this modification assisting in the attachment of CSPalpha to hydrophobic membranes including synaptic vesicles (Greaves et al., 2012). The percentage of palmitoylated CSPalpha protein (upper band) was compared to total CSPalpha (upper band + lower band) to determine whether in AD hippocampus, the levels of this protein modification are altered. It was found that almost half of CSPalpha protein in both control and AD brain was palmitoylated, however there were no observable differences in the amounts of CSPalpha palmitoylation between control (58.08 ± 4.95) and severe AD brain (57.27 ± 2.80) (t=0.1429, p=0.888 (Fig 4.1e). This suggests that in late-stage AD, CSPalpha is likely to be both palmitoylated and not palmitoylated.

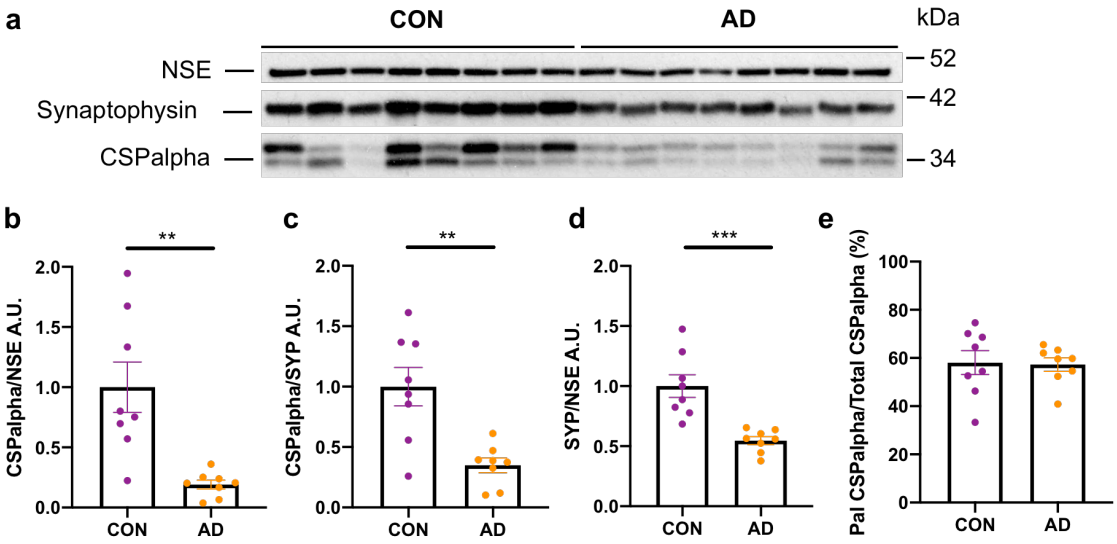

Figure 4.1. CSPalpha protein expression is reduced in AD hippocampus.

a) Western blots showing protein expression of CSPalpha (~35 kDa), NSE (47 kDa) and synaptophysin (38 kDa) in control (CON) (Braak 0-II) and AD (Braak VI) post-mortem hippocampal brain. Bar charts show relative levels (arbitrary units (A.U.)) of CSPalpha when normalised to **b)** the neuronal marker protein NSE and **c)** the synaptic marker protein synaptophysin, **d)** synaptophysin amounts relative to NSE. Following D'Agostino and Pearson normality testing, data were analysed using a two-tailed independent t-test. Data are expressed as fold change of control. **e)** percentage palmitoylated CSPalpha (upper band) compared to total CSPalpha levels (upper and lower bands). Data shown is mean ± S.E.M. [n = 8 cases per group]. ** $p<0.001$, ***$p<0.0001$.

4.4.2 CSPalpha expression is unaltered in mixed dementia

It is conceivable that CSPalpha protein expression may be also be reduced in cases of mixed dementia, similar to findings observed in AD hippocampus where synaptic loss is also apparent. Hence, CSPalpha expression in post-mortem hippocampal samples from cases with a pathological diagnosis of mixed dementia with amyloid angiopathy either as primary or secondary neuropathological diagnosis in comparison to the same control subjects were investigated. Immunoblotting results show a commonly found double band of CSPalpha at ~ 35 kDa. Bands were measured as total protein intensity of upper and lower bands and normalised to NSE and synaptophysin marker proteins (Fig 4.2a), as described above. There were no statistically significant changes in mixed dementia relative to controls in CSPalpha expression when normalised to NSE (mixed dementia (0.51 ± 0.19) and control (1.00 ± 0.21) ($U = 15$, $p = 0.152$ (Fig 4.2b)) or synaptophysin (mixed dementia (0.63 ± 0.11) and control (1.00 ± 0.19) ($t = 1.595$, $p = 0.135$ (Fig 4.2c)). However, the mean levels of CSPalpha appeared higher in controls than in mixed dementia, but this was not significant possibly due to the variability between samples. Synaptophysin levels were unchanged when normalised to NSE (mixed dementia (0.81 ± 0.14) and control (1.00 ± 0.04) ($t = 1.248$, $p = 0.232$ (Fig. 4.2c). This data shows that CSPalpha, although statistically unaltered, may be lost in hippocampus of mixed dementia brains, a region in which no loss of the presynaptic protein synaptophysin was detected.

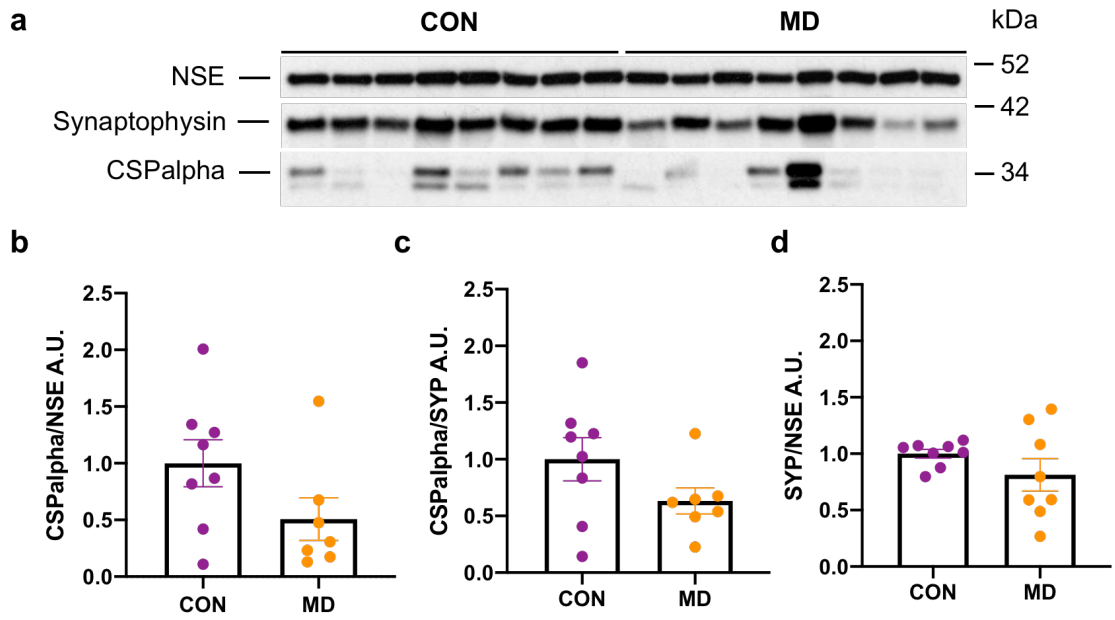

Figure 4.2. CSPalpha expression is unchanged in mixed dementia.

a) Western blots showing protein expression of CSPalpha, NSE and synaptophysin in control and mixed dementia (MD) post-mortem hippocampal brains. **b)** Bar chart show levels of CSPalpha were unchanged when normalised to NSE. Following D'Agostino and Pearson normality testing, data were analysed using non-parametric two-tailed Mann Whitney U test. **c)** Levels of CSPalpha were unchanged when normalised to synaptophysin. **d)** Levels of synaptophysin were unaltered in mixed dementia hippocampus when normalised to NSE. Following D'Agostino and Pearson normality testing, data were analysed using a parametric two-tailed independent t-test. Data are expressed as fold change of control. Data shown is mean ± S.E.M. [n = 8 cases per group].

4.4.3 CSPalpha expression is reduced in FTLD

FTLD is a distinct form of dementia affecting the frontotemporal region, which includes the hippocampus, and is also characterised by neurodegeneration. Here, CSPalpha expression changes were examined by comparing post-mortem samples from patients with a pathological diagnosis of FTLD-TDP (Subtypes A-C) with control subjects. CSPalpha was significantly reduced in the hippocampus of FTLD brains (0.21 ± 0.04) and relative to controls (1.00 ± 0.19) following normalisation of protein amounts to NSE ($t = 3.742$, $p = 0.0025$ (Fig 4.3a-b)) and to synaptophysin (FTLD (0.26 ± 0.01) and control (1.00 ± 0.17)) ($t = 4.037$, $p = 0.0014$ (Fig 4.3a, c)). This result suggests that in cases of FTLD, CSPalpha protein levels are reduced in remaining neurons of the hippocampus. The reduction of CSPalpha against synaptophysin levels, suggests that CSPalpha is not a downstream effect of synaptic loss in this region. However unlike in AD, synaptophysin levels were unaltered when normalised to NSE (FTLD (0.85 ± 0.13) and control (1.00 ± 0.07)) ($t = 1.060$, $p = 0.307$ (Fig 4.3d)) suggesting that the resulting CSPalpha loss occurs prior to early synaptic dysfunction and synapse loss in FTLD.

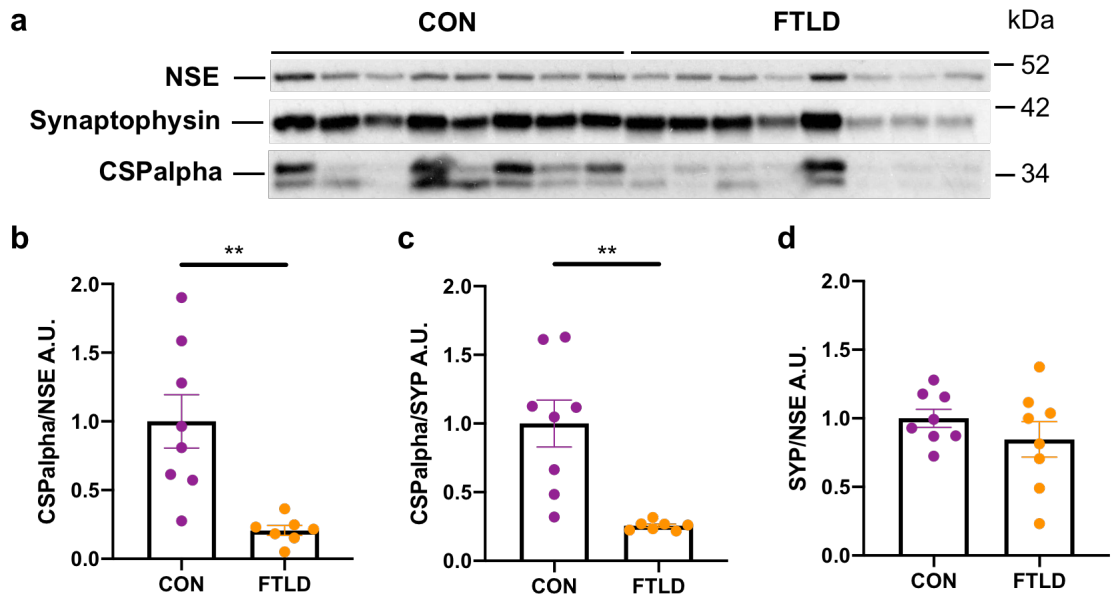

Figure 4.3. CSPalpha expression is downregulated in FTLD.

a) Western blots showing protein expression of CSPalpha, NSE and synaptophysin in control and FTLD post-mortem hippocampal brains. **b)** Bar charts show levels of CSPalpha significantly reduced in FTLD when normalised to the housekeeping protein NSE and **c)** synaptophysin. **d)** Levels of synaptophysin were unaltered in FTLD hippocampus when normalised to NSE. Following Shapiro-Wilk's normality testing, data were analysed using a parametric two-tailed independent t-test. Data are expressed as fold change of control. Data shown is mean ± S.E.M. [n = 8 cases per group]. ** $p<0.001$.

4.4.4 CSPalpha expression is unaltered in DLB

CSPalpha protein expression changes were next determined in post-mortem DLB hippocampus relative to control samples. Here, no significant changes were found in CSPalpha protein levels between DLB (1.28 ± 0.47) and controls (1.00 ± 0.21) when normalised to NSE ($t = 0.547$, $p = 0.593$ (Fig 4.4a-b)) or to synaptophysin (DLB (1.41 ± 0.37) and control (1.00 ± 0.16)) ($t = 1.001$, $p = 0.334$ (Fig 4.4a, c)). The apparent elevation of CSPalpha amounts observed however, may be due to the variability of samples, but the possibility of a valid result cannot be excluded. Synaptophysin levels were also unchanged when normalised to NSE (DLB (0.97 ± 0.19) and control (1.00 ± 0.11)) ($t = 0.1571$, $p = 0.877$ (Fig 4.4d). Some of the DLB cases were also reported to be diagnosed with mixed AD-like Braak pathology. However, when examined separately, CSPalpha amounts were not altered in DLB-AD cases relative to controls [n=4]. This suggests that CSPalpha amounts are not dysregulated in DLB, at least in the hippocampus. With a potential elevation in CSPalpha in remaining neurons, it can be suggested that there may be a greater preservation of synapses within the hippocampal region of DLB brain.

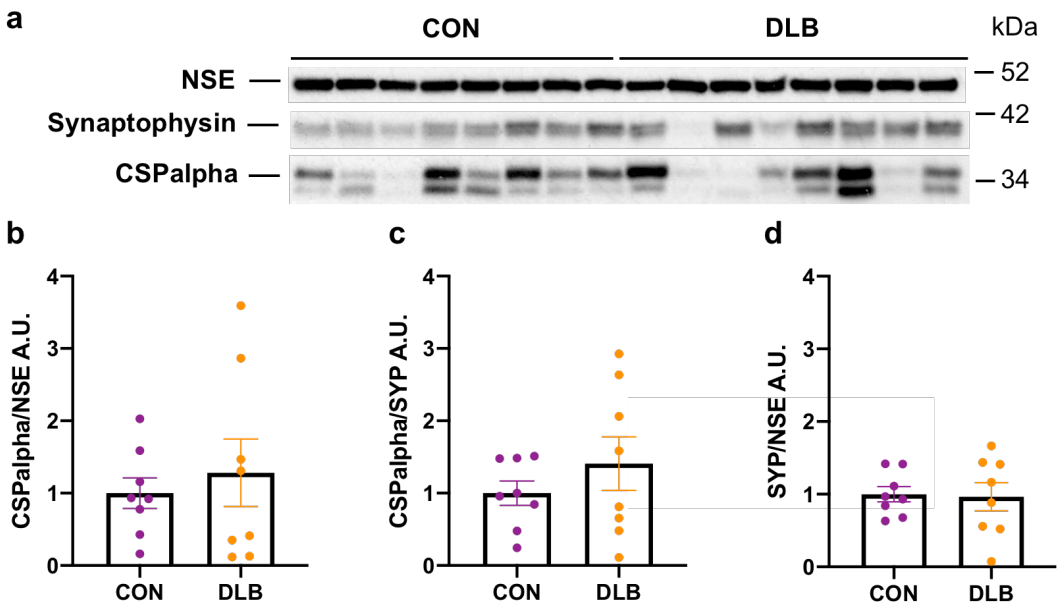

Figure 4.4. CSPalpha expression is unchanged in DLB.

a) Western blots showing protein expression of CSPalpha, NSE and synaptophysin in control and DLB post-mortem hippocampal brains. **b)** Bar charts show levels of CSPalpha unchanged when normalised to NSE and **c)** synaptophysin. **d)** Levels of synaptophysin were unaltered in DLB hippocampus when normalised to NSE. Following D'Agostino and Pearson normality testing, data were analysed using a two-tailed independent t-test. Data are expressed as fold change of control. Data shown is mean ± S.E.M. [n = 8 cases per group].

To summarise these immunoblotting results, significant reduction in CSPalpha protein amounts were observed in AD and FTLD brain compared to healthy control brain. This reduction was evident when normalized to NSE suggesting that CSPalpha is lost prior to neuron loss. Similarly, normalization to synaptophysin in AD suggests that CSPalpha is reduced before the loss of remaining synapses. This suggests that CSPalpha may play a role in presynaptic dysfunction in the hippocampus of both AD and FTLD. However, unlike AD, synapses in the hippocampus in FTLD brains are not lost, suggesting that CSPalpha reduction may be caused by an alternative mechanism. A non-significant reduction of CSPalpha was also found in cases of mixed dementia similar to AD. No significant changes in CSPalpha protein amounts were evident in DLB. The data obtained from these analyses are summarized below (Table 4.2). Due to some degree of variability between post-mortem brain samples, changes between control and disease states were not always possible to define definitively. Correlation analysis might provide more informative data regarding the relationship between CSPalpha and synapse/neuron loss.

Table 4.2. Summary of mean ± S.E.M. reduction (↓) and elevation (↑) of total protein amounts in disease (AD, mixed dementia, FTLD and DLB) relative to control samples.

Data normalisation of CSPalpha to NSE and synaptophysin (SYP) and SYP normalisation to NSE. ** $p<0.001$, ***$p<0.0001$.

Disease	CSPalpha/NSE	CSPalpha/SYP	SYP/NSE
AD	0.81 ± 0.21 (↓) **	0.65 ± 0.17 (↓) **	0.45 ± 0.10 (↓) ***
Mixed Dementia	0.49 ± 0.02 (↓)	0.37 ± 0.23 (↓)	0.19 ± 0.15 (↓)
FTLD	0.79 ± 0.21 (↓) **	0.74 ± 0.18 (↓) **	0.15 ± 0.15 (↓)
DLB	0.28 ± 0.51 (↑)	0.41 ± 0.41 (↑)	0.03 ± 0.22 (↓)

4.4.5 Plaque-associated CSPalpha accumulations are a common feature in amyloid diseases and tissues with Aβ deposition

Previously in Chapter 3, it was shown that in AD post-mortem brain and in the brain of the 5xFAD mouse model, CSPalpha accumulates in the presence of Aβ plaques. Since CSPalpha expression was found to be altered in different dementia forms other than AD, it was next important to determine whether in these diseased brains CSPalpha also accumulates and, if so, whether such accumulations are associated with the presence of Aβ plaques. This would enable a greater insight into whether this abnormal change in CSPalpha protein is linked to either general synaptic failure within these diseases or is in fact a process specific to dysfunctional APP processing.

To confirm this idea, the notion that plaque associated CSPalpha accumulations were evident not only in AD but may also be present in other neurodegenerative disease with mixed pathologies was explored. Using a subset of brains (n=5) from the samples used in western blotting analysis (n=8), it was first attempted to understand whether CSPalpha accumulations were present in healthy brains with and without Aβ deposition, including brains from known Aβ associated diseases such as AD and mixed dementia. Here, immunofluorescence techniques were used to co-label post-mortem human brains from the temporal cortex region with antibodies specific to CSPalpha and Aβ. Brains from control (Braak 0-II), AD (Braak VI) and mixed dementia (Braak VI) were compared.

Diffuse staining of CSPalpha in the neuropil was found in all tissue sections within the gray matter of the temporal cortex, confirming its presynaptic localisation. Three control cases (Braak stage 0-II) were identified with frequent sparse accumulations of CSPalpha in proximity with diffuse and neuritic cored Aβ plaques (Fig 4.5b, Table 4.3). In contrast, two other control cases (Braak stage I-II) did not show positive labelling of either protein (Fig 4.5a, Table 4.3). This confirmed the previous findings

(Chapter 3, Section 3.4.6) that cases with no pathological deposition of Aβ, do not present with abnormal CSPalpha accumulations, yet cases which show Aβ deposits also show deposition of CSPalpha, likely some of which are likely a part of presynaptic dystrophies.

Similar to previous results in BA9 and hippocampus (Chapter 3, Section 3.4.6), numerous CSPalpha accumulations decorating diffuse and neuritic cored plaques in the temporal cortex of severe AD were found (Fig 4.5c). Immunoreactivity of amorphous CSPalpha deposits was observed in the periphery of each plaque in the same region of mixed dementia brain (Fig 4.5d). This was predictable due to the majority of coexisting pathologies between mixed dementia and AD cases. This is not only supported by a possible reduction in CSPalpha expression in mixed dementia brain which precedes synapse loss, but also the accumulation and/or potential release of CSPalpha protein that is sequestered within Aβ deposits. Interestingly, in cases of both mixed dementia and AD, CSPalpha accumulations were found to associate with cerebrovascular Aβ-deposits in some cortical arteries and arterioles, with evidence of dysphoric angiopathy (flamelike Aβ deposits that radiate into the neuropil from the vessel wall) (Fig 4.6a, b, Chapter 6, Fig 6.2). This suggests that Aβ transport between the neuropil and blood circulation may be involved in early synaptic changes that culminate in synaptic dysfunction and loss. It can be suggested that even though the causal mechanisms that lead to Aβ plaque formation may differ between parenchymal Aβ and Aβ-CAA, the downstream effect of toxic aggregated Aβ species may lead to synaptic dysfunction in both. These data further suggest that CSPalpha accumulations may be a suitable marker for both early-stage synaptic dysfunction and late-stage synapse loss within Aβ-related dementias.

Table 4.3. Qualitative characterisation of control brain hippocampus.

Comparisons of the presence of Aβ plaques and Braak staging with CSPalpha deposits in control brain. Numbers in parentheses refer to cases from Chapter 2, Section 2.3, Table 2.5.

Control Brain	Amyloid Diagnosis	Braak Stage	Amyloid Plaques Present?	CSPalpha Deposits Present?
1	Mild focal amyloid angiopathy	0	Many diffuse and some neuritic cored plaques	Frequent (dispersed)
3	-	II	Diffuse and neuritic cored plaques	Frequent (clustered)
4	Age-related changes	II	None	None
6	Age-related changes	II	Some diffuse plaques	Sparse
8	Mild age-related changes	I	None	None

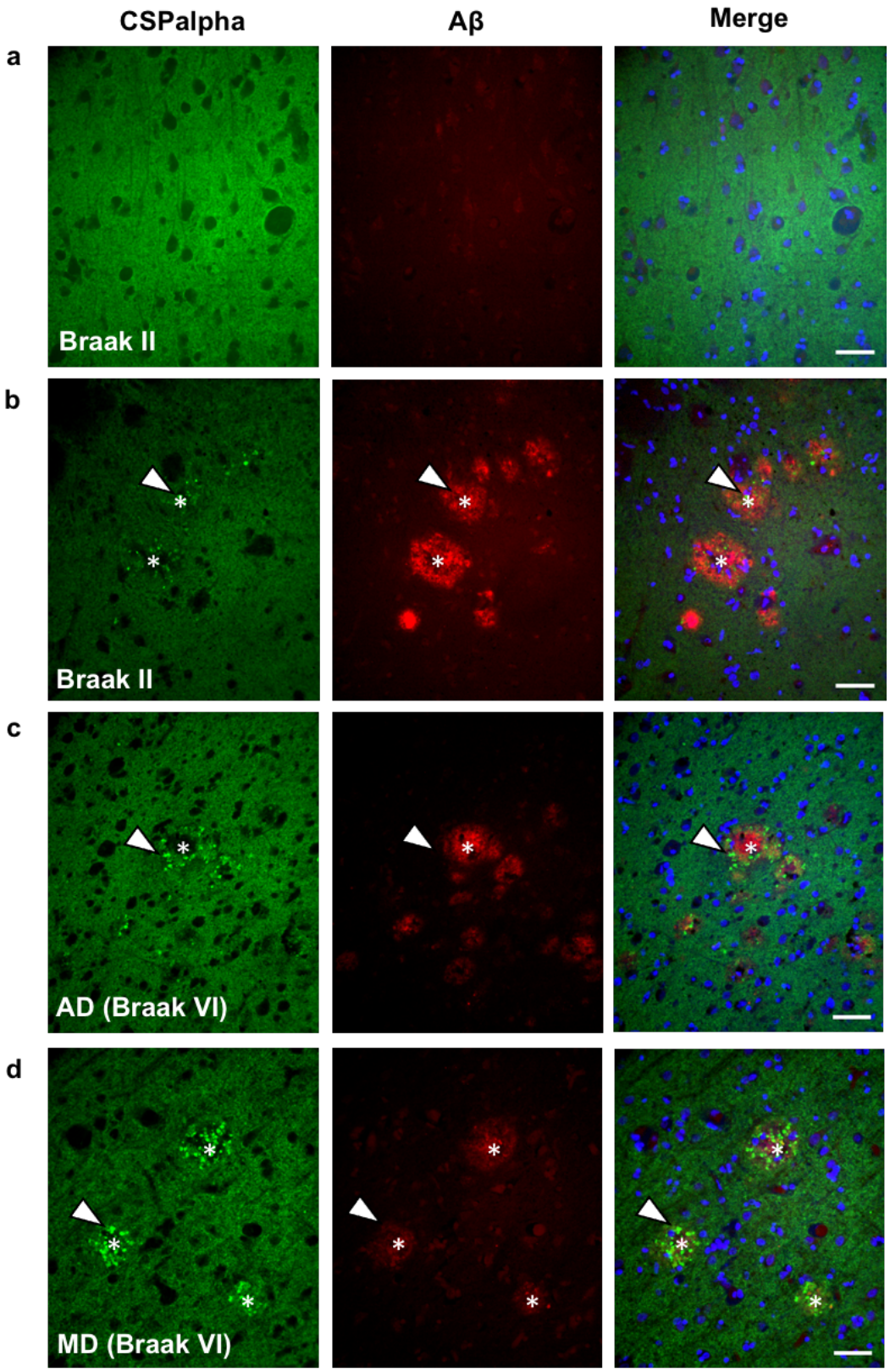
CSPalpha
Aβ
Merge
a
Braak II
b
Braak II
c
AD (Braak VI)
d
MD (Braak VI)

Figure 4.5. Plaque associated CSPalpha accumulations present in early Braak stage and amyloid diseases.

Representative immunofluorescence co-labelling of post-mortem temporal cortex brains sections for **a)** control (Braak II) without Aβ plaques, **b)** control (Braak II) with Aβ plaques, **c)** AD (Braak stage VI) and **d)** mixed dementia (MD) (Braak stage VI). Sections labelled with CSPalpha (*green*) and Aβ (*red*) antibodies. DAPI (*blue*) was used to stain nuclei [n=5 per group]. *Arrows* indicative of CSPalpha accumulations and *asterisks* label the Aβ plaque core. Magnification 40x. Scale bar 50 μm.

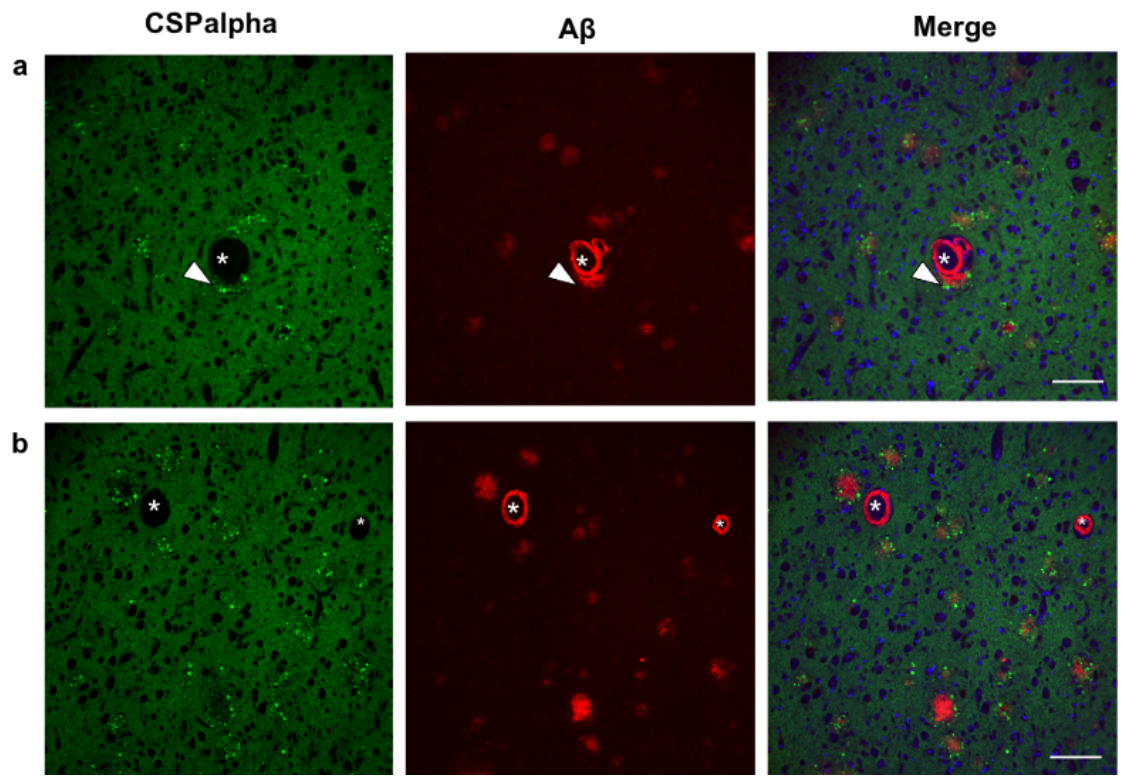

Figure 4.6. CSPalpha accumulations surround Aβ-CAA-associated blood vessels and parenchymal Aβ plaques

Representative immunofluorescence co-labelling of post-mortem temporal cortex for **a)** mixed dementia (Braak VI) with CSPalpha surrounding Aβ plaques and CAA in small arterioles and **b)** mixed dementia (Braak VI) with CAA that are not associated with CSPalpha accumulations. Sections labelled with CSPalpha (*green*) and Aβ (*red*) antibodies. DAPI (*blue*) was used to stain nuclei. *Triangular arrows* indicative of CSPalpha accumulations and *asterisks* label the Aβ-lined vessel centre. Magnification 20x. Scale bar 100 μm.

4.4.6 Plaque-associated CSPalpha accumulations are present in FTLD and DLB brains

The next aim was to explore the localisation and distribution of CSPalpha in FTLD and DLB brains, including those cases with and without mixed-AD amyloid pathologies (Table 4.4). This would answer the question as to whether accumulations of CSPalpha are specific to Aβ related diseases or are found in diseases where general synapse loss is profound. Tissue sections of temporal cortex were co-labelled with an anti-CSPalpha and anti-Aβ antibody. DAPI was applied to mark cellular nuclei. Specific CSPalpha background staining was evident within each tissue section. Interestingly, three FTLD and DLB brains were found to contain amyloid plaque deposits in line with their mixed pathological diagnosis and these cases also showed CSPalpha immunoreactive deposits, the density of which was substantially lower than observed in AD (Fig 4.7a, c). On the other hand, two FTLD and DLB brains did not show either protein accumulation (Fig 4.7b, d). This suggests that CSPalpha accumulations are Aβ plaque-associated but may not be determined by disease-specific changes. CSPalpha labelling was absent in negative controls, confirming the specificity of staining (Fig 4.8).

Table 4.4. Qualitative characterisation of FTLD and DLB brains.

Comparisons of the presence of Aβ plaques and Braak staging with CSPalpha deposits in FTLD and DLB brains. Numbers in parentheses refer to cases from Chapter 2, Section 2.3, Table 2.5.

FTLD Brain No.	Amyloid Diagnosis	Braak Stage	Amyloid Plaques Present?	CSPalpha Aggregates Present?
27	Amyloid angiopathy	V	Diffuse plaques and neuritic cored plaques	Frequent
29	Mild to moderate vascular pathology	III	Diffuse plaques and neuritic cored plaques	Frequent
30	-	-	None	None
31	-	-	None	None
32	Mild amyloid angiopathy	IV	Diffuse plaques and neuritic cored plaques	Frequent

DLB Brain No.	Amyloid Diagnosis	Braak Stage	Amyloid Plaques Present?	CSPalpha Aggregates Present?
34	-	III	Few small diffuse plaques	Few and sparse
35	-	-	Diffuse plaques	Frequent and sparse
36	-	-	None	None
37	Moderate amyloid angiopathy	IV	Few	Frequent and sparse
40	-	II	None	None

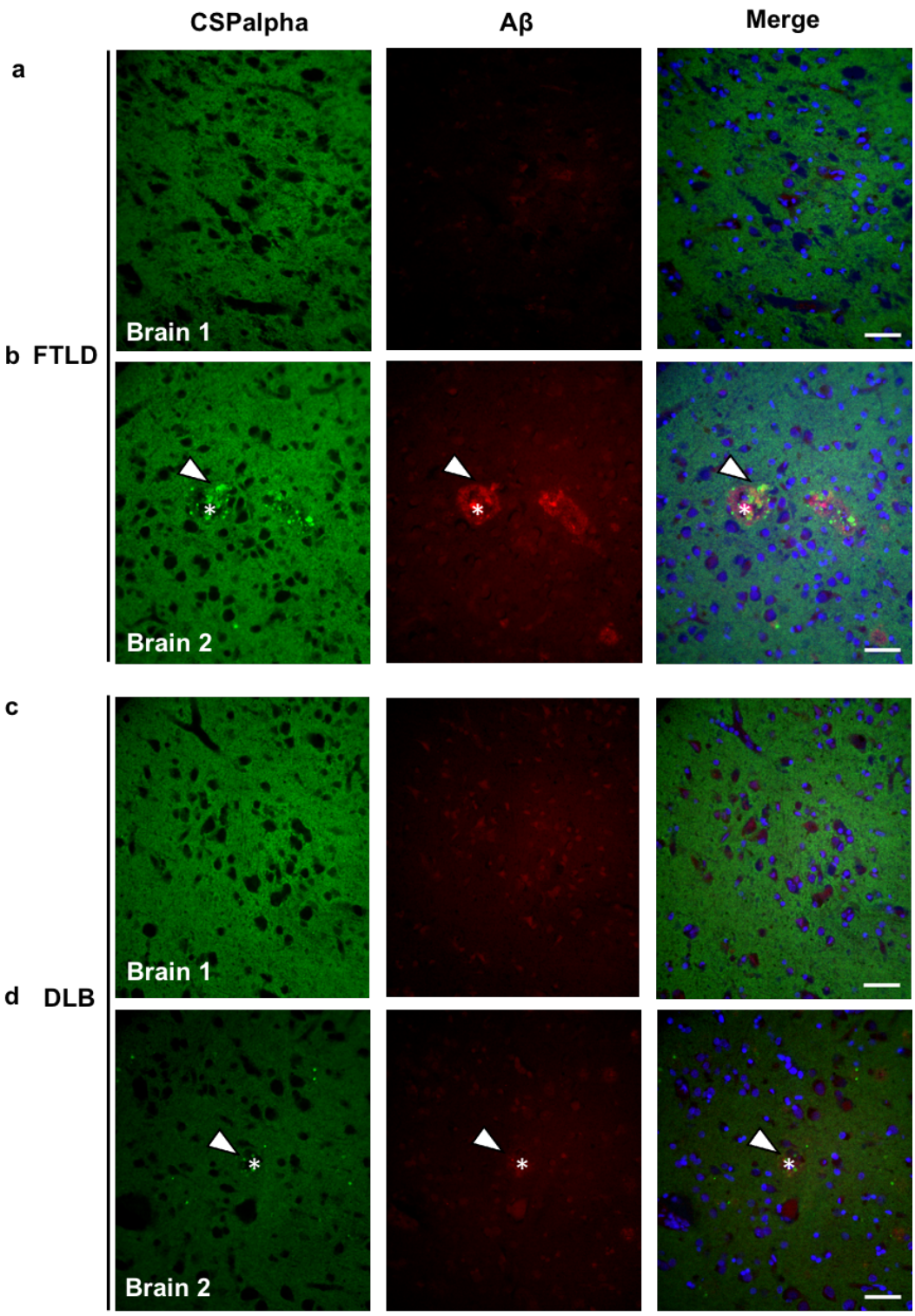
CSPalpha
Aβ
Merge
a
b FTLD
Brain 1
Brain 2
c
d DLB
Brain 1
Brain 2

Figure 4.7. Evidence of CSPalpha accumulations in FTLD and DLB brains in the presence of amyloid plaques.

Representative immunofluorescence images of post-mortem temporal cortex brains sections in **a)** FTLD without Aβ plaques, **b)** FTLD with Aβ plaques, **c)** DLB without Aβ plaques and **d)** DLB with Aβ plaques. Sections were immunolabelled with antibodies against CSPalpha (green), Aβ (*red*) and DAPI (*blue*) [n=5 per group]. *Arrows* indicative of CSPalpha accumulations and *asterisks* label the Aβ plaque core. Magnification 40x. Scale bar 50 μm.

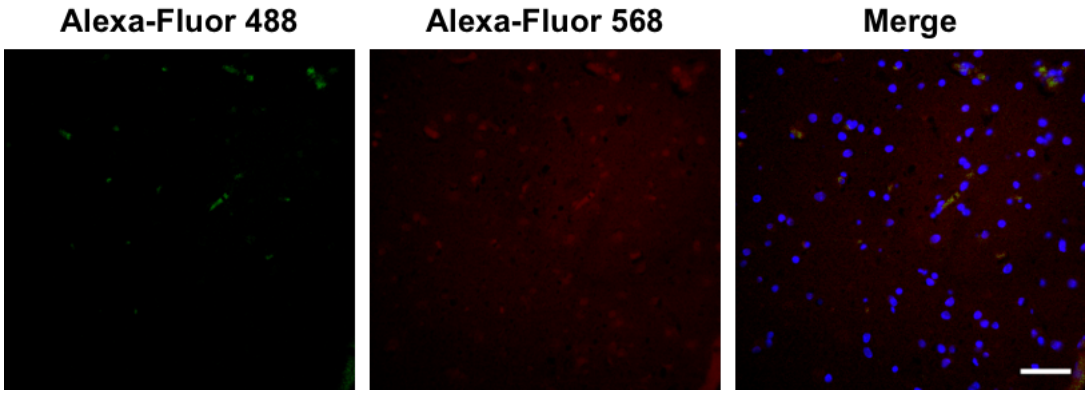

Figure 4.8. Negative control for CSPalpha antibody staining of post-mortem human brain.

Representative images of negative control of post-mortem temporal cortex brains sections. Sections were probed only with secondary antibodies for alexa-fluor 488 (*green*), alexa-fluor 568 (*red*) and DAPI (*blue*), where only slight background staining is visible. Magnification 40x. Scale bar 50 μm.

4.4.7 CSPalpha accumulations are not evident in tauopathy brains unless Aβ deposits are present

Having confirmed that CSPalpha accumulations are associated with Aβ deposits and are not disease specific, it was important to further explore this discovery by investigating diseases that do not show Aβ pathology, and also to further investigate any association with hallmark tau pathologies. Tauopathies are a family of neurodegenerative disorders characterised by the abnormal deposition of tau protein in the brain. Tissue from two primary tauopathies, namely PiD and PSP were examined. PiD is a 3R-tau predominant tauopathy that is characterized by spherical tau-positive intraneuronal “Pick bodies” and glial inclusions through limbic and neocortical regions (Irwin, 2016). Tau pathology is most prominent in the frontotemporal neocortex, but also significant sub-cortical tau pathology can accumulate in the basal ganglia and WM. PSP on the other hand is a 4R tau-linked tauopathy with characteristic hallmark pathologies of globose tau inclusions mainly located in brainstem and subcortical neurons, NFTs present in gray matter, “tufted astrocytes” and oligodendrocytic “coiled bodies” in the WM of the neocortex (Irwin, 2016).

Temporal cortex from PSP and PiD were co-labelled for CSPalpha, hyperphosphorylated tau (AT8 – sites Ser202, Thr 205) and for Aβ (6E10). The temporal cortex is severely affected within these diseases and severe atrophy is evident. Here, diffuse labelling of CSPalpha was found within the neuropil confirming its presynaptic localisation (Fig 4.9a-b). Characteristic tau pathology was identified in the temporal cortex of both PiD with the presence of AT8-positive Pick’s bodies along with sharply circumscribed neuronal cell bodies and tufted astrocytes (Fig 4.9a). PSP cases presented with abnormal tau changes with argyrophilic tau inclusions confirmed in all cases including globose NFTs and neuropil threads (Fig 4.9b).

In PiD, no evidence of any CSPalpha accumulations was identified amongst spherical cytoplasmic Pick's bodies or any evidence of Aβ deposition using the Aβ antibody (Fig 4.9a). This is in line with the current hypothesis since it was not expected to find CSPalpha accumulations within these cases. However, one out of two PSP cases showed Aβ deposition along with CSPalpha accumulations in the surrounding peripheral area (Fig 4.9b). This case had been pathologically diagnosed with early Alzheimer changes, which may account for the occurrence of Aβ deposition. The second case showed no staining for either CSPalpha or Aβ. These results provide further evidence that CSPalpha accumulations are not related to pathological tau changes and provides stronger support for an Aβ-associated synaptotoxic mechanism underlying CSPalpha accumulation in neurodegenerative diseases.

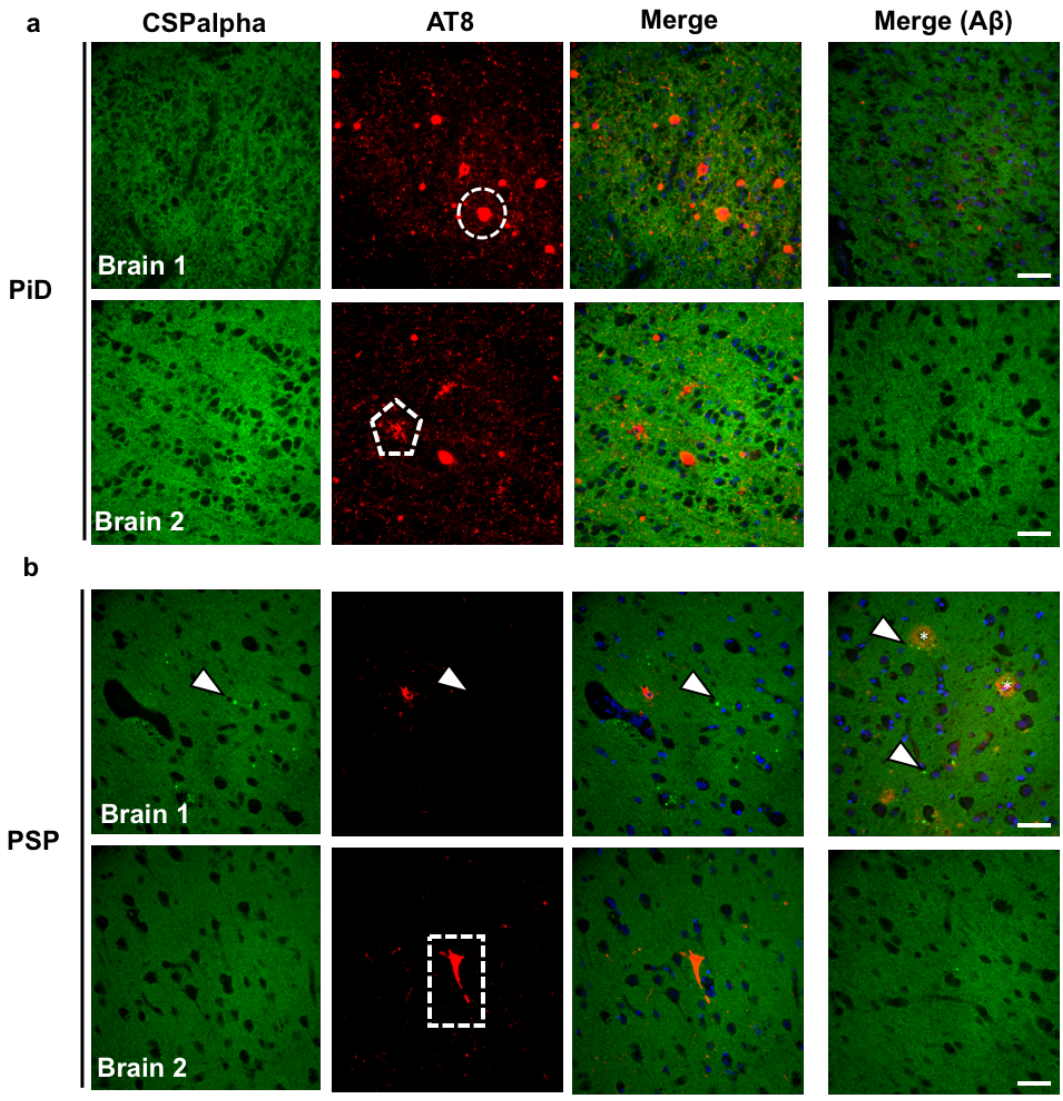

Figure 4.9. Plaque-localised CSPalpha accumulations found in some PSP but not in Pick's disease brains.

Representative immunofluorescence images of post-mortem temporal cortex from **a)** PiD and **b)** PSP. Sections were immunolabelled with antibodies against CSPalpha (green), AT8 (red), Aβ (red) and DAPI (blue). *Arrows* - CSPalpha accumulations, *asterisks* - plaque core, *dashed circle* - Pick's bodies in PiD brain, *dashed pentagon* – ramified astrocyte and *dashed rectangle* – NFT. Magnification 40x. Scale bar 50 μm. [n=2 per group].

4.4.8 CSPalpha accumulations are not evident in ANCL brain

ANCL is an autosomal dominant lysosomal storage disorder that is also characterised by dementia and neurodegenerative phenotypes (Kohlschütter et al., 2019). CSPalpha is known to be directly linked to this disorder, as mutations in the *DNAJC5* gene, which encodes CSPalpha, cause ANCL (Nosková et al., 2011). Interestingly, it has been reported in the literature that CSPalpha forms intracellular accumulations in ANCL, although this has only been shown biochemically and not through visual assays such as immunohistochemistry (Benitez et al., 2015). Hence, Aβ plaque-associated CSPalpha accumulations found in AD and other neurodegenerative diseases, could be linked to the intracellular aggregates of CSPalpha found in ANCL.

To explore this possibility and add a better mechanistic insight to the current findings, tissue was obtained from an ANCL case, harbouring a L115R mutation, whereby a leucine amino acid is altered to an arginine in the *DNAJC5 gene*. This mutation in CSPalpha lies within the CSD and has been reported to cause disruption to CSPalpha palmitoylation thereby altering the hydrophobicity of the protein and its association with membranes (Greaves et al., 2012). The precise functional effects of this mutation on CSPalpha function has not been fully established.

Tissue sections of BA9 and temporal cortex from ANCL brain were immunolabelled and compared to a healthy age-matched control. Sections were probed with an antibody against CSPalpha and co-stained with DAPI. Examination of the cortical brain sections revealed a marked enlargement of the cortical pyramidal neurons, not mistaken as ‘larger nuclei’ or holes caused by antigen retrieval methods which can disrupt the tissue (Fig 4.10). In ANCL affected swollen neurons, there was also evidence of nuclei displacement to the base of the apical dendrite and a markedly swollen cell body compared to the typical pyramidal shape of neurons in healthy

control brain (Fig 4.10). Diffuse CSPalpha neuropil staining was confirmed in both ANCL and healthy control tissues, consistent with synaptic localisation of CSPalpha in BA9 and temporal cortex. However, the intensity of staining was markedly reduced in ANCL brain (Fig 4.10). This is in line with only one other study that has shown reduced immunofluorescence labelling of CSPalpha in tissue from an ANCL case with an L115R mutation (Henderson et al., 2016). Another study showed, with biochemical characterisation, reduced CSPalpha protein amounts in a similar case when compared to healthy controls (Nosková et al., 2011; Henderson et al., 2016).

In both BA9 and temporal cortex, neurons were found containing auto fluorescent storage material (AFSM) evident at both 460 nm and 519 nm emission wavelengths. This is common in NCLs and is widely reported (Seehafer and Pearce, 2009; Benitez et al., 2015). No evidence of possible CSPalpha accumulations were found as previously characterised in AD and other neurodegenerative diseases, confirming that Aβ plaque-associated CSPalpha deposits are not present in ANCL tissues. This suggests that the mechanism by which intracellular oligomerisation of CSPalpha occurs in ANCL may be different to Aβ plaque-associated CSPalpha deposition, although it remains unknown whether the biophysical structure of these CSPalpha accumulations differ.

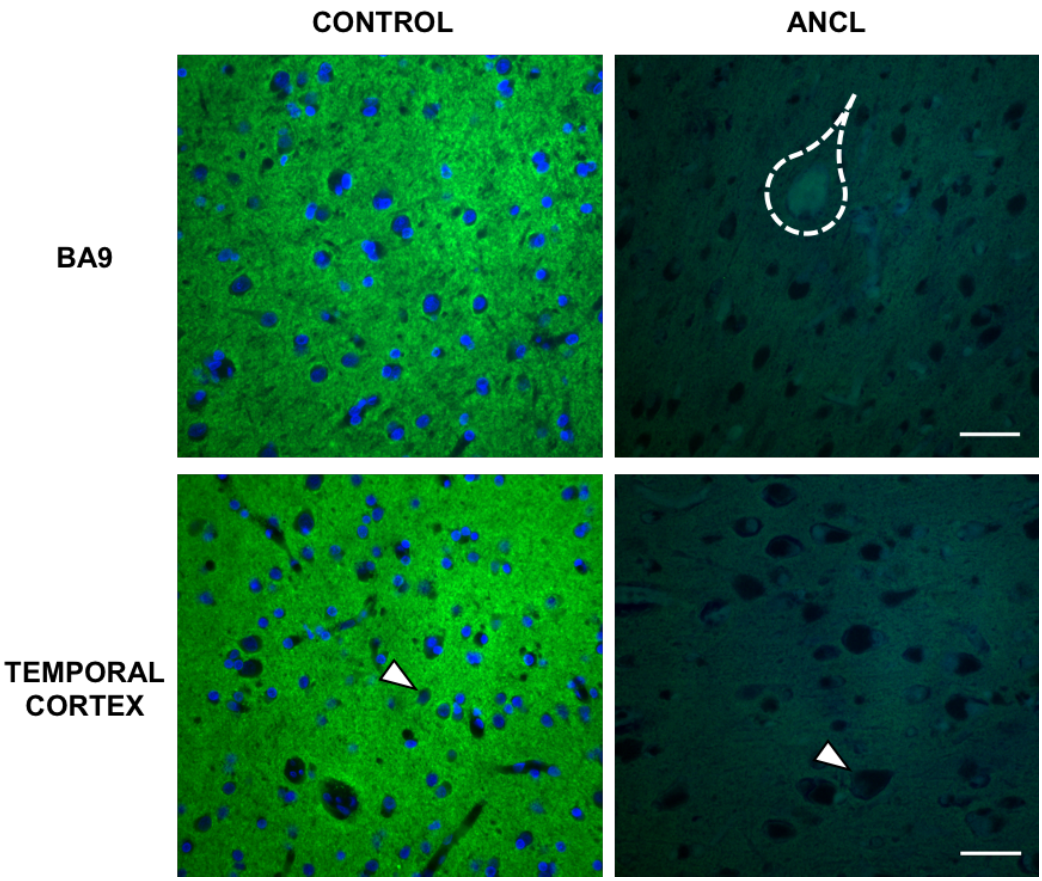

Figure 4.10. Immunostaining of tissue from an ANCL case with a *DNAJC5* L115R mutation.

Representative images from post-mortem BA9 and temporal cortex brain sections from a healthy control and ANCL tissue. Sections were immunolabelled for CSPalpha (*green*) and stained with DAPI to label nuclei (*blue*). *Dashed neuron* – Enlarged neuron in BA9 tissue containing stored lipopigment which is auto fluorescent and was only observed in ANCL tissue. *Arrows* – A typical pyramidal neuron in the control tissue compared to an enlarged cortical pyramidal neuron in tissue from the ANCL mutation carrier. Magnification 40x. Scale bar 50 μm. [n=1 case per group].

4.5 Discussion

The main aim of this chapter was to investigate the association of CSPalpha proteins with presynaptic dysfunction in neurodegenerative diseases other than AD. CSPalpha was examined by immunoblotting and immunohistochemistry in post-mortem human tissue samples from the hippocampus and temporal cortex, respectively. The main findings of this study are that 1) expression of CSPalpha is reduced in hippocampus in AD and FTLD, a non-significant reduction of CSPalpha levels was apparent in mixed dementia hippocampus and levels were unchanged in DLB, 2) Novel CSPalpha accumulations are Aβ plaque-associated in several neurodegenerative diseases, and are not related to tau pathology in tauopathies, and 3) CSPalpha accumulations in these neurodegenerative diseases are different to intracellular accumulations of CSPalpha found in genetically caused ANCL.

The multifunctional co-chaperone protein CSPalpha has previously been shown to be downregulated in AD (Zhang et al., 2012; Tiwari et al., 2015), a neurodegenerative disorder characterized by synaptic and neuronal loss. Impairment of synaptic activity is detrimental for synapses and CSPalpha is thought to be implicated in this process as evidenced by human *DNAJC5* gene mutations leading to hereditary neurodegenerative diseases such as ANCL (Benitez et al., 2011). It was therefore hypothesized that a loss of CSPalpha protein results in synaptic dysfunction. Evidence to support this hypothesis was found by replicating findings showing reduced CSPalpha expression in the hippocampus of severe AD cases when normalized to neuronal and synaptic markers. These findings further complement previous literature showing reductions in synaptosomal proteins in AD compared to controls, in particular proteins involved in vesicle trafficking, synaptic structure and signal transduction (Wiedenmann and Franke, 1985; Shimohama et al., 1997; Counts et al., 2006; Love et al., 2006; Tannenberg et al., 2006). Furthermore, it appears that

these reductions are not the result of neuronal and synaptic loss but in fact may precede such effects.

The mechanistic consequences of a dysregulation in CSPalpha leading to synaptic dysfunction are not completely understood. CSPalpha normally functions within a trimeric complex at the presynaptic terminal to mediate vesicular exocytotic interactions with SNARE proteins (Burgoyne and Morgan, 2015). A downregulation of CSPalpha may lead to fewer vesicles binding to presynaptic membranes thereby affecting activity-dependent synaptic transmission. Furthermore, CSPalpha-dependent interactions with dynamin-1 facilitate its polymerization for endocytotic vesicle fission to allow vesicles to be readily available for the next release cycle (Rozas et al., 2012; Zhang et al., 2012). It can therefore be speculated that such defects in recycling machinery that normally regulate endocytosis might lead to modulation of the exocytotic process. This may further support observations in CSPalpha KO mice whereby SNARE proteins such as SNAP-25 are reduced (Chandra et al., 2005; Sharma et al., 2012a) as well as in AD and PD post-mortem brain samples (Sharma et al., 2012b). This can contribute to the instability of synapses, reduced memory formation and neurodegeneration. Moreover, having reduced CSPalpha expression may also lead to an increase in the density of calcium-activated K+ channels (BK channels), which normally regulate the level of excitability at presynaptic terminals (Kyle et al., 2013). This is supported by increased BK channel expression in CSPalpha KO mice, that also show abnormal synaptic activity that may contribute to synaptic degeneration and neuronal loss (Ahrendt et al., 2014).

CSPalpha protein expression changes in other dementia types were investigated to establish whether such alterations may represent a common feature of neurodegeneration. In FTLD brains, reduced amounts of CSPalpha protein were observed even though synaptophysin levels were unchanged. This suggests that

CSPalpha may be implicated in early synaptic dysfunction in FTLD, however this may not be sufficient to lead to synaptic loss. Further evidence to support this result comes from observations in heterozygous KO mice that have a 50% reduction in CSPalpha and similar reductions in SNAP-25, a trans-SNARE protein vital for exocytosis, however mice are phenotypically normal (Burgoyne and Morgan, 2015). Hence, there may be possible alternative mechanisms involving CSPalpha, different to those in AD, that may contribute to eventual synaptic loss in FTLD. It may also imply that loss of synapse pathology may be delayed in the hippocampus of FTLD brain in comparison to the earliest observations of AD pathology in this region. Similarly, spared synaptophysin levels have been reported in the striatum region of FTLD brains (Riku et al., 2017). Interestingly, genetic analysis of CSPalpha in well-defined Drosophila mutants reveal that the loss of CSPalpha may in fact be neuroprotective and can delay degeneration in axonal and synaptic compartments of neurons in *vivo* (Wishart et al., 2012). CSPalpha may hence be a critical regulator of synaptic stability and can modulate neurodegeneration pathways, possibly linked to the hippocampus of FTLD brain. Only one known study by Tiwari and Colleagues (2015) has examined CSPalpha expression in FTLD, in particular within the cerebellum which is suggested to be affected by pathology, unlike in AD where the cerebellum is mostly spared from neurodegeneration (Al-Sarraj et al., 2011; Troakes et al., 2012; King et al., 2013; Tiwari et al., 2015). The underlying molecular mechanisms for such neuroprotection are not known, but one possibility is that CSPalpha has a synaptoprotective effect in the AD cerebellum to prevent neurodegeneration, the mechanisms for which are not fully known. CSPalpha levels were found to be unchanged in FTLD cerebellum, in contrast to AD where levels were elevated, a potentially specific change to AD (Tiwari et al., 2015). Hence, CSPalpha may not be neuroprotective within FTLD cerebellum, yet there may be a preservation of synapses within other FTLD affected areas within intact populations of neurons which merits further investigation.

A non-significant reduction of CSPalpha was observed in mixed dementia brains, (with either a primary or secondary neuropathological diagnosis of vascular pathology) in comparison to healthy controls. As such, synaptic loss is an early event in both AD and FBD, characterised by CAA pathology, preceded by changes in synaptic function (Revesz et al., 1999; Mead et al., 2000; Cantlon et al., 2015). As such, Tg-FDD mice, a model for CAA development, show disruption in the organization of GABAergic markers for inhibitory synapses. Interestingly, CSPalpha KO neuronal cultures show degeneration of GABAergic synapses, possibly due to reduced transport of GABA by CSPalpha to synaptic vesicles, physiologically important for stability of protein complexes between GABA-synthesizing enzymes (GAD65 and GAD67) and the vesicular GABA transporter (Hsu et al., 2000; García-Junco-Clemente et al., 2010). Hence, in cases of mixed dementia, exploration into synaptic sub-types may offer better sensitivity into CSPalpha expression changes. This finding also aligns with the reduction of presynaptic proteins shown in the literature, particularly synaptophysin and SNAP-25 within VaD brains (Zhan et al., 1993, 1994). However, the mechanisms between vascular pathology in mixed dementia and synaptotoxicity and reduction are yet to be established.

The development of vascular changes in mixed dementia and AD correlates with Braak staging, Aβ-deposition and the degree of dementia (Thal et al., 2003; Attems, 2005; Attems et al., 2007). Hence, comparable mechanisms at the synaptic level may operate in association with these coexisting pathologies. Evidence of reduced cerebral blood flow occurs with AD progression (Zhang et al., 2007; Zhiyou et al., 2009) and conversely Aβ accumulation in AD contributes to small vessel disease via CAA development, and can enhance vasoconstriction (Iadecola and Gorelick, 2003; Thal et al., 2008; Miners et al., 2011, 2014). As such, up to 50% of dementia cases show an overlap of AD neuropathology and cerebrovascular lesions including atherosclerosis, lacunar infarcts and microbleeds (Jellinger, 2013). Alterations in the

neurovascular unit may play a significant role that ultimately leads to reduced synaptic function and loss. The vascular hypothesis suggests that amyloid which originates in neurons, is transported along the perivascular interstitial fluid pathway and is deposited into blood vessels (Weller et al., 2008). Here, amyloid accumulation can impair the blood–brain barrier, reduce cerebral blood flow caused by dysfunction of the neurovascular unit and vessel rupture (Cisternas et al., 2019). This can lead to Aβ leakage and accumulation in the areas surrounding vessels and neuropil that can cause neuroinflammation and direct synaptic damage (Zlokovic, 2011), potentially leading to reduced CSPalpha expression and neurodegeneration (Cisternas et al., 2019). Albeit, the non-significant outcome of this study may be reflected by low sample numbers as CSPalpha has not been previously examined in these diseases and so power calculations were used on the basis of previous AD studies.

In DLB, no change was found in the levels of both CSPalpha and synaptophysin. Unlike in AD, DLB brains show spared atrophy and preservation within regions of the medial temporal, frontal, and parietal lobes (Oppedal et al., 2019). This supports the findings within the hippocampus of unchanged synaptic levels when normalized to neuronal content. Interestingly, DLB cases are known to show increasing burden of Lewy bodies and neurites within limbic and neocortical brains regions, specifically in the temporal lobe and *Cornu Ammonis* area 2 of the hippocampus (Walker et al., 2019). Along with alpha synuclein pathology, 28% of DLB cases also show hyperphosphorylated tau and Aβ deposition and may be given a secondary neuropathological diagnosis of AD (Walker et al., 2019). Such concomitant pathologies may be associated with a more rapid decline in cognition, however the contribution of each pathology over disease progression is still unclear, particularly in different brain regions that may show selective vulnerabilities to specific protein aggregations. As such, another study has shown that clinical outcomes of DLB are

closely related to alpha synuclein pathology and negatively associated with hyperphosphorylated tau, with no effect of Aβ (Tiraboschi et al., 2015). It is possible that such resilience within the hippocampus in DLB brains may be a compensatory effect of CSPalpha to overcome the alpha synuclein loss and/or accumulation into Lewy Bodies, as alpha synuclein has been shown to compensate for CSPalpha loss in CSPalpha KO mice (Chandra et al., 2005). Interestingly young triple alpha synuclein KO mice present an age-dependent increase in CSPalpha protein (Burré et al., 2010). Furthermore, degenerating synapse-enriched fractions of mice modelling aspects of HD and spinocerebellar ataxia type 5 show increased levels of CSPalpha, suggesting that the molecular pathways underlying neurodegeneration may be conserved (Wishart et al., 2012). This could also reflect a change in synaptic vesicle turnover or vesicle targeting, with elevated levels of CSPalpha (Hark et al., 2021). Similarly, even though reduced levels of synaptophysin have been reported in PD brains (Sharma et al., 2012b), it is possible that the minimal change of synaptic protein expression observed in DLB brains may act to compensate for the reduced ability of SNARE protein retrieval following exocytosis, as synaptophysin is reported to regulate the reinternalization of VAMP2 after exocytosis (Gordon et al., 2011). In order to assess such the impact of synaptic resilience within hippocampus, comparisons with other affected DLB brain regions such as the neocortex, subcortical nuclei and brainstem would be required (McKeith et al., 1996).

However, a main limitation to these sets of experiments is the ECL 'semi-quantitative' method for immunoblotting (an indirect method to assess protein levels) (Zellner et al., 2008). Due to the narrow dynamic range of ECL, the cumulative luminescence detected does not correlate linearly with the abundance of proteins and has limited quantitative reproducibility. A further challenge is signal saturation as each HRP bound secondary antibody has multiple binding sites that can interact with ECL substrates and so the signal amplification reaches plateau over a shorter period of

time. An alternative and more sensitive method would be fluorescence-based immunoblotting which has a greater quantifiable linear dynamic range and stability so that the signal correlates better with protein abundance (Gingrich et al., 2000; Lo et al., 2015).

The second main findings support the results in Chapter 3, of immunolabelled swollen, bulbous-shaped CSPalpha accumulations in several other neurodegenerative diseases in close proximity to Aβ plaques. This was observed in mixed dementia, FTLD, DLB, AD and healthy control tissues, but only when Aβ was deposited, both parenchymal and in the vasculature. This is the first study that has examined CSPalpha accumulations in relation to particular neurodegenerative diseases and/or amyloid plaque formation. As such, this study sheds light on the possibility that Aβ deposition is a prerequisite for the occurrence of altered CSPalpha structures. This notion is supported by a number of investigations that demonstrate Aβ as a primary pathological event that causes synapse loss and dysfunction across several neurodegenerative diseases (Woodhouse et al., 2005; Shankar et al., 2007; Li et al., 2009; Serrano-Pozo et al., 2011; Jackson et al., 2019a), although a precise mechanism for Aβ facilitating the formation of such CSPalpha clusters is unclear.

Interestingly, the temporal cortex of PiD and PSP brain were free of swollen CSPalpha accumulations unless Aβ was present. While CSPalpha deposits did not colocalise with aberrant tau pathology, other forms of neuritic degeneration cannot be excluded as evidenced in other diseases. Although, there may not be any association between CSPalpha accumulations and tau unlike previously suggested, (Fontaine et al., 2016; Deng et al., 2017), Xu and colleagues (2018) showed that the overexpression of CSPalpha results in extracellular release of tau and alpha synuclein, however this only occurred when the Hsc70 was intact (Xu et al., 2018),

the expression of which has not been fully characterised in these diseases.

It is interesting to note that having found a characteristic loss of presynaptic CSPalpha within the temporal cortex of some neurodegenerative diseases, it is yet unclear how this may be linked to the process of CSPalpha accumulations, not reflected within the immunoblotting results. Analysis of FTLD brains with no amyloid in comparison to FTLD brains with amyloid showed reduced presynaptically localised CSPalpha, whereas DLB brains with no Aβ deposits showed increased CSPalpha content relative to DLB cases with Aβ deposits. Reported studies show that CSPalpha, along with other neurodegenerative disease related proteins, can be released from the presynaptic terminal under physiological conditions (Deng et al., 2017; Xu et al., 2018). It is not clear how these mechanisms are affected in disease, but it is possible that reduced intracellular CSPalpha levels correlate with deposition of potentially extracellular CSPalpha proteins in association with Aβ plaques, the nature of which requires further investigation. However, due to the small sample number examined here, along with variability between samples, it is difficult at this stage to determine any correlation between intracellular CSPalpha levels and its extracellular accumulation.

It is also important to consider that deposits of CSPalpha may not have been captured after extensive tissue homogenisation and differential centrifugation of samples. Additionally, one out of three FTLD cases with CSPalpha accumulations (Table 4.4) was considered as an outlier in immunoblotting due to its variability. Furthermore, staining intensity could not be correlated with immunoblotting intensity due to the uneven nature of tissue sections which does not provide an accurate reflection of protein expression changes.

Although the Aβ peptide was the main focus of CSPalpha accumulation associated with different neurodegenerative diseases, other types of amyloid species found in different diseases may also present the same pathological effects on synapses and hence warrants further investigation. This includes conditions such as FDD, characterised by CAA due to ADan amyloid accumulation, a ~4 kDa Danish amyloid subunit derived from the 277-amino-acid ADan precursor protein (Garringer et al., 2010). WT neurons incubated with ADan oligomers reduce levels and colocalization between presynaptic (synapsin-1) and postsynaptic (PSD-95) protein clusters and puncta (You et al., 2019), and may relate to changes in both CSPalpha puncta and/or CSPalpha deposits. Furthermore, GABAergic synaptic markers colocalise with ADan and Aβ vascular amyloid deposits in 18-month-old-Tg-FDD mice, which suggests that CSPalpha, also found in GABAergic synapses, may localise with other Aβ species other than the Aβ peptide and may be implicated within a potential mechanism of synaptic damage (You et al., 2019). FBD is another inherited neurodegenerative disease, resulting from a mutation in the *BRI2* gene producing a 23- and 34- amino acid termed Bri and ABri, respectively (Vidal et al., 1999). The ABri peptide is the molecular equivalent of the AD-associated Aβ peptide and is found in both perivascular and parenchymal deposits in the brain of affected individuals (Cantlon et al., 2015). Although the sequence and innate biophysical properties of ABri and Aβ may be different, the neuropathological presentation is similar to that in AD, and so typical changes of CSPalpha accumulation may also be present in cases of FBD in association with another amyloid species (Cantlon et al., 2015). A further Aβ species is the amyloid-β precursor protein (AβPP), produced by an arctic (p. E693G) mutation that leads an autosomal dominant disease with a similar clinical profile typical of AD (Philipson et al., 2012). AβPP promotes the formation of Aβ protofibrils deposited in parenchymal plaque structures that resemble cotton wool plaques in AD, many of which may have the propensity to associate with CSPalpha accumulations (Philipson et al., 2012; Kalimo et al., 2013; Shi et al., 2017b). Hence, investigation into diseases

harbouring different Aβ species, will provide further confirmation as to the specificity of CSPalpha accumulation and the toxicity of such species that can lead to eventual synapse loss and presynaptic protein accrual.

The mechanistic pathway leading to CSPalpha deposition is still unknown. As previously discussed, some swellings of CSPalpha coalesce as part of synaptic dystrophies, a hallmark AD pathology, which may shed some light into at least part of the puzzle. Several in *vitro* and in *vivo* experiments indicate that Aβ may be synapto- and neuro-toxic (Kowall et al., 1991; Mucke and Selkoe, 2012; Westmark, 2013). As such, some of these CSPalpha clusters that form a part of swollen neurites may be the result of Aβ deposition as shown in AD, which can promote abnormal sprouting of presynaptic fibres (Masliah et al., 1991). Aside from direct effects of parenchymal Aβ deposition, blood brain barrier dysfunction can lead to leakage of plasma proteins into the brain perivascular space and contribute to the formation of amyloid plaques and the development of dystrophic neurites as punctate, bulbous structures that emanate near capillaries (Zlokovic, 2011). Interestingly, these results show CSPalpha deposits in proximity to amyloid plaques that surround few, but not many vascular structures. On the other hand, aside from amyloid-associated dystrophic structures in FTLD, it has been previously been show that TDP-43 positive neurites containing ubiquitin inclusions are also present and are not associated with any other neuropathological proteins (Neumann et al., 2007; Hatanpaa et al., 2008). Since CSPalpha accumulations were generally not found in areas that did not contain plaques, this suggests that these pathological features are also not correlated with CSPalpha deposition (Forman et al., 2006; Mackenzie and Neumann, 2016). In the mThy1 alpha synuclein transgenic mouse model, an abundance of clusters of dystrophic neurites have been shown in areas of the neocortex, dentate gyrus and CA3 hippocampus along with striatum and pons, and these are immunoreactive for

alpha synuclein as shown with the SYN105 antibody (Games et al., 2013). This study suggests that dystrophic neurites are also a feature of DLB. These studies reinforce the need to further explore the possibility of an association between CSPalpha accumulations and other neurotoxic aggregates which include TDP-43 and alpha synuclein to determine dystrophic neurite composition in these diseases, and whether or not CSPalpha accumulates in these dystrophies.

The final aim attempted to deepen the understanding into the mechanistic basis for the formation of plaque associated CSPalpha accumulations found in several neurodegenerative diseases. Post-mortem human tissue of an ANCL case with the L115R mutation showed both AFSM and a reduced level of total CSPalpha expression but did not present with globular CSPalpha accumulations. CSPalpha accumulations may have been present, however a limitation to these observations by immunofluorescence was the use of Sudan Black, used to quench lipofuscin autofluorescence, and may have had a significant effect at masking low level CSPalpha signals that were below the level of detectability. This would therefore require a suitable negative control without the use of Sudan Black with the availability of more tissue sections, as the number of ANCL cases available was also limited. This result was however corroborated with a previous study by Henderson and colleagues (2016) identifying a 17% signal of CSPalpha immunofluorescence in comparison to controls, having used $CuSO_4$ treatment to quench autofluorescence (Henderson et al., 2016). Moreover, due to the young age of the individuals from which tissues were obtained (controls – 55 years, ANCL – 58 years), the formation of CSPalpha accumulations may not have emerged at this early stage of development.

It is widely reported that although CSPalpha mRNA levels remain constant, CSPalpha protein amounts are severely reduced in ANCL tissues, especially in L115R mutants (Nosková et al., 2011; Henderson et al., 2016). However, CSPalpha has the tendency

to form intracellular neuronal aggregates (Greaves et al., 2012; Benitez et al., 2015), which are potentially toxic to the synapse. It has been reported that 250 kDa molecular weight oligomers of CSPalpha may be linked to lysosomal dysfunction early in disease (Zhang and Chandra, 2014), however unlike many of the other mutant proteins known to cause ANCL, CSPalpha does not have a known lysosomal function nor has it been linked to lysosomal trafficking/sorting. Interestingly, ANCL brains show massive synaptic degeneration at end stage of disease, suggesting that neuronal dysfunction at the level of lysosomes may occur prior to onset of synaptotoxic effects with the loss of functional monomeric CSPalpha and the build-up of intracellular aggregated dysfunctional CSPalpha (Lopez-Ortega et al., 2017). This is however in contrast to observations of Aβ plaque associated CSPalpha aggregates, some of which may possibly be extracellular to the synapse. Hence, the mechanisms underlying CSPalpha dysfunction in ANCL in comparison to other dementias may be different, and some effects may be specific to mutated CSPalpha. It would be interesting to further understand whether there is a difference in the biophysical and structural properties of CSPalpha in different diseases since this may help to understand the nature of this protein and its relation to presynaptic dysfunction.

In conclusion, these collective findings provide evidence that CSPalpha accumulations may be a novel marker of presynaptic dysfunction suitable for post-mortem analysis in several neurodegenerative dementias that show Aβ deposition. Large immunolabelled CSPalpha protein accumulations that are frequently observed in AD brains are unique to regions of Aβ plaque formation, most likely forming in response to Aβ deposition. Aβ deposition is believed to be an essential component leading to synaptic dysfunction and ultimately synapse loss. This reinforces the fact that at the level of the synapse, toxic proteins in the progression of disease and in

particular regions of the brain are not merely the by-product of a more generalised process of neuronal degeneration. It is reasonable to suggest that CSPalpha, not only as a presynaptic protein but as a marker of pathological change may offer insight as a potential biomarker for early changes that occur in neurodegenerative diseases. This is likely to be beneficial in the understanding of early presynaptic degeneration, eventual synapse loss and cognitive decline.

Chapter 5: Discussion

Synapse loss which precedes neurodegeneration is the best-known correlate for cognitive decline and deficits in memory in AD (Arendt, 2009). The mechanisms pertaining to synaptotoxicity are not fully understood. This is mainly because this process occurs much earlier in life, well before symptoms of the disease become known and a diagnosis is given. The overarching theme of this PhD study was to investigate the involvement of CSPalpha, a presynaptic chaperone important for synaptic survival in synapse health and disease (Fernández-Chacón et al., 2004; Burgoyne and Morgan, 2015). CSPalpha alterations in AD were first reported by Tiwari and colleagues (2015), using post-mortem human studies, who generated data suggesting that CSPalpha is involved not only in synaptic degeneration, but also in neuroprotection in AD (Tiwari et al., 2015). The basis of this PhD study was to further investigate synaptic dysfunction in AD which involves CSPalpha. During the course of western blotting, immunohistochemistry and array tomography experiments, it was observed that CSPalpha may not only play a key role in synapse loss in several neurodegenerative diseases, but also can also form abnormal, extracellular accumulations. This suggests the hypothesis that CSPalpha undergoes disease-specific changes during AD progression and warranted further investigation.

The specific aims of the project were as follows:

1. Investigate whether alterations in CSPalpha abundance/ and or localisation are a sensitive marker of synaptic protection or degeneration during AD progression.

2. Characterise CSPalpha protein accumulations in relation to AD pathology.

3. Examine the association of altered or modified CSPalpha with synapses.

4. Determine the specificity of CSPalpha accumulations in AD in comparison to other neurodegenerative diseases.

A summary of the main findings and their relation to the aims of each chapter is given below:

5.1 CSPalpha in Alzheimer's Disease

Chapter 3 explored the abundance and distribution of CSPalpha in AD. Here, the BA9 brain region was studied as a late affected brain region in AD and hence provided insight into possible events that contribute to synaptic dysfunction and loss. CSPalpha protein levels were found to be roughly equivalent in early (Braak stages 0-II) and moderate (Braak stages III-IV) AD, possibly due to only a mild synaptic loss in this region combined with synaptic compensation mechanisms (DeKosky and Scheff, 1990). CSPalpha protein levels were reduced at late Braak stages, when synapse degeneration first becomes apparent in this region. This is in-line with previously published data on presynaptic proteins (Mukaetova-Ladinska et al., 2000; Vallortigara et al., 2014; Kurbatskaya et al., 2016), yet the changes in CSPalpha occur

before marked synapse loss, endorsing CSPalpha a as sensitive marker of presynaptic changes early in disease. The distribution of CSPalpha painted a similar picture, as CSPalpha with a typical synaptic labelling pattern was reduced in the vicinity of Aβ plaque deposits using both immunohistochemistry and array tomography. This is aligned with previously reported data showing that synapse loss is greatest in areas within and around Aβ plaques, being particularly related to the local concentration of oligomeric Aβ (Koffie et al., 2009). In addition, presynaptic terminals showed increased colocalization of CSPalpha and Aβ in the vicinity of Aβ plaques. The outcome of these results hence supports the notion that CSPalpha is a sensitive molecular marker of synapse loss in AD.

Whilst investigating the distribution of CSPalpha, plaque-associated globular accumulations of CSPalpha were discovered by immunohistochemistry. CSPalpha solubility was shown to be altered between control and AD samples, suggesting the possibility that CSPalpha may have an altered conformation, making it more resistant to extraction by harsh detergents. CSPalpha deposits were found in BA9, hippocampal and cerebellar regions of AD brain that decorated the periphery of neuritic cored Aβ plaques and surrounding diffuse Aβ plaques. These accumulations associated with some but not all tau pathology, a microglial marker and a marker for phosphorylated neurofilament protein in axonal dystrophy, suggesting that these accumulations may be mislocalised from their normal localisation of CSPalpha protein in presynaptic terminals. Interestingly, these accumulations varied in size, similar to that as described for dystrophic neurites (Sanchez-Varo et al., 2012). The presence of synaptic accumulations, indicative of presynaptic dystrophies was further examined. CSPalpha accumulations were found to co-localise with some, but not all presynaptic dystrophies, marked by synaptophysin and SNAP-25 positivity as well as an interacting partner, Hsc70. Using array tomography, the presence of both

CSPalpha accumulations and synaptophysin-positive presynaptic dystrophies were confirmed, both of which also positively immunolabelled with antibodies against Aβ. However, these presynaptic dystrophies were localised <10 μm from the Aβ plaque core, unlike CSPalpha deposits which were found to be dispersed up to a greater distance of 20 μm from the core. These findings were corroborated in the 5xFAD mouse model where CSPalpha accumulations were found at 3 months of age when Aβ is first deposited and increased up to 12 months of age when Aβ plaque burden is more profound. Combined, these findings indicate a close link between CSPalpha and Aβ deposition. CSPalpha accumulations were associated with some presynaptic dystrophies in the mouse model and shared similar qualitative spread from the plaque core as observed with array tomography in post-mortem human tissues. CSPalpha accumulations also labelled with an antibody against CSPalpha phosphorylated at Ser10, suggesting that CSPalpha phosphorylation status may be conserved after structural conformations, and/or that phosphorylated CSPalpha preferentially deposits. These data suggest that the mechanisms of CSPalpha accumulation may be different to those underlying presynaptic dystrophies. The CSPalpha accumulations found closer to the plaque centre that overlap with some dystrophies suggests that these complexes may form at a later stage in-line with synaptic die back theories.

5.2 CSPalpha in Other Neurodegenerative Diseases

Chapter 4 explored the hypothesis that CSPalpha may be altered in other neurodegenerative diseases in which synapse loss is prevalent and that CSPalpha accumulations that surround Aβ plaques may not be AD-specific but rather are associated with all diseases in which Aβ deposition is apparent. Using immunoblotting, Tiwari and colleagues (2015) reported that CSPalpha protein levels are altered in AD hippocampus (Tiwari et al., 2015). This study replicated the same

altered CSPalpha protein levels in AD, but also in FTLD hippocampus. However, unlike AD hippocampus, FTLD brain samples did not show reduced expression of synaptophysin suggesting that the mechanisms of CSPalpha-dependent presynaptic dysfunction may differ between AD and FTLD. Mixed dementia brains were found to show a non-significant reduction in CSPalpha, and no changes in CSPalpha amounts were found in DLB brain relative to controls. These findings support the notion that CSPalpha protein alterations may be different across neurodegenerative diseases.

Next, using immunohistochemistry, CSPalpha accumulations were labelled together with Aβ in sections from AD, FTLD, mixed dementia and DLB brain, where it was observed that deposits of CSPalpha were present in sections that contained both parenchymal and vascular Aβ deposits. No CSPalpha accumulations were present in brains that did not have amyloid deposition. Interestingly, control tissues that were determined to show some age-related Aβ plaque pathology validated the hypothesis. To determine if CSPalpha accumulations are specific for Aβ pathology, and not related to tau, sections from PSP and PiD were labelled with CSPalpha and tau antibodies. Similar to previous results, no CSPalpha deposits were observed in these tauopathies, but were identified on the rare occasion when Aβ plaques were detected. Finally, to explore a possible mechanism by which CSPalpha may accumulate, tissue sections from an ANCL brain with a L115R mutation, where CSPalpha is known to aggregate intracellularly, were examined. Here, CSPalpha accumulations were not observed, although intracellular AFSM was present. This data confirms that CSPalpha accumulations are related to Aβ pathology and these may develop as a result of Aβ-related changes in the brain. Structural changes of intracellular CSPalpha aggregates found in ANCL may be different to possible extracellular accumulations of CSPalpha found in other diseases and so this also alludes to a novel mechanism

by which CSPalpha is mislocalised and is structurally different from the monomeric CSPalpha proteins found within presynaptic terminals.

5.3 A Potential Mechanism of CSPalpha Accumulation

As suggested by the results in this PhD study, it is possible that CSPalpha accumulations are linked to dysfunctional APP processing that leads to increased Aβ production and deposition across several neurodegenerative diseases. It has been suggested that soluble oligomeric forms of Aβ plays a critical role in AD pathogenesis (Vickers et al., 2016). A halo of toxic Aβ oligomers directly affect presynaptic terminals near the edge of the Aβ plaque core (Koffie et al., 2009). Toxic diffusible Aβ oligomers associate with synaptosomes and leads to synaptic deterioration in primary neuronal cultures (Lacor et al., 2007). An inverse correlation between levels of Aβ oligomers and synaptic proteins has been shown (Pham et al., 2010). Interestingly, soluble oligomeric Aβ fragments extracted from the frontal cortex of AD brain, resulted in the dose-dependent reduction of CSPalpha when applied to neurons, a result confirmed when CSPalpha protein amounts were not altered when extracts were depleted of Aβ, thus further suggesting an Aβ toxicity-dependent effect on synaptic CSPalpha (Bate and Williams, 2018).

Mechanisms of Aβ-toxicity are also linked with tau hyperphosphorylation (Wu et al., 2018), axonal transport disruption (Decker et al., 2010) and failure of anterograde organelle trafficking via altered GSK3β signalling (Hooper et al., 2008). In fact, direct interaction between Aβ and the axonal plasma membrane can create a blockade through calcium-mediated signals (Wu et al., 2010a). Aβ oligomers can inhibit protein degradation mechanisms, important for the prominent functional role of CSPalpha within the synapse (Yerbury et al., 2016). More so, CSPalpha protein turnover has been reported to be impaired in cortical glutamatergic synapses of *App*$^{NL-F/NL-F}$ mice (Hark et al., 2021). Additionally, Aβ oligomers may also reduce levels of p25, known to regulate CSPalpha expression, by reducing calcium signaling, causing an internalization of desensitized NMDA receptors (Palop and Mucke, 2010; Paula-Lima

et al., 2013; Giese, 2014). Hence, disruption of these processes by Aβ oligomers may well be a contributing factor to the underlying mechanisms of inhibiting intraneuronal movements of synaptic vesicle proteins such as CSPalpha (Marsh and Alifragis, 2018), overall enlarging the synaptic vesicle pool and forming synaptic accumulations (Fornasiero et al., 2018).

In support of these mechanisms, this PhD study has reported, in line with previous studies, the presence of presynaptic accumulation-filled dystrophies in the close vicinity of Aβ plaques that are immunoreactive for synaptic proteins (Kandalepas et al., 2013; Sadleir et al., 2016; Ovsepian et al., 2019). CSPalpha colocalization with some of these dystrophic terminals suggests that these synaptic remnants represent late-stage dead and/or dying synapses that may be encapsulated within vesicular membranes. The molecular mechanisms that determine the formation of presynaptic swellings are not yet elucidated but may involve the accrual of vesicle-associated proteins such as CSPalpha, synaptophysin and SNAP-25 along with others that can no longer be released from the terminal. The findings in this study also reveal possible localisation of CSPalpha accumulations to reactive Iba-1-positive microglia in proximity to Aβ plaques. Microglia have been reported to aberrantly engulf synapses via ‘eat me’ signals as shown in mouse models of AD-like pathology (Hong et al., 2016; Shi et al., 2017a; Wu et al., 2019). Moreover, synaptic remnants in greater amounts have been described in these reactive microglia from post-mortem human AD tissues compared to non-diseased tissue (Tzioras et al., 2019). In fact, Aβ oligomer deposition at the synapse may induce microglial recruitment but also, promote engulfment of synaptic structures (Rajendran and Paolicelli, 2018). Furthermore, it may also be the case that microglia only ‘snip’ dying, protein filled synapses leaving behind synaptic remnant that becomes trapped within the milieu of toxic proteinaceous deposits (Weinhard et al., 2018). It would hence appeal that investigations into CSPalpha accumulation also determine the role of glial activation

and neuroinflammation in the development of presynaptic dystrophies that characterise early stages of disease (Gomez-Arboledas et al., 2018).

5.4 An Alternative Mechanism of CSPalpha Accumulation

A recent study by Hark and colleagues (2021) described the variability in overlap of presynaptic protein localisation with Aβ, more so in close proximity than direct overlap in the *App*$^{NL-F/NL-F}$ mouse. Synaptic proteins, those which had impaired turnover, appeared to accumulate extracellularly with others accumulating in swollen axon terminals and dystrophic neurites that surrounding Aβ plaques (Hark et al., 2021).

This underlies several interesting questions that currently remain in the field, more aligned with the notion that CSPalpha release may be associated with the prion-like propagation of misfolded proteins and more so the extracellular deposition of CSPalpha (Fontaine et al., 2016; Deng et al., 2017). Could it be that dysfunctional APP processing leads to the secretion of CSPalpha into the extracellular space and what does this mean for synapses? Using mechanistic theories of Aβ-dependent synaptic dysfunction, a new model of synaptic dysfunction and loss is proposed in the context of observed changes in CSPalpha and CSPalpha accumulations.

This alternative and novel hypothesis is in line with recently reported studies of CSPalpha release. CSPalpha accumulations may be formed in the early stages of disease before the consolidation of synaptic debris as presynaptic dystrophies that are concomitant with the development of Aβ plaque pathology. When amyloid deposition first occurs, a non-toxic plaque nidus forms within the parenchyma. After Aβ deposition, plaques increase in size and become closely associated with axons and presynaptic terminals causing a cascade of events by a dynamic equilibrium of high concentrations of neurotoxic soluble Aβ oligomers (Ferreira et al., 2015).

Furthermore, and in line with a potential protein release hypothesis, Aβ increases the formation of SNARE-complexes, elevates calcium levels inside the presynapse for synaptic vesicle fusion and may eventually lead to the exocytotic release of CSPalpha (Mattson et al., 1992; Demuro et al., 2005; Kuchibhotla et al., 2008; Zempel et al., 2010; Hudry et al., 2012). Aβ-meditated toxicity may also be linked with defects in endocytosis and its recovery due to inactivated dynamin and compromised vesicle mobility and redistribution back in the terminal, overall depleting vesicle reserve pools from the synapse (Kelly et al., 2005; Kelly and Ferreira, 2007; Parodi et al., 2010; Marsh and Alifragis, 2018). Interestingly, Aβ oligomers have been reported to damage the endo-lysosomal pathway (Marshall et al., 2020), either causing disruption to membranes and lysosomal leakage, a pathway used for CSPalpha-mediated clearance of misfolded proteins from the presynaptic terminal.

Increased excitatory activity results in the release of CSPalpha from the presynaptic terminal into the neuropil where it can then bind with high affinity to Aβ oligomers. This can be either due to increased exocytosis of the vesicle pool or via the endo-lysosomal pathway as previously reported (Xu et al., 2018). CSPalpha self-association may be influenced by the extracellular milieau and pH of the brain parenchyma enabling CSPalpha to be sequestered within the Aβ plaque periphery (Fig 5.1). This may occur at the earliest stages of Aβ deposition when plaques begin to form, and synapses are still alive but may no longer be functionally viable.

In the late stages of disease, when synapses become dysfunctional, vesicles trafficked for endo- and exo- cytosis can detach from microtubules and begin to accumulate as autophagic vacuoles with electron dense endosomes and lysosomal proteins as shown in humans AD brains and AD-like models (Masliah et al., 1991; Gowrishankar et al., 2015). As such, it has been reported that autophagic compartments, that participate in APP processing and Aβ peptide production (Yang

et al., 2011), can cause presynaptic swellings adjacent to Aβ plaques. As previously reported in in *vitro* neuronal cultures, Aβ oligomers can increase the size of synaptophysin-positive presynaptic terminals after 6 hours of treatment, where large synaptic bouton sizes possibly imply bigger presynaptic vesicle pools (Lacor et al., 2007). These accumulating vesicles consist of several proteins which include complexed synaptic proteins including CSPalpha and synaptophysin, APP and BACE-1 which elevate APP processing and generation and can hence promote enlargement of the plaque; thus leading to an enhanced feed forward loop of increased dystrophy that ultimately proceeds to neuronal loss and cognitive decline (Fig 5.1) (Zhao et al., 2007; Sanchez-Varo et al., 2012; Gomez-Arboledas et al., 2018).

The question as to whether some of the accumulating CSPalpha may lose its functional role within these peri-plaque dystrophies is yet to be elucidated however as previously reported, lack of the active zone structural proteins, bassoon, suggests that these terminals may have impaired synaptic transmission and also lack in synaptic machinery (Sadleir et al., 2016). This is in-line with the occurrence of dystrophies when depletion of synaptophysin is first observed (Adalbert et al., 2009). This supports the hypothesis of this thesis that CSPalpha may be a more sensitive pathological marker for early synaptic dysfunction in neurodegenerative diseases characterised by Aβ pathology. This does also raise further questions: Is CSPalpha release involved in the prion-like trans-synaptic propagation of misfolded proteins? and how might this relate to the regulation of synaptic health in disease? Are CSPalpha accumulations a possible form of neuroprotection from the build-up of misfolded proteins that threaten synaptic dysfunction? It is however conceivable that CSPalpha accumulations may compensate for presynaptic dysfunction, however this also requires further investigation.

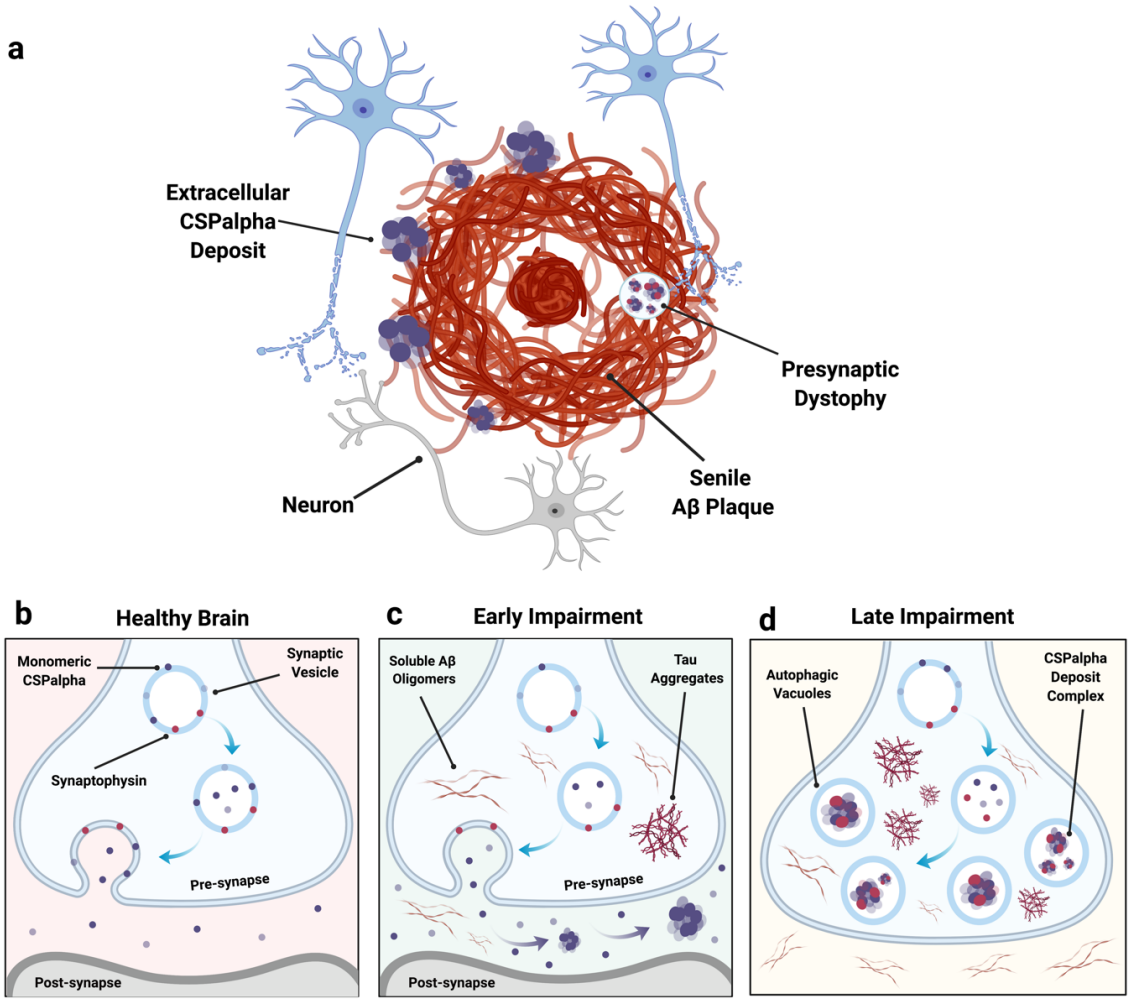
a
Extracellular
CSPalpha
Deposit
Presynaptic
Dystophy
Senile
Aβ Plaque
Neuron
b
Healthy Brain
Monomeric
CSPalpha
Synaptic
Vesicle
Synaptophysin
Pre-synapse
Post-synapse
c
Early Impairment
Soluble Aβ
Oligomers
Tau
Aggregates
Pre-synapse
Post-synapse
d
Late Impairment
Autophagic
Vacuoles
CSPalpha
Deposit
Complex

Figure 5.1. A proposed mechanism of CSPalpha accumulation in amyloid-related diseases.

a) Possible appearance of extracellular CSPalpha accumulations and presynaptic dystrophy in proximity to a neuritic cored Aβ plaque. **b)** *Healthy brain* - CSPalpha and synaptophysin localise to presynaptic vesicles. CSPalpha is important for exocytosis and chaperone of misfolded proteins from the presynaptic terminal. CSPalpha is also released from the terminal via MAPS pathway. **c)** *Early impairment* - In early stage of Aβ plaque formation, toxic soluble Aβ oligomers localise to the presynaptic terminal. This disrupts the normal endo- and exocytotic processes and physiological release of CSPalpha is exacerbated. Tau phosphorylation is also aggravated forming toxic tau aggregates. Once outside the presynaptic terminal, monomeric CSPalpha begins to self-associate, accumulates and is deposited in the vicinity of the growing Aβ plaque. **c)** *Late impairment* - As synaptic dysfunction worsens in later stages of disease, synapses can no longer function, and release of misfolded proteins is halted. Vesicular membranes build-up within the presynaptic terminal in areas closer to the Aβ plaque core and synaptic proteins including CSPalpha and synaptophysin, form complexes. Eventually synapses begin to die back leaving behind the synaptic remnant as a presynaptic dystrophy filled with vacuoles of synaptic proteins. *Arrows* indicate movement or transfer of proteins or molecular compartments. Created with Biorender.com.

This model is based on the amyloid cascade hypothesis, but it is acknowledged that many would argue against this hypothesis. The tau hypothesis of synaptic degeneration and cognitive decline has however gained much attention, where altered and mislocalised tau can lead to synaptic degeneration (Hoover et al., 2010; Crimins et al., 2013). Tau phosphorylation, including the presence of Aβ (Wu et al., 2018), allows fyn-tau interactions and tau mislocalisation leading to deficits in AMPA receptor clustering, and NMDA receptor related excitotoxicity all of which can lead to dysfunctional synapses (Bhaskar et al., 2005; Ittner et al., 2010; Miller et al., 2014). Whether this determines a pathological cascade or whether it is likely that tau changes occur via a different mechanism are still unknown. Mutant tau has however been reported in fly and neurons to associate with presynaptic vesicles via synaptopgyrin-3, causing defects in vesicular mobility and overall reduces synaptic transmission (Zhou et al., 2017; McInnes et al., 2018; Largo-Barrientos et al., 2021). Similarly, tau can bind to CSPalpha indirectly via Hsc70 and can be exported out of the cell by CSPalpha, possible relation to tau propagation (Fontaine et al., 2016; Deng et al., 2017). However, whether changes in CSPalpha abundance at pre-synapses influences the amount of tau release during pathological tau spread and the effect tau changes may have on CSPalpha in disease are questions yet to be explored. The results presented in this thesis, however, found only some association between CSPalpha and tau in AD or related tauopathies and so it can be suggested that CSPalpha may not be suitable marker for tau related synaptic degeneration.

In order to validate the proposed hypothesis, several experiments can be conducted which include:

- Co-immunoprecipitation of CSPalpha and synaptic Aβ peptides from synapses captured from post-mortem human tissue to determine their interaction at the synaptic level.
- Co-labelling of post-mortem tissues for CSPalpha with extracellular protein markers including synaptic, chaperone and exosome markers, as previously described (Deng et al., 2017) to confirm the extracellular nature of these deposits.
- Oligomeric Aβ treated primary cortical neurons in *vitro* may promote CSPalpha release which can be quantified using ELISA assay. Additionally, and overtime, abnormal synaptic changes can be visualised including blockade of anterograde transport, neuritic beading, synaptic failure and redistribution of CSPalpha into vesicular compartments, confirmed with lysosomal markers (LAMP-1/ CAT-D) (Sadleir et al., 2016).

5.4 Limitations of This PhD Study

The data presented within this thesis has been well designed and controlled experimentally, although there are important limitations of this work that require further discussion.

5.4.1 Post-mortem Human Brain Tissues

This PhD thesis has used post-mortem human brain samples to investigate the synaptic changes that occur in several neurodegenerative diseases as described by experiments in Chapters 3 and 4. The advantage of this approach is the direct relevance to human disease. Post-mortem tissues provide an excellent validation for cellular and animal models of disease which provide important mechanistic insights into signalling cascades and causes for disease progression, but which do not fully replicate human disease.

There are, however, limitations to the use of post-mortem tissues, many of which were considered before commencement of these studies, especially during interpretation of experimental results:

5.4.1.1 Technical Factors

As human tissues are obtained post-mortem, only a glimpse of the changes that have occurred at the end stage of life can be measured. Even though it is possible to determine the development of disease events by examining tissues from different brains distinguished into individual Braak stages, this does not however offer a longitudinal view for each individual brain. Furthermore, due to the heterogeneity of AD and complexity with multiple pathologies, it is challenging to interpret the mechanistic basis of findings without assessing the contribution of other neuropathologies.

Another factor is the PMD, which is the time (hours) from death to brain processing and the length of time can have a significant effect on the quality of brain tissues. For example, Wang and colleagues (2000), found that degradation of proteins, including the NR2A and 2B subunits of the NMDA receptor, were found rapidly reduced following death and up to 18 hours post-mortem (Wang et al., 2000b). Protein degradation may not be the same between samples and this may also vary depending on the vulnerability of proteins. For example, synaptophysin has much greater resistance to degradation when compared to other synaptic proteins such as synucleins and syntaxins (Liu and Brun, 1995; Siew et al., 2004). PMD may also have an effect on posttranslational modifications and protein-protein interactions in disease states (Ferrer et al., 2008). The pH of brain tissue has also been found to have a profound effect on the variation of gene expression (Li et al., 2004). Additionally, pH is valuable as a quality marker, perhaps better than PMD, brain region and storage time and as an indicator of pre-mortem events (Monoranu et al., 2009). However, details of pH along with factors which include storage and brain collection were not detailed in parts of this study, which may account for some of the variability found here.

A final limitation arises in the variation between brain regions, which may affect the way in which data is collected. As such, subregion variability is as important when investigating regional differences due to the specificity of pathology burden within these areas. The use of specific brain hemispheres may also be a contributing factor as interhemispheric differences of vascular and AD burden have been reported (Giannakopoulos et al., 2009). Also, the availability of particular tissues can be limiting, such as the hippocampus which is a popular region of study across several neurodegenerative diseases.

5.4.1.2 Genetic Factors

Genetic factors can underlie the aetiology of neurodegenerative disease. The ApoE ε4 allele is the strongest genetic risk factor for sporadic AD, and is associated with synapse loss and accrual of oligomeric Aβ within synapses (Koffie et al., 2012; Hesse et al., 2019). As such, accounting for ApoE genotype is important as this may account for underlying differences between samples and may have an overall effect on the outcome of results. This was not however taken into account within this study, although ApoE status was only reported for array tomography data (Chapter 2, Section 2.3, Table 2.4).

5.4.1.3 Environmental Factors

Pre-mortem events and lifelong choices can have an overall impact on disease along with changes observed post-mortem. This can include confounding factors such as previous illnesses, seizures, multiple diagnoses (in addition to main disease diagnosis), medications and with lifestyle factors that include smoking, substance abuse and socio-economic factors (McKhann et al., 2011). This may well have an

effect on the development of disease, cause of death and overall outcome of this study, but the effects are usually relatively small and only observable with larger sample sizes.

5.4.2 Time constraints of the study

The array tomography study that took place in the Spires-Jones lab at the University of Edinburgh was undertaken as part of an exceptional training opportunity funded by the MRC Flexible supplement. This was a month-long placement to undertake a study that would not only enhance this PhD but to develop scientific training methods. This placement was however time-constrained due to the number of elements that needed completion. This included training of AT methods, study design, post-mortem human tissue processing (Dr Jamie Rose, University of Edinburgh), antibody optimisation, tissue labelling, array scope imaging and training in analysis methods. This was accounting for little error in the technical procedures. It also meant that the study could not have been expanded to investigate other interesting pathological or synaptic markers that would enhance the results of the study.

Due to the recent Covid-19 pandemic and lockdown, this had meant closures of the laboratory. This proved as a limitation to the expansion of the overall study and meant that experiments that were initially planned as part of proof of concept were not pursued that would further support the data presented in this thesis. These include:

- Similar to immunoblotting and quantification of CSPalpha abundance in BA9 post-mortem human tissues, to investigate CSPalpha expression changes in other non-affected regions such as the cerebellum to complement immunofluorescence data.

- Thorough investigation of CSPalpha accumulations associated with Aβ plaques in affected and non-affected areas which include the hippocampus and cerebellum, respectively.
- Qualitative characterisation and co-labelling of CSPalpha deposits in different neurodegenerative diseases with a variety of sensitive markers of axonal dystrophies including APP and BACE1, oligomeric and monomeric Aβ to determine Aβ species, lysosomal proteins to identify whether CSPalpha deposits form due to lysosomal dysfunction and due to the heterogeneity of synapses, use of excitatory (VGLUT-1)/inhibitory (GABA/GAD) synaptic markers to define synapse type to provide more information on early presynaptic dysfunction with respect to CSPalpha.
- Previous reports suggest elevation in the level of CSPalpha phosphorylation at Ser10 in cortical synaptoneurosomes of APP/PS1 mice (Wu et al., 2018). Hence it would have been valuable to assess the abundance of CSPalpha phosphorylation at Ser10 in synaptoneurosomes from BA9 AD post-mortem tissues compared to controls using CSPalpha pSer10 antiserum in comparison to total CSPalpha protein in order evaluate differences in CSPalpha post-translational modifications at the synapse.

5.5. Future Studies

The data presented in this thesis proposes the findings that CSPalpha protein associates with presynaptic dystrophies in AD brain and possibly mislocalises from its physiological localisation at the presynaptic terminal and accumulates extracellularly, accumulations that are present in several neurodegenerative diseases that develop Aβ plaques and the 5xFAD mouse model. These events occur in proximity to Aβ plaque deposits and may be linked to a mechanism involving oligomeric Aβ toxicity. Development of advanced techniques and with more time, future experiments could investigate the mechanisms involving CSPalpha association with synaptic degeneration in health and disease along with understanding the functional changes of this significant presynaptic protein. Outlined below are possible avenues that could be explored in order to extend the work presented in this thesis:

5.5.1 Which proteins interact with CSPalpha accumulations?

This study has shown peri-plaque deposits of CSPalpha which in part co-localise with the synaptic protein, synaptophysin and CSPalpha-interacting partners, SNAP-25 and Hsc70. However, there may be many other interacting proteins, including pathological markers of disease. Using immunohistochemistry alone would take too long to identify other proteins and so faster, more advanced and unbiased approaches will be beneficial. Firstly, to understand the CSPalpha accumulation complex better, post-mortem human tissues could be processed for high performance liquid chromatography, to separate the deposit/aggregate fraction from monomeric CSPalpha. Next, to better determine the proteins that may complex with CSPalpha, fractions can undergo proteomic screen using mass spectrometry. This can then be followed up with coimmunoprecipitation assays to validate the interaction between

proteins, and extend the observations to compare the monomeric to deposit fractions, and control and disease tissues. In order to visualise this interaction, use of proximity ligation assays, which have been used in post-mortem human tissues (Lau et al., 2020), can also be used to determine the localisation of interactions at a distance of <40 nm. Additionally, mass spectrometry imaging can be used to investigate the spatial distribution of thousands of molecules in a single experiment (Buchberger et al., 2018). By understanding which proteins interact and whether there is a change in this interaction will provide a better mechanistic insight into the molecular changes within the synapse in health and disease.

5.5.2 Are CSPalpha posttranslational modifications altered across neurodegenerative diseases?

This thesis reports that CSPalpha pSer10 is evident in control and AD hippocampus and BA9 brain, including the presence of CSPalpha pSer10 in CSPalpha accumulations. It would be valuable to examine this further biochemically by quantifying the amount of CSPalpha phosphorylation across several neurodegenerative diseases relative to total CSPalpha amounts. This will provide a molecular understanding of post-translational changes in CSPalpha that may offer insight into possible structural and functional changes of CSPalpha in disease.

CSPalpha palmitoylation is also important for the binding of CSPalpha to plasma membranes. It has also been shown that CSPalpha aggregation is maintained by palmitoylation (Greaves et al., 2012). Differential extraction of control and AD BA9 samples in detergents showed that most CSPalpha is solubilised from the plasma membrane after exposure to the HS-TX detergent, as expected. It was also found in AD and control hippocampus that there is no change in the percentage of CSPalpha palmitoylation. This was calculated by measuring the abundance of the upper band of CSPalpha ~35 kDa, which is known to be palmitoylated. Due to time constraints,

this could not be validated. However, to do so brain samples can be treated with hydroxylamine, which can depalmitoylate CSPalpha causing a 7 kDa shift in molecular weight in the upper band. Studies to show that palmitoylation is important for CSPalpha to accumulate in AD would be important for understanding the mechanisms by which this process occurs. This could be achieved by the inhibition of pamitoyltranferase proteins that normally palmitoylate CSPalpha such as DHHC17 and may prevent CSPalpha accumulation (Greaves et al., 2008). If CSPalpha palmitoylation is altered, then this could be further investigated by labelling the interaction of palmitoyl transferase proteins with CSPalpha protein in post-mortem studies.

5.5.3 Could these accumulations be aggregates of CSPalpha?

During this study, it was considered that CSPalpha accumulations may in fact be putative aggregates. The time constraint of the study meant that investigating this would not have been possible. To better understand the nature of these deposits using a more sophisticated technique would be to undertake immuno-electron microscopy or structural analysis. Nuclear magnetic resonance spectroscopy can provide a better understanding of CSPalpha accumulation structure and dynamic stability in their natural milieu. Electron microscopy has been previously used to validate presynaptic dystrophies in the presence of Aβ plaques (Gowrishankar et al., 2015; De Rossi et al., 2019). Immunogold-labelling of post-mortem tissues would provide a more in-depth analysis of these accumulations. The use of post-mortem tissues however may prove difficult due to the quality of tissue required for this technique. Instead, use of 5xFAD mice would be preferable from which fresh tissues can be obtained and where CSPalpha accumulations have been observed. Furthermore, techniques such as Clear Lipid-exchanged Acrylamide-hybridized Rigid Imaging may improve molecular probing of CSPalpha accumulations, as shown previously in the study for Lewy body inclusions (Liu et al., 2016).

5.5.4 Can overexpression of CSPalpha provide neuroprotection?

Synapses are lost from otherwise viable neurons, and so efforts to prevent neuronal death may be too late in the development of the disease to provide a possible therapeutic rescue. Any form of 'synaptoprotective' therapy may be much more effective, but this would need to be administered much earlier, and so identifying a suitable molecular target for therapeutic intervention is key (Coleman et al., 2004). Studies that have investigated the role of CSPalpha in synaptic survival have experimentally modelled a downregulation of CSPalpha using CSPalpha KO models to highlight the impact on synaptic function (Fernández-Chacón et al., 2004; Burgoyne and Morgan, 2015). Very few studies have explored CSPalpha overexpression in *vitro* in addition to the finding by Tiwari and colleagues (2015) who found an elevation of CSPalpha in the AD cerebellum, a protected region in AD (Tiwari et al., 2015). The Giese group have previously cloned a CSPalpha lentiviral overexpressing plasmid (a gift from Professor Thomas Südhof). This plasmid could be injected into the hippocampus of the 5xFAD mouse model to determine whether an overexpression of CSPalpha may rescue dysfunctional synapses and/or reverse the formation of CSPalpha accumulation.

5.6 Future Perspective

It can be proposed that CSPalpha may be the most sensitive marker for presynaptic dysfunction for use by neuropathologists to investigate the pathological hallmarks of synapse loss in several neurodegenerative diseases. This is in comparison to traditionally used markers of synapse health such as synaptophysin, that has been shown not to be as important for synaptic survival as CSPalpha (Fernández-Chacón et al., 2004). Furthermore, as synapse loss is known to correlate with cognitive decline, this provides precedent for use of CSPalpha biomarkers as a means of detecting early synaptic and cognitive changes (DeKosky and Scheff, 1990; Blennow et al., 1996; De Wilde et al., 2016; Colom-Cadena et al., 2020).

It has recently been reported that synapses can be visualised in the living brain using synaptic vesicle glycoprotein 2A with [^{11}C]UCB-J positron emission tomography (PET) ligand (Finnema et al., 2016; Constantinescu et al., 2019; Li et al., 2019), with further ligands in the development phase (Colom-Cadena et al., 2020). A 40% signal reduction was observed in AD hippocampus compared to controls (Chen et al., 2018). This, along with CSF markers and advanced imaging techniques may offer a strong indicator of synapse degeneration in the brain. Interestingly, there are several studies now investigating synaptic CSF biomarkers which include SNAP-25 and synaptotagmin (Davidsson et al., 1996; Brinkmalm et al., 2014). More aligned with this study, CSPalpha has also been observed in CSF from brains with no clinical diagnosis of CSPalpha related pathology (Deng et al., 2017). Additionally, with the possibility that CSPalpha may be secreted within exosomes, development of neuron-derived blood exosomes assays may allow measurement of exosomal CSPalpha which might provide a better reflection of early synaptic damage in disease (Winston et al., 2016; Lashley et al., 2018). Hence, the use of CSPalpha as a biomarker of

synapse damage and loss may hold great promise as a biological indicator of synapse dysfunction and cognitive decline in AD.

5.7 Conclusions

Synapse loss is a primary event occurring prior to neuronal loss in several neurodegenerative diseases and is closely associated with cognitive decline. The data presented in this PhD study have revealed accumulations of CSPalpha, a presynaptic chaperone protein, in AD and other neurodegenerative diseases that are found in proximity to Aβ plaques. This has been evidenced using both post-mortem human tissues and the 5xFAD mouse model. CSPalpha accrual is also shown at presynaptic dystrophies at a stage when synapse loss is at its greatest. These results have led to a novel possible mechanism of early toxicity of synapses by either the possible secretion of CSPalpha that can then be deposited as larger globular structures or CSPalpha accumulation within remnant synapses that decorate the outskirts of Aβ plaques. Furthermore, CSPalpha expression changes were altered in different neurodegenerative diseases such as FTLD, warranting further exploration into the mechanisms of synapse loss within multiple diseases. These data together shed light on CSPalpha as being a sensitive marker for early synaptic changes in health and disease, likely more so than traditionally used synaptic protein markers. Furthermore, the knowledge offered by this PhD will provide a new perspective when investigating the mechanisms underlying synaptic degeneration in several neurodegenerative diseases in the future.

Chapter 6: Appendix

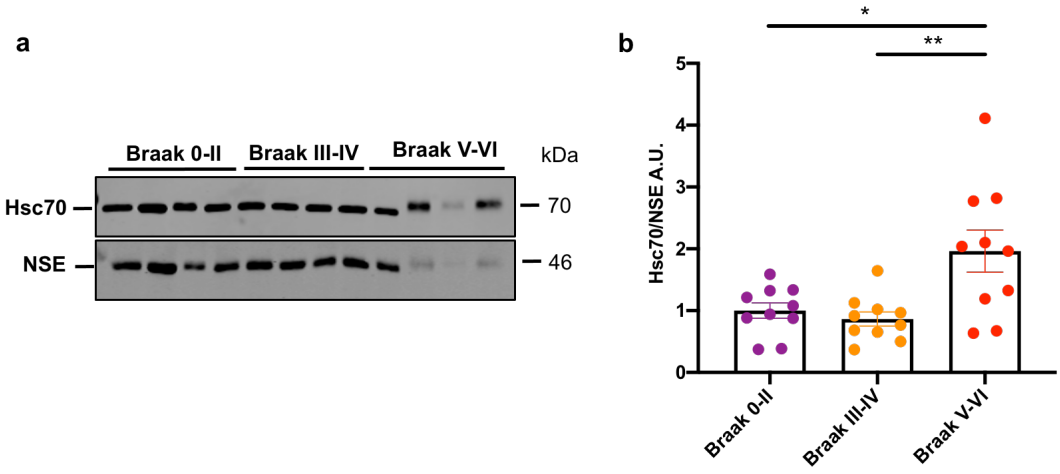

Figure 6.1. Hsc70 protein levels are elevated in AD BA9.

a) Representative western blots of homogenates from Braak stages 0-II, III-IV and V-VI post-mortem BA9 immunoblotted for Hsc70 (70 kDa) and NSE as a neuronal loading control. **b)** Bar charts show quantification of Hsc70 relative to NSE. Hsc70 protein levels were significant across Braak stages ($F(2, 27)=4.926$, $p=0.0027$), and elevated in severe AD (Braak V-VI) relative to Braak III-IV ($p=0.004$), and Braak 0-II ($p=0.01$). Following D'Agostino and Pearson normality testing, data were analysed using a One-way ANOVA with Tukey's multiple comparison test. Data shown are mean ± SEM expressed as a fold average of control. [n=10 cases per group].

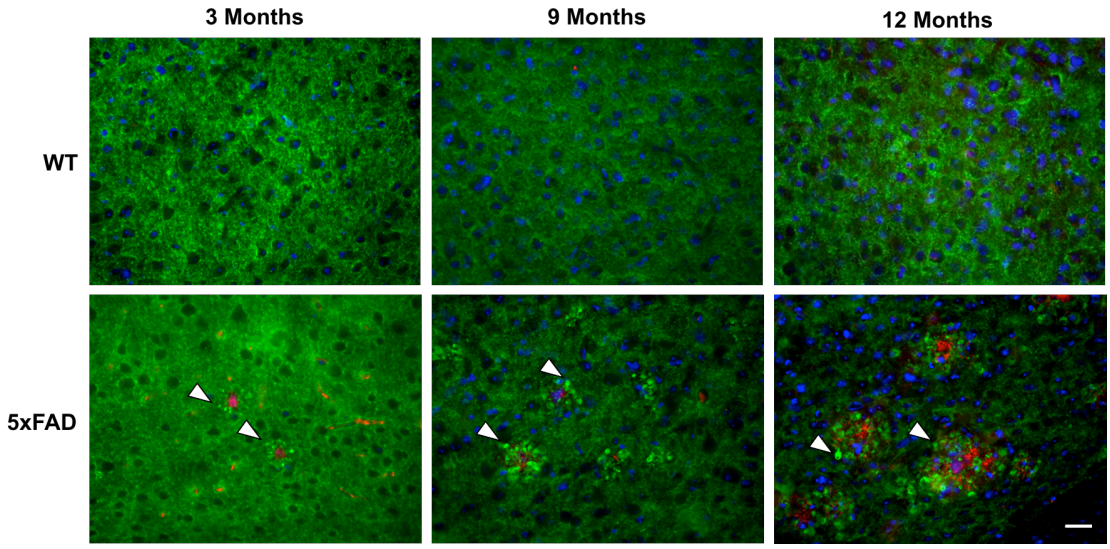

Figure 6.2. Aβ plaque-associated CSPalpha accumulations in 3, 9 and 12 month old 5xFAD mice.

Representative low magnification images of unmatched cortical sections from female WT and 5xFAD transgenic mouse brains at 3, 9 and 12 months of age co-labelled with CSPalpha (*green*) and Aβ (*red*) antibodies. DAPI (*blue*) was used to stain nuclei. *White arrowheads* indicative of CSPalpha accumulations. Magnification 40x. Scale 25 μm. [n=1 mouse per age group].

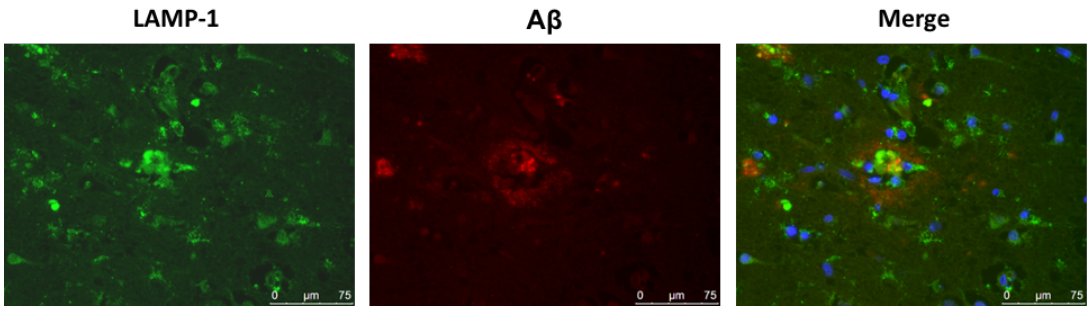

Figure 6.3. LAMP-1 accumulates within Aβ plaques.

Representative images of BA9 brain sections of Braak stage IV human post-mortem AD brain co-labelled with antibodies against **a)** LAMP-1 (*green*) and Aβ (*red*). DAPI (*blue*) was used to stain nuclei. Magnification 20x. Scale bar 75 µm. [n=1 case].

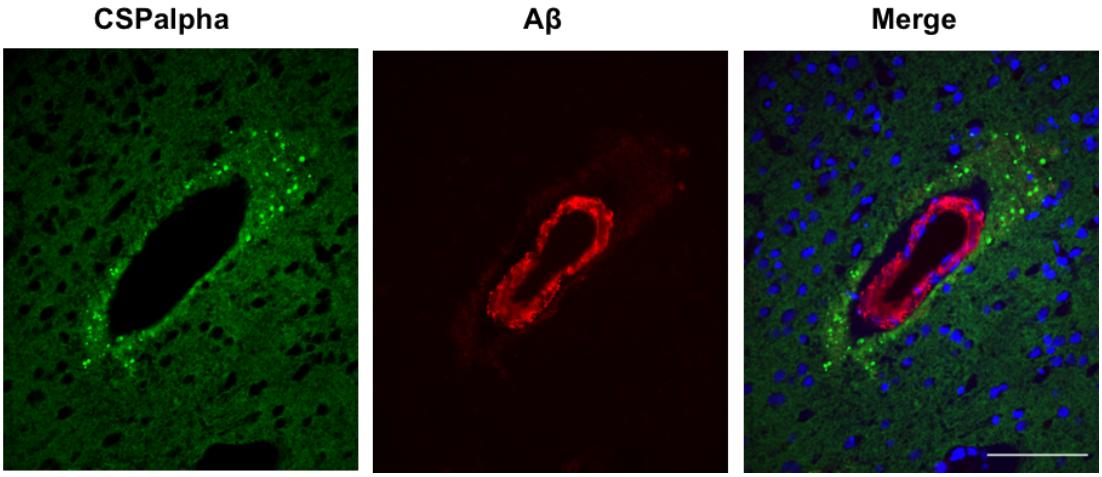

Figure 6.4. CSPalpha accumulations surround Aβ vascular pathology in AD.

Representative image of a temporal cortical brain section from Braak stage VI human post-mortem AD brain depicting CSPalpha accumulations in proximity to an artery with its vessel wall disrupted Aβ deposits and dysphoric angiopathy. Tissue section co-labelled with antibodies against CSPalpha (*green*) and Aβ (*red*). DAPI (*blue*) was used to stain nuclei. Magnification 40x. Scale bar 100 µm.

Chapter 7: References

2020 Alzheimer's disease facts and figures (2020). *Alzheimer's Dement.* 16, 391–460.

Abramov, E., Dolev, I., Fogel, H., Ciccotosto, G. D., Ruff, E., and Slutsky, I. (2009). Amyloid-B as a positive endogenous regulator of release probability at hippocampal synapses. *Nat. Neurosci.* 12, 1567–1576.

Adalbert, R., Nogradi, A., Babetto, E., Janeckova, L., Walker, S. A., Kerschensteiner, M., Misgeld, T., and Coleman, M. P. (2009). Severely dystrophic axons at amyloid plaques remain continuous and connected to viable cell bodies. *Brain* 132, 402–416.

Ahmed, Z., Cooper, J., Murray, T. K., Garn, K., McNaughton, E., Clarke, H., Parhizkar, S., Ward, M. A., Cavallini, A., Jackson, S., Bose, S., Clavaguera, F., Tolnay, M., Lavenir, I., Goedert, M., Hutton, M. L., and O'Neill, M. J. (2014). A novel in vivo model of tau propagation with rapid and progressive neurofibrillary tangle pathology: The pattern of spread is determined by connectivity, not proximity. *Acta Neuropathol.* 127, 667–683.

Ahrendt, E., Kyle, B., Braun, A. P., and Braun, J. E. A. (2014). Cysteine string protein limits expression of the large conductance, calcium-activated K+ (BK) channel. *PLoS One* 9, 1–9.

Al-Sarraj, S., King, A., Troakes, C., Smith, B., Maekawa, S., Bodi, I., Rogelj, B., Al-Chalabi, A., Hortobágyi, T., and Shaw, C. E. (2011). P62 positive, TDP-43 negative, neuronal cytoplasmic and intranuclear inclusions in the cerebellum and hippocampus define the pathology of C9orf72-linked FTLD and MND/ALS. *Acta Neuropathol.* 122, 691–702.

Albert, M. S., DeKosky, S. T., Dickson, D., Dubois, B., Feldman, H. H., Fox, N. C., Gamst, A., Holtzman, D. M., Jagust, W. J., Petersen, R. C., Snyder, P. J., Carrillo, M. C., Thies, B., and Phelps, C. H. (2011). The diagnosis of mild cognitive impairment due to Alzheimer's disease: recommendations from the National Institute on Aging-Alzheimer's Association workgroups on diagnostic guidelines for Alzheimer's disease. *Alzheimers. Dement.* 7, 270–279.

Allen, B., Ingram, E., Takao, M., Smith, M. J., Jakes, R., Virdee, K., Yoshida, H., Holzer, M., Craxton, M., Emson, P. C., Atzori, C., Migheli, A., Anthony Crowther, R., Ghetti, B., Spillantini, M. G., and Goedert, M. (2002). Abundant tau filaments and nonapoptotic neurodegeneration in transgenic mice

expressing human P301s tau protein. *J. Neurosci.* 22, 9340–9351.

Alonso, A. D., Cohen, L. S., Corbo, C., Morozova, V., ElIdrissi, A., Phillips, G., and Kleiman, F. E. (2018). Hyperphosphorylation of Tau Associates with changes in its function beyond microtubule stability. *Front. Cell. Neurosci.* 12, 1–11.

Amador-Ortiz, C., Lin, W.-L., Ahmed, Z., Personett, D., Davies, P., Duara, R., Graff-Radford, N. R., Hutton, M. L., and Dickson, D. W. (2007). TDP-43 immunoreactivity in hippocampal sclerosis and Alzheimer's disease. *Ann. Neurol.* 61, 435–445.

Amar, F., Sherman, M. A., Rush, T., Larson, M., Boyle, G., Chang, L., Götz, J., Buisson, A., and Lesné, S. E. (2017). The amyloid-β oligomer Aβ∗56 induces specific alterations in neuronal signaling that lead to tau phosphorylation and aggregation. *Sci. Signal.* 10.

Amorim, I. S., Mitchell, N. L., Palmer, D. N., Sawiak, S. J., Mason, R., Wishart, T. M., and Gillingwater, T. H. (2015). Molecular neuropathology of the synapse in sheep with CLN5 Batten disease. *Brain Behav.* 5, 1–12.

Andorfer, C., Kress, Y., Espinoza, M., De Silva, R., Tucker, K. L., Barde, Y. A., Duff, K., and Davies, P. (2003). Hyperphosphorylation and aggregation of tau in mice expressing normal human tau isoforms. *J. Neurochem.* 86, 582–590.

Andreadis, A., Brown, W. M., and Kosik, K. S. (1992). Structure and Novel Exons of the Human τ Gene. *Biochemistry* 31, 10626–10633.

Andrew, R. J., Kellett, K. A. B., Thinakaran, G., and Hooper, N. M. (2016). A Greek tragedy: The growing complexity of Alzheimer amyloid precursor protein proteolysis. *J. Biol. Chem.* 291, 19235–19244.

Arai, H., Lee, V. M. -., Messinger, M. L., Greenberg, B. D., Lowery, D. E., and Trojanowski, J. Q. (1991). Expression patterns of β-amyloid precursor protein (β-APP) in neural and nonneural human tissues from alzheimer's disease and control subjects. *Ann. Neurol.* 30, 686–693.

Arai, T., Hasegawa, M., Akiyama, H., Ikeda, K., Nonaka, T., Mori, H., Mann, D., Tsuchiya, K., Yoshida, M., Hashizume, Y., and Oda, T. (2006). TDP-43 is a component of ubiquitin-positive tau-negative inclusions in frontotemporal lobar degeneration and amyotrophic lateral sclerosis. *Biochem. Biophys. Res. Commun.* 351, 602–611.

Arai, T., Mackenzie, I. R. A., Hasegawa, M., Nonoka, T., Niizato, K., Tsuchiya, K., Iritani, S., Onaya, M., and Akiyama, H. (2009). Phosphorylated TDP-43 in Alzheimer's disease and dementia with Lewy bodies. *Acta Neuropathol.* 117, 125–136.

Arbel-Ornath, M., Hudry, E., Boivin, J. R., Hashimoto, T., Takeda, S., Kuchibhotla,

K. V., Hou, S., Lattarulo, C. R., Belcher, A. M., Shakerdge, N., Trujillo, P. B., Muzikansky, A., Betensky, R. A., Hyman, B. T., and Bacskai, B. J. (2017). Soluble oligomeric amyloid-β induces calcium dyshomeostasis that precedes synapse loss in the living mouse brain. *Mol. Neurodegener.* 12, 1–14.

Arber, C., Toombs, J., Lovejoy, C., Ryan, N. S., Paterson, R. W., Willumsen, N., Gkanatsiou, E., Portelius, E., Blennow, K., Heslegrave, A., Schott, J. M., Hardy, J., Lashley, T., Fox, N. C., Zetterberg, H., and Wray, S. (2020). Familial Alzheimer's disease patient-derived neurons reveal distinct mutation-specific effects on amyloid beta. *Mol. Psychiatry* 25, 2919–2931.

Arendt, T. (2009). Synaptic degeneration in Alzheimer's disease. *Acta Neuropathol.* 118, 167–179.

Arnold, S. E., Hyman, B. T., Flory, J., Damasio, A. R., and Van Hoesen, G. W. (1991). The topographical and neuroanatomical distribution of neurofibrillary tangles and neuritic plaques in the cerebral cortex of patients with alzheimer's disease. *Cereb. Cortex* 1, 103–116.

Arrasate, M., Pérez, M., and Avila, J. (2000). Tau dephosphorylation at Tau-1 site correlates with its association to cell membrane. *Neurochem. Res.* 25, 43–50.

Arriagada, P. V., Growdon, J. H., Hedley-Whyte, E. T., and Hyman, B. T. (1992). Neurofibrillary tangles but not senile plaques parallel duration and severity of Alzheimer's disease. *Neurology* 42, 631–639.

Arvanitakis, Z., Capuano, A. W., Leurgans, S. E., Bennett, D. A., and Schneider, J. A. (2016). Relation of cerebral vessel disease to Alzheimer's disease dementia and cognitive function in elderly people: a cross-sectional study. *Lancet. Neurol.* 15, 934–943.

Asai, H., Ikezu, S., Tsunoda, S., Medalla, M., Luebke, J., Haydar, T., Wolozin, B., Butovsky, O., Kügler, S., and Ikezu, T. (2015). Depletion of microglia and inhibition of exosome synthesis halt tau propagation. *Nat. Neurosci.* 18, 1584–1593.

Attems, J. (2005). Sporadic cerebral amyloid angiopathy: pathology, clinical implications, and possible pathomechanisms. *Acta Neuropathol.* 110, 345–359.

Attems, J., Quass, M., Jellinger, K. A., and Lintner, F. (2007). Topographical distribution of cerebral amyloid angiopathy and its effect on cognitive decline are influenced by Alzheimer disease pathology. *J. Neurol. Sci.* 257, 49–55.

Aziz, W., Kraev, I., Mizuno, K., Kirby, A., Fang, T., Rupawala, H., Kasbi, K., Rothe, S., Jozsa, F., Rosenblum, K., Stewart, M. G., and Giese, K. P. (2019). Multi-input Synapses, but Not LTP-Strengthened Synapses, Correlate with Hippocampal Memory Storage in Aged Mice. *Curr. Biol.* 29, 3600–3610.

Bahia, V. S., Takada, L. T., and Deramecourt, V. (2013). Neuropathology of frontotemporal lobar degeneration: a review. *Dement. Neuropsychol.* 7, 19–26.

Bahmanyar, S., Higgins, G. A., Goldgaber, D., Lewis, D. A., Morrison, J. H., Wilson, M. C., Shankar, S. K., and Gajdusek, D. C. (1987). Localization of amyloid β protein messenger RNA in brains from patients with Alzheimer's disease. *Science (80-.).* 237, 77–80.

Bai, B., Hales, C. M., Chen, P. C., Gozal, Y., Dammer, E. B., Fritz, J. J., Wang, X., Xia, Q., Duong, D. M., Street, C., Cantero, G., Cheng, D., Jones, D. R., Wu, Z., Li, Y., Diner, I., Heilman, C. J., Rees, H. D., Wu, H., Lin, L., Szulwach, K. E., Gearing, M., Mufson, E. J., Bennett, D. A., Montine, T. J., Seyfried, N. T., Wingo, T. S., Sun, Y. E., Jin, P., Hanfelt, J., Willcock, D. M., Levey, A., Lah, J. J., and Peng, J. (2013). U1 small nuclear ribonucleoprotein complex and RNA splicing alterations in Alzheimer's disease. *Proc. Natl. Acad. Sci. U. S. A.* 110, 16562–16567.

Baker, S., Polanco, J. C., and Götz, J. (2016). Extracellular Vesicles Containing P301L Mutant Tau Accelerate Pathological Tau Phosphorylation and Oligomer Formation but Do Not Seed Mature Neurofibrillary Tangles in ALZ17 Mice. *J. Alzheimer's Dis.* 54, 1207–1217.

Bancher, C., Braak, H., Fischer, P., and Jellinger, K. A. (1993). Neuropathological staging of Alzheimer lesions and intellectual status in Alzheimer's and Parkinson's disease patients. *Neurosci. Lett.* 162, 179–182.

Barker, W. W., Luis, C. A., Kashuba, A., Luis, M., Harwood, D. G., Loewenstein, D., Waters, C., Jimison, P., Shepherd, E., Sevush, S., Graff-Radford, N., Newland, D., Todd, M., Miller, B., Gold, M., Heilman, K., Doty, L., Goodman, I., Robinson, B., Pearl, G., Dickson, D., and Duara, R. (2002). Relative frequencies of Alzheimer disease, Lewy body, vascular and frontotemporal dementia, and hippocampal sclerosis in the State of Florida Brain Bank. *Alzheimer Dis. Assoc. Disord.* 16, 203–212.

Barry, A. E., Klyubin, I., McDonald, J. M., Mably, A. J., Farrell, M. A., Scott, M., Walsh, D. M., and Rowan, M. J. (2011). Alzheimer's disease brain-derived amyloid-β-mediated inhibition of LTP In Vivo is prevented by immunotargeting cellular prion protein. *J. Neurosci.* 31, 7259–7263.

Barthélemy, N. R., Fenaille, F., Hirtz, C., Sergeant, N., Schraen-Maschke, S., Vialaret, J., Buée, L., Gabelle, A., Junot, C., Lehmann, S., and Becher, F. (2016). Tau Protein Quantification in Human Cerebrospinal Fluid by Targeted Mass Spectrometry at High Sequence Coverage Provides Insights into Its Primary Structure Heterogeneity. *J. Proteome Res.* 15, 667–676.

Bass, J. J., Wilkinson, D. J., Rankin, D., Phillips, B. E., Szewczyk, N. J., Smith, K., and Atherton, P. J. (2017). An overview of technical considerations for Western blotting applications to physiological research. *Scand. J. Med. Sci. Sport.* 27, 4–25.

Bate, C., and Williams, A. (2018). Monomeric amyloid-β reduced amyloid-β oligomer-induced synapse damage in neuronal cultures. *Neurobiol. Dis.* 111, 48–58.

Bateman, R. J., Munsell, L. Y., Morris, J. C., Swarm, R., Yarasheski, K. E., and Holtzman, D. M. (2006). Human amyloid-β synthesis and clearance rates as measured in cerebrospinal fluid in vivo. *Nat. Med.* 12, 856–861.

Baumann, K., Mandelkow, E. M., Biernat, J., Piwnica-Worms, H., and Mandelkow, E. (1993). Abnormal Alzheimer-like phosphorylation of tau-protein by cyclin-dependent kinases cdk2 and cdk5. *FEBS Lett.* 336, 417–424.

Bayés, À., Collins, M. O., Galtrey, C. M., Simonnet, C., Roy, M., Croning, M. D. R., Gou, G., Van De Lagemaat, L. N., Milward, D., Whittle, I. R., Smith, C., Choudhary, J. S., and Grant, S. G. N. (2014). Human post-mortem synapse proteome integrity screening for proteomic studies of postsynaptic complexes. *Mol. Brain* 7, 1–11.

Beach, T. G., Walker, R., and McGeer, E. G. (1989). Patterns of gliosis in alzheimer's disease and aging cerebrum. *Glia* 2, 420–436.

Begcevic, I., Kosanam, H., Martínez-Morillo, E., Dimitromanolakis, A., Diamandis, P., Kuzmanov, U., Hazrati, L. N., and Diamandis, E. P. (2013). Semiquantitative proteomic analysis of human hippocampal tissues from alzheimer's disease and age-matched control brains. *Clin. Proteomics* 10, 1–7.

Bekris, L. M., Yu, C. E., Bird, T. D., and Tsuang, D. W. (2010). Review article: Genetics of Alzheimer disease. *J. Geriatr. Psychiatry Neurol.* 23, 213–227.

Benilova, I., Karran, E., and De Strooper, B. (2012). The toxic Aβ oligomer and Alzheimer's disease: An emperor in need of clothes. *Nat. Neurosci.* 15, 349–357.

Benitez, B. A., Alvarado, D., Cai, Y., Mayo, K., Chakraverty, S., Norton, J., Morris, J. C., Sands, M. S., Goate, A., and Cruchaga, C. (2011). Exome-sequencing confirms DNAJC5 mutations as cause of adult neuronal ceroid-lipofuscinosis. *PLoS One* 6, 1–11.

Benitez, B. A., Cairns, N. J., Schmidt, R. E., Morris, J. C., Norton, J. B., Cruchaga, C., Sands, M. S., Haltia, M., Goebel, H., Anderson, G., Goebel, H., Simonati, A., Sadzot, B., Reznik, M., Arrese-Estrada, J., Franck, G., Josephson, S., Schmidt, R., Millsap, P., McManus, D., Morris, J., Benitez, B., Alvarado, D.,

Cai, Y., Mayo, K., Chakraverty, S., Norton, J., Morris, J., Sands, M., Goate, A., Cruchaga, C., Noskova, L., Stranecky, V., Hartmannova, H., Pristoupilova, A., Baresova, V., Ivanek, R., Hulkova, H., Jahnova, H., Zee, J., Staropoli, J., Sims, K., Tyynela, J., Broeckhoven, C., Nijssen, P., Mole, S., Elleder, M., Kmoch, S., Velinov, M., Dolzhanskaya, N., Gonzalez, M., Powell, E., Konidari, I., Hulme, W., Staropoli, J., Xin, W., Wen, G., Barone, R., Coppel, S., Sims, K., Brown, W., Zuchner, S., Zinsmaier, K., Fernandez-Chacon, R., Wolfel, M., Nishimune, H., Tabares, L., Schmitz, F., Castellano-Munoz, M., Rosenmund, C., Montesinos, M., Sanes, J., Schneggenburger, R., Sudhof, T., Chandra, S., Gallardo, G., Fernandez-Chacon, R., Schluter, O., Sudhof, T., Donnelier, J., Braun, J., Zhang, Y., Henderson, M., Colangelo, C., Ginsberg, S., Bruce, C., Wu, T., Chandra, S., Sharma, M., Burre, J., Bronk, P., Zhang, Y., Xu, W., Sudhof, T., Sharma, M., Burre, J., Sudhof, T., Donnelier, J., Braun, S., Dolzhanskaya, N., Ahrendt, E., Braun, A., Velinov, M., Braun, J., Cairns, N., Perrin, R., Franklin, E., Carter, D., Vincent, B., Xie, M., Bateman, R., Benzinger, T., Friedrichsen, K., Brooks, W., Halliday, G., McLean, C., Ghetti, B., Morris, J., Williams, R., Aberg, L., Autti, T., Goebel, H., Kohlschütter, A., Lönnqvist, T., Shyng, C., Sands, M., Fraldi, A., Annunziata, F., Lombardi, A., Kaiser, H., Medina, D., Spampanato, C., Fedele, A., Polishchuk, R., Sorrentino, N., Simons, K., Ballabio, A., Kielar, C., Wishart, T., Palmer, A., Dihanich, S., Wong, A., Macauley, S., Chan, C., Sands, M., Pearce, D., Cooper, J., Gillingwater, T., Pressey, S., Smith, D., Wong, A., Platt, F., Cooper, J., Song, J., Misgeld, T., Kang, H., Knecht, S., Lu, J., Cao, Y., Cotman, S., Bishop, D., Lichtman, J., Greaves, J., Lemonidis, K., Gorleku, O., Cruchaga, C., Grefen, C., Chamberlain, L., Evans, G., Morgan, A., Brown, H., Larsson, O., Branstrom, R., Yang, S., Leibiger, B., Leibiger, I., Fried, G., Moede, T., Deeney, J., Brown, G., Jacobsson, G., Rhodes, C., Braun, J., Scheller, R., Corkey, B., Berggren, P., Meister, B., Chamberlain, L., Burgoyne, R., Chamberlain, L., Henry, J., Burgoyne, R., Greaves, J., Salaun, C., Fukata, Y., Fukata, M., Chamberlain, L., Greaves, J., Chamberlain, L., Luzio, J., Pryor, P., and Bright, N. (2015). Clinically early-stage CSPα mutation carrier exhibits remarkable terminal stage neuronal pathology with minimal evidence of synaptic loss. *Acta Neuropathol. Commun.* 3, 1–10.

Benitez, B. A., and Sands, M. S. (2017). Primary fibroblasts from CSPα mutation carriers recapitulate hallmarks of the adult onset neuronal ceroid lipofuscinosis. *Sci. Rep.* 7, 1–15.

Bennett, D. A., Schneider, J. A., Arvanitakis, Z., and Wilson, R. S. (2012a).

Overview and findings from the religious orders study. *Curr. Alzheimer Res.* 9, 628–645.

Bennett, D. A., Schneider, J. A., Buchman, A. S., Barnes, L. L., Boyle, P. A., and Wilson, R. S. (2012b). Overview and findings from the rush Memory and Aging Project. *Curr. Alzheimer Res.* 9, 646–663.

Bentahir, M., Nyabi, O., Verhamme, J., Tolia, A., Horré, K., Wiltfang, J., Esselmann, H., and De Strooper, B. (2006). Presenilin clinical mutations can affect γ-secretase activity by different mechanisms. *J. Neurochem.* 96, 732–742.

Benzing, W. C., and Mufson, E. J. (1995). Apolipoprotein E immunoreactivity within neurofibrillary tangles: relationship to tau and PHF in Alzheimer's disease. *Exp. Neurol.* 132, 162–171.

Benzing, W. C., Mufson, E. J., and Armstrong, D. M. (1993). Alzheimer's disease-like dystrophic neurites characteristically associated with senile plaques are not found within other neurodegenerative disease unless amyloid β-protein deposition is present. *Brain Res.* 606, 10–18.

Bereczki, E., Francis, P. T., Howlett, D., Pereira, J. B., Höglund, K., Bogstedt, A., Cedazo-Minguez, A., Baek, J. H., Hortobágyi, T., Attems, J., Ballard, C., and Aarsland, D. (2016). Synaptic proteins predict cognitive decline in Alzheimer's disease and Lewy body dementia. *Alzheimer's Dement.* 12, 1149–1158.

Berger, Z., Roder, H., Hanna, A., Carlson, A., Rangachari, V., Yue, M., Wszolek, Z., Ashe, K., Knight, J., Dickson, D., Andorfer, C., Rosenberry, T. L., Lewis, J., Hutton, M., and Janus, C. (2007). Accumulation of pathological tau species and memory loss in a conditional model of tauopathy. *J. Neurosci.* 27, 3650–3662.

Bergström, P., Agholme, L., Nazir, F. H., Satir, T. M., Toombs, J., Wellington, H., Strandberg, J., Bontell, T. O., Kvartsberg, H., Holmström, M., Boreström, C., Simonsson, S., Kunath, T., Lindahl, A., Blennow, K., Hanse, E., Portelius, E., Wray, S., and Zetterberg, H. (2016). Amyloid precursor protein expression and processing are differentially regulated during cortical neuron differentiation. *Sci. Rep.* 6, 1–14.

Bhaskar, K., Yen, S. H., and Lee, G. (2005). Disease-related modifications in tau affect the interaction between Fyn and tau. *J. Biol. Chem.* 280, 35119–35125.

Biernat, J., and Mandelkow, E. M. (1999). The development of cell processes induced by tau protein requires phosphorylation of serine 262 and 356 in the repeat domain and is inhibited by phosphorylation in the proline-rich domains. *Mol. Biol. Cell* 10, 727–740.

Binder, L. I., Frankfurter, A., and Rebhun, L. I. (1985). The distribution of tau in the

mammalian central nervous central nervous. *J. Cell Biol.* 101, 1371–1378.

Binder, L. I., Guillozet-Bongaarts, A. L., Garcia-Sierra, F., and Berry, R. W. (2005). Tau, tangles, and Alzheimer's disease. *Biochim. Biophys. Acta - Mol. Basis Dis.* 1739, 216–223.

Bittner, T., Fuhrmann, M., Burgold, S., Ochs, S. M., Hoffmann, N., Mitteregger, G., Kretzschmar, H., LaFerla, F. M., and Herms, J. (2010). Multiple Events Lead to Dendritic Spine Loss in Triple Transgenic Alzheimer's Disease Mice. *PLoS One* 5, 1–9.

Blennow, K., Bogdanovic, N., Alafuzoff, I., Ekman, R., and Davidsson, P. (1996). Synaptic pathology in Alzheimer's disease: Relation to severity of dementia, but not to senile plaques, neurofibrillary tangles, or the ApoE4 allele. *J. Neural Transm.* 103, 603–618.

Blennow, K., and Zetterberg, H. (2018). Biomarkers for Alzheimer's disease: current status and prospects for the future. *J. Intern. Med.* 284, 643–663.

Boal, F., Zhang, H., Tessier, C., Scotti, P., and Lang, J. (2004). The Variable C-Terminus of Cysteine String Proteins Modulates Exocytosis and Protein-Protein Interactions. *Biochemistry* 43, 16212–16223.

Bobkova, N. V., Garbuz, D. G., Nesterova, I., Medvinskaya, N., Samokhin, A., Alexandrova, I., Yashin, V., Karpov, V., Kukharsky, M. S., Ninkina, N. N., Smirnov, A. A., Nudler, E., and Evgen'Ev, M. (2014). Therapeutic effect of exogenous Hsp70 in mouse models of Alzheimer's disease. *J. Alzheimer's Dis.* 38, 425–435.

Borlikova, G. G., Trejo, M., Mably, A. J., Mc Donald, J. M., Sala Frigerio, C., Regan, C. M., Murphy, K. J., Masliah, E., and Walsh, D. M. (2013). Alzheimer brain-derived amyloid β-protein impairs synaptic remodeling and memory consolidation. *Neurobiol. Aging* 34, 1315–1327.

Boutajangout, A., Authelet, M., Blanchard, V., Touchet, N., Tremp, G., Pradier, L., and Brion, J. P. (2004). Characterisation of cytoskeletal abnormalities in mice transgenic for wild-type human tau and familial Alzheimer's disease mutants of APP and presenilin-1. *Neurobiol. Dis.* 15, 47–60.

Bouvier, D. S., Jones, E. V., Quesseveur, G., Davoli, M. A., Ferreira, T. A., Quirion, R., Mechawar, N., and Murai, K. K. (2016). High Resolution Dissection of Reactive Glial Nets in Alzheimer's Disease. *Sci. Rep.* 6, 1–15.

Boyle, P. A., Yu, L., Nag, S., Leurgans, S., Wilson, R. S., Bennett, D. A., and Schneider, J. A. (2015). Cerebral amyloid angiopathy and cognitive outcomes in community-based older persons. *Neurology* 85, 1930–1936.

Boyle, P. A., Yu, L., Wilson, R. S., Leurgans, S. E., Schneider, J. A., and Bennett,

D. A. (2018). Person-specific contribution of neuropathologies to cognitive loss in old age. *Ann. Neurol.* 83, 74–83.

Braak, E., Braak, H., and Mandelkow, E. M. (1994). A sequence of cytoskeleton changes related to the formation of neurofibrillary tangles and neuropil threads. *Acta Neuropathol.* 87, 554–567.

Braak, H., and Braak, E. (1991). Neuropathological stageing of Alzheimer-related changes. *Acta Neuropathol.* 82, 239–259.

Braak, H., and Braak, E. (1995). Staging of alzheimer's disease-related neurofibrillary changes. *Neurobiol. Aging* 16, 271–278.

Braak, H., Del Tredici, K., Rüb, U., De Vos, R. A. I., Jansen Steur, E. N. H., and Braak, E. (2003). Staging of brain pathology related to sporadic Parkinson's disease. *Neurobiol. Aging* 24, 197–211.

Brandt, R., Hundelt, M., and Shahani, N. (2005). Tau alteration and neuronal degeneration in tauopathies: Mechanisms and models. *Biochim. Biophys. Acta - Mol. Basis Dis.* 1739, 331–354.

Brandt, R., and Lee, G. (1994). Orientation, assembly, and stability of microtubule bundles induced by a fragment of tau protein. *Cell Motil. Cytoskeleton* 28, 143–154.

Braun, J. E. A., and Scheller, R. H. (1995). Cysteine string protein, a DnaJ family member, is present on diverse secretory vesicles. *Neuropharmacology* 34, 1361–1369.

Braun, J. E., Wilbanks, S. M., and Scheller, R. H. (1996). The cysteine string secretory vesicle protein activates Hsc70 ATPase. *J. Biol. Chem.* 271, 25989–25993.

Bridi, J. C., and Hirth, F. (2018). Mechanisms of α-Synuclein induced synaptopathy in parkinson's disease. *Front. Neurosci.* 12, 1–18.

Brinkmalm, A., Brinkmalm, G., Honer, W. G., Frölich, L., Hausner, L., Minthon, L., Hansson, O., Wallin, A., Zetterberg, H., Blennow, K., and Öhrfelt, A. (2014). SNAP-25 is a promising novel cerebrospinal fluid biomarker for synapse degeneration in Alzheimer's disease. *Mol. Neurodegener.* 9, 1–13.

Brion, J. P., Couck, A. M., Bruce, M., Anderton, B., and Flament-Durand, J. (1991). Synaptophysin and chromogranin A immunoreactivities in senile plaques of Alzheimer's disease. *Brain Res.* 539, 143–150.

Broe, M., Hodges, J. R., Schofield, E., Shepherd, C. E., Kril, J. J., and Halliday, G. M. (2003). Staging disease severity in pathologically confirmed cases of frontotemporal dementia. *Neurology* 60, 1005–1011.

Bronk, P., Nie, Z., Klose, M. K., Dawson-Scully, K., Zhang, J., Robertson, R. M.,

Atwood, H. L., and Zinsmaier, K. E. (2005). The multiple functions of cysteine-string protein analyzed at Drosophila nerve terminals. *J. Neurosci.* 25, 2204–2214.

Brown, H., Larsson, O., Bränström, R., Yang, S. N., Leibiger, B., Leibiger, I., Fried, G., Moede, T., Deeney, J. T., Brown, G. R., Jacobsson, G., Rhodes, C. J., Braun, J. E. A., Scheller, R. H., Corkey, B. E., Berggren, P. O., and Meister, B. (1998). Cysteine string protein (CSP) is an insulin secretory granule-associated protein regulating β-cell exocytosis. *EMBO J.* 17, 5048–5058.

Brun, A., Liu, X., and Erikson, C. (1995). Synapse loss and gliosis in the molecular layer of the cerebral cortex in Alzheimer's disease and in frontal lobe degeneration. *Neurodegeneration* 4, 171–177.

Buchberger, A. R., DeLaney, K., Johnson, J., and Li, L. (2018). Mass Spectrometry Imaging: A Review of Emerging Advancements and Future Insights. *Anal. Chem.* 90, 240–265.

Buchner, E., and Gundersen, C. (1997). The DnaJ-like cysteine string protein and exocytotic neurotransmitter release. *Trends Neurosci.* 20, 223–227.

Burgoyne, R. D., and Morgan, A. (2015). Cysteine string protein (CSP) and its role in preventing neurodegeneration. *Semin. Cell Dev. Biol.* 40, 153–159.

Burns, M. P., Noble, W. J., Olm, V., Gaynor, K., Casey, E., LaFrancois, J., Wang, L., and Duff, K. (2003). Co-localization of cholesterol, apolipoprotein E and fibrillar Aβ in amyloid plaques. *Mol. Brain Res.* 110, 119–125.

Burré, J., Sharma, M., Tsetsenis, T., Buchman, V., Etherton, M. R., and Südhof, T. C. (2010). α-Synuclein promotes SNARE-complex assembly in vivo and in vitro. *Science (80-.).* 329, 1663–1667.

Busche, M. A., Wegmann, S., Dujardin, S., Commins, C., Schiantarelli, J., Klickstein, N., Kamath, T. V., Carlson, G. A., Nelken, I., and Hyman, B. T. (2019). Tau impairs neural circuits, dominating amyloid-β effects, in Alzheimer models in vivo. *Nat. Neurosci.* 22, 57–64.

Bussière, T., Giannakopoulos, P., Bouras, C., Perl, D. P., Morrison, J. H., and Hof, P. R. (2003). Progressive degeneration of nonphosphorylated neurofilament protein-enriched pyramidal neurons predicts cognitive impairment in Alzheimer's disease: Stereologic analysis of prefrontal cortex area 9. *J. Comp. Neurol.* 463, 281–302.

Cadieux-Dion, M., Andermann, E., Lachance-Touchette, P., Ansorge, O., Meloche, C., Barnab, A., Kuzniecky, R. I., Andermann, F., Faught, E., Leonberg, S., Damiano, J. A., Berkovic, S. F., Rouleau, G. A., and Cossette, P. (2013). Recurrent mutations in DNAJC5 cause autosomal dominant Kufs disease. *Clin.*

Genet. 83, 571–575.

Calabrese, B., Shaked, G. M., Tabarean, I. V., Braga, J., Koo, E. H., and Halpain, S. (2007). Rapid, concurrent alterations in pre- and postsynaptic structure induced by naturally-secreted amyloid-β protein. *Mol. Cell. Neurosci.* 35, 183–193.

Caló, L., Hidari, E., Wegrzynowicz, M., Dalley, J. W., Schneider, B. L., Anichtchik, O., Carlson, E., Klenerman, D., and Spillantini, M. G. (2020). CSPα reduces aggregates and rescues striatal dopamine release in αsynuclein transgenic mice. *bioRxiv*. doi:10.1101/2020.07.31.229153.

Cantlon, A., Frigerio, C. S., Freir, D. B., Boland, B., Jin, M., and Walsh, D. M. (2015). The Familial British Dementia Mutation Promotes Formation of Neurotoxic Cystine Cross-linked Amyloid Bri (ABri) Oligomers *. *J. Biol. Chem.* 290, 16502–16516.

Castellano, J. M., Kim, J., Stewart, F. R., Jiang, H., DeMattos, R. B., Patterson, B. W., Fagan, A. M., Morris, J. C., Mawuenyega, K. G., Cruchaga, C., Goate, A. M., Bales, K. R., Paul, S. M., Bateman, R. J., and Holtzman, D. M. (2011). Human apoE isoforms differentially regulate brain amyloid-β peptide clearance. *Sci. Transl. Med.* 3, 1–21.

Chai, X., Dage, J. L., and Citron, M. (2012). Constitutive secretion of tau protein by an unconventional mechanism. *Neurobiol. Dis.* 48, 356–366.

Chamberlain, L. H., and Burgoyne, R. D. (1996). Identification of a novel cysteine string protein variant and expression of cysteine string proteins in non-neuronal cells. *J. Biol. Chem.* 271, 7320–7323.

Chamberlain, L. H., and Burgoyne, R. D. (1997). Activation of the ATPase activity of heat-shock proteins Hsc70/Hsp70 by cysteine-string protein. *Biochem. J.* 322, 853–858.

Chamberlain, L. H., and Burgoyne, R. D. (2000). Cysteine-string protein: The chaperone at the synapse. *J. Neurochem.* 74, 1781–1789.

Chandra, S., Gallardo, G., Fernández-Chacón, R., Schlüter, O. M., and Südhof, T. C. (2005). α-Synuclein cooperates with CSPα in preventing neurodegeneration. *Cell* 123, 383–396.

Chapuis, J., Hansmannel, F., Gistelinck, M., Mounier, A., Van Cauwenberghe, C., Kolen, K. V., Geller, F., Sottejeau, Y., Harold, D., Dourlen, P., Grenier-Boley, B., Kamatani, Y., Delepine, B., Demiautte, F., Zelenika, D., Zommer, N., Hamdane, M., Bellenguez, C., Dartigues, J. F., Hauw, J. J., Letronne, F., Ayral, A. M., Sleegers, K., Schellens, A., Broeck, L. V., Engelborghs, S., De Deyn, P. P., Vandenberghe, R., O'Donovan, M., Owen, M., Epelbaum, J., Mercken, M.,

Karran, E., Bantscheff, M., Drewes, G., Joberty, G., Campion, D., Octave, J. N., Berr, C., Lathrop, M., Callaerts, P., Mann, D., Williams, J., Buée, L., Dewachter, I., Van Broeckhoven, C., Amouyel, P., Moechars, D., Dermaut, B., and Lambert, J. C. (2013). Increased expression of BIN1 mediates Alzheimer genetic risk by modulating tau pathology. *Mol. Psychiatry* 18, 1225–1234.

Chen, M. K., Mecca, A. P., Naganawa, M., Finnema, S. J., Toyonaga, T., Lin, S. F., Najafzadeh, S., Ropchan, J., Lu, Y., McDonald, J. W., Michalak, H. R., Nabulsi, N. B., Arnsten, A. F. T., Huang, Y., Carson, R. E., and Van Dyck, C. H. (2018). Assessing Synaptic Density in Alzheimer Disease with Synaptic Vesicle Glycoprotein 2A Positron Emission Tomographic Imaging. *JAMA Neurol.* 75, 1215–1224.

Chévez-Gutiérrez, L., Bammens, L., Benilova, I., Vandersteen, A., Benurwar, M., Borgers, M., Lismont, S., Zhou, L., Van Cleynenbreugel, S., Esselmann, H., Wiltfang, J., Serneels, L., Karran, E., Gijsen, H., Schymkowitz, J., Rousseau, F., Broersen, K., and De Strooper, B. (2012). The mechanism of γ-Secretase dysfunction in familial Alzheimer disease. *EMBO J.* 31, 2261–2274.

Chiang, N., Hsiao, Y.-T., Yang, H.-J., Lin, Y.-C., Lu, J.-C., and Wang, C.-T. (2014). Phosphomimetic Mutation of Cysteine String Protein-α Increases the Rate of Regulated Exocytosis by Modulating Fusion Pore Dynamics in PC12 Cells. *PLoS One* 9, 1–13.

Choi, H. Y., Liu, Y., Tennert, C., Sugiura, Y., Karakatsani, A., Kröger, S., Johnson, E. B., Hammer, R. E., Lin, W., and Herz, J. (2013). APP interacts with LRP4 and agrin to coordinate the development of the neuromuscular junction in mice. *Elife*.

Chow, V. W., Mattson, M. P., Wong, P. C., and Gleichmann, M. (2010). An overview of APP processing enzymes and products. *Neuromolecular Med.* 12, 1–12.

Choy, R. W. Y., Cheng, Z., and Schekman, R. (2012). Amyloid precursor protein (APP) traffics from the cell surface via endosomes for amyloid β (Aβ) production in the trans-Golgi network. *Proc. Natl. Acad. Sci. U. S. A.* 109, 11914–11915.

Chu, T. H., Cummins, K., Sparling, J. S., Tsutsui, S., Brideau, C., Nilsson, K. P. R., Joseph, J. T., and Stys, P. K. (2017). Axonal and myelinic pathology in 5xFAD Alzheimer's mouse spinal cord. *PLoS One* 12, 1–22.

Chun, W., Waldo, G. S., and Johnson, G. V. W. (2007). Split GFP complementation assay: A novel approach to quantitatively measure aggregation of tau in situ: Effects of GSK3β activation and caspase 3 cleavage. *J. Neurochem.* 103, 2529–2539.

Cissé, M., Halabisky, B., Harris, J., Devidze, N., Dubal, D. B., Sun, B., Orr, A., Lotz, G., Kim, D. H., Hamto, P., Ho, K., Yu, G. Q., and Mucke, L. (2011). Reversing EphB2 depletion rescues cognitive functions in Alzheimer model. *Nature* 469, 47–52.

Cisternas, P., Taylor, X., and Lasagna-Reeves, C. A. (2019). The Amyloid-Tau-Neuroinflammation Axis in the Context of Cerebral Amyloid Angiopathy. *Int. J. Mol. Sci.* 20, 6319.

Cisternas, P., Taylor, X., Perkins, A., Maldonado, O., Allman, E., Cordova, R., Marambio, Y., Munoz, B., Pennington, T., Xiang, S., Zhang, J., Vidal, R., Atwood, B., and Lasagna-Reeves, C. A. (2020). Vascular amyloid accumulation alters the gabaergic synapse and induces hyperactivity in a model of cerebral amyloid angiopathy. *Aging Cell* 19.

Citron, M., Eckman, C. B., Diehl, T. S., Corcoran, C., Ostaszewski, B. L., Xia, W., Levesque, G., Hyslop, P. S. G., Younkin, S. G., and Selkoe, D. J. (1998). Additive effects of PS1 and APP mutations on secretion of the 42- residue amyloid β-protein. *Neurobiol. Dis.* 5, 107–116.

Citron, M., Westaway, D., Xia, W., Carlson, G., Diehl, T., Levesque, G., Johnson-Wood, K., Lee, M., Seubert, P., Davis, A., Kholodenko, D., Motter, R., Sherrington, R., Perry, B., Yao, H., Strome, R., Lieberburg, I., Rommens, J., Kim, S., Schenk, D., Fraser, P., St. George Hyslop, P., and Selkoe, D. J. (1997). Mutant presenilins of Alzheimer's disease increase production of 42-residue amyloid β-protein in both transfected cells and transgenic mice. *Nat. Med.* 3, 67–72.

Clare, R., King, V. G., Wirenfeldt, M., and Vinters, H. V. (2010). Synapse loss in dementias. *J. Neurosci. Res.* 88, 2083–2090.

Clark, R. F., Hutton, M., Fuldner, M., Froelich, S., Karran, E., Talbot, C., Crook, R., Lendon, C., Prihar, G., He, C., Korenblat, K., Martinez, A., Wragg, M., Busfield, F., Behrens, M. I., Myers, A., Norton, J., Morris, J., Mehta, N., Pearson, C., Lincoln, S., Baker, M., Duff, K., Zehr, C., Perez-Tur, J., Houlden, H., Ruiz, A., Ossa, J., Lopera, F., Arcos, M., Madrigal, L., Collinge, J., Humphreys, C., Ashworth, A., Sarner, S., Fox, N., Harvey, R., Kennedy, A., Roques, P., Cline, R. T., Philips, C. A., Venter, J. C., Forsell, L., Axelman, K., Lilius, L., Johnston, J., Cowburn, R., Viitanen, M., Winblad, B., Kosik, K., Haltia, M., Poyhonen, M., Dickson, D., Mann, D., Neary, D., Snowden, J., Lantos, P., Lannfelt, L., Rossor, M., Roberts, G. W., Adams, M. D., Hardy, J., and Goate, A. (1995). The structure of the presenilin 1 (S182) gene and identification of six novel mutations in early onset AD families. *Nat. Genet.* 11, 219–222.

Clavaguera, F., Akatsu, H., Fraser, G., Crowther, R. A., Frank, S., Hench, J., Probst, A., Winkler, D. T., Reichwald, J., Staufenbiel, M., Ghetti, B., Goedert, M., and Tolnay, M. (2013). Brain homogenates from human tauopathies induce tau inclusions in mouse brain. *Proc. Natl. Acad. Sci. U. S. A.* 110, 9535–9540.

Clavaguera, F., Bolmont, T., Crowther, R. A., Abramowski, D., Frank, S., Probst, A., Fraser, G., Stalder, A. K., Beibel, M., Staufenbiel, M., Jucker, M., Goedert, M., and Tolnay, M. (2009). Transmission and spreading of tauopathy in transgenic mouse brain. *Nat. Cell Biol.* 11, 909–913.

Clavaguera, F., Hench, J., Lavenir, I., Schweighauser, G., Frank, S., Goedert, M., and Tolnay, M. (2014). Peripheral administration of tau aggregates triggers intracerebral tauopathy in transgenic mice. *Acta Neuropathol.* 127, 299–301.

Cleary, J. P., Walsh, D. M., Hofmeister, J. J., Shankar, G. M., Kuskowski, M. A., Selkoe, D. J., and Ashe, K. H. (2005). Natural oligomers of the amyloid-β protein specifically disrupt cognitive function. *Nat. Neurosci.* 8, 79–84.

Cleveland, D. W., Hwo, S. Y., and Kirschner, M. W. (1977). Purification of tau, a microtubule-associated protein that induces assembly of microtubules from purified tubulin. *J. Mol. Biol.* 116, 207–225.

Clinton, J., Blackman, S. E. A., Royston, M. C., and Roberts, G. W. (1994). Differential synaptic loss in the cortex in Alzheimer's disease: A study using archival material. *Neuroreport* 5, 497–500.

Cohen, R. S., Blomberg, F., Berzins, K., and Siekevitz, P. (1977). The structure of postsynaptic densities isolated from dog cerebral cortex. I. Overall morphology and protein composition. *J. Cell Biol.* 74, 181–203.

Coleman, P. D., and Yao, P. J. (2003). Synaptic slaughter in Alzheimer's disease. *Neurobiol. Aging* 24, 1023–1027.

Coleman, P., Federoff, H., and Kurlan, R. (2004). A focus on the synapse for neuroprotection in Alzheimer disease and other dementias. *Neurology* 63, 1155–1162.

Colom-Cadena, M., Pegueroles, J., Herrmann, A. G., Henstridge, C. M., Muñoz, L., Querol-Vilaseca, M., Martín-Paniello, C. S., Luque-Cabecerans, J., Clarimon, J., Belbin, O., Núñez-Llaves, R., Blesa, R., Smith, C., McKenzie, C. A., Frosch, M. P., Roe, A., Fortea, J., Andilla, J., Loza-Alvarez, P., Gelpi, E., Hyman, B. T., Spires-Jones, T. L., and Lleó, A. (2017). Synaptic phosphorylated α-synuclein in dementia with Lewy bodies. *Brain* 140, 3204–3214.

Colom-Cadena, M., Spires-Jones, T., Zetterberg, H., Blennow, K., Caggiano, A., Dekosky, S. T., Fillit, H., Harrison, J. E., Schneider, L. S., Scheltens, P., De Haan, W., Grundman, M., Van Dyck, C. H., Izzo, N. J., and Catalano, S. M.

(2020). The clinical promise of biomarkers of synapse damage or loss in Alzheimer's disease. *Alzheimer's Res. Ther.* 12, 1–12.

Coma, M., Serenó, L., Da Rocha-Souto, B., Scotton, T. C., España, J., Sánchez, M. B., Rodríguez, M., Agulló, J., Guardia-Laguarta, C., Garcia-Alloza, M., Borrelli, L. A., Clarimón, J., Lleó, A., Bacskai, B. J., Saura, C. A., Hyman, B. T., and Gómez-Isla, T. (2010). Triflusal reduces dense-core plaque load, associated axonal alterations and inflammatory changes, and rescues cognition in a transgenic mouse model of Alzheimer's disease. *Neurobiol. Dis.* 38, 482–491.

Condello, C., Schain, A., and Grutzendler, J. (2011). Multicolor time-stamp reveals the dynamics and toxicity of amyloid deposition. *Sci. Rep.* 1, 1–12.

Constantinescu, C. C., Tresse, C., Zheng, M. Q., Gouasmat, A., Carroll, V. M., Mistico, L., Alagille, D., Sandiego, C. M., Papin, C., Marek, K., Seibyl, J. P., Tamagnan, G. D., and Barret, O. (2019). Development and In Vivo Preclinical Imaging of Fluorine-18-Labeled Synaptic Vesicle Protein 2A (SV2A) PET Tracers. *Mol. Imaging Biol.* 21, 509–518.

Coppola, T., and Gundersen, C. (1996). Widespread expression of human cysteine string proteins. *FEBS Lett.* 391, 269–272.

Corder, E. H., Saunders, A. M., Strittmatter, W. J., Schmechel, D. E., Gaskell, P. C., Small, G. W., Roses, A. D., Haines, J. L., and Pericak-Vance, M. A. (1993). Gene dose of apolipoprotein E type 4 allele and the risk of Alzheimer's disease in late onset families. *Science (80-.).* 261, 921–923.

Counts, S. E., Nadeem, M., Lad, S. P., Wuu, J., and Mufson, E. J. (2006). Differential expression of synaptic proteins in the frontal and temporal cortex of elderly subjects with mild cognitive impairment. *J. Neuropathol. Exp. Neurol.* 65, 592–601.

Cowan, C. M., and Mudher, A. (2013). Are tau aggregates toxic or protective in tauopathies? *Front. Neurol.* 4, 1–13.

Coyne, A. N., Lorenzini, I., Chou, C. C., Torvund, M., Rogers, R. S., Starr, A., Zaepfel, B. L., Levy, J., Johannesmeyer, J., Schwartz, J. C., Nishimune, H., Zinsmaier, K., Rossoll, W., Sattler, R., and Zarnescu, D. C. (2017). Post-transcriptional Inhibition of Hsc70-4/HSPA8 Expression Leads to Synaptic Vesicle Cycling Defects in Multiple Models of ALS. *Cell Rep.* 21, 110–125.

Crimins, J. L., Pooler, A., Polydoro, M., Luebke, J. I., and Spires-Jones, T. L. (2013). The intersection of amyloid beta and tau in glutamatergic synaptic dysfunction and collapse in Alzheimer's disease. *Ageing Res. Rev.* 12, 757–763.

Croft, C. L., Wade, M. A., Kurbatskaya, K., Mastrandreas, P., Hughes, M. M.,

Phillips, E. C., Pooler, A. M., Perkinton, M. S., Hanger, D. P., and Noble, W. (2017). Membrane association and release of wild-type and pathological tau from organotypic brain slice cultures. *Cell Death Dis.* 8, 1–10.

Cruz, J. C., Tseng, H. C., Goldman, J. A., Shih, H., and Tsai, L. H. (2003). Aberrant Cdk5 activation by p25 triggers pathological events leading to neurodegeneration and neurofibrillary tangles. *Neuron* 40, 471–483.

D'Amore, J. D., Kajdasz, S. T., McLellan, M. E., Bacskai, B. J., Stern, E. A., and Hyman, B. T. (2003). In Vivo Multiphoton Imaging of a Transgenic Mouse Model of Alzheimer Disease Reveals Marked Thioflavine-S-Associated Alterations in Neurite Trajectories. *J. Neuropathol. Exp. Neurol.* 62, 137–145.

DaRocha-Souto, B., Coma, M., Pérez-Nievas, B. G., Scotton, T. C., Siao, M., Sánchez-Ferrer, P., Hashimoto, T., Fan, Z., Hudry, E., Barroeta, I., Serenó, L., Rodríguez, M., Sánchez, M. B., Hyman, B. T., and Gómez-Isla, T. (2012). Activation of glycogen synthase kinase-3 beta mediates β-amyloid induced neuritic damage in Alzheimer's disease. *Neurobiol. Dis.* 45, 425–437.

Davidsson, P., Jahn, R., Bergquist, J., Ekman, R., and Blennow, K. (1996). Synaptotagmin, a synaptic vesicle protein, is present in human cerebrospinal fluid - A new biochemical marker for synaptic pathology in Alzheimer disease? *Mol. Chem. Neuropathol.* 27, 195–210.

Davies, C. A., Mann, D. M. A., Sumpter, P. Q., and Yates, P. O. (1987). A quantitative morphometric analysis of the neuronal and synaptic content of the frontal and temporal cortex in patients with Alzheimer's disease. *J. Neurol. Sci.* 78, 151–164.

Dawkins, E., and Small, D. H. (2014). Insights into the physiological function of the β-amyloid precursor protein: Beyond Alzheimer's disease. *J. Neurochem.* 129, 756–769.

Dawson, G. R., Seabrook, G. R., Zheng, H., Smith, D. W., Graham, S., O'Dowd, G., Bowery, B. J., Boyce, S., Trumbauer, M. E., Chen, H. Y., Van Der Ploeg, L. H. T., and Sirinathsinghji, D. J. S. (1999). Age-related cognitive deficits, impaired long-term potentiation and reduction in synaptic marker density in mice lacking the β-amyloid precursor protein. *Neuroscience* 90, 1–13.

Dawson, H. N., Ferreira, A., Eyster, M. V, Ghoshal, N., Binder, L. I., and Vitek, M. P. (2001). Inhibition of neuronal maturation in primary hippocampal neurons from τ deficient mice. *J. Cell Sci.* 114, 1179–1187.

De Calignon, A., Polydoro, M., Suárez-Calvet, M., William, C., Adamowicz, D. H., Kopeikina, K. J., Pitstick, R., Sahara, N., Ashe, K. H., Carlson, G. A., Spires-Jones, T. L., and Hyman, B. T. (2012). Propagation of Tau Pathology in a

Model of Early Alzheimer's Disease. *Neuron* 73, 685–697.

De Rossi, P., Andrew, R. J., Musial, T. F., Buggia-Prevot, V., Xu, G., Ponnusamy, M., Ly, H., Krause, S. V., Rice, R. C., de l'Estoile, V., Valin, T., Salem, S., Despa, F., Borchelt, D. R., Bindokas, V. P., Nicholson, D. A., and Thinakaran, G. (2019). Aberrant accrual of BIN1 near Alzheimer's disease amyloid deposits in transgenic models. *Brain Pathol.* 29, 485–501.

De Strooper, B., and Annaert, W. (2000). Proteolytic processing and cell biological functions of the amyloid precursor protein. *J. Cell Sci.* 113, 1857–1870.

De Strooper, B., and Annaert, W. (2010). Novel Research Horizons for Presenilins and γ-Secretases in Cell Biology and Disease. *Annu. Rev. Cell Dev. Biol.* 26, 235–260.

De Wilde, M. C., Overk, C. R., Sijben, J. W., and Masliah, E. (2016). Meta-analysis of synaptic pathology in Alzheimer's disease reveals selective molecular vesicular machinery vulnerability. *Alzheimer's Dement.* 12, 633–644.

Decker, H., Lo, K. Y., Unger, S. M., Ferreira, S. T., and Silverman, M. A. (2010). Amyloid-β peptide oligomers disrupt axonal transport through an NMDA receptor-dependent mechanism that is mediated by glycogen synthase kinase 3β in primary cultured hippocampal neurons. *J. Neurosci.* 30, 9166–9171.

Dejanovic, B., Huntley, M. A., De Mazière, A., Meilandt, W. J., Wu, T., Srinivasan, K., Jiang, Z., Gandham, V., Friedman, B. A., Ngu, H., Foreman, O., Carano, R. A. D., Chih, B., Klumperman, J., Bakalarski, C., Hanson, J. E., and Sheng, M. (2018). Changes in the Synaptic Proteome in Tauopathy and Rescue of Tau-Induced Synapse Loss by C1q Antibodies. *Neuron* 100, 1322–1336.

DeKosky, S. T., and Scheff, S. W. (1990). Synapse loss in frontal cortex biopsies in Alzheimer's disease: Correlation with cognitive severity. *Ann. Neurol.* 27, 457–464.

DeKosky, S. T., Scheff, S. W., and Styren, S. D. (1996). Structural correlates of cognition in dementia: Quantification and assessment of synapse change. *Neurodegeneration* 5, 417–421.

Demuro, A., Mina, E., Kayed, R., Milton, S. C., Parker, I., and Glabe, C. G. (2005). Calcium dysregulation and membrane disruption as a ubiquitous neurotoxic mechanism of soluble amyloid oligomers. *J. Biol. Chem.* 280, 17294–17300.

Demuro, A., Smith, M., and Parker, I. (2011). Single-channel Ca2+ imaging implicates Aβ 1-42 amyloid pores in Alzheimer's disease pathology. *J. Cell Biol.* 195, 515–524.

Deng, J., Koutras, C., Donnelier, J., Alshehri, M., Fotouhi, M., Girard, M., Casha, S., McPherson, P. S., Robbins, S. M., and Braun, J. E. A. (2017). Neurons Export

Extracellular Vesicles Enriched in Cysteine String Protein and Misfolded Protein Cargo. *Sci. Rep.* 7, 1–12.

Derkinderen, P., Scales, T. M. E., Hanger, D. P., Leung, K. Y., Byers, H. L., Ward, M. A., Lenz, C., Price, C., Bird, I. N., Perera, T., Kellie, S., Williamson, R., Noble, W., Van Etten, R. A., Leroy, K., Brion, J. P., Reynolds, C. H., and Anderton, B. H. (2005). Tyrosine 394 is phosphorylated in Alzheimer's paired helical filament tau and in fetal tau with c-Abl as the candidate tyrosine kinase. *J. Neurosci.* 25, 6584–6593.

Devi, L., and Ohno, M. (2010). Phospho-eIF2α level is important for determining abilities of BACE1 reduction to rescue cholinergic neurodegeneration and memory defects in 5XFAD mice. *PLoS One* 5, 1–10.

DeVos, S. L., Corjuc, B. T., Oakley, D. H., Nobuhara, C. K., Bannon, R. N., Chase, A., Commins, C., Gonzalez, J. A., Dooley, P. M., Frosch, M. P., and Hyman, B. T. (2018). Synaptic tau seeding precedes tau pathology in human Alzheimer's disease brain. *Front. Neurosci.* 12, 1–15.

Dickson, D. W. (1997). The pathogenesis of senile plaques. *J. Neuropathol. Exp. Neurol.* 56, 321–339.

Dinamarca, M. C., Ríos, J. A., and Inestrosa, N. C. (2012). Postsynaptic receptors for amyloid-β oligomers as mediators of neuronal damage in Alzheimer's disease. *Front. Physiol.* 3, 1–7.

Diner, I., Hales, C. M., Bishof, I., Rabenold, L., Duong, D. M., Yi, H., Laur, O., Gearing, M., Troncoso, J., Thambisetty, M., Lah, J. J., Levey, A. I., and Seyfried, N. T. (2014). Aggregation properties of the small nuclear ribonucleoprotein U1-70K in Alzheimer disease. *J. Biol. Chem.* 289, 35296–35313.

Diner, I., Nguyen, T., and Seyfried, N. T. (2017). Enrichment of detergent-insoluble protein aggregates from human postmortem brain. *J. Vis. Exp.* 2017, 1–8.

Ding, Y., Zhao, J., Zhang, X., Wang, S., Viola, K. L., Chow, F. E., Zhang, Y., Lippa, C., Klein, W. L., and Gong, Y. (2019). Amyloid Beta Oligomers Target to Extracellular and Intracellular Neuronal Synaptic Proteins in Alzheimer's Disease. *Front. Neurol.* 10, 1–16.

Dixit, R., Ross, J. L., Goldman, Y. E., and Holzbaur, E. L. F. (2008). Differential regulation of dynein and kinesin motor proteins by tau. *Science (80-.).* 319, 1086–1089.

Drubin, D. G., and Kirschner, M. W. (1986). Tau protein function in living cells. *J. Cell Biol.* 103, 2739–2746.

Dubois, B., Feldman, H. H., Jacova, C., Cummings, J. L., Dekosky, S. T.,

Barberger-Gateau, P., Delacourte, A., Frisoni, G., Fox, N. C., Galasko, D., Gauthier, S., Hampel, H., Jicha, G. A., Meguro, K., O'Brien, J., Pasquier, F., Robert, P., Rossor, M., Salloway, S., Sarazin, M., de Souza, L. C., Stern, Y., Visser, P. J., and Scheltens, P. (2010). Revising the definition of Alzheimer's disease: a new lexicon. *Lancet. Neurol.* 9, 1118–1127.

Dubois, B., Feldman, H. H., Jacova, C., Hampel, H., Molinuevo, J. L., Blennow, K., DeKosky, S. T., Gauthier, S., Selkoe, D., Bateman, R., Cappa, S., Crutch, S., Engelborghs, S., Frisoni, G. B., Fox, N. C., Galasko, D., Habert, M.-O., Jicha, G. A., Nordberg, A., Pasquier, F., Rabinovici, G., Robert, P., Rowe, C., Salloway, S., Sarazin, M., Epelbaum, S., de Souza, L. C., Vellas, B., Visser, P. J., Schneider, L., Stern, Y., Scheltens, P., and Cummings, J. L. (2014). Advancing research diagnostic criteria for Alzheimer's disease: the IWG-2 criteria. *Lancet. Neurol.* 13, 614–629.

Duff, K., Eckman, C., Zehr, C., Yu, X., Prada, C. M., Perez-Tur, J., Hutton, M., Buee, L., Harigaya, Y., Yager, D., Morgan, D., Gordon, M. N., Holcomb, L., Refolo, L., Zenk, B., Hardy, J., and Younkin, S. (1996). Increased amyloid-β42(43) in brains of mice expressing mutant presenilin 1. *Nature* 383, 710–713.

Dugger, B. N., Adler, C. H., Shill, H. A., Caviness, J., Jacobson, S., Driver-Dunckley, E., and Beach, T. G. (2014). Concomitant pathologies among a spectrum of parkinsonian disorders. *Park. Relat. Disord.* 20, 525–529.

Dujardin, S., Bégard, S., Caillierez, R., Lachaud, C., Delattre, L., Carrier, S., Loyens, A., Galas, M.-C., Bousset, L., Melki, R., Aurégan, G., Hantraye, P., Brouillet, E., Buée, L., and Colin, M. (2014). Ectosomes: A New Mechanism for Non-Exosomal Secretion of Tau Protein. *PLoS One* 9, 1–10.

Eberle, K. K., Zinsmaier, K. E., Buchner, S., Gruhn, M., Jenni, M., Arnold, C., Leibold, C., Reisch, D., Walter, N., Hafen, E., Hofbauer, A., Pflugfelder, G. O., and Buchner, E. (1998). Wide distribution of the cysteine string proteins in Drosophila tissues revealed by targeted mutagenesis. *Cell Tissue Res.* 294, 203–217.

Ebneth, A., Godemann, R., Stamer, K., Illenberger, S., Trinczek, B., Mandelkow, E. M., and Mandelkow, E. (1998). Overexpression of tau protein inhibits kinesin-dependent trafficking of vesicles, mitochondria, and endoplasmic reticulum: Implications for Alzheimer's disease. *J. Cell Biol.* 143, 777–794.

Eckert, A., Nisbet, R., Grimm, A., and Götz, J. (2014). March separate, strike together - Role of phosphorylated TAU in mitochondrial dysfunction in Alzheimer's disease. *Biochim. Biophys. Acta - Mol. Basis Dis.* 1842, 1258–

1266.

Eckman, C. B., Mehta, N. D., Crook, R., Perez-tur, J., Prihar, G., Pfeiffer, E., Graff-Radford, N., Hinder, P., Yager, D., Zenk, B., Refolo, L. M., Prada, C. M., Younkin, S. G., Hutton, M., and Hardy, J. (1997). A new pathogenic mutation in the APP gene (1716V) increases the relative proportion of Aβ42(43). *Hum. Mol. Genet.* 6, 2087–2089.

Eimer, W. A., and Vassar, R. (2013). Neuron loss in the 5XFAD mouse model of Alzheimer's disease correlates with intraneuronal Aβ42 accumulation and Caspase-3 activation. *Mol. Neurodegener.* 8, 1–12.

Ekinci, F. J., and Shea, T. B. (2000). Phosphorylation of tau alters its association with the plasma membrane. *Cell. Mol. Neurobiol.* 20, 497–508.

Engmann, O., Hortobágyi, T., Thompson, A. J., Guadagno, J., Troakes, C., Soriano, S., Al-Sarraj, S., Kim, Y., and Giese, K. P. (2011). Cyclin-dependent kinase 5 activator p25 Is generated during memory formation and is reduced at an early stage in Alzheimer's disease. *Biol. Psychiatry* 70, 159–168.

Evans, C. G., Wisén, S., and Gestwicki, J. E. (2006). Heat shock proteins 70 and 90 inhibit early stages of amyloid β-(1-42) aggregation in vitro. *J. Biol. Chem.* 281, 33182–33191.

Evans, G. J. O., and Morgan, A. (2002). Phosphorylation-dependent interaction of the synaptic vesicle proteins cysteine string protein and synaptotagmin I. *Biochem. J.* 364, 343–347.

Evans, G. J. O., and Morgan, A. (2003). Regulation of the exocytotic machinery by cAMP-dependent protein kinase: Implications for presynaptic plasticity. *Biochem. Soc. Trans.* 31, 824–827.

Evans, G. J. O., and Morgan, A. (2005). Phosphorylation of cysteine string protein in the brain: developmental, regional and synaptic specificity. *Eur. J. Neurosci.* 21, 2671–2680.

Evans, G. J. O., Wilkinson, M. C., Graham, M. E., Turner, K. M., Chamberlain, L. H., Burgoyne, R. D., and Morgan, A. (2001). Phosphorylation of cysteine string protein by protein kinase A: Implications for the modulation of exocytosis. *J. Biol. Chem.* 276, 47877–47885.

Eybalin, M., Renard, N., Aure, F., and Safieddine, S. (2002). Cysteine-string protein in inner hair cells of the organ of Corti: Synaptic expression and upregulation at the onset of hearing. *Eur. J. Neurosci.* 15, 1409–1420.

Farrer, L. A. (1997). Effects of Age, Sex, and Ethnicity on the Association Between Apolipoprotein E Genotype and Alzheimer Disease. *JAMA* 278, 1349–1349.

Fath, T., Eidenmüller, J., and Brandt, R. (2002). Tau-mediated cytotoxicity in a

pseudohyperphosphorylation model of Alzheimer's disease. *J. Neurosci.* 22, 9733–9741.

Fein, J. A., Sokolow, S., Miller, C. A., Vinters, H. V., Yang, F., Cole, G. M., and Gylys, K. H. (2008). Co-localization of amyloid beta and tau pathology in Alzheimer's disease synaptosomes. *Am. J. Pathol.* 172, 1683–1692.

Fernández-Chacón, R., Wölfel, M., Nishimune, H., Tabares, L., Schmitz, F., Castellano-Muñoz, M., Rosenmund, C., Montesinos, M. L., Sanes, J. R., Schneggenburger, R., and Südhof, T. C. (2004). The synaptic vesicle protein CSPα prevents presynaptic degeneration. *Neuron* 42, 237–251.

Fernandez, M. A., Biette, K. M., Dolios, G., Seth, D., Wang, R., and Wolfe, M. S. (2016). Transmembrane Substrate Determinants for γ-Secretase Processing of APP CTFβ. *Biochemistry* 55, 5675–5688.

Ferreira, I. L., Bajouco, L. M., Mota, S. I., Auberson, Y. P., Oliveira, C. R., and Rego, A. C. (2012). Amyloid beta peptide 1-42 disturbs intracellular calcium homeostasis through activation of GluN2B-containing N-methyl-d-aspartate receptors in cortical cultures. *Cell Calcium* 51, 95–106.

Ferreira, S. T., Lourenco, M. V., Oliveira, M. M., and De Felice, F. G. (2015). Soluble amyloid-β oligomers as synaptotoxins leading to cognitive impairment in Alzheimer's disease. *Front. Cell. Neurosci.* 9, 1–17.

Ferrer, I. (1999). Neurons and their dendrites in frontotemporal dementia. *Dement. Geriatr. Cogn. Disord.* 10, 55–60.

Ferrer, I., Martinez, A., Boluda, S., Parchi, P., and Barrachina, M. (2008). Brain banks: Benefits, limitations and cautions concerning the use of post-mortem brain tissue for molecular studies. *Cell Tissue Bank.* 9, 181–194.

Fiandaca, M. S., Kapogiannis, D., Mapstone, M., Boxer, A., Eitan, E., Schwartz, J. B., Abner, E. L., Petersen, R. C., Federoff, H. J., Miller, B. L., and Goetzl, E. J. (2015). Identification of preclinical Alzheimer's disease by a profile of pathogenic proteins in neurally derived blood exosomes: A case-control study. *Alzheimer's Dement.* 11, 600–607.

Finnema, S. J., Nabulsi, N. B., Eid, T., Detyniecki, K., Lin, S. F., Chen, M. K., Dhaher, R., Matuskey, D., Baum, E., Holden, D., Spencer, D. D., Mercier, J., Hannestad, J., Huang, Y., and Carson, R. E. (2016). Imaging synaptic density in the living human brain. *Sci. Transl. Med.* 8, 1–10.

Flanigan, T. J., Xue, Y., Rao, S. K., Dhanushkodi, A., and McDonald, M. P. (2014). Abnormal vibrissa-related behavior and loss of barrel field inhibitory neurons in 5xFAD transgenics. *Genes, Brain Behav.* 13, 488–500.

Folstein, M. F., Folstein, S. E., and McHugh, P. R. (1975). "Mini-mental state": A

practical method for grading the cognitive state of patients for the clinician. *J. Psychiatr. Res.* 12, 189–198.

Fontaine, S. N., Zheng, D., Sabbagh, J. J., Martin, M. D., Chaput, D., Darling, A., Trotter, J. H., Stothert, A. R., Nordhues, B. A., Lussier, A., Baker, J., Shelton, L., Kahn, M., Blair, L. J., Stevens, S. M., and Dickey, C. A. (2016). DnaJ/Hsc70 chaperone complexes control the extracellular release of neurodegenerative-associated proteins. *EMBO J.* 35, 1537–1549.

Forman, M. S., Farmer, J., Johnson, J. K., Clark, C. M., Arnold, S. E., Coslett, H. B., Chatterjee, A., Hurtig, H. I., Karlawish, J. H., Rosen, H. J., Van Deerlin, V., Lee, V. M. Y., Miller, B. L., Trojanowski, J. Q., and Grossman, M. (2006). Frontotemporal dementia: Clinicopathological correlations. *Ann. Neurol.* 59, 952–962.

Fornasiero, E. F., Mandad, S., Wildhagen, H., Alevra, M., Rammner, B., Keihani, S., Opazo, F., Urban, I., Ischebeck, T., Sakib, M. S., Fard, M. K., Kirli, K., Centeno, T. P., Vidal, R. O., Rahman, R. U., Benito, E., Fischer, A., Dennerlein, S., Rehling, P., Feussner, I., Bonn, S., Simons, M., Urlaub, H., and Rizzoli, S. O. (2018). Precisely measured protein lifetimes in the mouse brain reveal differences across tissues and subcellular fractions. *Nat. Commun.* 9, 1–17.

Friedhoff, P., Schneider, A., Mandelkow, E. M., and Mandelkow, E. (1998). Rapid assembly of Alzheimer-like paired helical filaments from microtubule-associated protein tau monitored by fluorescence in solution. *Biochemistry* 37, 10223–10230.

Frost, B., Jacks, R. L., and Diamond, M. I. (2009). Propagation of Tau misfolding from the outside to the inside of a cell. *J. Biol. Chem.* 284, 12845–12852.

Furman, J. L., Vaquer-Alicea, J., White, C. L., Cairns, N. J., Nelson, P. T., and Diamond, M. I. (2017). Widespread tau seeding activity at early Braak stages. *Acta Neuropathol.* 133, 91–100.

Fuster-Matanzo, A., Hernández, F., and Ávila, J. (2018). Tau spreading mechanisms; Implications for dysfunctional tauopathies. *Int. J. Mol. Sci.* 19, 1–14.

Fuster, J. M. (2001). The prefrontal cortex - An update: Time is of the essence. *Neuron* 30, 319–333.

Gamblin, T. C., Chen, F., Zambrano, A., Abraha, A., Lagalwar, S., Guillozet, A. L., Lu, M., Fu, Y., Garcia-Sierra, F., LaPointe, N., Miller, R., Berry, R. W., Binder, L. I., and Cryns, V. L. (2003). Caspase cleavage of tau: Linking amyloid and neurofibrillary tangles in Alzheimer's disease. *Proc. Natl. Acad. Sci. U. S. A.*

100, 10032–10037.

Games, D., Seubert, P., Rockenstein, E., Patrick, C., Trejo, M., Ubhi, K., Ettle, B., Ghassemiam, M., Barbour, R., Schenk, D., Nuber, S., and Masliah, E. (2013). Axonopathy in an α-synuclein transgenic model of Lewy body disease is associated with extensive accumulation of c-terminal-truncated α-synuclein. *Am. J. Pathol.* 182, 940–953.

García-Junco-Clemente, P., Cantero, G., Gómez-Sánchez, L., Linares-Clemente, P., Martínez-López, J. A., Luján, R., and Fernández-Chacón, R. (2010). Cysteine String Protein-α Prevents Activity-Dependent Degeneration in GABAergic Synapses. *J. Neurosci.* 30, 7377–7391.

Garringer, H. J., Murrell, J., D'Adamio, L., Ghetti, B., and Vidal, R. (2010). Modeling familial British and Danish dementia. *Brain Struct. Funct.* 214, 235–244.

Ghosh, A., and Giese, K. P. (2015). Calcium/calmodulin-dependent kinase II and Alzheimer's disease. *Mol. Brain* 8, 1–7.

Ghosh, A., Mizuno, K., Tiwari, S. S., Proitsi, P., Gomez Perez-Nievas, B., Glennon, E., Martinez-Nunez, R. T., and Giese, K. P. (2020). Alzheimer's disease-related dysregulation of mRNA translation causes key pathological features with ageing. *Transl. Psychiatry* 10, 1–18.

Giannakopoulos, P., Herrmann, F. R., Bussière, T., Bouras, C., Kövari, E., Perl, D. P., Morrison, J. H., Gold, G., and Hof, P. R. (2003). Tangle and neuron numbers, but not amyloid load, predict cognitive status in Alzheimer's disease. *Neurology* 60, 1495–1500.

Giannakopoulos, P., Kövari, E., Herrmann, F. R., Hof, P. R., and Bouras, C. (2009). Interhemispheric distribution of Alzheimer disease and vascular pathology in brain aging. *Stroke* 40, 983–986.

Gibbons, G. S., Banks, R. A., Kim, B., Xu, H., Changolkar, L., Leight, S. N., Riddle, D. M., Li, C., Gathagan, R. J., Brown, H. J., Zhang, B., Trojanowski, J. Q., and Lee, V. M. Y. (2017). GFP-mutant human tau transgenic mice develop tauopathy following CNS injections of Alzheimer's brain-derived pathological tau or synthetic mutant human tau fibrils. *J. Neurosci.* 37, 11485–11494.

Giese, K. P. (2014). Generation of the Cdk5 activator p25 is a memory mechanism that is affected in early Alzheimer's disease. *Front. Mol. Neurosci.* 7, 1–4.

Gillingwater, T. H., and Wishart, T. M. (2013). Mechanisms underlying synaptic vulnerability and degeneration in neurodegenerative disease. *Neuropathol. Appl. Neurobiol.* 39, 320–334.

Gingrich, J. C., Davis, D. R., and Nguyen, Q. (2000). Multiplex Detection and Quantitation of Proteins on Western Blots Using Fluorescent Probes.

Biotechniques 29, 636–642.

Glennon, E. B., Lau, D. H. W., Gabriele, R. M. C., Taylor, M. F., Troakes, C., Opie-Martin, S., Elliott, C., Killick, R., Hanger, D. P., Perez-Nievas, B. G., and Noble, W. (2020). Bridging integrator 1 protein loss in Alzheimer's disease promotes synaptic tau accumulation and disrupts tau release. *Brain Commun.* 2, 1–16.

Goate, A., Chartier-Harlin, M. C., Mullan, M., Brown, J., Crawford, F., Fidani, L., Giuffra, L., Haynes, A., Irving, N., James, L., Mant, R., Newton, P., Rooke, K., Roques, P., Talbot, C., Pericak-Vance, M., Roses, A., Williamson, R., Rossor, M., Owen, M., and Hardy, J. (1991). Segregation of a missense mutation in the amyloid precursor protein gene with familial Alzheimer's disease. *Nature* 349, 704–706.

Goedert, M., Spillantini, M. G., Cairns, N. J., and Crowther, R. A. (1992a). Tau proteins of Alzheimer paired helical filaments: abnormal phosphorylation of all six brain isoforms. *Neuron* 8, 159–168.

Goedert, M., Spillantini, M. G., and Crowther, R. A. (1992b). Cloning of a big tau microtubule-associated protein characteristic of the peripheral nervous system. *Proc. Natl. Acad. Sci. U. S. A.* 89, 1983–1987.

Goedert, M., Spillantini, M. G., Jakes, R., Rutherford, D., and Crowther, R. A. (1989a). Multiple isoforms of human microtubule-associated protein tau: sequences and localization in neurofibrillary tangles of Alzheimer's disease. *Neuron* 3, 519–526.

Goedert, M., Spillantini, M. G., Potier, M. C., Ulrich, J., and Crowther, R. A. (1989b). Cloning and sequencing of the cDNA encoding an isoform of microtubule-associated protein tau containing four tandem repeats: differential expression of tau protein mRNAs in human brain. *EMBO J.* 8, 393–399.

Gomez-Arboledas, A., Davila, J. C., Sanchez-Mejias, E., Navarro, V., Nuñez-Diaz, C., Sanchez-Varo, R., Sanchez-Mico, M. V., Trujillo-Estrada, L., Fernandez-Valenzuela, J. J., Vizuete, M., Comella, J. X., Galea, E., Vitorica, J., and Gutierrez, A. (2018). Phagocytic clearance of presynaptic dystrophies by reactive astrocytes in Alzheimer's disease. *Glia* 66, 637–653.

Gómez-Isla, T., Hollister, R., West, H., Mui, S., Growdon, J. H., Petersen, R. C., Parisi, J. E., and Hyman, B. T. (1997). Neuronal loss correlates with but exceeds neurofibrillary tangles in Alzheimer's disease. *Ann. Neurol.* 41, 17–24.

Gordon, S. L., Leube, R. E., and Cousin, M. A. (2011). Synaptophysin Is Required for Synaptobrevin Retrieval during Synaptic Vesicle Endocytosis. *J. Neurosci.* 31, 14032–14036.

Gorenberg, E. L., and Chandra, S. S. (2017). The role of co-chaperones in synaptic

proteostasis and neurodegenerative disease. *Front. Neurosci.* 11, 1–16.

Gorenberg, E., Zhao, H., Bishai, J., Chou, V., Wirak, G., Lam, T., and Chandra, S. (2020). Identification of palmitoyl protein thioesterase 1 substrates defines roles for synaptic depalmitoylation. *bioRxiv*. doi:10.1101/2020.05.02.074302.

Gorleku, O. A., and Chamberlain, L. H. (2010). Palmitoylation and testis-enriched expression of the cysteine-string protein β isoform. *Biochemistry* 49, 5308–5313.

Götz, J., Chen, F., Van Dorpe, J., and Nitsch, R. M. (2001). Formation of neurofibrillary tangles in P301L tau transgenic mice induced by Aβ42 fibrils. *Science (80-.).* 293, 1491–1495.

Gowrishankar, S., Yuan, P., Wu, Y., Schrag, M., Paradise, S., Grutzendler, J., De Camilli, P., and Ferguson, S. M. (2015). Massive accumulation of luminal protease-deficient axonal lysosomes at Alzheimer's disease amyloid plaques. *Proc. Natl. Acad. Sci. U. S. A.* 112, 3699–3708.

Gozal, Y. M., Duong, D. M., Gearing, M., Cheng, D., Hanfelt, J. J., Funderburk, C., Peng, J., Lah, J. J., and Levey, A. I. (2009). Proteomics analysis reveals novel components in the detergent-insoluble subproteome in Alzheimer's disease. *J. Proteome Res.* 8, 5069–5079.

Greaves, J., and Chamberlain, L. H. (2006). Dual Role of the Cysteine-String Domain in Membrane Binding and Palmitoylation-dependent Sorting of the Molecular Chaperone Cysteine-String Protein. *Mol. Biol. Cell* 17, 4748–4759.

Greaves, J., Lemonidis, K., Gorleku, O. A., Cruchaga, C., Grefen, C., and Chamberlain, L. H. (2012). Palmitoylation-induced aggregation of cysteine-string protein mutants that cause neuronal ceroid lipofuscinosis. *J. Biol. Chem.* 287, 37330–37339.

Greaves, J., Salaun, C., Fukata, Y., Fukata, M., and Chamberlain, L. H. (2008). Palmitoylation and Membrane Interactions of the Neuroprotective Chaperone Cysteine-string Protein. *J. Biol. Chem.* 283, 25014–25026.

Greten-Harrison, B., Polydoro, M., Morimoto-Tomita, M., Diao, L., Williams, A. M., Nie, E. H., Makani, S., Tian, N., Castillo, P. E., Buchman, V. L., and Chandra, S. S. (2010). αβγ-Synuclein triple knockout mice revealage-dependent neuronal dysfunction. *Proc. Natl. Acad. Sci. U. S. A.* 107, 19573–19578.

Groemer, T. W., Thiel, C. S., Holt, M., Riedel, D., Hua, Y., Hüve, J., Wilhelm, B. G., and Klingauf, J. (2011). Amyloid precursor protein is trafficked and secreted via synaptic vesicles. *PLoS One* 6.

Grünberg, J., Walter, J., Eckman, C., Capell, A., Schindzielorz, A., Younkin, S., Mehta, N., Hardy, J., and Haass, C. (1998). Truncated presenilin 2 derived

from differentially spliced mRNAs does not affect the ratio of amyloid β-peptide 1-42/1-40. *Neuroreport* 9, 3293–3299.

Grundke-Iqbal, I., Iqbal, K., Tung, Y. C., Quinlan, M., Wisniewski, H. M., and Binder, L. I. (1986). Abnormal phosphorylation of the microtubule-associated protein tau (tau) in Alzheimer cytoskeletal pathology. *Proc. Natl. Acad. Sci. U. S. A.* 83, 4913–4917.

Guerreiro, R., Wojtas, A., Bras, J., Carrasquillo, M., Rogaeva, E., Majounie, E., Cruchaga, C., Sassi, C., Kauwe, J. S. K., Younkin, S., Hazrati, L., Collinge, J., Pocock, J., Lashley, T., Williams, J., Lambert, J.-C., Amouyel, P., Goate, A., Rademakers, R., Morgan, K., Powell, J., St. George-Hyslop, P., Singleton, A., and Hardy, J. (2013). TREM2 Variants in Alzheimer's Disease. *N. Engl. J. Med.* 368, 117–127.

Guerrero-Muñoz, M. J., Gerson, J., and Castillo-Carranza, D. L. (2015). Tau oligomers: The toxic player at synapses in Alzheimer's disease. *Front. Cell. Neurosci.* 9, 1–10.

Guix, F. X., Corbett, G. T., Cha, D. J., Mustapic, M., Liu, W., Mengel, D., Chen, Z., Aikawa, E., Young-Pearse, T., Kapogiannis, D., Selkoe, D. J., and Walsh, D. M. (2018). Detection of aggregation-competent tau in neuron-derived extracellular vesicles. *Int. J. Mol. Sci.* 19, 1–23.

Gundersen, C. B. (2020). Cysteine string proteins. *Prog. Neurobiol.* 188.

Gundersen, C. B., Mastrogiacomot, A., Faull, K., and Umbach, J. A. (1994). Extensive lipidation of a Torpedo cysteine string protein. *J. Biol. Chem.* 269, 19197–19199.

Gundersen, C. B., and Umbach, J. A. (1992). Suppression cloning of the cDNA for a candidate subunit of a presynaptic calcium channel. *Neuron* 9, 527–537.

Guo, J. L., and Lee, V. M. Y. (2011). Seeding of normal tau by pathological tau conformers drives pathogenesis of Alzheimer-like tangles. *J. Biol. Chem.* 286, 15317–15331.

Guo, J. L., Narasimhan, S., Changolkar, L., He, Z., Stieber, A., Zhang, B., Gathagan, R. J., Iba, M., McBride, J. D., Trojanowski, J. Q., and Lee, V. M. Y. (2016). Unique pathological tau conformers from alzheimer's brains transmit tau pathology in nontransgenic mice. *J. Exp. Med.* 213, 2635–2654.

Guo, T., Noble, W., and Hanger, D. P. (2017). Roles of tau protein in health and disease. *Acta Neuropathol.* 133, 665–704.

Haass, C., Kaether, C., Thinakaran, G., and Sisodia, S. (2012). Trafficking and proteolytic processing of APP. *Cold Spring Harb. Perspect. Med.* 2, 1–25.

Haass, C., Koo, E. H., Mellon, A., Hung, A. Y., and Selkoe, D. J. (1992). Targeting

of cell-surface β-amyloid precursor protein to lysosomes: Alternative processing into amyloid-bearing fragments. *Nature* 357, 500–503.

Haass, C., and Mandelkow, E. (2010). Fyn-tau-amyloid: A toxic triad. *Cell* 142, 356–358.

Haass, C., and Selkoe, D. J. (1993). Cellular processing of β-amyloid precursor protein and the genesis of amyloid β-peptide. *Cell* 75, 1039–1042.

Haass, C., and Selkoe, D. J. (2007). Soluble protein oligomers in neurodegeneration: Lessons from the Alzheimer's amyloid β-peptide. *Nat. Rev. Mol. Cell Biol.* 8, 101–112.

Hadley, K. C., Rakhit, R., Guo, H., Sun, Y., Jonkman, J. E. N., McLaurin, J., Hazrati, L. N., Emili, A., and Chakrabartty, A. (2015). Determining composition of micron-scale protein deposits in neurodegenerative disease by spatially targeted optical microproteomics. *Elife* 4, 1–21.

Hales, C. M., Dammer, E. B., Deng, Q., Duong, D. M., Gearing, M., Troncoso, J. C., Thambisetty, M., Lah, J. J., Shulman, J. M., Levey, A. I., and Seyfried, N. T. (2016). Changes in the detergent-insoluble brain proteome linked to amyloid and tau in Alzheimer's Disease progression. *Proteomics* 16, 3042–3053.

Hamanaka, Y., and Meinertzhagen, I. A. (2010). Immunocytochemical localization of synaptic proteins to photoreceptor synapses of Drosophila melanogaster. *J. Comp. Neurol.* 518, 1133–1155.

Hamley, I. W. (2012). The amyloid beta peptide: A chemist's perspective. role in Alzheimer's and fibrillization. *Chem. Rev.* 112, 5147–5192.

Hanger, D. P., Anderton, B. H., and Noble, W. (2009). Tau phosphorylation: the therapeutic challenge for neurodegenerative disease. *Trends Mol. Med.* 15, 112–119.

Hanger, D. P., Hughes, K., Woodgett, J. R., Brion, J. P., and Anderton, B. H. (1992). Glycogen synthase kinase-3 induces Alzheimer's disease-like phosphorylation of tau: Generation of paired helical filament epitopes and neuronal localisation of the kinase. *Neurosci. Lett.* 147, 58–62.

Hanger, D. P., and Noble, W. (2011). Functional implications of glycogen synthase kinase-3-mediated tau phosphorylation. *Int. J. Alzheimers. Dis.* 2011, 1–11.

Hanger, D. P., and Wray, S. (2010). Tau cleavage and tau aggregation in neurodegenerative disease. *Biochem. Soc. Trans.* 38, 1016–1020.

Hannon, E., Shireby, G. L., Brookes, K., Attems, J., Sims, R., Cairns, N. J., Love, S., Thomas, A. J., Morgan, K., Francis, P. T., and Mill, J. (2020). Genetic risk for Alzheimer's disease influences neuropathology via multiple biological pathways. *Brain Commun.* 2, 1–13.

Haque, A., Polcyn, R., Matzelle, D., and Banik, N. L. (2018). New insights into the role of neuron-specific enolase in neuro-inflammation, neurodegeneration, and neuroprotection. *Brain Sci.* 8, 1–12.

Hardy, J. (2009). The amyloid hypothesis for Alzheimer's disease: A critical reappraisal. *J. Neurochem.* 110, 1129–1134.

Hardy, J. A., and Higgins, G. A. (1992). Alzheimer's disease: The amyloid cascade hypothesis. *Science (80-.).* 256, 184–185.

Hardy, J., and Selkoe, D. J. (2002). The amyloid hypothesis of Alzheimer's disease: Progress and problems on the road to therapeutics. *Science (80-.).* 297, 353–356.

Hark, T. J., Rao, N. R., Castillon, C., Basta, T., Smukowski, S., Bao, H., Upadhyay, A., Bomba-Warczak, E., Nomura, T., O'Toole, E. T., Morgan, G. P., Ali, L., Saito, T., Guillermier, C., Saido, T. C., Steinhauser, M. L., Stowell, M. H. B., Chapman, E. R., Contractor, A., and Savas, J. N. (2021). Pulse-Chase Proteomics of the App Knockin Mouse Models of Alzheimer's Disease Reveals that Synaptic Dysfunction Originates in Presynaptic Terminals. *Cell Syst.* 12, 141-158.e9.

Harris, J. A., Koyama, A., Maeda, S., Ho, K., Devidze, N., Dubal, D. B., Yu, G. Q., Masliah, E., and Mucke, L. (2012). Human P301L-Mutant Tau Expression in Mouse Entorhinal-Hippocampal Network Causes Tau Aggregation and Presynaptic Pathology but No Cognitive Deficits. *PLoS One* 7, 1–16.

Harwell, C. S., and Coleman, M. P. (2016). Synaptophysin depletion and intraneuronal Aβ in organotypic hippocampal slice cultures from huAPP transgenic mice. *Mol. Neurodegener.* 11, 1–16.

Hasegawa, M., Fujiwara, H., Nonaka, T., Wakabayashi, K., Takahashi, H., Lee, V. M. Y., Trojanowski, J. Q., Mann, D., and Iwatsubo, T. (2002). Phosphorylated α-synuclein is ubiquitinated in α-synucleinopathy lesions. *J. Biol. Chem.* 277, 49071–49076.

Hasegawa, M., Watanabe, S., Kondo, H., Akiyama, H., Mann, D. M. A., Saito, Y., and Murayama, S. (2014). 3R and 4R tau isoforms in paired helical filaments in Alzheimer's disease. *Acta Neuropathol.* 127, 303–305.

Hashimoto, T., Serrano-Pozo, A., Hori, Y., Adams, K. W., Takeda, S., Banerji, A. O., Mitani, A., Joyner, D., Thyssen, D. H., Bacskai, B. J., Frosch, M. P., Spires-Jones, T. L., Finn, M. B., Holtzman, D. M., and Hyman, B. T. (2012). Apolipoprotein e, especially apolipoprotein E4, increases the oligomerization of amyloid β peptide. *J. Neurosci.* 32, 15181–15192.

Hatanpaa, K. J., Bigio, E. H., Cairns, N. J., Womack, K. B., Weintraub, S., Morris, J.

C., Foong, C., Xiao, G., Hladik, C., Mantanona, T. Y., and White, C. L. (2008). TAR DNA-binding protein 43 immunohistochemistry reveals extensive neuritic pathology in FTLD-U: A midwest-southwest consortium for FTLD study. *J. Neuropathol. Exp. Neurol.* 67, 271–279.

He, Y., Wei, M., Wu, Y., Qin, H., Li, W., Ma, X., Cheng, J., Ren, J., Shen, Y., Chen, Z., Sun, B., Huang, F. De, Shen, Y., and Zhou, Y. D. (2019). Amyloid β oligomers suppress excitatory transmitter release via presynaptic depletion of phosphatidylinositol-4,5-bisphosphate. *Nat. Commun.* 10, 1–18.

Head, E., Corrada, M. M., Kahle-Wrobleski, K., Kim, R. C., Sarsoza, F., Goodus, M., and Kawas, C. H. (2009). Synaptic proteins, neuropathology and cognitive status in the oldest-old. *Neurobiol. Aging* 30, 1125–1134.

Head, E., T. Lott, I., M. Wilcock, D., and A. Lemere, C. (2015). Aging in Down Syndrome and the Development of Alzheimer's Disease Neuropathology. *Curr. Alzheimer Res.* 13, 18–29.

Hebb, C. O., and Whittaker, V. P. (1958). Intracellular distributions of acetylcholine and choline acetylase. *J. Physiol.* 142, 187–196.

Henderson, M. X., Cornblath, E. J., Li, H. L., Changolkar, L., Zhang, B., Brown, H. J., Gathagan, R. J., Olufemi, M. F., Bassett, D. S., Trojanowski, J. Q., and Lee, V. M. Y. (2020). Tau pathology spreads between anatomically-connected regions of the brain and is modulated by a LRRK2 mutation. *bioRxiv*. doi:10.1101/2020.10.13.337857.

Henderson, M. X., Wirak, G. S., Zhang, Y. quan, Dai, F., Ginsberg, S. D., Dolzhanskaya, N., Staropoli, J. F., Nijssen, P. C. G., Lam, T. K. T., Roth, A. F., Davis, N. G., Dawson, G., Velinov, M., and Chandra, S. S. (2016). Neuronal ceroid lipofuscinosis with DNAJC5/CSPα mutation has PPT1 pathology and exhibit aberrant protein palmitoylation. *Acta Neuropathol.* 131, 621–637.

Heneka, M. T., Carson, M. J., Khoury, J. El, Landreth, G. E., Brosseron, F., Feinstein, D. L., Jacobs, A. H., Wyss-Coray, T., Vitorica, J., Ransohoff, R. M., Herrup, K., Frautschy, S. A., Finsen, B., Brown, G. C., Verkhratsky, A., Yamanaka, K., Koistinaho, J., Latz, E., Halle, A., Petzold, G. C., Town, T., Morgan, D., Shinohara, M. L., Perry, V. H., Holmes, C., Bazan, N. G., Brooks, D. J., Hunot, S., Joseph, B., Deigendesch, N., Garaschuk, O., Boddeke, E., Dinarello, C. A., Breitner, J. C., Cole, G. M., Golenbock, D. T., and Kummer, M. P. (2015). Neuroinflammation in Alzheimer's disease. *Lancet Neurol.* 14, 388–405.

Henkins, K. M., Sokolow, S., Miller, C. A., Vinters, H. V., Poon, W. W., Cornwell, L. B., Saing, T., and Gylys, K. H. (2012). Extensive p-Tau pathology and SDS-

stable p-Tau oligomers in Alzheimer's cortical synapses. *Brain Pathol.* 22, 826–833.

Henstridge, C. M., Hyman, B. T., and Spires-Jones, T. L. (2019). Beyond the neuron–cellular interactions early in Alzheimer disease pathogenesis. *Nat. Rev. Neurosci.* 20, 94–108.

Henstridge, C. M., Pickett, E., and Spires-Jones, T. L. (2016). Synaptic pathology: A shared mechanism in neurological disease. *Ageing Res. Rev.* 28, 72–84.

Hesse, R., Hurtado, M. L., Jackson, R. J., Eaton, S. L., Herrmann, A. G., Colom-Cadena, M., Tzioras, M., King, D., Rose, J., Tulloch, J., McKenzie, C. A., Smith, C., Henstridge, C. M., Lamont, D., Wishart, T. M., and Spires-Jones, T. L. (2019). Comparative profiling of the synaptic proteome from Alzheimer's disease patients with focus on the APOE genotype. *Acta Neuropathol. Commun.* 7, 214.

Himmler, A., Drechsel, D., Kirschner, M. W., and Martin, D. W. (1989). Tau consists of a set of proteins with repeated C-terminal microtubule-binding domains and variable N-terminal domains. *Mol. Cell. Biol.* 9, 1381–1388.

Hippius, H., and Neundörfer, G. (2003). The discovery of Alzheimer's disease. *Dialogues Clin. Neurosci.* 5, 101–108.

Hof, P. R., Morrison, J. H., and Cox, K. (1990). Quantitative analysis of a vulnerable subset of pyramidal neurons in Alzheimer's disease: I. Superior frontal and inferior temporal cortex. *J. Comp. Neurol.* 301, 44–54.

Holcomb, L., Gordon, M. N., Mcgowan, E., Yu, X., Benkovic, S., Jantzen, P., Wright, K., Saad, I., Mueller, R., Morgan, D., Sanders, S., Zehr, C., O'Campo, K., Hardy, J., Prada, C. M., Eckman, C., Younkin, S., Hsiao, K., and Duff, K. (1998). Accelerated Alzheimer-type phenotype in transgenic mice carrying both mutant amyloid precursor protein and presenilin 1 transgenes. *Nat. Med.* 4, 97–100.

Hollingsworth, E. B., Mcneal, E. T., Burton, J. L., Williams, R. J., Daly, J. W., and Creveling, C. R. (1985). Biochemical characterization of a filtered synaptoneurosome preparation from guinea pig cerebral cortex: Cyclic adenosine 3':5'-monophosphate-generating systems, receptors, and enzymes. *J. Neurosci.* 5, 2240–2253.

Holtzman, D. M., Morris, J. C., and Goate, A. M. (2011). Alzheimer's disease: the challenge of the second century. *Sci. Transl. Med.* 3, 1–35.

Honer, W. G. (2003). Pathology of presynaptic proteins in Alzheimer's disease: More than simple loss of terminals. in *Neurobiology of Aging*, 1047–1062.

Hong, S., Beja-Glasser, V. F., Nfonoyim, B. M., Frouin, A., Li, S., Ramakrishnan, S.,

Merry, K. M., Shi, Q., Rosenthal, A., Barres, B. A., Lemere, C. A., Selkoe, D. J., and Stevens, B. (2016). Complement and microglia mediate early synapse loss in Alzheimer mouse models. *Science (80-.).* 352, 712–716.

Honig, L. S., Vellas, B., Woodward, M., Boada, M., Bullock, R., Borrie, M., Hager, K., Andreasen, N., Scarpini, E., Liu-Seifert, H., Case, M., Dean, R. A., Hake, A., Sundell, K., Poole Hoffmann, V., Carlson, C., Khanna, R., Mintun, M., DeMattos, R., Selzler, K. J., and Siemers, E. (2018). Trial of Solanezumab for Mild Dementia Due to Alzheimer's Disease. *N. Engl. J. Med.* 378, 321–330.

Hooper, C., Killick, R., and Lovestone, S. (2008). The GSK3 hypothesis of Alzheimer's disease. *J. Neurochem.* 104, 1433–1439.

Hoover, B. R., Reed, M. N., Su, J., Penrod, R. D., Kotilinek, L. A., Grant, M. K., Pitstick, R., Carlson, G. A., Lanier, L. M., Yuan, L. L., Ashe, K. H., and Liao, D. (2010). Tau Mislocalization to Dendritic Spines Mediates Synaptic Dysfunction Independently of Neurodegeneration. *Neuron* 68, 1067–1081.

Howlett, D. R., Whitfield, D., Johnson, M., Attems, J., O'Brien, J. T., Aarsland, D., Lai, M. K. P., Lee, J. H., Chen, C., Ballard, C., Hortobágyi, T., and Francis, P. T. (2015). Regional Multiple Pathology Scores Are Associated with Cognitive Decline in Lewy Body Dementias. *Brain Pathol.* 25, 401–408.

Hsiao, K., Chapman, P., Nilsen, S., Eckman, C., Harigaya, Y., Younkin, S., Yang, F., and Cole, G. (1996). Correlative memory deficits, Abeta elevation, and amyloid plaques in transgenic mice. *Science (80-.).* 274, 99–102.

Hsieh, H., Boehm, J., Sato, C., Iwatsubo, T., Tomita, T., Sisodia, S., and Malinow, R. (2006). AMPAR Removal Underlies Aβ-Induced Synaptic Depression and Dendritic Spine Loss. *Neuron* 52, 831–843.

Hsu, C.-C., Davis, K. M., Jin, H., Foos, T., Floor, E., Chen, W., Tyburski, J. B., Yang, C.-Y., Schloss, J. V, and Wu, J.-Y. (2000). Association of l-Glutamic Acid Decarboxylase to the 70-kDa Heat Shock Protein as a Potential Anchoring Mechanism to Synaptic Vesicles *. *J. Biol. Chem.* 275, 20822–20828.

Hu, N. W., Nicoll, A. J., Zhang, D., Mably, A. J., O'Malley, T., Purro, S. A., Terry, C., Collinge, J., Walsh, D. M., and Rowan, M. J. (2014). MGlu5 receptors and cellular prion protein mediate amyloid-β- facilitated synaptic long-term depression in vivo. *Nat. Commun.* 5, 1–13.

Hu, S., Xiang, Y., Qiu, L., Wang, M., and Zhang, Y. (2020). Activation of the membrane-bound Nrf1 transcription factor by USP19, a tail-anchored ubiquitin-specific protease in the endoplasmic reticulum. *bioRxiv*. doi:10.1101/2020.10.05.326363.

Hu, W. T., Josephs, K. A., Knopman, D. S., Boeve, B. F., Dickson, D. W., Petersen, R. C., and Parisi, J. E. (2008). Temporal lobar predominance of TDP-43 neuronal cytoplasmic inclusions in Alzheimer disease. *Acta Neuropathol.* 116, 215.

Hudry, E., Wu, H. Y., Arbel-Ornath, M., Hashimoto, T., Matsouaka, R., Fan, Z., Spires-Jones, T. L., Betensky, R. A., Bacskai, B. J., and Hyman, B. T. (2012). Inhibition of the NFAT pathway alleviates amyloid beta neurotoxicity in a mouse model of Alzheimer's disease. *J. Neurosci.* 32, 3176–3192.

Hutton, M., Lendon, C. L., Rizzu, P., Baker, M., Froelich, S., Houlden, H., Pickering-Brown, S., Chakraverty, S., Isaacs, A., Grover, A., Hackett, J., Adamson, J., Lincoln, S., Dickson, D., Davies, P., Petersen, R. C., Stevens, M., de Graaff, E., Wauters, E., van Baren, J., Hillebrand, M., Joosse, M., Kwon, J. M., Nowotny, P., Che, L. K., Norton, J., Morris, J. C., Reed, L. A., Trojanowski, J., Basun, H., Lannfelt, L., Neystat, M., Fahn, S., Dark, F., Tannenberg, T., Dodd, P. R., Hayward, N., Kwok, J. B. J., Schofield, P. R., Andreadis, A., Snowden, J., Craufurd, D., Neary, D., Owen, F., Oostra, B. A., Hardy, J., Goate, A., van Swieten, J., Mann, D., Lynch, T., and Heutink, P. (1998). Association of missense and 5′-splice-site mutations in tau with the inherited dementia FTDP-17. *Nature* 393, 702–705.

Huynh, T. P. V., Liao, F., Francis, C. M., Robinson, G. O., Serrano, J. R., Jiang, H., Roh, J., Finn, M. B., Sullivan, P. M., Esparza, T. J., Stewart, F. R., Mahan, T. E., Ulrich, J. D., Cole, T., and Holtzman, D. M. (2017). Age-Dependent Effects of apoE Reduction Using Antisense Oligonucleotides in a Model of β-amyloidosis. *Neuron* 96, 1013–1023.

Hyman, B. T., Phelps, C. H., Beach, T. G., Bigio, E. H., Cairns, N. J., Carrillo, M. C., Dickson, D. W., Duyckaerts, C., Frosch, M. P., Masliah, E., Mirra, S. S., Nelson, P. T., Schneider, J. A., Thal, D. R., Thies, B., Trojanowski, J. Q., Vinters, H. V., and Montine, T. J. (2012). National Institute on Aging-Alzheimer's Association guidelines for the neuropathologic assessment of Alzheimer's disease. *Alzheimer's Dement.* 8, 1–13.

Iadecola, C. (2010). The overlap between neurodegenerative and vascular factors in the pathogenesis of dementia. *Acta Neuropathol.* 120, 287–296.

Iadecola, C., and Gorelick, P. B. (2003). Converging pathogenic mechanisms in vascular and neurodegenerative dementia. *Stroke* 34, 335–337.

Iba, M., McBride, J. D., Guo, J. L., Zhang, B., Trojanowski, J. Q., and Lee, V. M. Y. (2015). Tau pathology spread in PS19 tau transgenic mice following locus coeruleus (LC) injections of synthetic tau fibrils is determined by the LC's

afferent and efferent connections. *Acta Neuropathol.* 130, 349–362.

Imler, E., Pyon, J. S., Kindelay, S., Torvund, M., Zhang, Y. Q., Chandra, S. S., and Zinsmaier, K. E. (2019). A drosophila model of neuronal ceroid lipofuscinosis CLN4 reveals a hypermorphic gain of function mechanism. *Elife* 8, 1–34.

Iqbal, K., and Grundke-Iqbal, I. (2002). Neurofibrillary pathology leads to synaptic loss and not the other way around in Alzheimer disease. *J. Alzheimer's Dis.* 4, 235–238.

Irwin, D. J. (2016). Tauopathies as clinicopathological entities. *Park. Relat. Disord.* 22, 29–33.

Itagaki, S., McGeer, P. L., Akiyama, H., Zhu, S., and Selkoe, D. (1989). Relationship of microglia and astrocytes to amyloid deposits of Alzheimer disease. *J. Neuroimmunol.* 24, 173–182.

Ittner, L. M., Ke, Y. D., Delerue, F., Bi, M., Gladbach, A., van Eersel, J., Wölfing, H., Chieng, B. C., Christie, M. J., Napier, I. A., Eckert, A., Staufenbiel, M., Hardeman, E., and Götz, J. (2010). Dendritic function of tau mediates amyloid-β toxicity in alzheimer's disease mouse models. *Cell* 142, 387–397.

Jack, C. R., Bennett, D. A., Blennow, K., Carrillo, M. C., Dunn, B., Haeberlein, S. B., Holtzman, D. M., Jagust, W., Jessen, F., Karlawish, J., Liu, E., Molinuevo, J. L., Montine, T., Phelps, C., Rankin, K. P., Rowe, C. C., Scheltens, P., Siemers, E., Snyder, H. M., Sperling, R., Elliott, C., Masliah, E., Ryan, L., and Silverberg, N. (2018). NIA-AA Research Framework: Toward a biological definition of Alzheimer's disease. *Alzheimer's Dement.* 14, 535–562.

Jack Jr, C. R., Albert, M. S., Knopman, D. S., McKhann, G. M., Sperling, R. A., Carrillo, M. C., Thies, B., and Phelps, C. H. (2011). Introduction to the recommendations from the National Institute on Aging-Alzheimer's Association workgroups on diagnostic guidelines for Alzheimer's disease. *Alzheimers. Dement.* 7, 257–262.

Jackson, J., Jambrina, E., Li, J., Marston, H., Menzies, F., Phillips, K., and Gilmour, G. (2019a). Targeting the Synapse in Alzheimer's Disease. *Front. Neurosci.* 13, 735.

Jackson, R. J., Rose, J., Tulloch, J., Henstridge, C., Smith, C., and Spires-Jones, T. L. (2019b). Clusterin accumulates in synapses in Alzheimer's disease and is increased in apolipoprotein E4 carriers. *Brain Commun.* 1, 1–12.

Jackson, R. J., Rudinskiy, N., Herrmann, A. G., Croft, S., Kim, J. M., Petrova, V., Ramos-Rodriguez, J. J., Pitstick, R., Wegmann, S., Garcia-Alloza, M., Carlson, G. A., Hyman, B. T., and Spires-Jones, T. L. (2016). Human tau increases amyloid β plaque size but not amyloid β-mediated synapse loss in a novel

mouse model of Alzheimer's disease. *Eur. J. Neurosci.* 44, 3056–3066.

Jadhav, S., Avila, J., Schöll, M., Kovacs, G. G., Kövari, E., Skrabana, R., Evans, L. D., Kontsekova, E., Malawska, B., de Silva, R., Buee, L., and Zilka, N. (2019). A walk through tau therapeutic strategies. *Acta Neuropathol. Commun.* 7, 1–31.

Jankowsky, J. L., and Zheng, H. (2017). Practical considerations for choosing a mouse model of Alzheimer's disease. *Mol. Neurodegener.* 12, 89.

Jedličková, I., Cadieux-Dion, M., Přistoupilová, A., Stránecký, V., Hartmannová, H., Hodaňová, K., Barešová, V., Hůlková, H., Sikora, J., Nosková, L., Mušálková, D., Vyleťal, P., Sovová, J., Cossette, P., Andermann, E., Andermann, F., and Kmoch, S. (2020). Autosomal-dominant adult neuronal ceroid lipofuscinosis caused by duplication in DNAJC5 initially missed by Sanger and whole-exome sequencing. *Eur. J. Hum. Genet.* 28, 783–789.

Jefferson, T., Čaušević, M., Auf Dem Keller, U., Schilling, O., Isbert, S., Geyer, R., Maier, W., Tschickardt, S., Jumpertz, T., Weggen, S., Bond, J. S., Overall, C. M., Pietrzik, C. U., and Becker-Pauly, C. (2011). Metalloprotease meprin β generates nontoxic N-terminal amyloid precursor protein fragments in vivo. *J. Biol. Chem.* 286, 27741–27750.

Jellinger, K. A. (2007). The enigma of vascular cognitive disorder and vascular dementia. *Acta Neuropathol.* 113, 349–388.

Jellinger, K. A. (2013). Pathology and pathogenesis of vascular cognitive impairment-a critical update. *Front. Aging Neurosci.* 5, 1–19.

Jellinger, K. A. (2020). Pathobiological Subtypes of Alzheimer Disease. *Dement. Geriatr. Cogn. Disord.* 49, 321–333.

Jellinger, K. A., and Attems, J. (2007). Neuropathological evaluation of mixed dementia. *J. Neurol. Sci.* 257, 80–87.

Jellinger, K. A., Wenning, G. K., and Seppi, K. (2007). Predictors of survival in dementia with Lewy bodies and Parkinson dementia. *Neurodegener. Dis.* 4, 428–430.

Jhou, J.-F., and Tai, H.-C. (2017). The Study of Postmortem Human Synaptosomes for Understanding Alzheimer's Disease and Other Neurological Disorders: A Review. *Neurol. Ther.* 6, 57–68.

Jiang, Q., Lee, C. Y. D., Mandrekar, S., Wilkinson, B., Cramer, P., Zelcer, N., Mann, K., Lamb, B., Willson, T. M., Collins, J. L., Richardson, J. C., Smith, J. D., Comery, T. A., Riddell, D., Holtzman, D. M., Tontonoz, P., and Landreth, G. E. (2008). ApoE Promotes the Proteolytic Degradation of Aβ. *Neuron* 58, 681–693.

Jiang, S., Li, Y., Zhang, X., Bu, G., Xu, H., and Zhang, Y. W. (2014). Trafficking regulation of proteins in Alzheimer's disease. *Mol. Neurodegener.* 9, 1–13.

Jimenez-Sanchez, M., Lam, W., Hannus, M., Sönnichsen, B., Imarisio, S., Fleming, A., Tarditi, A., Menzies, F., Ed Dami, T., Xu, C., Gonzalez-Couto, E., Lazzeroni, G., Heitz, F., Diamanti, D., Massai, L., Satagopam, V. P., Marconi, G., Caramelli, C., Nencini, A., Andreini, M., Sardone, G. L., Caradonna, N. P., Porcari, V., Scali, C., Schneider, R., Pollio, G., O'Kane, C. J., Caricasole, A., and Rubinsztein, D. C. (2015). SiRNA screen identifies QPCT as a druggable target for Huntington's disease. *Nat. Chem. Biol.* 11, 347–354.

Jin, M., Shepardson, N., Yang, T., Chen, G., Walsh, D., and Selkoe, D. J. (2011). Soluble amyloid β-protein dimers isolated from Alzheimer cortex directly induce Tau hyperphosphorylation and neuritic degeneration. *Proc. Natl. Acad. Sci. U. S. A.* 108, 5819–5824.

Joachim, C. L., Morris, J. H., and Selkoe, D. J. (1989). Diffuse senile plaques occur commonly in the cerebellum in Alzheimer's disease. *Am. J. Pathol.* 135, 309–319.

Johnen, A., and Bertoux, M. (2019). Psychological and cognitive markers of behavioral variant frontotemporal dementia - A clinical neuropsychologist's view on diagnostic criteria and beyond. *Front. Neurol.* 10, 1–24.

Jonsson, T., Atwal, J. K., Steinberg, S., Snaedal, J., Jonsson, P. V., Bjornsson, S., Stefansson, H., Sulem, P., Gudbjartsson, D., Maloney, J., Hoyte, K., Gustafson, A., Liu, Y., Lu, Y., Bhangale, T., Graham, R. R., Huttenlocher, J., Bjornsdottir, G., Andreassen, O. A., Jonsson, E. G., Palotie, A., Behrens, T. W., Magnusson, O. T., Kong, A., Thorsteinsdottir, U., Watts, R. J., and Stefansson, K. (2012). A mutation in APP protects against Alzheimer's disease and age-related cognitive decline. *Nature* 488, 96–99.

Jonsson, T., Stefansson, H., Steinberg, S., Jonsdottir, I., Jonsson, P. V., Snaedal, J., Bjornsson, S., Huttenlocher, J., Levey, A. I., Lah, J. J., Rujescu, D., Hampel, H., Giegling, I., Andreassen, O. A., Engedal, K., Ulstein, I., Djurovic, S., Ibrahim-Verbaas, C., Hofman, A., Ikram, M. A., van Duijn, C. M., Thorsteinsdottir, U., Kong, A., and Stefansson, K. (2013). Variant of TREM2 Associated with the Risk of Alzheimer's Disease. *N. Engl. J. Med.* 368, 107–116.

Jorissen, E., Prox, J., Bernreuther, C., Weber, S., Schwanbeck, R., Serneels, L., Snellinx, A., Craessaerts, K., Thathiah, A., Tesseur, I., Bartsch, U., Weskamp, G., Blobel, C. P., Glatzel, M., De Strooper, B., and Saftig, P. (2010). The disintegrin/metalloproteinase ADAM10 is essential for the establishment of the

brain cortex. *J. Neurosci.* 30, 4833–4844.

Josephs, K. A., Hodges, J. R., Snowden, J. S., Mackenzie, I. R., Neumann, M., Mann, D. M., and Dickson, D. W. (2011). Neuropathological background of phenotypical variability in frontotemporal dementia. *Acta Neuropathol.* 122, 137–153.

Josephs, K. A., Murray, M. E., Whitwell, J. L., Parisi, J. E., Petrucelli, L., Jack, C. R., Petersen, R. C., and Dickson, D. W. (2014). Staging TDP-43 pathology in Alzheimer's disease. *Acta Neuropathol.* 127, 441–450.

Josephs, K. A., Whitwell, J. L., Knopman, D. S., Hu, W. T., Stroh, D. A., Baker, M., Rademakers, R., Boeve, B. F., Parisi, J. E., Smith, G. E., Ivnik, R. J., Petersen, R. C., Jack Jr, C. R., and Dickson, D. W. (2008). Abnormal TDP-43 immunoreactivity in AD modifies clinicopathologic and radiologic phenotype. *Neurology* 70, 1850–1857.

Jucker, M., and Walker, L. C. (2013). Self-propagation of pathogenic protein aggregates in neurodegenerative diseases. *Nature* 501, 45–51.

Kalimo, H., Lalowski, M., Bogdanovic, N., Philipson, O., Bird, T. D., Nochlin, D., Schellenberg, G. D., Brundin, R., Olofsson, T., Soliymani, R., Baumann, M., Wirths, O., Bayer, T. A., Nilsson, L. N. G., Basun, H., Lannfelt, L., and Ingelsson, M. (2013). The Arctic AβPP mutation leads to Alzheimer's disease pathology with highly variable topographic deposition of differentially truncated Aβ. *Acta Neuropathol. Commun.* 1, 60.

Kamenetz, F., Tomita, T., Hsieh, H., Seabrook, G., Borchelt, D., Iwatsubo, T., Sisodia, S., and Malinow, R. (2003). APP Processing and Synaptic Function. *Neuron* 37, 925–937.

Kandalepas, P. C., Sadleir, K. R., Eimer, W. A., Zhao, J., Nicholson, D. A., and Vassar, R. (2013). The Alzheimer's β-secretase BACE1 localizes to normal presynaptic terminals and to dystrophic presynaptic terminals surrounding amyloid plaques. *Acta Neuropathol.* 126, 329–352.

Kang, J., Lemaire, H. G., Unterbeck, A., Salbaum, J. M., Masters, C. L., Grzeschik, K. H., Multhaup, G., Beyreuther, K., and Müller-Hill, B. (1987). The precursor of Alzheimer's disease amyloid A4 protein resembles a cell-surface receptor. *Nature* 325, 733–736.

Kanno, T., Tsuchiya, A., and Nishizaki, T. (2014). Hyperphosphorylation of Tau at Ser396 occurs in the much earlier stage than appearance of learning and memory disorders in 5XFAD mice. *Behav. Brain Res.* 274, 302–306.

Kantarci, K., Weigand, S. D., Przybelski, S. A., Shiung, M. M., Whitwell, J. L., Negash, S., Knopman, D. S., Boeve, B. F., O'Brien, P. C., Petersen, R. C., and

Jack Jr, C. R. (2009). Risk of dementia in MCI: combined effect of cerebrovascular disease, volumetric MRI, and 1H MRS. *Neurology* 72, 1519–1525.

Kapasi, A., DeCarli, C., and Schneider, J. A. (2017). Impact of multiple pathologies on the threshold for clinically overt dementia. *Acta Neuropathol.* 134, 171–186.

Karch, C. M., and Goate, A. M. (2015). Alzheimer's disease risk genes and mechanisms of disease pathogenesis. *Biol. Psychiatry* 77, 43–51.

Kashani, A., Lepicard, È., Poirel, O., Videau, C., David, J. P., Fallet-Bianco, C., Simon, A., Delacourte, A., Giros, B., Epelbaum, J., Betancur, C., and El Mestikawy, S. (2008). Loss of VGLUT1 and VGLUT2 in the prefrontal cortex is correlated with cognitive decline in Alzheimer disease. *Neurobiol. Aging* 29, 1619–1630.

Kashyap, S. S., Johnson, J. R., McCue, H. V., Chen, X., Edmonds, M. J., Ayala, M., Graham, M. E., Jenn, R. C., Barclay, J. W., Burgoyne, R. D., and Morgan, A. (2014). Caenorhabditis elegans dnj-14, the orthologue of the DNAJC5 gene mutated in adult onset neuronal ceroid lipofuscinosis, provides a new platform for neuroprotective drug screening and identifies a SIR-2.1-independent action of resveratrol. *Hum. Mol. Genet.* 23, 5916–5927.

Kay, K. R., Smith, C., Wright, A. K., Serrano-Pozo, A., Pooler, A. M., Koffie, R., Bastin, M. E., Bak, T. H., Abrahams, S., Kopeikina, K. J., McGuone, D., Frosch, M. P., Gillingwater, T. H., Hyman, B. T., and Spires-Jones, T. L. (2013). Studying synapses in human brain with array tomography and electron microscopy. *Nat. Protoc.* 8, 1366–1380.

Kayed, R., Head, E., Sarsoza, F., Saing, T., Cotman, C. W., Necula, M., Margol, L., Wu, J., Breydo, L., Thompson, J. L., Rasool, S., Gurlo, T., Butler, P., and Glabe, C. G. (2007). Fibril specific, conformation dependent antibodies recognize a generic epitope common to amyloid fibrils and fibrillar oligomers that is absent in prefibrillar oligomers. *Mol. Neurodegener.* 2, 18.

Keller, J. N., Lauderback, C. M., Butterfield, D. A., Kindy, M. S., Yu, J., and Markesbery, W. R. (2000). Amyloid β-peptide effects on synaptosomes from apolipoprotein E- deficient mice. *J. Neurochem.* 74, 1579–1586.

Kelly, B. L., and Ferreira, A. (2007). Beta-amyloid disrupted synaptic vesicle endocytosis in cultured hippocampal neurons. *Neuroscience* 147, 60–70.

Kelly, B. L., Vassar, R., and Ferreira, A. (2005). β-amyloid-induced dynamin 1 depletion in hippocampal neurons: A potential mechanism for early cognitive decline in Alzheimer disease. *J. Biol. Chem.* 280, 31746–31753.

Kennedy, M. B., Bennett, M. K., and Erondu, N. E. (1983). Biochemical and

immunochemical evidence that the “major postsynaptic density protein” is a subunit of a calmodulin-dependent protein kinase. *Proc. Natl. Acad. Sci. U. S. A.* 80, 7357–7361.

Kfoury, N., Holmes, B. B., Jiang, H., Holtzman, D. M., and Diamond, M. I. (2012). Trans-cellular propagation of Tau aggregation by fibrillar species. *J. Biol. Chem.* 287, 19440–19451.

Khanahmadi, M., Farhud, D. D., and Malmir, M. (2015). Genetic of Alzheimer’s disease: A narrative review article. *Iran. J. Public Health* 44, 892–901.

Khatoon, S., Grundke-Iqbal, I., and Iqbal, K. (1994). Levels of normal and abnormally phosphorylated tau in different cellular and regional compartments of Alzheimer disease and control brains. *FEBS Lett.* 351, 80–84.

Kim, J., Basak, J. M., and Holtzman, D. M. (2009). The Role of Apolipoprotein E in Alzheimer’s Disease. *Neuron* 63, 287–303.

Kim, J., Gee, H. Y., and Lee, M. G. (2018). Unconventional protein secretion – new insights into the pathogenesis and therapeutic targets of human diseases. *J. Cell Sci.* 131, 1–11.

Kim, Y. E., Hipp, M. S., Bracher, A., Hayer-Hartl, M., and Ulrich Hartl, F. (2013). Molecular chaperone functions in protein folding and proteostasis. *Annu. Rev. Biochem.* 82, 323–355.

Kimura, A., Hata, S., and Suzuki, T. (2016). Alternative selection of site APP-cleaving enzyme 1 (BACE1) cleavage sites in amyloid β-protein precursor (APP) harboring protective and pathogenic mutations within the Aβ sequence. *J. Biol. Chem.* 291, 24041–24053.

Kimura, R., and Ohno, M. (2009). Impairments in remote memory stabilization precede hippocampal synaptic and cognitive failures in 5XFAD Alzheimer mouse model. *Neurobiol. Dis.* 33, 229–235.

King, A., Al-Sarraj, S., Troakes, C., Smith, B. N., Maekawa, S., Iovino, M., Spillantini, M. G., and Shaw, C. E. (2013). Mixed tau, TDP-43 and p62 pathology in FTLD associated with a C9ORF72 repeat expansion and p.Ala239Thr MAPT (tau) variant. *Acta Neuropathol.* 125, 303–310.

Kins, S., Crameri, A., Evans, D. R. H., Hemmings, B. A., Nitsch, R. M., and Götz, J. (2001). Reduced Protein Phosphatase 2A Activity Induces Hyperphosphorylation and Altered Compartmentalization of Tau in Transgenic Mice. *J. Biol. Chem.* 276, 38193–38200.

Klein, W. L. (2013). Synaptotoxic amyloid-β oligomers: A molecular basis for the cause, diagnosis, and treatment of Alzheimer’s disease? *J. Alzheimer’s Dis.* 33, 49–65.

Knowles, R. B., Wyart, C., Buldyrev, S. V., Cruz, L., Urbanc, B., Hasselmo, M. E., Stanley, H. E., and Hyman, B. T. (1999). Plaque-induced neurite abnormalities: Implications for disruption of neural networks in Alzheimer's disease. *Proc. Natl. Acad. Sci. U. S. A.* 96, 5274–5279.

Koffie, R. M., Hashimoto, T., Tai, H. C., Kay, K. R., Serrano-Pozo, A., Joyner, D., Hou, S., Kopeikina, K. J., Frosch, M. P., Lee, V. M., Holtzman, D. M., Hyman, B. T., and Spires-Jones, T. L. (2012). Apolipoprotein E4 effects in Alzheimer's disease are mediated by synaptotoxic oligomeric amyloid-β. *Brain* 135, 2155–2168.

Koffie, R. M., Hyman, B. T., and Spires-Jones, T. L. (2011). Alzheimer's disease: Synapses gone cold. *Mol. Neurodegener.* 6, 1–9.

Koffie, R. M., Meyer-Luehmann, M., Hashimoto, T., Adams, K. W., Mielke, M. L., Garcia-Alloza, M., Micheva, K. D., Smith, S. J., Kim, M. L., Lee, V. M., Hyman, B. T., and Spires-Jones, T. L. (2009). Oligomeric amyloid β associates with postsynaptic densities and correlates with excitatory synapse loss near senile plaques. *Proc. Natl. Acad. Sci. U. S. A.* 106, 4012–4017.

Kohan, S. A., Pescatori, M., Brecha, N. C., Mastrogiacomo, A., Umbach, J. A., and Gundersen, C. B. (1995). Cysteine string protein immunoreactivity in the nervous system and adrenal gland of rat. *J. Neurosci.* 15, 6230–6238.

Kohlschütter, A., Schulz, A., Bartsch, U., and Storch, S. (2019). Current and Emerging Treatment Strategies for Neuronal Ceroid Lipofuscinoses. *CNS Drugs* 33, 315–325.

Koleske, A. J. (2013). Molecular mechanisms of dendrite stability. *Nat. Rev. Neurosci.* 14, 536–550.

Koo, E. H., Squazzo, S. L., Selkoe, D. J., and Koo, C. H. (1996). Trafficking of cell-surface amyloid beta-protein precursor. I. Secretion, endocytosis and recycling as detected by labeled monoclonal antibody. *J. Cell Sci.* 109, 991–998.

Kopeikina, K. J., Carlson, G. A., Pitstick, R., Ludvigson, A. E., Peters, A., Luebke, J. I., Koffie, R. M., Frosch, M. P., Hyman, B. T., and Spires-Jones, T. L. (2011). Tau accumulation causes mitochondrial distribution deficits in neurons in a mouse model of tauopathy and in human Alzheimer's disease brain. *Am. J. Pathol.* 179, 2071–2082.

Kopeikina, K. J., Hyman, B. J., and Spires-Jones, T. L. (2012). Soluble forms of tau are toxic in alzheimer's disease. *Transl. Neurosci.* 3, 223–233.

Kopeikina, K. J., Wegmann, S., Pitstick, R., Carlson, G. A., Bacskai, B. J., Betensky, R. A., Hyman, B. T., and Spires-Jones, T. L. (2013). Tau Causes Synapse Loss without Disrupting Calcium Homeostasis in the rTg4510 Model of

Tauopathy. *PLoS One* 8, 1–8.

Koutras, C., and Braun, J. E. A. (2014). J protein mutations and resulting proteostasis collapse. *Front. Cell. Neurosci.* 8, 1–7.

Kovacs, G. G., Alafuzoff, I., Al-Sarraj, S., Arzberger, T., Bogdanovic, N., Capellari, S., Ferrer, I., Gelpi, E., Kövari, V., Kretzschmar, H., Nagy, Z., Parchi, P., Seilhean, D., Soininen, H., Troakes, C., and Budka, H. (2008). Mixed brain pathologies in dementia: The BrainNet Europe consortium experience. *Dement. Geriatr. Cogn. Disord.* 26, 343–350.

Kovacs, G. G., Milenkovic, I., Wöhrer, A., Höftberger, R., Gelpi, E., Haberler, C., Hönigschnabl, S., Reiner-Concin, A., Heinzl, H., Jungwirth, S., Krampla, W., Fischer, P., and Budka, H. (2013). Non-Alzheimer neurodegenerative pathologies and their combinations are more frequent than commonly believed in the elderly brain: A community-based autopsy series. *Acta Neuropathol.* 126, 365–384.

Kowall, N. W., Beal, M. F., Busciglio, J., Duffy, L. K., and Yankner, B. A. (1991). An in vivo model for the neurodegenerative effects of β amyloid and protection by substance P. *Proc. Natl. Acad. Sci. U. S. A.* 88, 7247–7251.

Kramer, M. L., and Schulz-Schaeffer, W. J. (2007). Presynaptic α-synuclein aggregates, not Lewy bodies, cause neurodegeneration in dementia with lewy bodies. *J. Neurosci.* 27, 1405–1410.

Kuchibhotla, K. V., Goldman, S. T., Lattarulo, C. R., Wu, H. Y., Hyman, B. T., and Bacskai, B. J. (2008). Aβ Plaques Lead to Aberrant Regulation of Calcium Homeostasis In Vivo Resulting in Structural and Functional Disruption of Neuronal Networks. *Neuron* 59, 214–225.

Kuhn, P. H., Wang, H., Dislich, B., Colombo, A., Zeitschel, U., Ellwart, J. W., Kremmer, E., Roßner, S., and Lichtenthaler, S. F. (2010). ADAM10 is the physiologically relevant, constitutive α-secretase of the amyloid precursor protein in primary neurons. *EMBO J.* 29, 3020–3032.

Kunkle, B. W., Grenier-Boley, B., Sims, R., Bis, J. C., Damotte, V., Naj, A. C., Boland, A., Vronskaya, M., van der Lee, S. J., Amlie-Wolf, A., Bellenguez, C., Frizatti, A., Chouraki, V., Martin, E. R., Sleegers, K., Badarinarayan, N., Jakobsdottir, J., Hamilton-Nelson, K. L., Moreno-Grau, S., Olaso, R., Raybould, R., Chen, Y., Kuzma, A. B., Hiltunen, M., Morgan, T., Ahmad, S., Vardarajan, B. N., Epelbaum, J., Hoffmann, P., Boada, M., Beecham, G. W., Garnier, J. G., Harold, D., Fitzpatrick, A. L., Valladares, O., Moutet, M. L., Gerrish, A., Smith, A. V., Qu, L., Bacq, D., Denning, N., Jian, X., Zhao, Y., Del Zompo, M., Fox, N. C., Choi, S. H., Mateo, I., Hughes, J. T., Adams, H. H.,

Malamon, J., Sanchez-Garcia, F., Patel, Y., Brody, J. A., Dombroski, B. A., Naranjo, M. C. D., Daniilidou, M., Eiriksdottir, G., Mukherjee, S., Wallon, D., Uphill, J., Aspelund, T., Cantwell, L. B., Garzia, F., Galimberti, D., Hofer, E., Butkiewicz, M., Fin, B., Scarpini, E., Sarnowski, C., Bush, W. S., Meslage, S., Kornhuber, J., White, C. C., Song, Y., Barber, R. C., Engelborghs, S., Sordon, S., Voijnovic, D., Adams, P. M., Vandenberghe, R., Mayhaus, M., Cupples, L. A., Albert, M. S., De Deyn, P. P., Gu, W., Himali, J. J., Beekly, D., Squassina, A., Hartmann, A. M., Orellana, A., Blacker, D., Rodriguez-Rodriguez, E., Lovestone, S., Garcia, M. E., Doody, R. S., Munoz-Fernadez, C., Sussams, R., Lin, H., Fairchild, T. J., Benito, Y. A., Holmes, C., Karamujić-Čomić, H., Frosch, M. P., Thonberg, H., Maier, W., Roschupkin, G., Ghetti, B., Giedraitis, V., Kawalia, A., Li, S., Huebinger, R. M., Kilander, L., Moebus, S., Hernández, I., Kamboh, M. I., Brundin, R. M., Turton, J., Yang, Q., Katz, M. J., Concari, L., Lord, J., Beiser, A. S., Keene, C. D., Helisalmi, S., Kloszewska, I., Kukull, W. A., Koivisto, A. M., Lynch, A., Tarraga, L., Larson, E. B., Haapasalo, A., Lawlor, B., Mosley, T. H., Lipton, R. B., Solfrizzi, V., Gill, M., Longstreth, W. T., Montine, T. J., Frisardi, V., Diez-Fairen, M., Rivadeneira, F., Petersen, R. C., Deramecourt, V., Alvarez, I., Salani, F., Ciaramella, A., Boerwinkle, E., Reiman, E. M., Fievet, N., Rotter, J. I., Reisch, J. S., Hanon, O., Cupidi, C., Andre Uitterlinden, A. G., Royall, D. R., Dufouil, C., Maletta, R. G., de Rojas, I., Sano, M., Brice, A., Cecchetti, R., George-Hyslop, P. S., Ritchie, K., Tsolaki, M., Tsuang, D. W., Dubois, B., Craig, D., Wu, C. K., Soininen, H., Avramidou, D., Albin, R. L., Fratiglioni, L., Germanou, A., Apostolova, L. G., Keller, L., Koutroumani, M., Arnold, S. E., Panza, F., Gkatzima, O., Asthana, S., Hannequin, D., Whitehead, P., Atwood, C. S., Caffarra, P., Hampel, H., Quintela, I., Carracedo, Á., Lannfelt, L., Rubinsztein, D. C., Barnes, L. L., Pasquier, F., Frölich, L., Barral, S., McGuinness, B., Beach, T. G., Johnston, J. A., Becker, J. T., Passmore, P., Bigio, E. H., Schott, J. M., Bird, T. D., Warren, J. D., Boeve, B. F., Lupton, M. K., Bowen, J. D., Proitsi, P., Boxer, A., Powell, J. F., Burke, J. R., Kauwe, J. S. K., Burns, J. M., Mancuso, M., Buxbaum, J. D., Bonuccelli, U., Cairns, N. J., McQuillin, A., Cao, C., Livingston, G., Carlson, C. S., Bass, N. J., Carlsson, C. M., Hardy, J., Carney, R. M., Bras, J., Carrasquillo, M. M., Guerreiro, R., Allen, M., Chui, H. C., Fisher, E., Masullo, C., Crocco, E. A., DeCarli, C., Bisceglio, G., Dick, M., Ma, L., Duara, R., Graff-Radford, N. R., Evans, D. A., Hodges, A., Faber, K. M., Scherer, M., Fallon, K. B., Riemenschneider, M., Fardo, D. W., Heun, R., Farlow, M. R., Kölsch, H., Ferris, S., Leber, M., Foroud, T. M., Heuser, I., Galasko, D. R., Giegling, I.,

Gearing, M., Hüll, M., Geschwind, D. H., Gilbert, J. R., Morris, J., Green, R. C., Mayo, K., Growdon, J. H., Feulner, T., Hamilton, R. L., Harrell, L. E., Drichel, D., Honig, L. S., Cushion, T. D., Huentelman, M. J., Hollingworth, P., Hulette, C. M., Hyman, B. T., Marshall, R., Jarvik, G. P., Meggy, A., Abner, E., Menzies, G. E., Jin, L. W., Leonenko, G., Real, L. M., Jun, G. R., Baldwin, C. T., Grozeva, D., Karydas, A., Russo, G., Kaye, J. A., Kim, R., Jessen, F., Kowall, N. W., Vellas, B., Kramer, J. H., Vardy, E., LaFerla, F. M., Jöckel, K. H., Lah, J. J., Dichgans, M., Leverenz, J. B., Mann, D., Levey, A. I., Pickering-Brown, S., Lieberman, A. P., Klopp, N., Lunetta, K. L., Wichmann, H. E., Lyketsos, C. G., Morgan, K., Marson, D. C., Brown, K., Martiniuk, F., Medway, C., Mash, D. C., Nöthen, M. M., Masliah, E., Hooper, N. M., McCormick, W. C., Daniele, A., McCurry, S. M., Bayer, A., McDavid, A. N., Gallacher, J., McKee, A. C., van den Bussche, H., Mesulam, M., Brayne, C., Miller, B. L., Riedel-Heller, S., Miller, C. A., Miller, J. W., Al-Chalabi, A., Morris, J. C., Shaw, C. E., Myers, A. J., Wiltfang, J., O'Bryant, S., Olichney, J. M., Alvarez, V., Parisi, J. E., Singleton, A. B., Paulson, H. L., Collinge, J., Perry, W. R., Mead, S., Peskind, E., Cribbs, D. H., Rossor, M., Pierce, A., Ryan, N. S., Poon, W. W., Nacmias, B., Potter, H., Sorbi, S., Quinn, J. F., Sacchinelli, E., Raj, A., Spalletta, G., Raskind, M., Caltagirone, C., Bossù, P., Orfei, M. D., Reisberg, B., Clarke, R., Reitz, C., Smith, A. D., Ringman, J. M., Warden, D., Roberson, E. D., Wilcock, G., Rogaeva, E., Bruni, A. C., Rosen, H. J., Gallo, M., Rosenberg, R. N., Ben-Shlomo, Y., Sager, M. A., Mecocci, P., Saykin, A. J., Pastor, P., Cuccaro, M. L., Vance, J. M., Schneider, J. A., Schneider, L. S., Slifer, S., Seeley, W. W., Smith, A. G., Sonnen, J. A., Spina, S., Stern, R. A., Swerdlow, R. H., Tang, M., Tanzi, R. E., Trojanowski, J. Q., Troncoso, J. C., Van Deerlin, V. M., Van Eldik, L. J., Vinters, H. V., Vonsattel, J. P., Weintraub, S., Welsh-Bohmer, K. A., Wilhelmsen, K. C., Williamson, J., Wingo, T. S., Woltjer, R. L., Wright, C. B., Yu, C. E., Yu, L., Saba, Y., Pilotto, A., Bullido, M. J., Peters, O., Crane, P. K., Bennett, D., Bosco, P., Coto, E., Boccardi, V., De Jager, P. L., Lleo, A., Warner, N., Lopez, O. L., Ingelsson, M., Deloukas, P., Cruchaga, C., Graff, C., Gwilliam, R., Fornage, M., Goate, A. M., Sanchez-Juan, P., Kehoe, P. G., Amin, N., Ertekin-Taner, N., Berr, C., Debette, S., Love, S., Launer, L. J., Younkin, S. G., Dartigues, J. F., Corcoran, C., Ikram, M. A., Dickson, D. W., Nicolas, G., Campion, D., Tschanz, J. A., Schmidt, H., Hakonarson, H., Clarimon, J., Munger, R., Schmidt, R., Farrer, L. A., Van Broeckhoven, C., C. O'Donovan, M., DeStefano, A. L., Jones, L., Haines, J. L., Deleuze, J. F., Owen, M. J., Gudnason, V., Mayeux, R., Escott-Price, V., Psaty, B. M.,

Ramirez, A., Wang, L. S., Ruiz, A., van Duijn, C. M., Holmans, P. A., Seshadri, S., Williams, J., Amouyel, P., Schellenberg, G. D., Lambert, J. C., and Pericak-Vance, M. A. (2019). Genetic meta-analysis of diagnosed Alzheimer's disease identifies new risk loci and implicates Aβ, tau, immunity and lipid processing. *Nat. Genet.* 51, 414–430.

Kurbatskaya, K., Phillips, E. C., Croft, C. L., Dentoni, G., Hughes, M. M., Wade, M. A., Al-Sarraj, S., Troakes, C., O'Neill, M. J., Perez-Nievas, B. G., Hanger, D. P., and Noble, W. (2016). Upregulation of calpain activity precedes tau phosphorylation and loss of synaptic proteins in Alzheimer's disease brain. *Acta Neuropathol. Commun.* 4, 1–15.

Kwong, L. K., Neumann, M., Sampathu, D. M., Lee, V. M. Y., and Trojanowski, J. Q. (2007). TDP-43 proteinopathy: The neuropathology underlying major forms of sporadic and familial frontotemporal lobar degeneration and motor neuron disease. *Acta Neuropathol.* 114, 63–70.

Kyle, B. D., Ahrendt, E., Braun, A. P., and Braun, J. E. A. (2013). The large conductance, calcium-activated K+ (BK) Channel is regulated by Cysteine String Protein. *Sci. Rep.* 3, 1–11.

Lacor, P. N., Buniel, M. C., Furlow, P. W., Clemente, A. S., Velasco, P. T., Wood, M., Viola, K. L., and Klein, W. L. (2007). Aβ oligomer-induced aberrations in synapse composition, shape, and density provide a molecular basis for loss of connectivity in Alzheimer's disease. *J. Neurosci.* 27, 796–807.

LaFerla, F. M., Green, K. N., and Oddo, S. (2007). Intracellular amyloid-β in Alzheimer's disease. *Nat. Rev. Neurosci.* 8, 499–509.

Laird, F. M., Cai, H., Savonenko, A. V., Farah, M. H., He, K., Melnikova, T., Wen, H., Chiang, H. C., Xu, G., Koliatsos, V. E., Borchelt, D. R., Price, D. L., Lee, H. K., and Wong, P. C. (2005). BACE1, a major determinant of selective vulnerability of the brain to amyloid-β amyloidogenesis, is essential for cognitive, emotional, and synaptic functions. *J. Neurosci.* 25, 11693–11709.

Lambert, J. C., Ibrahim-Verbaas, C. A., Harold, D., Naj, A. C., Sims, R., Bellenguez, C., Jun, G., DeStefano, A. L., Bis, J. C., Beecham, G. W., Grenier-Boley, B., Russo, G., Thornton-Wells, T. A., Jones, N., Smith, A. V., Chouraki, V., Thomas, C., Ikram, M. A., Zelenika, D., Vardarajan, B. N., Kamatani, Y., Lin, C. F., Gerrish, A., Schmidt, H., Kunkle, B., Fiévet, N., Amouyel, P., Pasquier, F., Deramecourt, V., De Bruijn, R. F. A. G., Amin, N., Hofman, A., Van Duijn, C. M., Dunstan, M. L., Hollingworth, P., Owen, M. J., O'Donovan, M. C., Jones, L., Holmans, P. A., Moskvina, V., Williams, J., Baldwin, C., Farrer, L. A., Choi, S. H., Lunetta, K. L., Fitzpatrick, A. L., Harris, T. B., Psaty, B. M., Gilbert, J. R.,

Hamilton-Nelson, K. L., Martin, E. R., Pericak-Vance, M. A., Haines, J. L., Gudnason, V., Jonsson, P. V., Eiriksdottir, G., Bihoreau, M. T., Lathrop, M., Valladares, O., Cantwell, L. B., Wang, L. S., Schellenberg, G. D., Ruiz, A., Boada, M., Reitz, C., Mayeux, R., Ramirez, A., Maier, W., Hanon, O., Kukull, W. A., Buxbaum, J. D., Campion, D., Wallon, D., Hannequin, D., Crane, P. K., Larson, E. B., Becker, T., Cruchaga, C., Goate, A. M., Craig, D., Johnston, J. A., Mc-Guinness, B., Todd, S., Passmore, P., Berr, C., Ritchie, K., Lopez, O. L., De Jager, P. L., Evans, D., Lovestone, S., Proitsi, P., Powell, J. F., Letenneur, L., Barberger-Gateau, P., Dufouil, C., Dartigues, J. F., Morón, F. J., Rubinsztein, D. C., St. George-Hyslop, P., Sleegers, K., Bettens, K., Van Broeckhoven, C., Huentelman, M. J., Gill, M., Brown, K., Morgan, K., Kamboh, M. I., Keller, L., Fratiglioni, L., Green, R., Myers, A. J., Love, S., Rogaeva, E., Gallacher, J., Bayer, A., Clarimon, J., Lleo, A., Tsuang, D. W., Yu, L., Bennett, D. A., Tsolaki, M., Bossù, P., Spalletta, G., Collinge, J., Mead, S., Sorbi, S., Nacmias, B., Sanchez-Garcia, F., Deniz Naranjo, M. C., Fox, N. C., Hardy, J., Bosco, P., Clarke, R., Brayne, C., Galimberti, D., Mancuso, M., Matthews, F., Moebus, S., Mecocci, P., Del Zompo, M., Hampel, H., Pilotto, A., Bullido, M., Panza, F., Caffarra, P., Mayhaus, M., Pichler, S., Gu, W., Riemenschneider, M., Lannfelt, L., Ingelsson, M., Hakonarson, H., Carrasquillo, M. M., Zou, F., Younkin, S. G., Beekly, D., Alvarez, V., Coto, E., Razquin, C., Pastor, P., Mateo, I., Combarros, O., Faber, K. M., Foroud, T. M., Soininen, H., Hiltunen, M., Blacker, D., Mosley, T. H., Graff, C., Holmes, C., Montine, T. J., Rotter, J. I., Brice, A., Nalls, M. A., Kauwe, J. S. K., Boerwinkle, E., Schmidt, R., Rujescu, D., Tzourio, C., Nöthen, M. M., Launer, L. J., and Seshadri, S. (2013). Meta-analysis of 74,046 individuals identifies 11 new susceptibility loci for Alzheimer's disease. *Nat. Genet.* 45, 1452–1458.

Lambert, M. P., Barlow, A. K., Chromy, B. A., Edwards, C., Freed, R., Liosatos, M., Morgan, T. E., Rozovsky, I., Trommer, B., Viola, K. L., Wals, P., Zhang, C., Finch, C. E., Krafft, G. A., and Klein, W. L. (1998). Diffusible, nonfibrillar ligands derived from Aβ1-42 are potent central nervous system neurotoxins. *Proc. Natl. Acad. Sci. U. S. A.* 95, 6448–6453.

Lane-Donovan, C., Wong, W. M., Durakoglugil, M. S., Wasser, C. R., Jiang, S., Xian, X., and Herz, J. (2016). Genetic restoration of plasma apoe improves cognition and partially restores synaptic defects in ApoE-deficient mice. *J. Neurosci.* 36, 10141–10150.

Largo-Barrientos, P., Apóstolo, N., Creemers, E., Callaerts-Vegh, Z., Swerts, J., Davies, C., McInnes, J., Wierda, K., De Strooper, B., Spires-Jones, T., de Wit,

J., Uytterhoeven, V., and Verstreken, P. (2021). Lowering Synaptogyrin-3 expression rescues Tau-induced memory defects and synaptic loss in the presence of microglial activation. *Neuron* 109, 767–777.

Larner, A. J. (1997). The Cerebellum in Alzheimer's Disease. *Dement. Geriatr. Cogn. Disord.* 8, 203–209.

Lasagna-Reeves, C. A., Castillo-Carranza, D. L., Sengupta, U., Clos, A. L., Jackson, G. R., and Kayed, R. (2011). Tau oligomers impair memory and induce synaptic and mitochondrial dysfunction in wild-type mice. *Mol. Neurodegener.* 6, 1–14.

Lashley, T., Schott, J. M., Weston, P., Murray, C. E., Wellington, H., Keshavan, A., Foti, S. C., Foiani, M., Toombs, J., Rohrer, J. D., Heslegrave, A., and Zetterberg, H. (2018). Molecular biomarkers of Alzheimer's disease: progress and prospects. *Dis. Model. Mech.* 11, 1–47.

Lau, D. H. W., Paillusson, S., Hartopp, N., Rupawala, H., Mórotz, G. M., Gomez-Suaga, P., Greig, J., Troakes, C., Noble, W., and Miller, C. C. J. (2020). Disruption of endoplasmic reticulum-mitochondria tethering proteins in post-mortem Alzheimer's disease brain. *Neurobiol. Dis.* 143.

Lazarev, V. F., Mikhaylova, E. R., Guzhova, I. V., and Margulis, B. A. (2017). Possible function of molecular chaperones in diseases caused by propagating amyloid aggregates. *Front. Neurosci.* 11, 1–8.

Le, R., Cruz, L., Urbanc, B., Knowles, R. B., Hsiao-Ashe, K., Duff, K., Irizarry, M. C., Stanley, H. E., and Hyman, B. T. (2001). Plaque-Induced Abnormalities in Neurite Geometry in Transgenic Models of Alzheimer Disease: Implications for Neural System Disruption. *J. Neuropathol. Exp. Neurol.* 60, 753–758.

Lee, E. B., Leng, L. Z., Zhang, B., Kwong, L., Trojanowski, J. Q., Abel, T., and Lee, V. M.-Y. (2006). Targeting Amyloid-β Peptide (Aβ) Oligomers by Passive Immunization with a Conformation-selective Monoclonal Antibody Improves Learning and Memory in Aβ Precursor Protein (APP) Transgenic Mice *. *J. Biol. Chem.* 281, 4292–4299.

Lee, G., Thangavel, R., Sharma, V. M., Litersky, J. M., Bhaskar, K., Fang, S. M., Do, L. H., Andreadis, A., Van Hoesen, G., and Ksiezak-Reding, H. (2004). Phosphorylation of Tau by Fyn: Implications for Alzheimer's Disease. *J. Neurosci.* 24, 2304–2312.

Lee, J. G., Takahama, S., Zhang, G., Tomarev, S. I., and Ye, Y. (2016). Unconventional secretion of misfolded proteins promotes adaptation to proteasome dysfunction in mammalian cells. *Nat. Cell Biol.* 18, 765–776.

Lee, J., Xu, Y., Zhang, T., Cui, L., Saidi, L., and Ye, Y. (2018). Secretion of

misfolded cytosolic proteins from mammalian cells is independent of chaperone-mediated autophagy. *J. Biol. Chem.* 293, 14359–14370.

Lee, K. J., Moussa, C. E. H., Lee, Y., Sung, Y., Howell, B. W., Turner, R. S., Pak, D. T. S., and Hoe, H. S. (2010). Beta amyloid-independent role of amyloid precursor protein in generation and maintenance of dendritic spines. *Neuroscience* 169, 344–356.

Lee, V. M. Y., Balin, B. J., Otvos, L., and Trojanowski, J. Q. (1991). A68: A major subunit of paired helical filaments and derivatized forms of normal tau. *Science (80-.).* 251, 675–678.

Lemere, C. A., Blusztajn, J. K., Yamaguchi, H., Wisniewski, T., Saido, T. C., and Selkoe, D. J. (1996). Sequence of deposition of heterogeneous amyloid β-peptides and APO E in down syndrome: Implications for initial events in amyloid plaque formation. *Neurobiol. Dis.* 3, 16–32.

Lemonidis, K., Sanchez-Perez, M. C., and Chamberlain, L. H. (2015). Identification of a novel sequence motif recognized by the ankyrin repeat domain of zDHHC17/13 S-acyltransferases. *J. Biol. Chem.* 290, 21939–21950.

Leveque, C., Pupier, S., Marqueze, B., Geslin, L., Kataoka, M., Takahashi, M., De Waard, M., and Seagar, M. (1998). Interaction of cysteine string proteins with the α1A Subunit of the P/Q-type calcium channel. *J. Biol. Chem.* 273, 13488–13492.

Levy-Lahad, E., Wasco, W., Poorkaj, P., Romano, D. M., Oshima, J., Pettingell, W. H., Yu, C. E., Jondro, P. D., Schmidt, S. D., Wang, K., Crowley, A. C., Fu, Y. H., Guenette, S. Y., Galas, D., Nemens, E., Wijsman, E. M., Bird, T. D., Schellenberg, G. D., and Tanzi, R. E. (1995). Candidate gene for the chromosome 1 familial Alzheimer's disease locus. *Science (80-.).* 269, 973–977.

Lewis, J., McGowan, E., Rockwood, J., Melrose, H., Nacharaju, P., Van Slegtenhorst, M., Gwinn-Hardy, K., Murphy, M. P., Baker, M., Yu, X., Duff, K., Hardy, J., Corral, A., Lin, W. L., Yen, S. H., Dickson, D. W., Davies, P., and Hutton, M. (2000). Neurofibrillary tangles, amyotrophy and progressive motor disturbance in mice expressing mutant (P301L)tau protein. *Nat. Genet.* 25, 402–405.

Li, J. M., Xue, Z. Q., Deng, S. H., Luo, X. G., Patrylo, P. R., Rose, G. W., Cai, H., Cai, Y., and Yan, X. X. (2013). Amyloid plaque pathogenesis in 5XFAD mouse spinal cord: Retrograde transneuronal modulation after peripheral nerve injury. *Neurotox. Res.* 24, 1–14.

Li, J. Z., Vawter, M. P., Walsh, D. M., Tomita, H., Evans, S. J., Choudary, P. V.,

Lopez, J. F., Avelar, A., Shokoohi, V., Chung, T., Mesarwi, O., Jones, E. G., Watson, S. J., Akil, H., Bunney, W. E., and Myers, R. M. (2004). Systematic changes in gene expression in postmortem human brains associated with tissue pH and terminal medical conditions. *Hum. Mol. Genet.* 13, 609–616.

Li, S., Cai, Z., Wu, X., Holden, D., Pracitto, R., Kapinos, M., Gao, H., Labaree, D., Nabulsi, N., Carson, R. E., and Huang, Y. (2019). Synthesis and in Vivo Evaluation of a Novel PET Radiotracer for Imaging of Synaptic Vesicle Glycoprotein 2A (SV2A) in Nonhuman Primates. *ACS Chem. Neurosci.* 10, 1544–1554.

Li, S., Hong, S., Shepardson, N. E., Walsh, D. M., Shankar, G. M., and Selkoe, D. (2009). Soluble Oligomers of Amyloid β Protein Facilitate Hippocampal Long-Term Depression by Disrupting Neuronal Glutamate Uptake. *Neuron* 62, 788–801.

Li, S., Jin, M., Koeglsperger, T., Shepardson, N. E., Shankar, G. M., and Selkoe, D. J. (2011). Soluble a β oligomers inhibit long-term potentiation through a mechanism involving excessive activation of extrasynaptic NR2B-containing NMDA receptors. *J. Neurosci.* 31, 6627–6638.

Li, Z., Jo, J., Jia, J. M., Lo, S. C., Whitcomb, D. J., Jiao, S., Cho, K., and Sheng, M. (2010). Caspase-3 activation via mitochondria is required for long-term depression and AMPA receptor internalization. *Cell* 141, 859–871.

Li, Z., Shue, F., Zhao, N., Shinohara, M., and Bu, G. (2020). APOE2: protective mechanism and therapeutic implications for Alzheimer's disease. *Mol. Neurodegener.* 15, 63.

Liao, L., Cheng, D., Wang, J., Duong, D. M., Losik, T. G., Gearing, M., Rees, H. D., Lah, J. J., Levey, A. I., and Peng, J. (2004). Proteomic characterization of postmortem amyloid plaques isolated by laser capture microdissection. *J. Biol. Chem.* 279, 37061–37068.

Liebsch, F., Kulic, L., Teunissen, C., Shobo, A., Ulku, I., Engelschalt, V., Hancock, M. A., van der Flier, W. M., Kunach, P., Rosa-Neto, P., Scheltens, P., Poirier, J., Saftig, P., Bateman, R. J., Breitner, J., Hock, C., and Multhaup, G. (2019). Aβ34 is a BACE1-derived degradation intermediate associated with amyloid clearance and Alzheimer's disease progression. *Nat. Commun.* 10, 1–15.

Linden, D. J., and Ahn, S. (1999). Activation of presynaptic cAMP-dependent protein kinase is required for induction of cerebellar long-term potentiation. *J. Neurosci.* 19, 10221–10227.

Lisman, J. (2017). Criteria for identifying the molecular basis of the engram (CaMKII, PKMzeta). *Mol. Brain* 10, 1–10.

Litvinchuk, A., Wan, Y. W., Swartzlander, D. B., Chen, F., Cole, A., Propson, N. E., Wang, Q., Zhang, B., Liu, Z., and Zheng, H. (2018). Complement C3aR Inactivation Attenuates Tau Pathology and Reverses an Immune Network Deregulated in Tauopathy Models and Alzheimer's Disease. *Neuron* 100, 1337–1353.

Liu, A. K. L., Hurry, M. E. D., Ng, O. T. W., DeFelice, J., Lai, H. M., Pearce, R. K. B., Wong, G. T. C., Chang, R. C. C., and Gentleman, S. M. (2016). Bringing CLARITY to the human brain: visualization of Lewy pathology in three dimensions. *Neuropathol. Appl. Neurobiol.* 42, 573–587.

Liu, C. C., Zhao, N., Fu, Y., Wang, N., Linares, C., Tsai, C. W., and Bu, G. (2017). ApoE4 Accelerates Early Seeding of Amyloid Pathology. *Neuron* 96, 1024–1032.

Liu, F., Grundke-Iqbal, I., Iqbal, K., and Gong, C. X. (2005). Contributions of protein phosphatases PP1, PP2A, PP2B and PP5 to the regulation of tau phosphorylation. *Eur. J. Neurosci.* 22, 1942–1950.

Liu, L., Drouet, V., Wu, J. W., Witter, M. P., Small, S. A., Clelland, C., and Duff, K. (2012). Trans-synaptic spread of tau pathology in vivo. *PLoS One* 7, 1–9.

Liu, X., and Brum, A. (1996). Regional and laminar synaptic pathology in frontal lobe degeneration of non-Alzheimer type. *Int. J. Geriatr. Psychiatry* 11, 47–55.

Liu, X., and Brun, A. (1995). Synaptophysin immunoveactivity is stable 36 h postmortem. *Dementia* 6, 211–217.

Liu, X., Passant, U., Risberg, J., Warkentin, S., and Brun, A. (1999). Synapse density related to cerebral blood flow and symptomatology in frontal lobe degeneration and Alzheimer's disease. *Dement. Geriatr. Cogn. Disord.* 10, 64–70.

Lo, C.-A., Kays, I., Emran, F., Lin, T.-J., Cvetkovska, V., and Chen, B. E. (2015). Quantification of Protein Levels in Single Living Cells. *Cell Rep.* 13, 2634–2644.

Löffler, J., and Huber, G. (1992). β-Amyloid Precursor Protein Isoforms in Various Rat Brain Regions and During Brain Development. *J. Neurochem.* 59, 1316–1324.

Lomen-Hoerth, C., Anderson, T., and Miller, B. (2002). The overlap of amyotrophic lateral sclerosis and frontotemporal dementia. *Neurology* 59, 1077–1079.

Lopez-Ortega, E., Ruiz, R., and Tabares, L. (2017). CSPα, a Molecular Co-chaperone Essential for Short and Long-Term Synaptic Maintenance. *Front. Neurosci.* 11, 1–6.

Lopez Sanchez, M. I. G., Wijngaarden, P., and Trounce, I. A. (2019). Amyloid

precursor protein-mediated mitochondrial regulation and Alzheimer's disease. *Br. J. Pharmacol.* 176, 3464–3474.

Louis, J. V., Martens, E., Borghgraef, P., Lambrecht, C., Sents, W., Longin, S., Zwaenepoel, K., Pijnenborg, R., Landrieu, I., Lippens, G., Ledermann, B., Götz, J., Van Leuven, F., Goris, J., and Janssens, V. (2011). Mice lacking phosphatase PP2A subunit PR61/B′δ (Ppp2r5d) develop spatially restricted tauopathy by deregulation of CDK5 and GSK3β. *Proc. Natl. Acad. Sci. U. S. A.* 108, 6957–6962.

Love, S., Siew, L. K., Dawbarn, D., Wilcock, G. K., Ben-Shlomo, Y., and Allen, S. J. (2006). Premorbid effects of APOE on synaptic proteins in human temporal neocortex. *Neurobiol. Aging* 27, 797–803.

Lovestone, S., Hartley, C. L., Pearce, J., and Anderton, B. H. (1996). Phosphorylation of tau by glycogen synthase kinase-3β in intact mammalian cells: The effects on the organization and stability of microtubules. *Neuroscience* 73, 1145–1157.

Lovestone, S., Reynolds, C. H., Latimer, D., Davis, D. R., Anderton, B. H., Gallo, J. M., Hanger, D., Mulot, S., Marquardt, B., Stabel, S., Woodgett, J. R., and Miller, C. C. J. (1994). Alzheimer's disease-like phosphorylation of the microtubule-associated protein tau by glycogen synthase kinase-3 in transfected mammalian cells. *Curr. Biol.* 4, 1077–1086.

Lowe, V. J., Wiste, H. J., Senjem, M. L., Weigand, S. D., Therneau, T. M., Boeve, B. F., Josephs, K. A., Fang, P., Pandey, M. K., Murray, M. E., Kantarci, K., Jones, D. T., Vemuri, P., Graff-Radford, J., Schwarz, C. G., Machulda, M. M., Mielke, M. M., Roberts, R. O., Knopman, D. S., Petersen, R. C., and Jack, C. R. (2018). Widespread brain tau and its association with ageing, Braak stage and Alzheimer's dementia. *Brain* 141, 271–287.

Lue, L. F., Kuo, Y. M., Roher, A. E., Brachova, L., Shen, Y., Sue, L., Beach, T., Kurth, J. H., Rydel, R. E., and Rogers, J. (1999). Soluble amyloid β peptide concentration as a predictor of synaptic change in Alzheimer's disease. *Am. J. Pathol.* 155, 853–862.

Maas, T., Eidenmüller, J., and Brandt, R. (2000). Interaction of tau with the neural membrane cortex is regulated by phosphorylation at sites that are modified in paired helical filaments. *J. Biol. Chem.* 275, 15733–15740.

Mackenzie, I. R. A., and Neumann, M. (2016). Molecular neuropathology of frontotemporal dementia: insights into disease mechanisms from postmortem studies. *J. Neurochem.* 138, 54–70.

Mackenzie, I. R. A., Neumann, M., Baborie, A., Sampathu, D. M., Du Plessis, D.,

Jaros, E., Perry, R. H., Trojanowski, J. Q., Mann, D. M. A., and Lee, V. M. Y. (2011). A harmonized classification system for FTLD-TDP pathology. *Acta Neuropathol.* 122, 111–113.

Mackenzie, I. R. A., Neumann, M., Bigio, E. H., Cairns, N. J., Alafuzoff, I., Kril, J., Kovacs, G. G., Ghetti, B., Halliday, G., Holm, I. E., Ince, P. G., Kamphorst, W., Revesz, T., Rozemuller, A. J. M., Kumar-Singh, S., Akiyama, H., Baborie, A., Spina, S., Dickson, D. W., Trojanowski, J. Q., and Mann, D. M. A. (2009). Nomenclature for neuropathologic subtypes of frontotemporal lobar degeneration: Consensus recommendations. *Acta Neuropathol.* 117, 15–18.

Magga, J. M., Jarvis, S. E., Arnot, M. I., Zamponi, G. W., and Braun, J. E. A. (2000). Cysteine string protein regulates G protein modulation of N-type calcium channels. *Neuron* 28, 195–204.

Mahley, R. W., Weisgraber, K. H., and Huang, Y. (2006). Apolipoprotein E4: A causative factor and therapeutic target in neuropathology, including Alzheimer's disease. *Proc. Natl. Acad. Sci. U. S. A.* 103, 5644–5651.

Mairet-Coello, G., Courchet, J., Pieraut, S., Courchet, V., Maximov, A., and Polleux, F. (2013). The CAMKK2-AMPK Kinase Pathway Mediates the Synaptotoxic Effects of Aβ Oligomers through Tau Phosphorylation. *Neuron* 78, 94–108.

Mandelkow, E. M., Biernat, J., Drewes, G., Gustke, N., Trinczek, B., and Mandelkow, E. (1995). Tau domains, phosphorylation, and interactions with microtubules. *Neurobiol. Aging* 16, 355–362.

Mandelkow, E. M., and Mandelkow, E. (1998). Tau in Alzheimer's disease. *Trends Cell Biol.* 8, 425–427.

Mandelkow, E. M., Stamer, K., Vogel, R., Thies, E., and Mandelkow, E. (2003). Clogging of axons by tau, inhibition of axonal traffic and starvation of synapses. *Neurobiol. Aging* 24, 1079–1085.

Mandybur, T. I., and Chuirazzi, C. C. (1990). Astrocytes and the plaques of alzheimer's disease. *Neurology* 40, 635–639.

Mannini, B., and Chiti, F. (2017). Chaperones as suppressors of protein misfolded oligomer toxicity. *Front. Mol. Neurosci.* 10, 1–8.

Månsson, C., Kakkar, V., Monsellier, E., Sourigues, Y., Härmark, J., Kampinga, H. H., Melki, R., and Emanuelsson, C. (2014). DNAJB6 is a peptide-binding chaperone which can suppress amyloid fibrillation of polyglutamine peptides at substoichiometric molar ratios. *Cell Stress Chaperones* 19, 227–239.

Marsh, J., and Alifragis, P. (2018). Synaptic dysfunction in Alzheimer's disease: The effects of amyloid beta on synaptic vesicle dynamics as a novel target for therapeutic intervention. *Neural Regen. Res.* 13, 616–623.

Marshall, K. E., Vadukul, D. M., Staras, K., and Serpell, L. C. (2020). Misfolded amyloid-β-42 impairs the endosomal–lysosomal pathway. *Cell. Mol. Life Sci.* 77, 5031–5043.

Martin, L., Latypova, X., Wilson, C. M., Magnaudeix, A., Perrin, M. L., Yardin, C., and Terro, F. (2013). Tau protein kinases: Involvement in Alzheimer's disease. *Ageing Res. Rev.* 12, 289–309.

Masliah, E., Mallory, M., Alford, M., DeTeresa, R., Hansen, L. A., McKeel, D. W., and Morris, J. C. (2001). Altered expression of synaptic proteins occurs early during progression of Alzheimer's disease. *Neurology* 56, 127–129.

Masliah, E., Mallory, M., Deerinck, T., Deteresa, R., Lamont, S., Miller, A., Terry, R. D., Carragher, B., and Ellisman, M. (1993). Re-evaluation of the structural organization of neuritic plaques in alzheimer's disease. *J. Neuropathol. Exp. Neurol.* 52, 619–632.

Masliah, E., Mallory, M., Hansen, L., Alford, M., Albright, T., DeTeresa, R., Terry, R., Baudier, J., and Saitoh, T. (1991). Patterns of aberrant sprouting in alzheimer's disease. *Neuron* 6, 729–739.

Masliah, E., Mallory, M., Hansen, L., Richard, D. T., Alford, M., and Terry, R. (1994). Synaptic and neuritic alterations during the progression of Alzheimer's disease. *Neurosci. Lett.* 174, 67–72.

Masliah, E., Terry, R. D., Mallory, M., Alford, M., and Hansen, L. A. (1990). Diffuse plaques do not accentuate synapse loss in Alzheimer's disease. *Am. J. Pathol.* 137, 1293–1297.

Mastrogiacomo, A., and Gundersen, C. B. (1995). The nucleotide and deduced amino acid sequence of a rat cysteine string protein. *Mol. Brain Res.* 28, 12–18.

Mastrogiacomo, A., Kornblum, H. I., Umbach, J. A., and Gundersen, C. B. (1998). A Xenopus cysteine string protein with a cysteine residue in the J domain. *Biochim. Biophys. Acta - Mol. Cell Res.* 1401, 239–241.

Mastrogiacomo, A., Parsons, S. M., Zampighi, G. A., Jenden, D. J., Umbach, J. A., and Gundersen, C. B. (1994). Cysteine string proteins: A potential link between synaptic vesicles and presynaptic Ca2+ channels. *Science (80-.).* 263, 981–982.

Matej, R., Tesar, A., and Rusina, R. (2019). Alzheimer's disease and other neurodegenerative dementias in comorbidity: A clinical and neuropathological overview. *Clin. Biochem.* 73, 26–31.

Mattson, M. P., Cheng, B., Davis, D., Bryant, K., Lieberburg, I., and Rydel, R. E. (1992). β-Amyloid peptides destabilize calcium homeostasis and render human

cortical neurons vulnerable to excitotoxicity. *J. Neurosci.* 12, 376–389.

Mattsson-Carlgren, N., Andersson, E., Janelidze, S., Ossenkoppele, R., Insel, P., Strandberg, O., Zetterberg, H., Rosen, H. J., Rabinovici, G., Chai, X., Blennow, K., Dage, J. L., Stomrud, E., Smith, R., Palmqvist, S., and Hansson, O. (2020). Aβ deposition is associated with increases in soluble and phosphorylated tau that precede a positive Tau PET in Alzheimer's disease. *Sci. Adv.* 6, 1–14.

McAleese, K. E., Walker, L., Erskine, D., Thomas, A. J., McKeith, I. G., and Attems, J. (2017). TDP-43 pathology in Alzheimer's disease, dementia with Lewy bodies and ageing. *Brain Pathol.* 27, 472–479.

McDonald, J. M., Cairns, N. J., Taylor-Reinwald, L., Holtzman, D., and Walsh, D. M. (2012). The levels of water-soluble and triton-soluble Aβ are increased in Alzheimer's disease brain. *Brain Res.* 1450, 138–147.

McInnes, J., Wierda, K., Snellinx, A., Bounti, L., Wang, Y. C., Stancu, I. C., Apóstolo, N., Gevaert, K., Dewachter, I., Spires-Jones, T. L., De Strooper, B., De Wit, J., Zhou, L., and Verstreken, P. (2018). Synaptogyrin-3 Mediates Presynaptic Dysfunction Induced by Tau. *Neuron* 97, 823–835.

McKeith, I. G., Galasko, D., Kosaka, K., Perry, E. K., Dickson, D. W., Hansen, L. A., Salmon, D. P., Lowe, J., Mirra, S. S., Byrne, E. J., Lennox, G., Quinn, N. P., Edwardson, J. A., Ince, P. G., Bergeron, C., Burns, A., Miller, B. L., Lovestone, S., Collerton, D., Jansen, E. N., Ballard, C., de Vos, R. A., Wilcock, G. K., Jellinger, K. A., and Perry, R. H. (1996). Consensus guidelines for the clinical and pathologic diagnosis of dementia with Lewy bodies (DLB): report of the consortium on DLB international workshop. *Neurology* 47, 1113–1124.

McKhann, G. M., Knopman, D. S., Chertkow, H., Hyman, B. T., Jack Jr, C. R., Kawas, C. H., Klunk, W. E., Koroshetz, W. J., Manly, J. J., Mayeux, R., Mohs, R. C., Morris, J. C., Rossor, M. N., Scheltens, P., Carrillo, M. C., Thies, B., Weintraub, S., and Phelps, C. H. (2011). The diagnosis of dementia due to Alzheimer's disease: recommendations from the National Institute on Aging-Alzheimer's Association workgroups on diagnostic guidelines for Alzheimer's disease. *Alzheimers. Dement.* 7, 263–269.

McLean, C. A., Cherny, R. A., Fraser, F. W., Fuller, S. J., Smith, M. J., Beyreuther, K., Bush, A. I., and Masters, C. L. (1999). Soluble pool of Aβ amyloid as a determinant of severity of neurodegeneration in Alzheimer's disease. *Ann. Neurol.* 46, 860–866.

Mead, S., James-Galton, M., Revesz, T., Doshi, R. B., Harwood, G., Pan, E. L., Ghiso, J., Frangione, B., and Plant, G. (2000). Familial British dementia with amyloid angiopathy: Early clinical, neuropsychological and imaging findings.

Brain 123, 975–991.

Medina, M., and Avila, J. (2014). The role of extracellular Tau in the spreading of neurofibrillary pathology. *Front. Cell. Neurosci.* 8, 1–7.

Menkes-Caspi, N., Yamin, H. G., Kellner, V., Spires-Jones, T. L., Cohen, D., and Stern, E. A. (2015). Pathological tau disrupts ongoing network activity. *Neuron* 85, 959–966.

Merezhko, M., Uronen, R. L., and Huttunen, H. J. (2020). The Cell Biology of Tau Secretion. *Front. Mol. Neurosci.* 13, 1–20.

Metaxas, A., Thygesen, C., Kempf, S. J., Anzalone, M., Vaitheeswaran, R., Petersen, S., Landau, A. M., Audrain, H., Teeling, J. L., Darvesh, S., Brooks, D. J., Larsen, M. R., and Finsen, B. (2018). Tauopathy in the APPswe/PS1ΔE9 mouse model of familial Alzheimer's disease. *bioRxiv*. doi:10.1101/405647.

Micheva, K. D., Busse, B., Weiler, N. C., O'Rourke, N., and Smith, S. J. (2010). Single-synapse analysis of a diverse synapse population: Proteomic imaging methods and markers. *Neuron* 68, 639–653.

Miller, E. C., Teravskis, P. J., Dummer, B. W., Zhao, X., Huganir, R. L., and Liao, D. (2014). Tau phosphorylation and tau mislocalization mediate soluble Aβ oligomer-induced AMPA glutamate receptor signaling deficits. *Eur. J. Neurosci.* 39, 1214–1224.

Miller, L. C., Swayne, L. A., Chen, L., Feng, Z. P., Wacker, J. L., Muchowski, P. J., Zamponi, G. W., and Braun, J. E. A. (2003). Cysteine String Protein (CSP) Inhibition of N-type Calcium Channels Is Blocked by Mutant Huntingtin. *J. Biol. Chem.* 278, 53072–53081.

Miners, J. S., Barua, N., Kehoe, P. G., Gill, S., and Love, S. (2011). Aβ-degrading enzymes: Potential for treatment of alzheimer disease. *J. Neuropathol. Exp. Neurol.* 70, 944–959.

Miners, J. S., Palmer, J. C., Tayler, H., Palmer, L. E., Ashby, E., Kehoe, P. G., and Love, S. (2014). Aβ degradation or cerebral perfusion? Divergent effects of multifunctional enzymes. *Front. Aging Neurosci.* 6, 1–13.

Mirra, S. S., Heyman, A., McKeel, D., Sumi, S. M., Crain, B. J., Brownlee, L. M., Vogel, F. S., Hughes, J. P., van Belle, G., Berg, L., Ball, M. J., Bierer, L. M., Claasen, D., Hansen, L. R., Hart, M., Hedreen, J., Baltimore, B., Hen Derson, V., Hyman, B. T., Joachim, C., Mark-Esbery, W., Mar Tinez, A. J., McKee, A., Miller, C., Moossy, J., Nochlin, D., Perl, D., Petito, C., Rao, G. R., Schelper, R. L., Slager, U., and Terry, R. D. (1991). The consortium to establish a registry for Alzheimer's disease (CERAD). Part II. Standardization of the neuropathologic assessment of Alzheimer's disease. *Neurology* 41, 479–486.

Mitchison, T., and Kirschner, M. (1984). Dynamic instability of microtubule growth. *Nature* 312, 237–242.

Moechars, D., Lorent, K., De Strooper, B., Dewachter, I., and Van Leuven, F. (1996). Expression in brain of amyloid precursor protein mutated in the α-secretase site causes disturbed behavior, neuronal degeneration and premature death in transgenic mice. *EMBO J.* 15, 1265–1274.

Moghekar, A., Rao, S., Li, M., Ruben, D., Mammen, A., Tang, X., and O'Brien, R. J. (2011). Large quantities of Aβ peptide are constitutively released during amyloid precursor protein metabolism in vivo and in vitro. *J. Biol. Chem.* 286, 15989–15997.

Monoranu, C. M., Apfelbacher, M., Grünblatt, E., Puppe, B., Alafuzoff, I., Ferrer, I., Al-Saraj, S., Keyvani, K., Schmitt, A., Falkai, P., Schittenhelm, J., Halliday, G., Kril, J., Harper, C., McLean, C., Riederer, P., and Roggendorf, W. (2009). PH measurement as quality control on human post mortem brain tissue: A study of the BrainNet Europe consortium. *Neuropathol. Appl. Neurobiol.* 35, 329–337.

Montagne, A., Nation, D. A., Sagare, A. P., Barisano, G., Sweeney, M. D., Chakhoyan, A., Pachicano, M., Joe, E., Nelson, A. R., D'Orazio, L. M., Buennagel, D. P., Harrington, M. G., Benzinger, T. L. S., Fagan, A. M., Ringman, J. M., Schneider, L. S., Morris, J. C., Reiman, E. M., Caselli, R. J., Chui, H. C., Tcw, J., Chen, Y., Pa, J., Conti, P. S., Law, M., Toga, A. W., and Zlokovic, B. V. (2020). APOE4 leads to blood–brain barrier dysfunction predicting cognitive decline. *Nature* 581, 71–76.

Montine, T. J., Phelps, C. H., Beach, T. G., Bigio, E. H., Cairns, N. J., Dickson, D. W., Duyckaerts, C., Frosch, M. P., Masliah, E., Mirra, S. S., Nelson, P. T., Schneider, J. A., Thal, D. R., Trojanowski, J. Q., Vinters, H. V., and Hyman, B. T. (2012). National institute on aging-Alzheimer's association guidelines for the neuropathologic assessment of Alzheimer's disease: A practical approach. *Acta Neuropathol.* 123, 1–11.

Moreno, H., Choi, S., Yu, E., Brusco, J., Avila, J., Moreira, J. E., Sugimori, M., and Llinás, R. R. (2011). Blocking effects of human tau on squid giant synapse transmission and its prevention by T-817 MA. *Front. Synaptic Neurosci.* 3, 1–8.

Morishima-Kawashima, M. (2014). Molecular mechanism of the intramembrane cleavage of the β-carboxyl terminal fragment of amyloid precursor protein by γ-Secretase. *Front. Physiol.* 5, 1–7.

Muchowski, P. J., Schaffar, G., Sittler, A., Wanker, E. E., Hayer-Hartl, M. K., and Hartl, F. U. (2000). Hsp70 and Hsp40 chaperones can inhibit self-assembly of polyglutamine proteins into amyloid-like fibrils. *Proc. Natl. Acad. Sci. U. S. A.*

97, 7841–7846.

Mucke, L., and Selkoe, D. J. (2012). Neurotoxicity of amyloid β-protein: Synaptic and network dysfunction. *Cold Spring Harb. Perspect. Med.* 2, 1–18.

Mudher, A., Shepherd, D., Newman, T. A., Mildren, P., Jukes, J. P., Squire, A., Mears, A., Berg, S., MacKay, D., Asuni, A. A., Bhat, R., and Lovestone, S. (2004). GSK-3β inhibition reverses axonal transport defects and behavioural phenotypes in Drosophila. *Mol. Psychiatry* 9, 522–530.

Mukaetova-Ladinska, E. B., Garcia-Siera, F., Hurt, J., Gertz, H. J., Xuereb, J. H., Hills, R., Brayne, C., Huppert, F. A., Paykel, E. S., McGee, M., Jakes, R., Honer, W. G., Harrington, C. R., and Wischik, C. M. (2000). Staging of cytoskeletal and β-amyloid changes in human isocortex reveals biphasic synaptic protein response during progression of Alzheimer's disease. *Am. J. Pathol.* 157, 623–636.

Mukherjee, A. B., Appu, A. P., Sadhukhan, T., Casey, S., Mondal, A., Zhang, Z., and Bagh, M. B. (2019). Emerging new roles of the lysosome and neuronal ceroid lipofuscinoses. *Mol. Neurodegener.* 14, 1–23.

Mullan, M., Crawford, F., Axelman, K., Houlden, H., Lilius, L., Winblad, B., and Lannfelt, L. (1992). A pathogenic mutation for probable Alzheimer's disease in the APP gene at the N–terminus of β–amyloid. *Nat. Genet.* 1, 345–347.

Müller, U. C., Deller, T., and Korte, M. (2017). Not just amyloid: Physiological functions of the amyloid precursor protein family. *Nat. Rev. Neurosci.* 18, 281–298.

Murray, M. E., Graff-Radford, N. R., Ross, O. A., Petersen, R. C., Duara, R., and Dickson, D. W. (2011). Neuropathologically defined subtypes of Alzheimer's disease with distinct clinical characteristics: a retrospective study. *Lancet Neurol.* 10, 785–796.

Murrell, J., Farlow, M., Ghetti, B., and Benson, M. D. (1991). A mutation in the amyloid precursor protein associated with hereditary Alzheimer's disease. *Science (80-.).* 254, 97–99.

Nagy, Z. S., Esiri, M. M., Jobst, K. A., Johnston, C., Litchfield, S., Sim, E., and Smith, A. D. (1995). Influence of the apolipoprotein E genotype on amyloid deposition and neurofibrillary tangle formation in Alzheimer's disease. *Neuroscience* 69, 757–761.

Nakashima-Yasuda, H., Uryu, K., Robinson, J., Xie, S. X., Hurtig, H., Duda, J. E., Arnold, S. E., Siderowf, A., Grossman, M., Leverenz, J. B., Woltjer, R., Lopez, O. L., Hamilton, R., Tsuang, D. W., Galasko, D., Masliah, E., Kaye, J., Clark, C. M., Montine, T. J., Lee, V. M. Y., and Trojanowski, J. Q. (2007). Co-

morbidity of TDP-43 proteinopathy in Lewy body related diseases. *Acta Neuropathol.* 114, 221–229.

Narasimhan, S., Guo, J. L., Changolkar, L., Stieber, A., McBride, J. D., Silva, L. V., He, Z., Zhang, B., Gathagan, R. J., Trojanowski, J. Q., and Lee, V. M. Y. (2017). Pathological tau strains from human brains recapitulate the diversity of tauopathies in nontransgenic mouse brain. *J. Neurosci.* 37, 11406–11423.

Naseri, N. N., Ergel, B., Kharel, P., Na, Y., Huang, Q., Huang, R., Dolzhanskaya, N., Burré, J., Velinov, M. T., and Sharma, M. (2020a). Aggregation of mutant cysteine string protein-α via Fe–S cluster binding is mitigated by iron chelators. *Nat. Struct. Mol. Biol.* 27, 192–201.

Naseri, N., Sharma, M., and Velinov, M. (2020b). Autosomal dominant neuronal ceroid lipofuscinosis: Clinical features and molecular basis. *Clin. Genet.*, 1–8.

Neuman, K. M., Molina-Campos, E., Musial, T. F., Price, A. L., Oh, K. J., Wolke, M. L., Buss, E. W., Scheff, S. W., Mufson, E. J., and Nicholson, D. A. (2015). Evidence for Alzheimer's disease-linked synapse loss and compensation in mouse and human hippocampal CA1 pyramidal neurons. *Brain Struct. Funct.* 220, 3143–3165.

Neumann, M., Kwong, L. K., Sampathu, D. M., Trojanowski, J. Q., and Lee, V. M. Y. (2007). TDP-43 proteinopathy in frontotemporal lobar degeneration and amyotrophic lateral sclerosis: Protein misfolding diseases without amyloidosis. *Arch. Neurol.* 64, 1388–1394.

Neumann, M., Sampathu, D. M., Kwong, L. K., Truax, A. C., Micsenyi, M. C., Chou, T. T., Bruce, J., Schuck, T., Grossman, M., Clark, C. M., McCluskey, L. F., Miller, B. L., Masliah, E., Mackenzie, I. R., Feldman, H., Feiden, W., Kretzschmar, H. A., Trojanowski, J. Q., and Lee, V. M. Y. (2006). Ubiquitinated TDP-43 in frontotemporal lobar degeneration and amyotrophic lateral sclerosis. *Science (80-.).* 314, 130–133.

Neve, R. L., Stewart, G. D., Newcomb, P., Van Keuren, M. L., Patterson, D., Drabkin, H. A., and Kurnit, D. M. (1986). Human chromosome 21-encoded cDNA clones. *Gene* 49, 361–369.

Nicoll, J. A. R., Buckland, G. R., Harrison, C. H., Page, A., Harris, S., Love, S., Neal, J. W., Holmes, C., and Boche, D. (2019). Persistent neuropathological effects 14 years following amyloid-β immunization in Alzheimer's disease. *Brain* 142, 2113–2126.

Nieto-González, J. L., Gómez-Sánchez, L., Mavillard, F., Linares-Clemente, P., Rivero, M. C., Valenzuela-Villatoro, M., Muñoz-Bravo, J. L., Pardal, R., and Fernández-Chacón, R. (2019). Loss of postnatal quiescence of neural stem

cells through mTOR activation upon genetic removal of cysteine string protein-α. *Proc. Natl. Acad. Sci. U. S. A.* 116, 8000–8009.

Nizhnikov, A. A., Alexandrov, A. I., Ryzhova, T. A., Mitkevich, O. V., Dergalev, A. A., Ter-Avanesyan, M. D., and Galkin, A. P. (2014). Proteomic screening for amyloid proteins. *PLoS One* 9, 1–18.

Noble, W., Hanger, D. P., Miller, C. C. J., and Lovestone, S. (2013). The importance of tau phosphorylation for neurodegenerative diseases. *Front. Neurol.* 4, 1–11.

Noble, W., Olm, V., Takata, K., Casey, E., Mary, O., Meyerson, J., Gaynor, K., LaFrancois, J., Wang, L., Kondo, T., Davies, P., Burns, M., Veeranna, Nixon, R., Dickson, D., Matsuoka, Y., Ahlijanian, M., Lau, L. F., and Duff, K. (2003). Cdk5 is a key factor in tau aggregation and tangle formation in vivo. *Neuron* 38, 555–565.

Nobuhara, C. K., DeVos, S. L., Commins, C., Wegmann, S., Moore, B. D., Roe, A. D., Costantino, I., Frosch, M. P., Pitstick, R., Carlson, G. A., Hock, C., Nitsch, R. M., Montrasio, F., Grimm, J., Cheung, A. E., Dunah, A. W., Wittmann, M., Bussiere, T., Weinreb, P. H., Hyman, B. T., and Takeda, S. (2017). Tau Antibody Targeting Pathological Species Blocks Neuronal Uptake and Interneuron Propagation of Tau in Vitro. *Am. J. Pathol.* 187, 1399–1412.

Nordstedt, C., Gandy, S. E., Alafuzoff, I., Caporaso, G. L., Iverfeldt, K., Grebb, J. A., Winblad, B., and Greengard, P. (1991). Alzheimer β/A4 amyloid precursor protein in human brain: Aging-associated increases in holoprotein and in a proteolytic fragment. *Proc. Natl. Acad. Sci. U. S. A.* 88, 8910–8914.

Nosková, L., Stránecký, V., Hartmannová, H., Přistoupilová, A., Barešová, V., Ivánek, R., Hlková, H., Jahnová, H., Van Der Zee, J., Staropoli, J. F., Sims, K. B., Tyynelä, J., Van Broeckhoven, C., Nijssen, P. C. G., Mole, S. E., Elleder, M., and Kmoch, S. (2011). Mutations in DNAJC5, encoding cysteine-string protein alpha, cause autosomal-dominant adult-onset neuronal ceroid lipofuscinosis. *Am. J. Hum. Genet.* 89, 241–252.

O'Brien, J. T., Erkinjuntti, T., Reisberg, B., Roman, G., Sawada, T., Pantoni, L., Bowler, J. V., Ballard, C., DeCarli, C., Gorelick, P. B., Rockwood, K., Burns, A., Gauthier, S., and DeKosky, S. T. (2003). Vascular cognitive impairment. *Lancet Neurol.* 2, 89–98.

O'Brien, J. T., and Thomas, A. (2015). Vascular dementia. *Lancet* 386, 1698–1706.

O'Brien, R. J., and Wong, P. C. (2011). Amyloid precursor protein processing and alzheimer's disease. *Annu. Rev. Neurosci.* 34, 185–204.

O'Leary, T. P., Robertson, A., Chipman, P. H., Rafuse, V. F., and Brown, R. E. (2018). Motor function deficits in the 12 month-old female 5xFAD mouse model

of Alzheimer's disease. *Behav. Brain Res.* 337, 256–263.

Oakley, H., Cole, S. L., Logan, S., Maus, E., Shao, P., Craft, J., Guillozet-Bongaarts, A., Ohno, M., Disterhoft, J., Van Eldik, L., Berry, R., and Vassar, R. (2006). Intraneuronal β-amyloid aggregates, neurodegeneration, and neuron loss in transgenic mice with five familial Alzheimer's disease mutations: Potential factors in amyloid plaque formation. *J. Neurosci.* 26, 10129–10140.

Oddo, S., Caccamo, A., Shepherd, J. D., Murphy, M. P., Golde, T. E., Kayed, R., Metherate, R., Mattson, M. P., Akbari, Y., and LaFerla, F. M. (2003). Triple-transgenic model of Alzheimer's Disease with plaques and tangles: Intracellular Aβ and synaptic dysfunction. *Neuron* 39, 409–421.

Ohyama, T., Verstreken, P., Ly, C. V., Rosenmund, T., Rajan, A., Tien, A. C., Haueter, C., Schulze, K. L., and Bellen, H. J. (2007). Huntingtin-interacting protein 14, a palmitoyl transferase required for exocytosis and targeting of CSP to synaptic vesicles. *J. Cell Biol.* 179, 1481–1496.

Oppedal, K., Ferreira, D., Cavallin, L., Lemstra, A. W., ten Kate, M., Padovani, A., Rektorova, I., Bonanni, L., Wahlund, L. O., Engedal, K., Nobili, F., Kramberger, M., Taylor, J. P., Hort, J., Snædal, J., Blanc, F., Walker, Z., Antonini, A., Westman, E., and Aarsland, D. (2019). A signature pattern of cortical atrophy in dementia with Lewy bodies: A study on 333 patients from the European DLB consortium. *Alzheimer's Dement.* 15, 400–409.

Outeiro, T. F., Koss, D. J., Erskine, D., Walker, L., Kurzawa-Akanbi, M., Burn, D., Donaghy, P., Morris, C., Taylor, J. P., Thomas, A., Attems, J., and McKeith, I. (2019). Dementia with Lewy bodies: An update and outlook. *Mol. Neurodegener.* 14, 1–18.

Overk, C. R., and Masliah, E. (2014). Pathogenesis of synaptic degeneration in Alzheimer's disease and Lewy body disease. *Biochem. Pharmacol.* 88, 508–516.

Ovsepian, S. V., O'Leary, V. B., Zaborszky, L., Ntziachristos, V., and Dolly, J. O. (2019). Amyloid Plaques of Alzheimer's Disease as Hotspots of Glutamatergic Activity. *Neuroscientist* 25, 288–297.

Palop, J. J., Chin, J., Roberson, E. D., Wang, J., Thwin, M. T., Bien-Ly, N., Yoo, J., Ho, K. O., Yu, G.-Q., Kreitzer, A., Finkbeiner, S., Noebels, J. L., and Mucke, L. (2007). Aberrant excitatory neuronal activity and compensatory remodeling of inhibitory hippocampal circuits in mouse models of Alzheimer's disease. *Neuron* 55, 697–711.

Palop, J. J., and Mucke, L. (2010). Amyloid-B-induced neuronal dysfunction in Alzheimer's disease: From synapses toward neural networks. *Nat. Neurosci.*

13, 812–818.

Pankiewicz, J. E., Guridi, M., Kim, J., Asuni, A. A., Sanchez, S., Sullivan, P. M., Holtzman, D. M., and Sadowski, M. J. (2014). Blocking the apoE/Aβ interaction ameliorates Aβ-related pathology in APOE ε2 and ε4 targeted replacement Alzheimer model mice. *Acta Neuropathol. Commun.* 2, 1–11.

Parameshwaran, K., Dhanasekaran, M., and Suppiramaniam, V. (2008). Amyloid beta peptides and glutamatergic synaptic dysregulation. *Exp. Neurol.* 210, 7–13.

Park, G., Nhan, H. S., Tyan, S. H., Kawakatsu, Y., Zhang, C., Navarro, M., and Koo, E. H. (2020). Caspase Activation and Caspase-Mediated Cleavage of APP Is Associated with Amyloid β-Protein-Induced Synapse Loss in Alzheimer's Disease. *Cell Rep.* 31, 1–18.

Park, J., Fang, S., Crews, A. L., Lin, K. W., and Adler, K. B. (2008). MARCKS regulation of mucin secretion by airway epithelium in vitro: Interaction with chaperones. *Am. J. Respir. Cell Mol. Biol.* 39, 68–76.

Parodi, J., Sepúlveda, F. J., Roa, J., Opazo, C., Inestrosa, N. C., and Aguayo, L. G. (2010). β-amyloid causes depletion of synaptic vesicles leading to neurotransmission failure. *J. Biol. Chem.* 285, 2506–2514.

Paschkowsky, S., Hsiao, J. M., Young, J. C., and Munter, L. M. (2019). The discovery of proteases and intramembrane proteolysis. *Biochem. Cell Biol.* 97, 265–269.

Patel, P., Prescott, G. R., Burgoyne, R. D., Lian, L. Y., and Morgan, A. (2016). Phosphorylation of Cysteine String Protein Triggers a Major Conformational Switch. *Structure* 24, 1380–1386.

Patterson, C. (2018). World Alzheimer Report 2018 - The state of the art of dementia research: New frontiers.

Paula-Lima, A. C., Brito-Moreira, J., and Ferreira, S. T. (2013). Deregulation of excitatory neurotransmission underlying synapse failure in Alzheimer's disease. *J. Neurochem.* 126, 191–202.

Peng, C., Gathagan, R. J., Covell, D. J., Medellin, C., Stieber, A., Robinson, J. L., Zhang, B., Pitkin, R. M., Olufemi, M. F., Luk, K. C., Trojanowski, J. Q., and Lee, V. M. Y. (2018). Cellular milieu imparts distinct pathological α-synuclein strains in α-synucleinopathies. *Nature* 557, 558–563.

Perez-Nievas, B. G., Stein, T. D., Tai, H. C., Dols-Icardo, O., Scotton, T. C., Barroeta-Espar, I., Fernandez-Carballo, L., De Munain, E. L., Perez, J., Marquie, M., Serrano-Pozo, A., Frosch, M. P., Lowe, V., Parisi, J. E., Petersen, R. C., Ikonomovic, M. D., López, O. L., Klunk, W., Hyman, B. T., and Gómez-

Isla, T. (2013). Dissecting phenotypic traits linked to human resilience to Alzheimer's pathology. *Brain* 136, 2510–2526.

Perl, D. P. (2010). Neuropathology of Alzheimer's disease. *Mt. Sinai J. Med.* 77, 32–42.

Perrin, R. J., Fagan, A. M., and Holtzman, D. M. (2009). Multimodal techniques for diagnosis and prognosis of Alzheimer's disease. *Nature* 461, 916–922.

Pham, E., Crews, L., Ubhi, K., Hansen, L., Adame, A., Cartier, A., Salmon, D., Galasko, D., Michael, S., Savas, J. N., Yates, J. R., Glabe, C., and Masliah, E. (2010). Progressive accumulation of amyloid-β oligomers in Alzheimer's disease and in amyloid precursor protein transgenic mice is accompanied by selective alterations in synaptic scaffold proteins. *FEBS J.* 277, 3051–3067.

Philipson, O., Lord, A., Lalowski, M., Soliymani, R., Baumann, M., Thyberg, J., Bogdanovic, N., Olofsson, T., Tjernberg, L. O., Ingelsson, M., Lannfelt, L., Kalimo, H., and Nilsson, L. N. G. (2012). The Arctic amyloid-β precursor protein (AβPP) mutation results in distinct plaques and accumulation of N- and C-truncated Aβ. *Neurobiol. Aging* 33.

Piccini, A., Russo, C., Gliozzi, A., Relini, A., Vitali, A., Borghi, R., Giliberto, L., Armirotti, A., D'Arrigo, C., Bachi, A., Cattaneo, A., Canale, C., Torrassa, S., Saido, T. C., Markesbery, W., Gambetti, P., and Tabaton, M. (2005). β-amyloid is different in normal aging and in Alzheimer disease. *J. Biol. Chem.* 280, 34186–34192.

Pickett, E. K., Herrmann, A. G., McQueen, J., Abt, K., Dando, O., Tulloch, J., Jain, P., Dunnett, S., Sohrabi, S., Fjeldstad, M. P., Calkin, W., Murison, L., Jackson, R. J., Tzioras, M., Stevenson, A., D'Orange, M., Hooley, M., Davies, C., Colom-Cadena, M., Anton-Fernandez, A., King, D., Oren, I., Rose, J., McKenzie, C. A., Allison, E., Smith, C., Hardt, O., Henstridge, C. M., Hardingham, G. E., and Spires-Jones, T. L. (2019). Amyloid Beta and Tau Cooperate to Cause Reversible Behavioral and Transcriptional Deficits in a Model of Alzheimer's Disease. *Cell Rep.* 29, 3592–3604.

Pickett, E. K., Koffie, R. M., Wegmann, S., Henstridge, C. M., Herrmann, A. G., Colom-Cadena, M., Lleo, A., Kay, K. R., Vaught, M., Soberman, R., Walsh, D. M., Hyman, B. T., and Spires-Jones, T. L. (2016). Non-Fibrillar Oligomeric Amyloid-β within Synapses. *J. Alzheimer's Dis.* 53, 787–800.

Pickett, E. K., Rose, J., McCrory, C., McKenzie, C. A., King, D., Smith, C., Gillingwater, T. H., Henstridge, C. M., and Spires-Jones, T. L. (2018). Region-specific depletion of synaptic mitochondria in the brains of patients with Alzheimer's disease. *Acta Neuropathol.* 136, 747–757.

Piedrahita, D., Castro-Alvarez, J. F., Boudreau, R. L., Villegas-Lanau, A., Kosik, K. S., Gallego-Gomez, J. C., and Cardona-GGómez, G. P. (2016). β-Secretase 1's targeting reduces hyperphosphorilated tau, implying autophagy actors in 3xTg-AD mice. *Front. Cell. Neurosci.* 9, 1–19.

Pink, D., Donnelier, J., Lewis, J., and Braun, J. E. A. (2018). Cargo-Loading of Misfolded Proteins into Extracellular Vesicles: The Role of J Proteins. *bioRxiv*. Available at: http://biorxiv.org/content/early/2018/05/08/310219.abstract.

Poirel, O., Mella, S., Videau, C., Ramet, L., Davoli, M. A., Herzog, E., Katsel, P., Mechawar, N., Haroutunian, V., Epelbaum, J., Daumas, S., and El Mestikawy, S. (2018). Moderate decline in select synaptic markers in the prefrontal cortex (BA9) of patients with Alzheimer's disease at various cognitive stages. *Sci. Rep.* 8, 1–14.

Polanco, J. C., Scicluna, B. J., Hill, A. F., and Götz, J. (2016). Extracellular vesicles isolated from the brains of rTg4510 mice seed tau protein aggregation in a threshold-dependent manner. *J. Biol. Chem.* 291, 12445–12466.

Pooler, A. M., and Hanger, D. P. (2010). Functional implications of the association of tau with the plasma membrane. *Biochem. Soc. Trans.* 38, 1012–1015.

Pooler, A. M., Noble, W., and Hanger, D. P. (2014). A role for tau at the synapse in Alzheimer's disease pathogenesis. *Neuropharmacology* 76, 1–8.

Pooler, A. M., Phillips, E. C., Lau, D. H. W., Noble, W., and Hanger, D. P. (2013a). Physiological release of endogenous tau is stimulated by neuronal activity. *EMBO Rep.* 14, 389–394.

Pooler, A. M., Polydoro, M., Maury, E. A., Nicholls, S. B., Reddy, S. M., Wegmann, S., William, C., Saqran, L., Cagsal-Getkin, O., Pitstick, R., Beier, D. R., Carlson, G. A., Spires-Jones, T. L., and Hyman, B. T. (2015). Amyloid accelerates tau propagation and toxicity in a model of early Alzheimer's disease. *Acta Neuropathol. Commun.* 3, 1–11.

Pooler, A. M., Polydoro, M., Wegmann, S., Nicholls, S. B., Spires-Jones, T. L., and Hyman, B. T. (2013b). Propagation of tau pathology in Alzheimer's disease: identification of novel therapeutic targets. *Alzheimers. Res. Ther.* 5, 49.

Pooler, A. M., Usardi, A., Evans, C. J., Philpott, K. L., Noble, W., and Hanger, D. P. (2012). Dynamic association of tau with neuronal membranes is regulated by phosphorylation. *Neurobiol. Aging* 33, 27–38.

Prescott, G. R., Jenkins, R. E., Walsh, C. M., and Morgan, A. (2008). Phosphorylation of cysteine string protein on Serine 10 triggers 14-3-3 protein binding. *Biochem. Biophys. Res. Commun.* 377, 809–814.

Prince, M., Albanese, E., Guerchet, M., and Prina, M. (2014). Alzheimer's Disease

International. Dementia and risk reduction: an analysis of protective and modifiable factors.

Purro, S. A., Dickins, E. M., and Salinas, P. C. (2012). The secreted Wnt antagonist dickkopf-1 is required for amyloid β-mediated synaptic loss. *J. Neurosci.* 32, 3492–3498.

Quinlan, E. M., Olstein, D. H., and Bear, M. F. (1999). Bidirectional, experience-dependent regulation of N-methyl-D-aspartate receptor subunit composition in the rat visual cortex during postnatal development. *Proc. Natl. Acad. Sci. U. S. A.* 96, 12876–12880.

Rabinovici, G. D., Carrillo, M. C., Forman, M., DeSanti, S., Miller, D. S., Kozauer, N., Petersen, R. C., Randolph, C., Knopman, D. S., Smith, E. E., Isaac, M., Mattsson, N., Bain, L. J., Hendrix, J. A., and Sims, J. R. (2017). Multiple comorbid neuropathologies in the setting of Alzheimer's disease neuropathology and implications for drug development. *Alzheimer's Dement. Transl. Res. Clin. Interv.* 3, 83–91.

Raiford, K. L., Park, J., Lin, K. W., Fang, S., Crews, A. L., and Adler, K. B. (2011). Mucin granule-associated proteins in human bronchial epithelial cells: The airway goblet cell "granulome." *Respir. Res.* 12, 1–10.

Rajendran, L., and Annaert, W. (2012). Membrane Trafficking Pathways in Alzheimer's Disease. *Traffic* 13, 759–770.

Rajendran, L., Honsho, M., Zahn, T. R., Keller, P., Geiger, K. D., Verkade, P., and Simons, K. (2006). Alzheimer's disease β-amyloid peptides are released in association with exosomes. *Proc. Natl. Acad. Sci. U. S. A.* 103, 11172–11177.

Rajendran, L., and Paolicelli, R. C. (2018). Microglia-mediated synapse loss in Alzheimer's disease. *J. Neurosci.* 38, 2911–2919.

Rapoport, M., Dawson, H. N., Binder, L. I., Vitek, M. P., and Ferreira, A. (2002). Tau is essential to β-amyloid-induced neurotoxicity. *Proc. Natl. Acad. Sci. U. S. A.* 99, 6364–6369.

Rauch, J. N., Luna, G., Guzman, E., Audouard, M., Challis, C., Sibih, Y. E., Leshuk, C., Hernandez, I., Wegmann, S., Hyman, B. T., Gradinaru, V., Kampmann, M., and Kosik, K. S. (2020). LRP1 is a master regulator of tau uptake and spread. *Nature* 580, 381–385.

Reddy, P. H. (2011). Abnormal tau, mitochondrial dysfunction, impaired axonal transport of mitochondria, and synaptic deprivation in Alzheimer's disease. *Brain Res.* 1415, 136–148.

Reddy, P. H., Mani, G., Park, B. S., Jacques, J., Murdoch, G., Whetsell, W., Kaye, J., and Manczak, M. (2005). Differential loss of synaptic proteins in Alzheimer's

disease: Implications for synaptic dysfunction. *J. Alzheimer's Dis.* 7, 103–117.

Renner, M., Lacor, P. N., Velasco, P. T., Xu, J., Contractor, A., Klein, W. L., and Triller, A. (2010). Deleterious Effects of Amyloid β Oligomers Acting as an Extracellular Scaffold for mGluR5. *Neuron* 66, 739–754.

Revesz, T., Holton, J. L., Doshi, B., Anderton, B. H., Scaravilli, F., and Plant, G. T. (1999). Cytoskeletal pathology in familial cerebral amyloid angiopathy (British type) with non-neuritic amyloid plaque formation. *Acta Neuropathol.* 97, 170–176.

Revuelta, G. J., Rosso, A., and Lippa, C. F. (2008). Neuritic pathology as a correlate of synaptic loss in dementia with Lewy bodies. *Am. J. Alzheimers. Dis. Other Demen.* 23, 97–102.

Reynolds, C. H., Garwood, C. J., Wray, S., Price, C., Kellie, S., Perera, T., Zvelebil, M., Yang, A., Sheppard, P. W., Varndell, I. M., Hanger, D. P., and Anderton, B. H. (2008). Phosphorylation regulates tau interactions with Src homology 3 domains of phosphatidylinositol 3-kinase, phospholipase Cγ1, Grb2, and Src family kinases. *J. Biol. Chem.* 283, 18177–18186.

Riku, Y., Watanabe, H., Yoshida, M., Mimuro, M., Iwasaki, Y., Masuda, M., Ishigaki, S., Katsuno, M., and Sobue, G. (2017). Pathologic involvement of glutamatergic striatal inputs from the cortices in TAR DNA-binding protein 43 kDa-related frontotemporal lobar degeneration and amyotrophic lateral sclerosis. *J. Neuropathol. Exp. Neurol.* 76, 759–768.

Rissman, R. A., Poon, W. W., Blurton-Jones, M., Oddo, S., Torp, R., Vitek, M. P., LaFerla, F. M., Rohn, T. T., and Cotman, C. W. (2004). Caspase-cleavage of tau is an early event in Alzheimer disease tangle pathology. *J. Clin. Invest.* 114, 121–130.

Rivera, S., Khrestchatisky, M., Kaczmarek, L., Rosenberg, G. A., and Jaworski, D. M. (2010). Metzincin proteases and their inhibitors: Foes or friends in nervous system physiology? *J. Neurosci.* 30, 15337–15357.

Robinson, J. L., Molina-Porcel, L., Corrada, M. M., Raible, K., Lee, E. B., Lee, V. M. Y., Kawas, C. H., and Trojanowski, J. Q. (2014). Perforant path synaptic loss correlates with cognitive impairment and Alzheimer's disease in the oldest-old. *Brain* 137, 2578–2587.

Rodríguez-Martín, T., Cuchillo-Ibáñez, I., Noble, W., Nyenya, F., Anderton, B. H., and Hanger, D. P. (2013). Tau phosphorylation affects its axonal transport and degradation. *Neurobiol. Aging* 34, 2146–2157.

Rogaeva, E., Meng, Y., Lee, J. H., Gu, Y., Kawarai, T., Zou, F., Katayama, T., Baldwin, C. T., Cheng, R., Hasegawa, H., Chen, F., Shibata, N., Lunetta, K. L.,

Pardossi-Piquard, R., Bohm, C., Wakutani, Y., Cupples, L. A., Cuenco, K. T., Green, R. C., Pinessi, L., Rainero, I., Sorbi, S., Bruni, A., Duara, R., Friedland, R. P., Inzelberg, R., Hampe, W., Bujo, H., Song, Y. Q., Andersen, O. M., Willnow, T. E., Graff-Radford, N., Petersen, R. C., Dickson, D., Der, S. D., Fraser, P. E., Schmitt-Ulms, G., Younkin, S., Mayeux, R., Farrer, L. A., and St. George-Hyslop, P. (2007). The neuronal sortilin-related receptor SORL1 is genetically associated with Alzheimer disease. *Nat. Genet.* 39, 168–177.

Rogers, J. T., Leiter, L. M., McPhee, J., Cahill, C. M., Zhan, S. S., Potter, H., and Nilsson, L. N. G. (1999). Translation of the Alzheimer amyloid precursor protein mRNA is up- regulated by interleukin-1 through 5'-untranslated region sequences. *J. Biol. Chem.* 274, 6421–6431.

Roh, S. E., Woo, J. A., Lakshmana, M. K., Uhlar, C., Ankala, V., Boggess, T., Liu, T., Hong, Y. H., Mook-Jung, I., Kim, S. J., and Kang, D. E. (2013). Mitochondrial dysfunction and calcium deregulation by the RanBP9-cofilin pathway. *FASEB J.* 27, 4776–4789.

Rönicke, R., Mikhaylova, M., Rönicke, S., Meinhardt, J., Schröder, U. H., Fändrich, M., Reiser, G., Kreutz, M. R., and Reymann, K. G. (2011). Early neuronal dysfunction by amyloid β oligomers depends on activation of NR2B-containing NMDA receptors. *Neurobiol. Aging* 32, 2219–2228.

Ross, C. A., and Poirier, M. A. (2004). Protein aggregation and neurodegenerative disease. *Nat. Med.* 10, 1–8.

Rozas, J. L., Gómez-Sánchez, L., Mircheski, J., Linares-Clemente, P., Nieto-González, J. L., Vázquez, E. M., Luján, R., and Fernández-Chacón, R. (2012). Motorneurons Require Cysteine String Protein-α to Maintain the Readily Releasable Vesicular Pool and Synaptic Vesicle Recycling. *Neuron* 74, 151–165.

Rustom, A., Saffrich, R., Markovic, I., Walther, P., and Gerdes, H. H. (2004). Nanotubular Highways for Intercellular Organelle Transport. *Science (80-.).* 303, 1007–1010.

Rüttiger, L., Sausbier, M., Zimmermann, U., Winter, H., Braig, C., Engel, J., Knirsch, M., Arntz, C., Langer, P., Hirt, B., Müller, M., Köpschall, I., Pfister, M., Münkner, S., Rohbock, K., Pfaff, I., Rüsch, A., Ruth, P., and Knipper, M. (2004). Deletion of the Ca2+-activated potassium (BK) α-subunit but not the BKβ1-subunit leads to progressive hearing loss. *Proc. Natl. Acad. Sci. U. S. A.* 101, 12922–12927.

Sadleir, K. R., Kandalepas, P. C., Buggia-Prévot, V., Nicholson, D. A., Thinakaran, G., and Vassar, R. (2016). Presynaptic dystrophic neurites surrounding

amyloid plaques are sites of microtubule disruption, BACE1 elevation, and increased Aβ generation in Alzheimer's disease. *Acta Neuropathol.* 132, 235–256.

Saito, T., Matsuba, Y., Mihira, N., Takano, J., Nilsson, P., Itohara, S., Iwata, N., and Saido, T. C. (2014). Single App knock-in mouse models of Alzheimer's disease. *Nat. Neurosci.* 17, 661–663.

Saman, S., Kim, W. H., Raya, M., Visnick, Y., Miro, S., Saman, S., Jackson, B., McKee, A. C., Alvarez, V. E., Lee, N. C. Y., and Hall, G. F. (2012). Exosome-associated tau is secreted in tauopathy models and is selectively phosphorylated in cerebrospinal fluid in early Alzheimer disease. *J. Biol. Chem.* 287, 3842–3849.

Sambri, I., D'Alessio, R., Ezhova, Y., Giuliano, T., Sorrentino, N. C., Cacace, V., De Risi, M., Cataldi, M., Annunziato, L., De Leonibus, E., and Fraldi, A. (2017). Lysosomal dysfunction disrupts presynaptic maintenance and restoration of presynaptic function prevents neurodegeneration in lysosomal storage diseases. *EMBO Mol. Med.* 9, 112–132.

Samuel, W., Alford, M., Hofstetter, C. R., and Hansen, L. (1997). Dementia with Lewy bodies versus pure Alzheimer disease: Differences in cognition, neuropathology, cholinergic dysfunction, and synapse density. *J. Neuropathol. Exp. Neurol.* 56, 499–508.

Sanchez-Varo, R., Trujillo-Estrada, L., Sanchez-Mejias, E., Torres, M., Baglietto-Vargas, D., Moreno-Gonzalez, I., De Castro, V., Jimenez, S., Ruano, D., Vizuete, M., Davila, J. C., Garcia-Verdugo, J. M., Jimenez, A. J., Vitorica, J., and Gutierrez, A. (2012). Abnormal accumulation of autophagic vesicles correlates with axonal and synaptic pathology in young Alzheimer's mice hippocampus. *Acta Neuropathol.* 123, 53–70.

Sanders, C. R. (2016). How γ-secretase hits a moving target. *Elife* 5, 1–4.

Sanders, D. W., Kaufman, S. K., DeVos, S. L., Sharma, A. M., Mirbaha, H., Li, A., Barker, S. J., Foley, A. C., Thorpe, J. R., Serpell, L. C., Miller, T. M., Grinberg, L. T., Seeley, W. W., and Diamond, M. I. (2014). Distinct tau prion strains propagate in cells and mice and define different tauopathies. *Neuron* 82, 1271–1288.

Sannerud, R., Esselens, C., Ejsmont, P., Mattera, R., Rochin, L., Tharkeshwar, A. K., De Baets, G., De Wever, V., Habets, R., Baert, V., Vermeire, W., Michiels, C., Groot, A. J., Wouters, R., Dillen, K., Vints, K., Baatsen, P., Munck, S., Derua, R., Waelkens, E., Basi, G. S., Mercken, M., Vooijs, M., Bollen, M., Schymkowitz, J., Rousseau, F., Bonifacino, J. S., Van Niel, G., De Strooper,

B., and Annaert, W. (2016). Restricted Location of PSEN2/γ-Secretase Determines Substrate Specificity and Generates an Intracellular Aβ Pool. *Cell* 166, 193–208.

Satizabal, C. L., Beiser, A. S., Chouraki, V., Chêne, G., Dufouil, C., and Seshadri, S. (2016). Incidence of Dementia over Three Decades in the Framingham Heart Study. *N. Engl. J. Med.* 374, 523–532.

Sato, N., Imaizumi, K., Manabe, T., Taniguchi, M., Hitomi, J., Katayama, T., Yoneda, T., Morihara, T., Yasuda, Y., Takagi, T., Kudo, T., Tsuda, T., Itoyama, Y., Makifuchi, T., Fraser, P. E., St George-Hyslop, P., and Tohyama, M. (2001). Increased production of β-amyloid and vulnerability to endoplasmic reticulum stress by an aberrant spliced form of presenilin 2*. *J. Biol. Chem.* 276, 2108–2114.

Scheff, S. W., DeKosky, S. T., and Price, D. A. (1990). Quantitative assessment of cortical synaptic density in Alzheimer's disease. *Neurobiol. Aging* 11, 29–37.

Scheff, S. W., Price, D. A., Schmitt, F. A., and Mufson, E. J. (2006). Hippocampal synaptic loss in early Alzheimer's disease and mild cognitive impairment. *Neurobiol. Aging* 27, 1372–1384.

Scheff, S. W., Price, D. A., Schmitt, F. A., Roberts, K. N., Ikonomovic, M. D., and Mufson, E. J. (2013). Synapse stability in the precuneus early in the progression of alzheimer's disease. *J. Alzheimer's Dis.* 35, 599–609.

Schellenberg, G. D., and Montine, T. J. (2012). The genetics and neuropathology of Alzheimer's disease. *Acta Neuropathol.* 124, 305–323.

Scheuner, D., Eckman, C., Jensen, M., Song, X., Citron, M., Suzuki, N., Bird, T. D., Hardy, J., Hutton, M., Kukull, W., Larson, E., Levy-Lahad, E., Viitanen, M., Peskind, E., Poorkaj, P., Schellenberg, G., Tanzi, R., Wasco, W., Lannfelt, L., Selkoe, D., and Younkin, S. (1996). Secreted amyloid β-protein similar to that in the senile plaques of Alzheimer's disease is increased in vivo by the presenilin 1 and 2 and APP mutations linked to familial Alzheimer's disease. *Nat. Med.* 2, 864–870.

Schmidt, B. Z., Watts, R. J., Aridor, M., and Frizzell, R. A. (2009). Cysteine string protein promotes proteasomal degradation of the cystic fibrosis transmembrane conductance regulator (CFTR) by increasing its interaction with the C terminus of Hsp70-interacting protein and promoting CFTR ubiquitylation. *J. Biol. Chem.* 284, 4168–4178.

Schmitz, F., Tabares, L., Khimich, D., Strenzke, N., De La Villa-Polo, P., Castellano-Muñoz, M., Bulankina, A., Moser, T., Fernández-Chacón, R., and Südhof, T. C. (2006). CSPα-deficiency causes massive and rapid photoreceptor

degeneration. *Proc. Natl. Acad. Sci. U. S. A.* 103, 2926–2931.

Schnaider, B. M., Haroutunian, V., Schmeidler, J., Sano, M., Fam, P., Kavanaugh, A., Barr, A. M., Honer, W. G., and Katsel, P. (2012). Synaptic protein deficits are associated with dementia irrespective of extreme old age. *Neurobiol. Aging* 33, 1–8.

Schneider, A., Biernat, J., Von Bergen, M., Mandelkow, E., and Mandelkow, E. M. (1999). Phosphorylation that detaches tau protein from microtubules (Ser262, Ser214) also protects it against aggregation into Alzheimer paired helical filaments. *Biochemistry* 38, 3549–3558.

Schneider, J. A., Arvanitakis, Z., Bang, W., and Bennett, D. A. (2007). Mixed brain pathologies account for most dementia cases in community-dwelling older persons. *Neurology* 69, 2197–2204.

Schneider, J. A., Arvanitakis, Z., Leurgans, S. E., and Bennett, D. A. (2009). The neuropathology of probable Alzheimer disease and mild cognitive impairment. *Ann. Neurol.* 66, 200–208.

Schneider, L. (2020). A resurrection of aducanumab for Alzheimer's disease. *Lancet Neurol.* 19, 111–112.

Schweers, O., Schönbrunn-Hanebeck, E., Marx, A., and Mandelkow, E. (1994). Structural studies of tau protein and Alzheimer paired helical filaments show no evidence for β-structure. *J. Biol. Chem.* 269, 24290–24297.

Seehafer, S. S., and Pearce, D. A. (2009). Spectral properties and mechanisms that underlie autofluorescent accumulations in Batten disease. *Biochem. Biophys. Res. Commun.* 382, 247–251.

Selkoe, D. J. (2001). Alzheimer's disease: Genes, proteins, and therapy. *Physiol. Rev.* 81, 741–766.

Selkoe, D. J. (2002). Alzheimer's disease is a synaptic failure. *Science (80-.).* 298, 789–791.

Selkoe, D. J., and Hardy, J. (2016). The amyloid hypothesis of Alzheimer's disease at 25 years. *EMBO Mol. Med.* 8, 595–608.

Selkoe, D. J., and Wolfe, M. S. (2007). Presenilin: Running with Scissors in the Membrane. *Cell* 131, 215–221.

Selkoe, D. J., Yamazaki, T., Citron, M., Podlisny, M. B., Koo, E. H., Teplow, D. B., and Haass, C. (1996). The role of APP processing and trafficking pathways in the formation of amyloid β-protein. in *Annals of the New York Academy of Sciences*, 57–64.

Selvaraj, P., Wen, J., Tanaka, M., and Zhang, Y. (2019). Therapeutic Effect of a Novel Fatty Acid Amide Hydrolase Inhibitor PF04457845 in the Repetitive

Closed Head Injury Mouse Model. *J. Neurotrauma* 36, 1655–1669.

Sengupta, U., Nilson, A. N., and Kayed, R. (2016). The Role of Amyloid-β Oligomers in Toxicity, Propagation, and Immunotherapy. *EBioMedicine* 6, 42–49.

Serrano-Pozo, A., Betensky, R. A., Frosch, M. P., and Hyman, B. T. (2016). Plaque-associated local toxicity increases over the clinical course of Alzheimer disease. *Am. J. Pathol.* 186, 375–384.

Serrano-Pozo, A., Frosch, M. P., Masliah, E., and Hyman, B. T. (2011). Neuropathological alterations in Alzheimer disease. *Cold Spring Harb. Perspect. Med.* 1, 1–23.

Seshadri, S., Fitzpatrick, A. L., Ikram, M. A., DeStefano, A. L., Gudnason, V., Boada, M., Bis, J. C., Smith, A. V., Carassquillo, M. M., Lambert, J. C., Harold, D., Schrijvers, E. M. C., Ramirez-Lorca, R., Debette, S., Longstreth, W. T., Janssens, A. C. J. W., Pankratz, V. S., Dartigues, J. F., Hollingworth, P., Aspelund, T., Hernandez, I., Beiser, A., Kuller, L. H., Koudstaal, P. J., Dickson, D. W., Tzourio, C., Abraham, R., Antunez, C., Du, Y., Rotter, J. I., Aulchenko, Y. S., Harris, T. B., Petersen, R. C., Berr, C., Owen, M. J., Lopez-Arrieta, J., Varadarajan, B. N., Becker, J. T., Rivadeneira, F., Nalls, M. A., Graff-Radford, N. R., Campion, D., Auerbach, S., Rice, K., Hofman, A., Jonsson, P. V., Schmidt, H., Lathrop, M., Mosley, T. H., Au, R., Psaty, B. M., Uitterlinden, A. G., Farrer, L. A., Lumley, T., Ruiz, A., Williams, J., Amouyel, P., Younkin, S. G., Wolf, P. A., Launer, L. J., Lopez, O. L., Van Duijn, C. M., and Breteler, M. M. B. (2010). Genome-wide analysis of genetic loci associated with Alzheimer disease. *JAMA - J. Am. Med. Assoc.* 303, 1832–1840.

Seyfried, N. T., Gozal, Y. M., Donovan, L. E., Herskowitz, J. H., Dammer, E. B., Xia, Q., Ku, L., Chang, J., Duong, D. M., Rees, H. D., Cooper, D. S., Glass, J. D., Gearing, M., Tansey, M. G., Lah, J. J., Feng, Y., Levey, A. I., and Peng, J. (2012). Quantitative analysis of the detergent-insoluble brain proteome in frontotemporal lobar degeneration using SILAC internal standards. *J. Proteome Res.* 11, 2721–2738.

Shankar, G. M., Bloodgood, B. L., Townsend, M., Walsh, D. M., Selkoe, D. J., and Sabatini, B. L. (2007). Natural oligomers of the Alzheimer amyloid-β protein induce reversible synapse loss by modulating an NMDA-type glutamate receptor-dependent signaling pathway. *J. Neurosci.* 27, 2866–2875.

Shankar, G. M., Li, S., Mehta, T. H., Garcia-Munoz, A., Shepardson, N. E., Smith, I., Brett, F. M., Farrell, M. A., Rowan, M. J., Lemere, C. A., Regan, C. M., Walsh, D. M., Sabatini, B. L., and Selkoe, D. J. (2008). Amyloid-β protein dimers

isolated directly from Alzheimer's brains impair synaptic plasticity and memory. *Nat. Med.* 14, 837–842.

Sharma, M., Burré, J., Bronk, P., Zhang, Y., Xu, W., and Südhof, T. C. (2012a). CSPα knockout causes neurodegeneration by impairing SNAP-25 function. *EMBO J.* 31, 829–841.

Sharma, M., Burré, J., and Südhof, T. C. (2011). CSPα promotes SNARE-complex assembly by chaperoning SNAP-25 during synaptic activity. *Nat. Cell Biol.* 13, 30–39.

Sharma, M., Burré, J., and Südhof, T. C. (2012b). Proteasome inhibition alleviates SNARE-dependent neurodegeneration. *Sci. Transl. Med.* 4, 1–10.

Shen, J., and Kelleher, R. J. (2007). The presenilin hypothesis of Alzheimer's disease: Evidence for a loss-of-function pathogenic mechanism. *Proc. Natl. Acad. Sci. U. S. A.* 104, 403–409.

Sheng, J., and Wu, L. G. (2012). Cysteine String Protein α: A New Role in Vesicle Recycling. *Neuron* 74, 6–8.

Sheng, M., Sabatini, B. L., and Südhof, T. C. (2012). Synapses and Alzheimer's disease. *Cold Spring Harb. Perspect. Biol.* 4, 1–18.

Sherrington, R., Rogaev, E. I., Liang, Y., Rogaeva, E. A., Levesque, G., Ikeda, M., Chi, H., Lin, C., Li, G., Holman, K., Tsuda, T., Mar, L., Foncin, J. F., Bruni, A. C., Montesi, M. P., Sorbi, S., Rainero, I., Pinessi, L., Nee, L., Chumakov, I., Pollen, D., Brookes, A., Sanseau, P., Polinsky, R. J., Wasco, W., Da Silva, H. A. R., Haines, J. L., Pericak-Vance, M. A., Tanzi, R. E., Roses, A. D., Fraser, P. E., Rommens, J. M., and St George-Hyslop, P. H. (1995). Cloning of a gene bearing missense mutations in early-onset familial Alzheimer's disease. *Nature* 375, 754–760.

Shi, Q., Chowdhury, S., Ma, R., Le, K. X., Hong, S., Caldarone, B. J., Stevens, B., and Lemere, C. A. (2017a). Complement C3 deficiency protects against neurodegeneration in aged plaque-rich APP/PS1 mice. *Sci. Transl. Med.* 9, 1–15.

Shi, Y., Gu, L., Alsharif, A. A., and Zhang, Z. (2017b). The Distinction of Amyloid-β Protein Precursor (AβPP) Ratio in Platelet Between Alzheimer's Disease Patients and Controls: A Systematic Review and Meta-Analysis. *J. Alzheimer's Dis.* 59, 1037–1044.

Shimohama, S., Kamiya, S., Taniguchi, T., Akagawa, K., and Kimura, J. (1997). Differential involvement of synaptic vesicle and presynaptic plasma membrane proteins in Alzheimer's disease. *Biochem. Biophys. Res. Commun.* 236, 239–242.

Shinohara, H., Inaguma, Y., Goto, S., Inagaki, T., and Kato, K. (1993). αB crystallin and HSP28 are enhanced in the cerebral cortex of patients with Alzheimer's disease. *J. Neurol. Sci.* 119, 203–208.

Shirafuji, T., Ueyama, T., Adachi, N., Yoshino, K. I., Sotomaru, Y., Uwada, J., Kaneoka, A., Ueda, T., Tanaka, S., Hide, I., Saito, N., and Sakai, N. (2018). The role of cysteine string protein α phosphorylation at serine 10 and 34 by protein kinase Cγ for presynaptic maintenance. *J. Neurosci.* 38, 278–290.

Siew, L. K., Love, S., Dawbarn, D., Wilcock, G. K., and Allen, S. J. (2004). Measurement of pre- and post-synaptic proteins in cerebral cortex: Effects of post-mortem delay. *J. Neurosci. Methods* 139, 153–159.

Sinclair, L. I., Tayler, H. M., and Love, S. (2015). Synaptic protein levels altered in vascular dementia. *Neuropathol. Appl. Neurobiol.* 41, 533–543.

Sjöbeck, M., and Englund, E. (2001). Alzheimer's disease and the cerebellum: A morphologic study on neuronal and glial changes. *Dement. Geriatr. Cogn. Disord.* 12, 211–218.

Smith, A. J., Duan, T., and Verkman, A. S. (2019). Aquaporin-4 reduces neuropathology in a mouse model of Alzheimer's disease by remodeling peri-plaque astrocyte structure. *Acta Neuropathol. Commun.* 7, 1–11.

Snyder, E. M., Nong, Y., Almeida, C. G., Paul, S., Moran, T., Choi, E. Y., Nairn, A. C., Salter, M. W., Lombroso, P. J., Gouras, G. K., and Greengard, P. (2005). Regulation of NMDA receptor trafficking by amyloid-β. *Nat. Neurosci.* 8, 1051–1058.

Snyder, H. M., Corriveau, R. A., Craft, S., Faber, J. E., Greenberg, S. M., Knopman, D., Lamb, B. T., Montine, T. J., Nedergaard, M., Schaffer, C. B., Schneider, J. A., Wellington, C., Wilcock, D. M., Zipfel, G. J., Zlokovic, B., Bain, L. J., Bosetti, F., Galis, Z. S., Koroshetz, W., and Carrillo, M. C. (2015). Vascular contributions to cognitive impairment and dementia including Alzheimer's disease. *Alzheimer's Dement.* 11, 710–717.

Sofroniew, M. V., and Vinters, H. V. (2010). Astrocytes: Biology and pathology. *Acta Neuropathol.* 119, 7–35.

Sperling, R. A., Aisen, P. S., Beckett, L. A., Bennett, D. A., Craft, S., Fagan, A. M., Iwatsubo, T., Jack Jr, C. R., Kaye, J., Montine, T. J., Park, D. C., Reiman, E. M., Rowe, C. C., Siemers, E., Stern, Y., Yaffe, K., Carrillo, M. C., Thies, B., Morrison-Bogorad, M., Wagster, M. V, and Phelps, C. H. (2011). Toward defining the preclinical stages of Alzheimer's disease: recommendations from the National Institute on Aging-Alzheimer's Association workgroups on diagnostic guidelines for Alzheimer's disease. *Alzheimers. Dement.* 7, 280–

292.

Spires-Jones, T. L., Attems, J., and Thal, D. R. (2017). Interactions of pathological proteins in neurodegenerative diseases. *Acta Neuropathol.* 134, 187–205.

Spires-Jones, T. L., and Hyman, B. (2014). The Intersection of Amyloid Beta and Tau at Synapses in Alzheimer's Disease. *Neuron* 82, 756–771.

Spires-Jones, T. L., Mielke, M. L., Rozkalne, A., Meyer-Luehmann, M., de Calignon, A., Bacskai, B. J., Schenk, D., and Hyman, B. T. (2009). Passive immunotherapy rapidly increases structural plasticity in a mouse model of Alzheimer disease. *Neurobiol. Dis.* 33, 213–220.

Spires, T. L., and Hyman, B. T. (2005). Transgenic models of Alzheimer's disease: Learning from animals. *NeuroRx* 2, 423–437.

Spires, T. L., Meyer-Luehmann, M., Stern, E. A., McLean, P. J., Skoch, J., Nguyen, P. T., Bacskai, B. J., and Hyman, B. T. (2005). Dendritic spine abnormalities in amyloid precursor protein transgenic mice demonstrated by gene transfer and intravital multiphoton microscopy. *J. Neurosci.* 25, 7278–7287.

Spittaels, K., Van Den Haute, C., Van Dorpe, J., Bruynseels, K., Vandezande, K., Laenen, I., Geerts, H., Mercken, M., Sciot, R., Van Lommel, A., Loos, R., and Van Leuven, F. (1999). Prominent axonopathy in the brain and spinal cord of transgenic mice overexpressing four-repeat human tau protein. *Am. J. Pathol.* 155, 2153–2165.

St. George-Hyslop, P. H., Tanzi, R. E., Polinsky, R. J., Haines, J. L., Nee, L., Watkins, P. C., Myers, R. H., Feldman, R. G., Pollen, D., Drachman, D., Growdon, J., Bruni, A., Foncin, J. F., Salmon, D., Frommelt, P., Amaducci, L., Sorbi, S., Piacentini, S., Stewart, G. D., Hobbs, W. J., Conneally, P. M., and Gusella, J. F. (1987). The genetic defect causing familial Alzheimer's disease maps on chromosome 21. *Science (80-.).* 235, 885–890.

Stahl, B., Tobaben, S., and Südhof, T. C. (1999). Two distinct domains in hsc70 are essential for the interaction with the synaptic vesicle cysteine string protein. *Eur. J. Cell Biol.* 78, 375–381.

Stamer, K., Vogel, R., Thies, E., Mandelkow, E., and Mandelkow, E. M. (2002). Tau blocks traffic of organelles, neurofilaments, and APP vesicles in neurons and enhances oxidative stress. *J. Cell Biol.* 156, 1051–1063.

Stelzmann, R. A., Norman Schnitzlein, H., and Reed Murtagh, F. (1995). An english translation of alzheimer's 1907 paper, "über eine eigenartige erkankung der hirnrinde." *Clin. Anat.* 8, 429–431.

Strassnig, M., and Ganguli, M. (2005). About a peculiar disease of the cerebral cortex: Alzheimer's original case revisited. *Psychiatry (Edgmont).* 2, 30–33.

Sultan, A., Nesslany, F., Violet, M., Bégard, S., Loyens, A., Talahari, S., Mansuroglu, Z., Marzin, D., Sergeant, N., Humez, S., Colin, M., Bonnefoy, E., Buée, L., and Galas, M. C. (2011). Nuclear Tau, a key player in neuronal DNA protection. *J. Biol. Chem.* 286, 4566–4575.

Suzuki, N., Cheung, T. T., Cai, X. D., Odaka, A., Otvos, L., Eckman, C., Golde, T. E., and Younkin, S. G. (1994). An increased percentage of long amyloid β protein secreted by familial amyloid β protein precursor (βAPP717) mutants. *Science (80-.).* 264, 1336–1340.

Swayne, L. A., Beck, K. E., and Braun, J. E. A. (2006). The cysteine string protein multimeric complex. *Biochem. Biophys. Res. Commun.* 348, 83–91.

Swayne, L. A., Blattler, C., Kay, J. G., and Braun, J. E. A. (2003). Oilgomerization characteristics of cysteine string protein. *Biochem. Biophys. Res. Commun.* 300, 921–926.

Szaruga, M., Munteanu, B., Lismont, S., Veugelen, S., Horré, K., Mercken, M., Saido, T. C., Ryan, N. S., De Vos, T., Savvides, S. N., Gallardo, R., Schymkowitz, J., Rousseau, F., Fox, N. C., Hopf, C., De Strooper, B., and Chávez-Gutiérrez, L. (2017). Alzheimer's-Causing Mutations Shift Aβ Length by Destabilizing γ-Secretase-Aβn Interactions. *Cell* 170, 443-456.e14.

Szczepanski, S. M., and Knight, R. T. (2014). Insights into Human Behavior from Lesions to the Prefrontal Cortex. *Neuron* 83, 1002–1018.

Tai, H.-C., Serrano-Pozo, A., Hashimoto, T., Frosch, M. P., Spires-Jones, T. L., and Hyman, B. T. (2012). The Synaptic Accumulation of Hyperphosphorylated Tau Oligomers in Alzheimer Disease Is Associated With Dysfunction of the Ubiquitin-Proteasome System. *Am. J. Pathol.* 181, 1426–1435.

Tai, H.-C., Wang, B. Y., Serrano-Pozo, A., Frosch, M. P., Spires-Jones, T. L., and Hyman, B. T. (2014). Frequent and symmetric deposition of misfolded tau oligomers within presynaptic and postsynaptic terminals in Alzheimer's disease. *Acta Neuropathol. Commun.* 2, 1–14.

Tai, L. M., Bilousova, T., Jungbauer, L., Roeske, S. K., Youmans, K. L., Yu, C., Poon, W. W., Cornwell, L. B., Miller, C. A., Vinters, H. V., Van Eldik, L. J., Fardo, D. W., Estus, S., Bu, G., Gylys, K. H., and LaDu, M. J. (2013). Levels of soluble apolipoprotein E/amyloid-β (Aβ) complex are reduced and oligomeric Aβ increased with APOE4 and alzheimer disease in a transgenic mouse model and human samples. *J. Biol. Chem.* 288, 5914–5926.

Takamori, S., Holt, M., Stenius, K., Lemke, E. A., Grønborg, M., Riedel, D., Urlaub, H., Schenck, S., Brügger, B., Ringler, P., Müller, S. A., Rammner, B., Gräter, F., Hub, J. S., De Groot, B. L., Mieskes, G., Moriyama, Y., Klingauf, J.,

Grubmüller, H., Heuser, J., Wieland, F., and Jahn, R. (2006). Molecular Anatomy of a Trafficking Organelle. *Cell* 127, 831–846.

Takeda, S., Commins, C., DeVos, S. L., Nobuhara, C. K., Wegmann, S., Roe, A. D., Costantino, I., Fan, Z., Nicholls, S. B., Sherman, A. E., Trisini Lipsanopoulos, A. T., Scherzer, C. R., Carlson, G. A., Pitstick, R., Peskind, E. R., Raskind, M. A., Li, G., Montine, T. J., Frosch, M. P., and Hyman, B. T. (2016). Seed-competent high-molecular-weight tau species accumulates in the cerebrospinal fluid of Alzheimer's disease mouse model and human patients. *Ann. Neurol.* 80, 355–367.

Takeuchi, T., Suzuki, M., Fujikake, N., Popiel, H. A., Kikuchi, H., Futaki, S., Wada, K., and Nagai, Y. (2015). Intercellular chaperone transmission via exosomes contributes to maintenance of protein homeostasis at the organismal level. *Proc. Natl. Acad. Sci.* 112, 2497–2506.

Tampellini, D., Rahman, N., Gallo, E. F., Huang, Z., Dumont, M., Capetillo-Zarate, E., Ma, T., Zheng, R., Lu, B., Nanus, D. M., Lin, M. T., and Gouras, G. K. (2009). Synaptic activity reduces intraneuronal Aβ, promotes APP transport to synapses, and protects against Aβ-related synaptic alterations. *J. Neurosci.* 29, 9704–9713.

Tannenberg, R. K., Scott, H. L., Tannenberg, A. E. G., and Dodd, P. R. (2006). Selective loss of synaptic proteins in Alzheimer's disease: Evidence for an increased severity with APOE ε4. *Neurochem. Int.* 49, 631–639.

Tanzi, R. E. (2012). The genetics of Alzheimer disease. *Cold Spring Harb. Perspect. Med.* 2, 1–10.

Tardivel, M., Bégard, S., Bousset, L., Dujardin, S., Coens, A., Melki, R., Buée, L., and Colin, M. (2016). Tunneling nanotube (TNT)-mediated neuron-to neuron transfer of pathological Tau protein assemblies. *Acta Neuropathol. Commun.* 4, 1–14.

Taylor, C. J., Ireland, D. R., Ballagh, I., Bourne, K., Marechal, N. M., Turner, P. R., Bilkey, D. K., Tate, W. P., and Abraham, W. C. (2008). Endogenous secreted amyloid precursor protein-α regulates hippocampal NMDA receptor function, long-term potentiation and spatial memory. *Neurobiol. Dis.* 31, 250–260.

Terry, R. D., Masliah, E., Salmon, D. P., Butters, N., DeTeresa, R., Hill, R., Hansen, L. A., and Katzman, R. (1991). Physical basis of cognitive alterations in alzheimer's disease: Synapse loss is the major correlate of cognitive impairment. *Ann. Neurol.* 30, 572–580.

Thal, D. R., Ghebremedhin, E., Orantes, M., and Wiestler, O. D. (2003). Vascular Pathology in Alzheimer Disease: Correlation of Cerebral Amyloid Angiopathy

and Arteriosclerosis/Lipohyalinosis with Cognitive Decline. *J. Neuropathol. Exp. Neurol.* 62, 1287–1301.

Thal, D. R., Griffin, W. S. T., de Vos, R. A. I., and Ghebremedhin, E. (2008). Cerebral amyloid angiopathy and its relationship to Alzheimer's disease. *Acta Neuropathol.* 115, 599–609.

Thal, D. R., Rüb, U., Orantes, M., and Braak, H. (2002). Phases of Aβ-deposition in the human brain and its relevance for the development of AD. *Neurology* 58, 1791–1800.

Thal, D. R., Walter, J., Saido, T. C., and Fändrich, M. (2015). Neuropathology and biochemistry of Aβ and its aggregates in Alzheimer's disease. *Acta Neuropathol.* 129, 167–182.

Thinakaran, G., and Koo, E. H. (2008). Amyloid precursor protein trafficking, processing, and function. *J. Biol. Chem.* 283, 29615–29619.

Thomas, D. X., Bajaj, S., McRae-McKee, K., Hadjichrysanthou, C., Anderson, R. M., and Collinge, J. (2020). Association of TDP-43 proteinopathy, cerebral amyloid angiopathy, and Lewy bodies with cognitive impairment in individuals with or without Alzheimer's disease neuropathology. *Sci. Rep.* 10, 14579.

Tiraboschi, P., Attems, J., Thomas, A., Brown, A., Jaros, E., Lett, D. J., Ossola, M., Perry, R. H., Ramsay, L., Walker, L., and McKeith, I. G. (2015). Clinicians' ability to diagnose dementia with Lewy bodies is not affected by β-amyloid load. *Neurology* 84, 496–499.

Tiwari, S. S. (2015). A study of putative p25 modulated synaptic molecules-CYFIP1, CYFIP2 and CSPα-in Alzheimer's Disease.

Tiwari, S. S., D'Orange, M., Troakes, C., Shurovi, B. N., Engmann, O., Noble, W., Hortobágyi, T., and Giese, K. P. (2015). Evidence that the presynaptic vesicle protein CSPalpha is a key player in synaptic degeneration and protection in Alzheimer's disease. *Mol. Brain* 8, 1–12.

Tiwari, S. S., Mizuno, K., Ghosh, A., Aziz, W., Troakes, C., Daoud, J., Golash, V., Noble, W., Hortobágyi, T., and Giese, K. P. (2016). Alzheimer-related decrease in CYFIP2 links amyloid production to tau hyperphosphorylation and memory loss. *Brain* 139, 2751–2765.

Tobaben, S., Thakur, P., Fernández-Chacón, R., Südhof, T. C., Rettig, J., and Stahl, B. (2001). A trimeric protein complex functions as a synaptic chaperone machine. *Neuron* 31, 987–999.

Tobaben, S., Varoqueaux, F., Brose, N., Stahl, B., and Meyer, G. (2003). A brain-specific isoform of small glutamine-rich tetratricopeptide repeat-containing protein binds to Hsc70 and the cysteine string protein. *J. Biol. Chem.* 278,

38376–38383.

Trepte, P., Kruse, S., Kostova, S., Hoffmann, S., Buntru, A., Tempelmeier, A., Secker, C., Diez, L., Schulz, A., Klockmeier, K., Zenkner, M., Golusik, S., Rau, K., Schnoegl, S., Garner, C. C., and Wanker, E. E. (2018). Lu TH y: a double-readout bioluminescence-based two-hybrid technology for quantitative mapping of protein–protein interactions in mammalian cells. *Mol. Syst. Biol.* 14, 1–20.

Troakes, C., Maekawa, S., Wijesekera, L., Rogelj, B., Siklós, L., Bell, C., Smith, B., Newhouse, S., Vance, C., Johnson, L., Hortobágyi, T., Shatunov, A., Al-Chalabi, A., Leigh, N., Shaw, C. E., King, A., and Al-Sarraj, S. (2012). An MND/ALS phenotype associated with C9orf72 repeat expansion: Abundant p62-positive, TDP-43-negative inclusions in cerebral cortex, hippocampus and cerebellum but without associated cognitive decline. *Neuropathology* 32, 505–514.

Trujillo-Estrada, L., Dávila, J. C., Sánchez-Mejias, E., Sánchez-Varo, R., Gomez-Arboledas, A., Vizuete, M., Vitorica, J., and Gutiérrez, A. (2014). Early neuronal loss and axonal/presynaptic damage is associated with accelerated amyloid-β accumulation in AβPP/PS1 Alzheimer's disease mice subiculum. *J. Alzheimer's Dis.* 42, 521–541.

Tu, S., Okamoto, S. ichi, Lipton, S. A., and Xu, H. (2014). Oligomeric Aβ-induced synaptic dysfunction in Alzheimer's disease. *Mol. Neurodegener.* 9, 1–12.

Tzioras, M., Daniels, M. J. D., King, D., Popovic, K., Holloway, R. K., Stevenson, A. J., Tulloch, J., Kandasamy, J., Sokol, D., Latta, C., Rose, J., Smith, C., Miron, V. E., Henstridge, C., McColl, B. W., and Spires-Jones, T. L. (2019). Altered synaptic ingestion by human microglia in Alzheimer's disease. *bioRxiv*, 1–25.

Uchihara, T., Nakamura, A., Yamazaki, M., and Mori, O. (2001). Evolution from pretangle neurons to neurofibrillary tangles monitored by thiazin red combined with Gallyas method and double immunofluorescence. *Acta Neuropathol.* 101, 535–539.

Uchikado, H., Lin, W.-L., DeLucia, M. W., and Dickson, D. W. (2006). Alzheimer disease with amygdala Lewy bodies: a distinct form of alpha-synucleinopathy. *J. Neuropathol. Exp. Neurol.* 65, 685–697.

Um, J. W., Kaufman, A. C., Kostylev, M., Heiss, J. K., Stagi, M., Takahashi, H., Kerrisk, M. E., Vortmeyer, A., Wisniewski, T., Koleske, A. J., Gunther, E. C., Nygaard, H. B., and Strittmatter, S. M. (2013). Metabotropic Glutamate Receptor 5 Is a Coreceptor for Alzheimer Aβ Oligomer Bound to Cellular Prion Protein. *Neuron* 79, 887–902.

Unger, C., Hedberg, M. M., Mustafiz, T., Svedberg, M. M., and Nordberg, A. (2005). Early changes in Aβ levels in the brain of APPswe transgenic mice - Implication on synaptic density, α7 neuronal nicotinic acetylcholine- and N-methyl-D-aspartate receptor levels. *Mol. Cell. Neurosci.* 30, 218–227.

Utton, M. A., Vandecandelaere, A., Wagner, U., Reynolds, C. H., Gibb, G. M., Miller, C. C. J., Bayley, P. M., and Anderton, B. H. (1997). Phosphorylation of tau by glycogen synthase kinase 3β affects the ability of tau to promote microtubule self-assembly. *Biochem. J.* 323, 741–747.

Vallortigara, J., Rangarajan, S., Whitfield, D., Alghamdi, A., Howlett, D., Hortobágyi, T., Johnson, M., Attems, J., Ballard, C., Thomas, A., O'Brien, J., Aarsland, D., and Francis, P. (2014). Dynamin1 concentration in the prefrontal cortex is associated with cognitive impairment in Lewy body dementia. *F1000Research* 3, 1–12.

Van Acker, Z. P., Bretou, M., and Annaert, W. (2019). Endo-lysosomal dysregulations and late-onset Alzheimer's disease: Impact of genetic risk factors. *Mol. Neurodegener.* 14, 1–20.

van der Flier, W. M., Pijnenburg, Y. Al, Fox, N. C., and Scheltens, P. (2011). Early-onset versus late-onset Alzheimer's disease: the case of the missing APOE ε4 allele. *Lancet. Neurol.* 10, 280–288.

Vandermeeren, M., Borgers, M., Van Kolen, K., Theunis, C., Vasconcelos, B., Bottelbergs, A., Wintmolders, C., Daneels, G., Willems, R., Dockx, K., Delbroek, L., Marreiro, A., Ver Donck, L., Sousa, C., Nanjunda, R., Lacy, E., Van De Casteele, T., Van Dam, D., De Deyn, P. P., Kemp, J. A., Malia, T. J., and Mercken, M. H. (2018). Anti-tau monoclonal antibodies derived from soluble and filamentous tau show diverse functional properties in vitro and in vivo. *J. Alzheimer's Dis.* 65, 265–281.

Vardarajan, B. N., Zhang, Y., Lee, J. H., Cheng, R., Bohm, C., Ghani, M., Reitz, C., Reyes-Dumeyer, D., Shen, Y., Rogaeva, E., St George-Hyslop, P., and Mayeux, R. (2015). Coding mutations in SORL1 and Alzheimer disease. *Ann. Neurol.* 77, 215–227.

Vassar, R., Bennett, B. D., Babu-Khan, S., Kahn, S., Mendiaz, E. A., Denis, P., Teplow, D. B., Ross, S., Amarante, P., Loeloff, R., Luo, Y., Fisher, S., Fuller, J., Edenson, S., Lile, J., Jarosinski, M. A., Biere, A. L., Curran, E., Burgess, T., Louis, J. C., Collins, F., Treanor, J., Rogers, G., and Citron, M. (1999). β-Secretase cleavage of Alzheimer's amyloid precursor protein by the transmembrane aspartic protease BACE. *Science (80-.).* 286, 735–741.

Vawter, M. P., Howard, A. L., Hyde, T. M., Kleinman, J. E., and Freed, W. J. (1999).

Alterations of hippocampal secreted N-CAM in bipolar disorder and synaptophysin in schizophrenia. *Mol. Psychiatry* 4, 467–475.

Velasco, L., Dublang, L., Moro, F., and Muga, A. (2019). The complex phosphorylation patterns that regulate the activity of Hsp70 and its cochaperones. *Int. J. Mol. Sci.* 20, 1–25.

Velinov, M., Dolzhanskaya, N., Gonzalez, M., Powell, E., Konidari, I., Hulme, W., Staropoli, J. F., Xin, W., Wen, G. Y., Barone, R., Coppel, S. H., Sims, K., Brown, W. T., and Zuchner, S. (2012). Mutations in the Gene DNAJC5 Cause Autosomal Dominant Kufs Disease in a Proportion of Cases: Study of the Parry Family and 8 Other Families. *PLoS One* 7, 1–8.

Veugelen, S., Saito, T., Saido, T. C., Chávez-Gutiérrez, L., and De Strooper, B. (2016). Familial Alzheimer's Disease Mutations in Presenilin Generate Amyloidogenic Aβ Peptide Seeds. *Neuron* 90, 410–416.

Vickers, J., Mitew, S., Woodhouse, A., Fernandez-Martos, C., Kirkcaldie, M., Canty, A., McCormack, G., and King, A. (2016). Defining the earliest pathological changes of Alzheimer's disease. *Curr. Alzheimer Res.* 13, 281–287.

Vidal, R., Calero, M., Piccardo, P., Farlow, M. R., Unverzagt, F. W., Méndez, E., Jiménez-Huete, A., Beavis, R., Gallo, G., Gomez-Tortosa, E., Ghiso, J., Hyman, B. T., Frangione, B., and Ghetti, B. (2000). Senile dementia associated with amyloid β protein angiopathy and tau perivascular pathology but not neuritic plaques in patients homozygous for the APOE-ε4 allele. *Acta Neuropathol.* 100, 1–12.

Vidal, R., Frangione, B., Rostagno, A., Mead, S., Révész, T., Plant, G., and Ghiso, J. (1999). A stop-codon mutation in the BRI gene associated with familial British dementia. *Nature* 399, 776–781.

Volpicelli-Daley, L. A., Luk, K. C., Patel, T. P., Tanik, S. A., Riddle, D. M., Stieber, A., Meaney, D. F., Trojanowski, J. Q., and Lee, V. M. Y. (2011). Exogenous α-Synuclein Fibrils Induce Lewy Body Pathology Leading to Synaptic Dysfunction and Neuron Death. *Neuron* 72, 57–71.

Walker, L., Stefanis, L., and Attems, J. (2019). Clinical and neuropathological differences between Parkinson's disease, Parkinson's disease dementia and dementia with Lewy bodies – current issues and future directions. *J. Neurochem.* 150, 467–474.

Walker, Z., Possin, K. L., Boeve, B. F., and Aarsland, D. (2015). Lewy body dementias. *Lancet* 386, 1683–1697.

Walsh, D. M., Klyubin, I., Fadeeva, J. V., Cullen, W. K., Anwyl, R., Wolfe, M. S., Rowan, M. J., and Selkoe, D. J. (2002). Naturally secreted oligomers of

amyloid β protein potently inhibit hippocampal long-term potentiation in vivo. *Nature* 416, 535–539.

Wang, H. Y., Lee, D. H. S., Davis, C. B., and Shank, R. P. (2000a). Amyloid peptide Aβ1-42 binds selectively and with picomolar affinity to α7 nicotinic acetylcholine receptors. *J. Neurochem.* 75, 1155–1161.

Wang, J., Dickson, D. W., Trojanowski, J. Q., and Lee, V. M. Y. (1999). The levels of soluble versus insoluble brain aβ distinguish Alzheimer's disease from normal and pathologic aging. *Exp. Neurol.* 158, 328–337.

Wang, J. Z., Wang, Z. H., and Tian, Q. (2014). Tau hyperphosphorylation induces apoptotic escape and triggers neurodegeneration in Alzheimer's disease. *Neurosci. Bull.* 30, 359–366.

Wang, X., Zhou, X., Li, G., Zhang, Y., Wu, Y., and Song, W. (2017a). Modifications and trafficking of APP in the pathogenesis of alzheimer's disease. *Front. Mol. Neurosci.* 10, 1–15.

Wang, Y., Balaji, V., Kaniyappan, S., Krüger, L., Irsen, S., Tepper, K., Chandupatla, R., Maetzler, W., Schneider, A., Mandelkow, E., and Mandelkow, E. M. (2017b). The release and trans-synaptic transmission of Tau via exosomes. *Mol. Neurodegener.* 12, 1–25.

Wang, Y., and Mandelkow, E. (2016). Tau in physiology and pathology. *Nat. Rev. Neurosci.* 17, 5–21.

Wang, Y., TesFaye, E., Yasuda, R. P., Mash, D. C., Armstrong, D. M., and Wolfe, B. B. (2000b). Effects of post-mortem delay on subunits of ionotropic glutamate receptors in human brain. *Mol. Brain Res.* 80, 123–131.

Wang, Z., Jackson, R. J., Hong, W., Taylor, W. M., Corbett, G. T., Moreno, A., Liu, W., Li, S., Frosch, M. P., Slutsky, I., Young-Pearse, T. L., Spires-Jones, T. L., and Walsh, D. M. (2017c). Human brain-derived Aβ oligomers bind to synapses and disrupt synaptic activity in a manner that requires APP. *J. Neurosci.* 37, 11947–11966.

Ward, M. W., Concannon, C. G., Whyte, J., Walsh, C. M., Corley, B., and Prehn, J. H. M. (2010). The amyloid precursor protein intracellular domain (AICD) disrupts actin dynamics and mitochondrial bioenergetics. *J. Neurochem.* 113, 275–284.

Wasco, W., Gurubhagavatula, S., Paradis, M. D., Romano, D. M., Sisodia, S. S., Hyman, B. T., Neve, R. L., and Tanzi, R. E. (1993). Isolation and characterization of APLP2 encoding a homologue of the alzheimer's associated amyloid β protein precursor. *Nat. Genet.* 5, 95–100.

Watanabe, A., Takio, K., and Ihara, Y. (1999). Deamidation and isoaspartate

formation in smeared tau in paired helical filaments: Unusual properties of the microtubule-binding domain of tau. *J. Biol. Chem.* 274, 7368–7378.

Waterston, R. H., Lindblad-Toh, K., Birney, E., Rogers, J., Abril, J. F., Agarwal, P., Agarwala, R., Ainscough, R., Alexandersson, M., An, P., Antonarakis, S. E., Attwood, J., Baertsch, R., Bailey, J., Barlow, K., Beck, S., Berry, E., Birren, B., Bloom, T., Bork, P., Botcherby, M., Bray, N., Brent, M. R., Brown, D. G., Brown, S. D., Bult, C., Burton, J., Butler, J., Campbell, R. D., Carninci, P., Cawley, S., Chiaromonte, F., Chinwalla, A. T., Church, D. M., Clamp, M., Clee, C., Collins, F. S., Cook, L. L., Copley, R. R., Coulson, A., Couronne, O., Cuff, J., Curwen, V., Cutts, T., Daly, M., David, R., Davies, J., Delehaunty, K. D., Deri, J., Dermitzakis, E. T., Dewey, C., Dickens, N. J., Diekhans, M., Dodge, S., Dubchak, I., Dunn, D. M., Eddy, S. R., Elnitski, L., Emes, R. D., Eswara, P., Eyras, E., Felsenfeld, A., Fewell, G. A., Flicek, P., Foley, K., Frankel, W. N., Fulton, L. A., Fulton, R. S., Furey, T. S., Gage, D., Gibbs, R. A., Glusman, G., Gnerre, S., Goldman, N., Goodstadt, L., Grafham, D., Graves, T. A., Green, E. D., Gregory, S., Guigó, R., Guyer, M., Hardison, R. C., Haussler, D., Hayashizaki, Y., LaHillier, D. W., Hinrichs, A., Hlavina, W., Holzer, T., Hsu, F., Hua, A., Hubbard, T., Hunt, A., Jackson, I., Jaffe, D. B., Johnson, L. S., Jones, M., Jones, T. A., Joy, A., Kamal, M., Karlsson, E. K., Karolchik, D., Kasprzyk, A., Kawai, J., Keibler, E., Kells, C., Kent, W. J., Kirby, A., Kolbe, D. L., Korf, I., Kucherlapati, R. S., Kulbokas, E. J., Kulp, D., Landers, T., Leger, J. P., Leonard, S., Letunic, I., Levine, R., Li, J., Li, M., Lloyd, C., Lucas, S., Ma, B., Maglott, D. R., Mardis, E. R., Matthews, L., Mauceli, E., Mayer, J. H., McCarthy, M., McCombie, W. R., McLaren, S., McLay, K., McPherson, J. D., Meldrim, J., Meredith, B., Mesirov, J. P., Miller, W., Miner, T. L., Mongin, E., Montgomery, K. T., Morgan, M., Mott, R., Mullikin, J. C., Muzny, D. M., Nash, W. E., Nelson, J. O., Nhan, M. N., Nicol, R., Ning, Z., Nusbaum, C., O'Connor, M. J., Okazaki, Y., Oliver, K., Overton-Larty, E., Pachter, L., Parra, G., Pepin, K. H., Peterson, J., Pevzner, P., Plumb, R., Pohl, C. S., Poliakov, A., Ponce, T. C., Ponting, C. P., Potter, S., Quail, M., Reymond, A., Roe, B. A., Roskin, K. M., Rubin, E. M., Rust, A. G., Santos, R., Sapojnikov, V., Schultz, B., Schultz, J., Schwartz, M. S., Schwartz, S., Scott, C., Seaman, S., Searle, S., Sharpe, T., Sheridan, A., Shownkeen, R., Sims, S., Singer, J. B., Slater, G., Smit, A., Smith, D. R., Spencer, B., Stabenau, A., Stange-Thomann, N., Sugnet, C., Suyama, M., Tesler, G., Thompson, J., Torrents, D., Trevaskis, E., Tromp, J., Ucla, C., Ureta-Vidal, A., Vinson, J. P., von Niederhausern, A. C., Wade, C. M., Wall, M., Weber, R. J., Weiss, R. B., Wendl, M. C., West, A. P., Wetterstrand,

K., Wheeler, R., Whelan, S., Wierzbowski, J., Willey, D., Williams, S., Wilson, R. K., Winter, E., Worley, K. C., Wyman, D., Yang, S., Yang, S. P., Zdobnov, E. M., Zody, M. C., and Lander, E. S. (2002). Initial sequencing and comparative analysis of the mouse genome. *Nature* 420, 520–562.

Waxman, E. A., Duda, J. E., and Giasson, B. I. (2008). Characterization of antibodies that selectively detect α-synuclein in pathological inclusions. *Acta Neuropathol.* 116, 37–46.

Wei, W., Nguyen, L. N., Kessels, H. W., Hagiwara, H., Sisodia, S., and Malinow, R. (2010). Amyloid beta from axons and dendrites reduces local spine number and plasticity. *Nat. Neurosci.* 13, 190–196.

Weiler, R., Lassmann, H., Fischer, P., Jellinger, K., and Winkler, H. (1990). A high ratio of chromogranin A to synaptin/synaptophysin is a common feature of brains in Alzheimer and Pick disease. *FEBS Lett.* 263, 337–339.

Weingarten, M. D., Lockwood, A. H., Hwo, S. Y., and Kirschner, M. W. (1975). A protein factor essential for microtubule assembly. *Proc. Natl. Acad. Sci. U. S. A.* 72, 1858–1862.

Weinhard, L., di Bartolomei, G., Bolasco, G., Machado, P., Schieber, N. L., Neniskyte, U., Exiga, M., Vadisiute, A., Raggioli, A., Schertel, A., Schwab, Y., and Gross, C. T. (2018). Microglia remodel synapses by presynaptic trogocytosis and spine head filopodia induction. *Nat. Commun.* 9, 1228.

Weisskopf, M. G., Castillo, P. E., Zalutsky, R. A., and Nicoll, R. A. (1994). Mediation of hippocampal mossy fiber long-term potentiation by cyclic AMP. *Science (80-.).* 265, 1878–1882.

Weller, R. O., Subash, M., Preston, S. D., Mazanti, I., and Carare, R. O. (2008). SYMPOSIUM: Clearance of Aβ from the Brain in Alzheimer's Disease: Perivascular Drainage of Amyloid-β Peptides from the Brain and Its Failure in Cerebral Amyloid Angiopathy and Alzheimer's Disease. *Brain Pathol.* 18, 253–266.

Weng, N., Baumler, M. D., Thomas, D. D. H., Falkowski, M. A., Swayne, L. A., Braun, J. E. A., and Groblewski, G. E. (2009). Functional role of J domain of cysteine string protein in Ca 2+-dependent secretion from acinar cells. *Am. J. Physiol. - Gastrointest. Liver Physiol.* 296, 1–10.

Westerman, M. A., Cooper-Blacketer, D., Mariash, A., Kotilinek, L., Kawarabayashi, T., Younkin, L. H., Carlson, G. A., Younkin, S. G., and Ashe, K. H. (2002). The relationship between Aβ and memory in the Tg2576 mouse model of Alzheimer's disease. *J. Neurosci.* 22, 1858–1867.

Westmark, C. J. (2013). What's hAPPening at synapses the role of amyloid β-

protein precursor and β-Amyloid in neurological disorders. *Mol. Psychiatry* 18, 425–434.

White, J. A., Krzystek, T. J., Hoffmar-Glennon, H., Thant, C., Zimmerman, K., Iacobucci, G., Vail, J., Thurston, L., Rahman, S., and Gunawardena, S. (2020). Excess Rab4 rescues synaptic and behavioral dysfunction caused by defective HTT-Rab4 axonal transport in Huntington's disease. *Acta Neuropathol. Commun.* 8, 1–22.

Whitson, J. S., Selkoe, D. J., and Cotman, C. W. (1989). Amyloid β protein enhances the survival of hippocampal neurons in vitro. *Science (80-.).* 243, 1488–1490.

Wiedenmann, B., and Franke, W. W. (1985). Identification and localization of synaptophysin, an integral membrane glycoprotein of Mr 38,000 characteristic of presynaptic vesicles. *Cell* 41, 1017–1028.

Wilhelm, B. G., Mandad, S., Truckenbrodt, S., Kroḧnert, K., Schäfer, C., Rammner, B., Koo, S. J., Claßen, G. A., Krauss, M., Haucke, V., Urlaub, H., and Rizzoli, S. O. (2014). Composition of isolated synaptic boutons reveals the amounts of vesicle trafficking proteins. *Science (80-.).* 344, 1023–1028.

Willem, M., Tahirovic, S., Busche, M. A., Ovsepian, S. V., Chafai, M., Kootar, S., Hornburg, D., Evans, L. D. B., Moore, S., Daria, A., Hampel, H., Müller, V., Giudici, C., Nuscher, B., Wenninger-Weinzierl, A., Kremmer, E., Heneka, M. T., Thal, D. R., Giedraitis, V., Lannfelt, L., Müller, U., Livesey, F. J., Meissner, F., Herms, J., Konnerth, A., Marie, H., and Haass, C. (2015). σ-Secretase processing of APP inhibits neuronal activity in the hippocampus. *Nature* 526, 443–447.

Wilson, R. S., Yu, L., Trojanowski, J. Q., Chen, E.-Y., Boyle, P. A., Bennett, D. A., and Schneider, J. A. (2013). TDP-43 Pathology, Cognitive Decline, and Dementia in Old Age. *JAMA Neurol.* 70, 1418–1424.

Winston, C. N., Goetzl, E. J., Akers, J. C., Carter, B. S., Rockenstein, E. M., Galasko, D., Masliah, E., and Rissman, R. A. (2016). Prediction of conversion from mild cognitive impairment to dementia with neuronally derived blood exosome protein profile. *Alzheimer's Dement. Diagnosis, Assess. Dis. Monit.* 3, 63–72.

Wishart, T. M., Parson, S. H., and Gillingwater, T. H. (2006). Synaptic vulnerability in neurodegenerative disease. *J. Neuropathol. Exp. Neurol.* 65, 733–739.

Wishart, T. M., Rooney, T. M., Lamont, D. J., Wright, A. K., Morton, A. J., Jackson, M., Freeman, M. R., and Gillingwater, T. H. (2012). Combining Comparative Proteomics and Molecular Genetics Uncovers Regulators of Synaptic and

Axonal Stability and Degeneration In Vivo. *PLOS Genet.* 8.

Wolters, F. J., and Arfan Ikram, M. (2019). Epidemiology of Vascular Dementia: Nosology in a Time of Epiomics. *Arterioscler. Thromb. Vasc. Biol.* 39, 1542–1549.

Woodhouse, A., West, A. K., Chuckowree, J. A., Vickers, J. C., and Dickson, T. C. (2005). Does β-amyloid plaque formation cause structural injury to neuronal processes? *Neurotox. Res.* 7, 5–15.

Wray, S., Saxton, M., Anderton, B. H., and Hanger, D. P. (2008). Direct analysis of tau from PSP brain identifies new phosphorylation sites and a major fragment of N-terminally cleaved tau containing four microtubule-binding repeats. *J. Neurochem.* 105, 2343–2352.

Wu, H.-Y., Kuo, P.-C., Wang, Y.-T., Lin, H.-T., Roe, A. D., Wang, B. Y., Han, C.-L., Hyman, B. T., Chen, Y.-J., and Tai, H.-C. (2018). β-Amyloid Induces Pathology-Related Patterns of Tau Hyperphosphorylation at Synaptic Terminals. *J. Neuropathol. Exp. Neurol.* 77, 814–826.

Wu, H. Y., Hudry, E., Hashimoto, T., Kuchibhotla, K., Rozkalne, A., Fan, Z., Spires-Jones, T., Xie, H., Arbel-Ornath, M., Grosskreutz, C. L., Bacskai, B. J., and Hyman, B. T. (2010a). Amyloid β induces the morphological neurodegenerative triad of spine loss, dendritic simplification, and neuritic dystrophies through calcineurin activation. *J. Neurosci.* 30, 2636–2649.

Wu, J. W., Breydo, L., Isas, J. M., Lee, J., Kuznetsov, Y. G., Langen, R., and Glabe, C. (2010b). Fibrillar oligomers nucleate the oligomerization of monomeric amyloid beta but do not seed fibril formation. *J. Biol. Chem.* 285, 6071–6079.

Wu, J. W., Herman, M., Liu, L., Simoes, S., Acker, C. M., Figueroa, H., Steinberg, J. I., Margittai, M., Kayed, R., Zurzolo, C., Di Paolo, G., and Duff, K. E. (2013). Small misfolded tau species are internalized via bulk endocytosis and anterogradely and retrogradely transported in neurons. *J. Biol. Chem.* 288, 1856–1870.

Wu, T., Dejanovic, B., Gandham, V. D., Gogineni, A., Edmonds, R., Schauer, S., Srinivasan, K., Huntley, M. A., Wang, Y., Wang, T.-M., Hedehus, M., Barck, K. H., Stark, M., Ngu, H., Foreman, O., Meilandt, W. J., Elstrott, J., Chang, M. C., Hansen, D. V, Carano, R. A. D., Sheng, M., and Hanson, J. E. (2019). Complement C3 Is Activated in Human AD Brain and Is Required for Neurodegeneration in Mouse Models of Amyloidosis and Tauopathy. *Cell Rep.* 28, 2111–2123.

Xiao, N. A., Zhang, J., Zhou, M., Wei, Z., Wu, X. L., Dai, X. M., Zhu, Y. G., and Chen, X. C. (2015). Reduction of glucose metabolism in olfactory bulb is an

earlier Alzheimer's disease-related biomarker in 5XFAD mice. *Chin. Med. J. (Engl).* 128, 2220–2227.

Xu, F., Proft, J., Gibbs, S., Winkfein, B., Johnson, J. N., Syed, N., and Braun, J. E. A. (2010). Quercetin targets cysteine string protein (CSPα) and impairs synaptic transmission. *PLoS One* 5, 1–13.

Xu, Y., Cui, L., Dibello, A., Wang, L., Lee, J., Saidi, L., Lee, J.-G., and Ye, Y. (2018). DNAJC5 facilitates USP19-dependent unconventional secretion of misfolded cytosolic proteins. *Cell Discov.* 4, 1–18.

Yamada, K. (2017). Extracellular tau and its potential role in the propagation of tau pathology. *Front. Neurosci.* 11, 1–5.

Yamada, K., Cirrito, J. R., Stewart, F. R., Jiang, H., Finn, M. B., Holmes, B. B., Binder, L. I., Mandelkow, E. M., Diamond, M. I., Lee, V. M. Y., and Holtzman, D. M. (2011). In vivo microdialysis reveals age-dependent decrease of brain interstitial fluid tau levels in P301S human tau transgenic mice. *J. Neurosci.* 31, 13110–13117.

Yanamandra, K., Kfoury, N., Jiang, H., Mahan, T. E., Ma, S., Maloney, S. E., Wozniak, D. F., Diamond, M. I., and Holtzman, D. M. (2013). Anti-tau antibodies that block tau aggregate seeding invitro markedly decrease pathology and improve cognition in vivo. *Neuron* 80, 402–414.

Yang, D. S., Stavrides, P., Mohan, P. S., Kaushik, S., Kumar, A., Ohno, M., Schmidt, S. D., Wesson, D., Bandyopadhyay, U., Jiang, Y., Pawlik, M., Peterhoff, C. M., Yang, A. J., Wilson, D. A., St George-Hyslop, P., Westaway, D., Mathews, P. M., Levy, E., Cuervo, A. M., and Nixon, R. A. (2011). Reversal of autophagy dysfunction in the TgCRND8 mouse model of Alzheimer's disease ameliorates amyloid pathologies and memory deficits. *Brain* 134, 258–277.

Yang, T., Li, S., Xu, H., Walsh, D. M., and Selkoe, D. J. (2017). Large soluble oligomers of amyloid β-protein from alzheimer brain are far less neuroactive than the smaller oligomers to which they dissociate. *J. Neurosci.* 37, 152–163.

Yang, X., and Tohda, C. (2018). Diosgenin restores Aβ-induced axonal degeneration by reducing the expression of heat shock cognate 70 (HSC70). *Sci. Rep.* 8, 1–10.

Yao, P. J., Zhu, M., Pyun, E. I., Brooks, A. I., Therianos, S., Meyers, V. E., and Coleman, P. D. (2003). Defects in expression of genes related to synaptic vesicle trafficking in frontal cortex of Alzheimer's disease. *Neurobiol. Dis.* 12, 97–109.

Yates, D., and McLoughlin, D. M. (2008). The molecular pathology of Alzheimer's

disease. *Psychiatry* 7, 1–5.

Ye, S., Huang, Y., Müllendorff, K., Dong, L., Giedt, G., Meng, E. C., Cohen, F. E., Kuntz, I. D., Weisgraber, K. H., and Mahley, R. W. (2005). Apolipoprotein (apo) E4 enhances amyloid β peptide production in cultured neuronal cells: ApoE structure as a potential therapeutic target. *Proc. Natl. Acad. Sci. U. S. A.* 102, 18700–18705.

Ye, X., Feng, T., Tammineni, P., Chang, Q., Jeong, Y. Y., Margolis, D. J., Cai, H., Kusnecov, A., and Cai, Q. (2017). Regulation of synaptic amyloid-β generation through bace1 retrograde transport in a mouse model of alzheimer's disease. *J. Neurosci.* 37, 2639–2655.

Ye, Y. (2018). Regulation of protein homeostasis by unconventional protein secretion in mammalian cells. *Semin. Cell Dev. Biol.* 83, 29–35.

Yerbury, J. J., Ooi, L., Dillin, A., Saunders, D. N., Hatters, D. M., Beart, P. M., Cashman, N. R., Wilson, M. R., and Ecroyd, H. (2016). Walking the tightrope: Proteostasis and neurodegenerative disease. *J. Neurochem.* 137, 489–505.

Yin, Y., Gao, D., Wang, Y., Wang, Z. H., Wang, X., Ye, J., Wu, D., Fang, L., Pi, G., Yang, Y., Wang, X. C., Lu, C., Ye, K., and Wang, J. Z. (2016). Tau accumulation induces synaptic impairment and memory deficit by calcineurin-mediated inactivation of nuclear CaMKIV/CREB signaling. *Proc. Natl. Acad. Sci. U. S. A.* 113, 3773–3781.

You, Y., Perkins, A., Cisternas, P., Muñoz, B., Taylor, X., You, Y., Garringer, H. J., Oblak, A. L., Atwood, B. K., Vidal, R., and Lasagna-Reeves, C. A. (2019). Tau as a mediator of neurotoxicity associated to cerebral amyloid angiopathy. *Acta Neuropathol. Commun.* 7, 26.

Young-Pearse, T. L., Bai, J., Chang, R., Zheng, J. B., Loturco, J. J., and Selkoe, D. J. (2007). A critical function for β-amyloid precursor protein in neuronal migration revealed by in utero RNA interference. *J. Neurosci.* 27, 14459–14469.

Young, J. J., Lavakumar, M., Tampi, D., Balachandran, S., and Tampi, R. R. (2018). Frontotemporal dementia: latest evidence and clinical implications. *Ther. Adv. Psychopharmacol.* 8, 33–48.

Yuksel, M., and Tacal, O. (2019). Trafficking and proteolytic processing of amyloid precursor protein and secretases in Alzheimer's disease development: An up-to-date review. *Eur. J. Pharmacol.* 856.

Zellner, M., Babeluk, R., Diestinger, M., Pirchegger, P., Skeledzic, S., and Oehler, R. (2008). Fluorescence-based Western blotting for quantitation of protein biomarkers in clinical samples. *Electrophoresis* 29, 3621–3627.

Zempel, H., Thies, E., Mandelkow, E., and Mandelkow, E. M. (2010). Aβ oligomers cause localized Ca2+ elevation, missorting of endogenous Tau into dendrites, Tau phosphorylation, and destruction of microtubules and spines. *J. Neurosci.* 30, 11938–11950.

Zhan, S. S., Beyreuther, K., and Schmitt, H. P. (1993). Vascular dementia in Spatz-Lindenberg's disease (SLD): cortical synaptophysin immunoreactivity as compared with dementia of Alzheimer type and non-demented controls. *Acta Neuropathol.* 86, 259–264.

Zhan, S. S., Beyreuther, K., and Schmitt, H. P. (1994). Synaptophysin immunoreactivity of the cortical neuropil in vascular dementia of binswanger type compared with the dementia of alzheimer type and nondemented controls. *Dement. Geriatr. Cogn. Disord.* 5, 79–87.

Zhang, H., Kelley, W. L., Chamberlain, L. H., Burgoyne, R. D., and Lang, J. (1999). Mutational analysis of cysteine-string protein function in insulin exocytosis. *J. Cell Sci.* 112, 1345–1351.

Zhang, W., Khan, A., Östenson, C. G., Berggren, P. O., Efendic, S., and Meister, B. (2002). Down-regulated expression of exocytotic proteins in pancreatic islets of diabetic GK rats. *Biochem. Biophys. Res. Commun.* 291, 1038–1044.

Zhang, X., Zhou, K., Wang, R., Cui, J., Lipton, S. A., Liao, F. F., Xu, H., and Zhang, Y. W. (2007). Hypoxia-inducible factor 1α (HIF-1α)-mediated hypoxia increases BACE1 expression and β-amyloid generation. *J. Biol. Chem.* 282, 10873–10880.

Zhang, Y. Q., Henderson, M. X., Colangelo, C. M., Ginsberg, S. D., Bruce, C., Wu, T., and Chandra, S. S. (2012). Identification of CSPα Clients Reveals a Role in Dynamin 1 Regulation. *Neuron* 74, 136–150.

Zhang, Y. quan, and Chandra, S. S. (2014). Oligomerization of Cysteine String Protein alpha mutants causing adult neuronal ceroid lipofuscinosis. *Biochim. Biophys. Acta - Mol. Basis Dis.* 1842, 2136–2146.

Zhang, Y. W., Thompson, R., Zhang, H., and Xu, H. (2011). APP processing in Alzheimer's disease. *Mol. Brain* 4, 1–13.

Zhang, Z., Song, M., Liu, X., Su Kang, S., Duong, D. M., Seyfried, N. T., Cao, X., Cheng, L., Sun, Y. E., Ping Yu, S., Jia, J., Levey, A. I., and Ye, K. (2015). Delta-secretase cleaves amyloid precursor protein and regulates the pathogenesis in Alzheimer's disease. *Nat. Commun.* 6, 1–16.

Zhao, C. M., Jacobsson, G., Chen, D., Håkanson, R., and Meister, B. (1997). Exocytotic proteins in enterochromaffin-like (ECL) cells of the rat stomach. *Cell Tissue Res.* 290, 539–551.

Zhao, J., Fu, Y., Yasvoina, M., Shao, P., Hitt, B., O'Connor, T., Logan, S., Maus, E., Citron, M., Berry, R., Binder, L., and Vassar, R. (2007). β-site amyloid precursor protein cleaving enzyme 1 levels become elevated in neurons around amyloid plaques: Implications for Alzheimer's disease pathogenesis. *J. Neurosci.* 27, 3639–3649.

Zhao, J., Liu, X., Xia, W., Zhang, Y., and Wang, C. (2020). Targeting Amyloidogenic Processing of APP in Alzheimer's Disease. *Front. Mol. Neurosci.* 13, 1–17.

Zhiyou, C., Yong, Y., Shanquan, S., Jun, Z., Liangguo, H., Ling, Y., and Jieying, L. (2009). Upregulation of BACE1 and β-amyloid protein mediated by chronic cerebral hypoperfusion contributes to cognitive impairment and pathogenesis of alzheimer's disease. *Neurochem. Res.* 34, 1226–1235.

Zhou, L., McInnes, J., Wierda, K., Holt, M., Herrmann, A. G., Jackson, R. J., Wang, Y. C., Swerts, J., Beyens, J., Miskiewicz, K., Vilain, S., Dewachter, I., Moechars, D., Strooper, B. De, Spires-Jones, T. L., Wit, J. De, and Verstreken, P. (2017). Tau association with synaptic vesicles causes presynaptic dysfunction. *Nat. Commun.* 8, 1–13.

Zinsmaier, K. E., Eberle, K. K., Buchner, E., Walter, N., and Benzer, S. (1994). Paralysis and early death in cysteine string protein mutants of Drosophila. *Science (80-.).* 263, 977–980.

Zinsmaier, K. E., Hofbauer, A., Heimbeck, G., Pflugfelder, G. O., Buchner, S., and Buchner, E. (1990). A cysteine-string protein is expressed in retina and brain of drosophila. *J. Neurogenet.* 7, 15–29.

Zlokovic, B. V. (2011). Neurovascular pathways to neurodegeneration in Alzheimer's disease and other disorders. *Nat. Rev. Neurosci.* 12, 723–738.

Zou, C., Montagna, E., Shi, Y., Peters, F., Blazquez-Llorca, L., Shi, S., Filser, S., Dorostkar, M. M., and Herms, J. (2015). Intraneuronal APP and extracellular Aβ independently cause dendritic spine pathology in transgenic mouse models of Alzheimer's disease. *Acta Neuropathol.* 129, 909–920.